MEDSI 2025
LUND • SWEDEN

THE 13th INTERNATIONAL CONFERENCE ON MECHANICAL ENGINEERING DESIGN OF SYNCHROTRON RADIATION EQUIPMENT AND INSTRUMENTATION

September 15 –19, 2025, Lund, Sweden

PROCEEDINGS at a glance

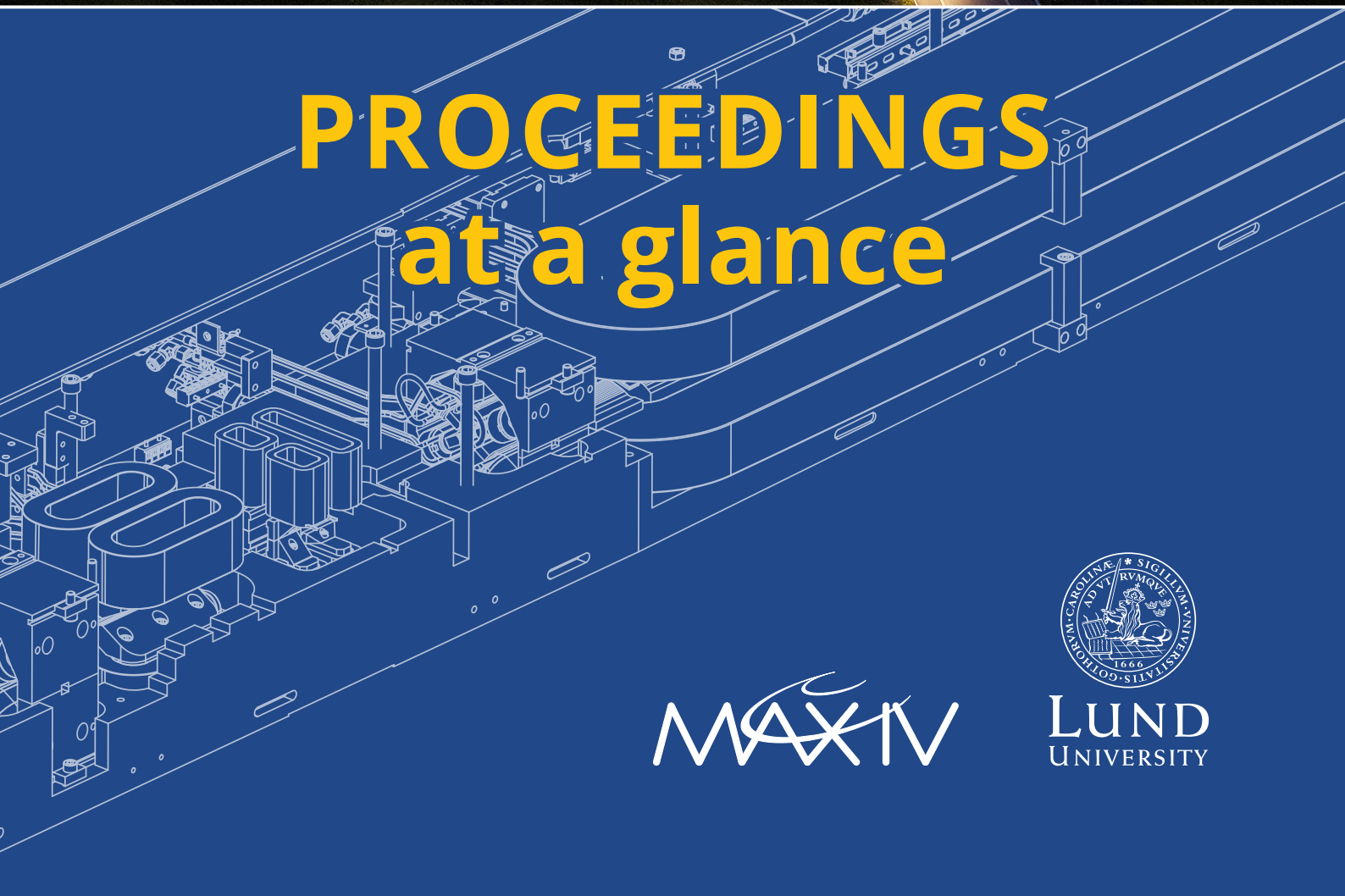

MAX IV

LUND UNIVERSITY

ISBN: 978-3-95450-263-9 ISSN: 2673-5520 doi: 10.18429/JACoW-MEDSI2025-TUOA01

APS UPGRADE - BEAMLINE ENGINEERING OVERVIEW*

O. Schmidt†, D. Capatina, J. Knopp, R. Winarski, Sunil Bean, Altaf Khan, M. Ramanathan
Argonne National Laboratory, Lemont, Illinois, USA

Abstract

The Advanced Photon Source Upgrade (APSU) has transformed the APS into a 4th generation light source. The new 6 GeV, 200 mA multi-bend achromat (MBA) storage ring, along with injector improvements and new front ends will provide an increased brightness and an orders-of-magnitude improvement in coherent flux over the current facility.

To take advantage of these new capabilities, we have designed and constructed nine new "feature beamlines" and implemented numerous additional beamline enhancements, all while ensuring the compatibility of existing programs. This paper will present a comprehensive overview of the APSU beamline scope, focusing on successes, challenges, and lessons learned.

FEATURE BEAMLINES

Nine "feature beamlines" were chosen to showcase "best in class" performance, taking full advantage of the new accelerator. The feature beamline scope included:

- New enclosures and utilities
- New Photon delivery systems
- New Optics
- New Beamline instrumentation
- New Controls systems

Figure 1: New Long Beamline Building (LBB).

Two of these beamlines, the InSitu Nanoprobe (ISN) and the High Energy X-ray Microscope (HEXM), extend into the new Long Beamline Building (Fig. 1) to enable long-distance optics, low-background environments, and enhanced stability for nanoscale focusing and high-energy diffraction/imaging.

The Coherent High Energy X-ray (CHEX) beamline has four independently operating branches with eight experimental stations from two canted undulators. The tunable-energy branch (28-ID-A/B/C) operates from 15-60 keV with a horizontally deflecting DCM. Three selectable-energy branches (28-ID-A/D/E, 28-ID-A/F, and 28-ID-A/G), operate at fixed energies between 15 to 60 keV utilizing single crystal monochromators.

The remaining feature beamlines include POLAR, XPCS, CSSI, 3DMN, ATOMIC, and PtychoProbe, spanning coherent imaging, high-energy scattering, time-resolved dynamics, and operando studies. The overall project Key Performance Parameters (KPPs) required demonstration of:

- Brightness at a defined energy and verification of the usable energy range.
- ISN: a 50 nm × 50 nm focal spot at the sample.

All feature beamlines met or exceeded their KPPs!

ENHANCEMENT BEAMLINES

Fifteen existing beamlines received major upgrades. The specific enhancements were chosen to get the best impact for money spent:

- Canted geometries to create independent branches, requiring new front-ends, shutters, primary slits, and branch enclosures; in most cases requiring significant redesign of their photon delivery system.
- New optics (monochromators, mirrors, multilayers, refractive lenses), upgraded absorbers and shielding.
- New/modernized instruments (diffractometers, detectors, sample environments).
- Controls and timing updates, beam-based alignment, and improved thermal–mechanical stability.

In total, approximately 60 instruments and about 30 optical subsystems were delivered or refurbished across the beamlines, leveraging reuse where appropriate.

BENDING MAGNET (BM) BEAMLINES

Due to the shift in the bending magnet source in the new storage ring, all BM beamlines were required to move inboard by 42 mm with an additional 0.5 mrad inboard angular shift. This realignment forced the existing components closer to the storage ring shielding wall in the first optical enclosures necessitating rerouting of utilities. The additional angular shift had a larger impact on downstream transport pipe, wall openings, and transitional shielding as the beam center deviated further from the original trajectory.

* Work supported by the U.S. Department of Energy, Office of Science, Basic Energy Sciences, under contract #DE-AC02-06CH11357.
† oschmidt@anl.gov

ISBN: 978-3-95450-263-9 ISSN: 2673-5520 doi: 10.18429/JACoW-MEDSI2025-TUOA02

DESIGN AND TECHNICAL COMMISSIONING OF THE IN SITU NANOPROBE ENDSTATION AND INSTRUMENT AT THE ADVANCED PHOTON SOURCE*

B. Davis†, Z. Cai, S. Kearney, B. Lai, J. Maser, P. Mercado-Lozano,
T. Mooney, L. Rebuffi, X. Shi, D. Shu, S. Wieghold
Advanced Photon Source, Argonne National Laboratory, Lemont, IL, USA

Abstract

The In Situ Nanoprobe (ISN) is a newly constructed, best-in-class experimental x-ray instrument at sector 19 of the upgraded Advanced Photon Source (APS-U). The new ISN beamline provides a 4.8-30 keV monochromatic x-ray beam, high coherence, and very high focused flux. Kirkpatrick-Baez (KB) mirror focusing offers a focal spot as low as 20 nm at a photon energy of 25 keV. The KB mirrors also provide a long working distance of 61 mm, to enable a versatile suite of sample environments: in-vacuum or in-air operation, heating to >1000 ˚C, cooling to 40 K, flow of liquids & gases, and applied electrical fields. The instrument supports fast fly-scanning of relatively large and heavy samples of ~10x10 mm and 2 kg at 1 mm/s. Measurement techniques include 2D and 3D x-ray fluorescent mapping, ptychographic coherent structural imaging, x-ray diffraction, x-ray excited optical luminescence and x-ray beam induced current and voltage measurements. This work presents the first mechanical results from the ongoing technical commissioning in Summer 2025, including the design and architecture of the endstation, vibrational and thermal management, beam conditioning, KB mirror design, vacuum chamber design, sample scanning, metrology, sample environments and detector systems design.

INTRODUCTION

The Advanced Photon Source (APS) at Argonne National Laboratory (ANL) has recently completed a major upgrade project (APS-U), increasing the brightness of the x-ray beams by up to 500 times with world-record beam emittance / coherence [1]. This upgrade will enable scientific discoveries across many disciplines.

The In Situ Nanoprobe (ISN) is a hard x-ray beamline [2] that was newly constructed, among many other APS-U beamlines, to take full advantage of the increased brightness and coherence. ISN is designed to operate with a very stable monochromatic x-ray beam of 4.8 to 30 keV. ISN was envisioned to study complex materials systems under *in-situ* and *operando* conditions across many lengths scales. This work details the numerous advancements in endstation and instrument engineering necessary to realize this goal and reports the first mechanical results from the ongoing technical commissioning.

* This research used resources of the Advanced Photon Source, a U.S. Department of Energy (DOE) Office of Science User Facility operated for the DOE Office of Science by Argonne National Laboratory under Contract No. DE-AC02-06CH11357
†bfdavis@anl.gov

ENDSTATION ENCLOSURE

The new ISN long beamline (see Fig. 1) is located at Sector 19-ID of APS and the ISN instrument is located in a satellite building at a distance of 220 m from the undulator source. The endstation enclosure is designed to isolate ambient and transient vibrations and mitigate thermal drifts, with the goal of maintaining stability of the nanofocusing mirrors and ultimately the x-ray focal spot.

Figure 1. ISN beamline and satellite building at APS, outlined in black.

Thermal stability is achieved with a passive system comprised of an intermediate air environment, vestibule, and laminar flow air socks (see Fig. 2). All HVAC supply and exhaust piping are routed through labyrinths in the ceiling and a vibration isolated exhaust fan is outside the enclosure. Hutch air temperature must stay within ±0.05 °C for 1 hr and the instrument surface temperature within ±0.01 °C for 1 hr.

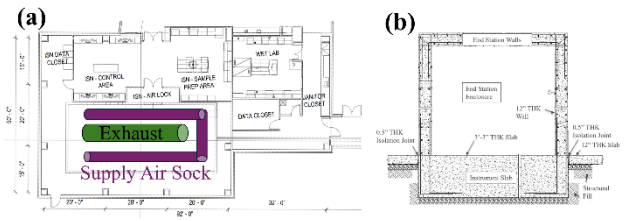

Figure 2. (a) Schematic layout of the ISN satellite building and endstation. (b) Cross-section view of the end station concrete foundation, isolation joint, and walls.

Vibrational stability is aided by a stand-alone concrete slab of thickness 1 m, with isolation joints damping from the surrounding floor. These construction specifications were made to meet a vibration criteria of VC-G, or 0.78 μm/s rms across 1-100 Hz band, based on similar facilities [3].

ISBN: 978-3-95450-263-9 ISSN: 2673-5520 doi: 10.18429/JACoW-MEDSI2025-TUOA04

ENGINEERING ADVANCEMENTS IN X-RAY PUMP–PROBE TECHNIQUES: DELAYLINE FOR ATTOSECOND SCIENCES AT LCLS

Hengzi Wang*, Taran Driver, Yoshio Ichii, Namrata Balakrishnan, Randy Whitney, James Cryan, Agostino Marinelli
SLAC National Accelerator Laboratory, Menlo Park, CA, USA

Abstract

X-ray pump–probe experiments at X-ray free-electron laser (XFEL) facilities, such as LCLS, enable investigation of ultrafast electronic and atomic dynamics. Central to these experiments are advanced delayline systems for generating X-ray pulse pairs with finely tunable time delays and precise alignment. In this work, we present background on delayline techniques and focus on the development of the next-generation Soft X-ray (SXR) delayline at LCLS. The SXR delayline delivers attosecond- to femtosecond-resolution timing, exceptional beam stability, and rapid mode switching, addressing the limitations of earlier technologies. We discuss its optical engineering challenges, control strategies, and scientific applications in ultrafast materials, chemistry, and quantum science.

INTRODUCTION

Ultrafast X-ray science, enabled by X-ray free-electron lasers (XFELs) such as the Linac Coherent Light Source (LCLS), has revolutionized our ability to observe atomic, molecular, and condensed matter dynamics at unprecedented time scales, extending into the attosecond regime [1]. Central to these advances are X-ray pump–probe experiments, which rely on precise control and generation of two time-delayed X-ray pulses to explore ultrafast phenomena that were previously inaccessible.

To achieve this precision, various delayline systems have been developed at LCLS, utilizing both magnetic chicane architectures and split-and-delay optics. Magnetic chicanes employ sequences of dipole magnets to introduce variable path length separations in the electron beam, thereby generating two X-ray pulses with adjustable temporal delays [2]. Split-and-delay optics utilize high-quality crystals and mirrors to split a single X-ray pulse into two, directing each along distinct optical paths with engineered delays before recombination at the sample [3]. Both technologies present important trade-offs in terms of achievable delay range, temporal resolution, and beam stability. Typically, these techniques can deliver delays from several femtoseconds to the nanosecond scale.

However, for attosecond science, new approaches are required. At LCLS, the XLEAP scheme was developed to deliver attosecond X-ray pulses; nevertheless, the pulse duration in XLEAP is not tunable, and the scheme lacks the ability to freely adjust delays across zero or to independently shape or steer both X-ray pulses. These limitations constrain its suitability for next-generation attosecond pump–probe experiments [4].

To address these needs, the Soft X-ray (SXR) delayline project was launched at LCLS, targeting the soft X-ray regime with tunable sub-femtosecond delays, robust operational stability, and rapid mode-switching capabilities. The SXR delay line is installed in the SXRSS section between the 3rd and 4th dipole magnets (see Fig. 1), providing tunable time separation for the generation of X-ray pulse pairs. Its optical path comprises a pair of ultra-precision mirrors mounted on translation stages, actively aligned via piezo actuators and monitored with two capacitive sensors, achieving attosecond timing fidelity.

This integrated system overcomes the limitations of both XLEAP and SXRSS, delivering attosecond-resolution delay tuning, high repeatability, and long-term stability. As a result, it enables new advances in attosecond-resolved studies of quantum materials, ultrafast chemical reactions, and nonlinear X-ray interactions.

SXR DELAYLINE: MOTIVATION AND SCIENCE DRIVERS

The SXR delayline is conceived to overcome key shortcomings and unlock new science opportunities:

- **Freely tunable delays crossing zero:** Crucial for time-resolved studies where both pump-before-probe and probe-before-pump processes are relevant.
- **Attosecond to few-femtosecond resolution:** Required to follow electron dynamics and transient structure formation.
- **Decoupled pulse properties:** Ability to independently specify the energy, arrival time, direction, and duration for both X-ray pulses, broadening the experimental toolkit.
- **Long-scale stability and repeatability:** Vital for extended beamlines (up to 100 m), where micron-scale misalignments can destroy time resolution and focal overlap.
- **Rapid mode switching:** Support for soft x-ray self-seeding (SXRSS), SXR delayline pump–probe, or normal SASE[1] operation.

* hengziwang@slac.stanford.edu

[1] SASE: Self-Amplified Spontaneous Emission Free-Electron Laser. SASE FELs generate intense coherent X-ray pulses via exponential amplification of spontaneous emission in an undulator, as the electron bunch propagates without external seeding.

ISBN: 978-3-95450-263-9 ISSN: 2673-5520 doi: 10.18429/JACoW-MEDSI2025-TUOA05

THE DESIGN OF SIBIPIRUNA – A CRYOGENIC SOFT X-RAY TOMOGRAPHY BEAMLINE WITH BSL2, BSL3 AND BSL4 COMPATIBILITY FOR SIRIUS AND ORION AT CNPEM

R. R. Geraldes*, G. G. Basilio, C. S. N. C. Bueno, V. B. Falchetto, M. O. E. Leal, F. R. Lena, M. O. de Lima, P. H. M. Lopes Silva, M. B. Machado, G. B. Z. L. Moreno, E. O. Pereira, A. C. Pinto, P. P. R. Proença, R. S. Rabelo, G. G. Ribeiro, G. L. M. P. Rodrigues, L. Sanfelici, J. S. C. A. Santos, G. A. de Souza, M. B. Cardoso, H. Westfahl Jr
Brazilian Center for Research in Energy and Materials, Campinas, Brazil

Abstract

Recent outbreaks of emerging infectious diseases have highlighted the need for enhanced biosafety measures and research capabilities. Addressing this, the Brazilian Center for Research in Energy and Materials (CNPEM) is spearheading the development of Orion, Latin America's first facility to host a Biosafety Level 4 (BSL4) laboratory. More ambitiously, Orion will pioneer a groundbreaking global achievement: the integration between BSL4 areas and synchrotron beamlines. A connection between Orion and the 4th-generation storage ring Sirius/LNLS will enable unprecedented X-ray bioimaging opportunities in soft, tender and hard X-rays, with a program covering cells, tissues up to entire organisms. At the lower energy range, the SIBIPIRUNA beamline will allow for 3D imaging of infected single cells using cryogenic soft X-ray tomography. With a resolution target of 30 nm, rapid full tomography time around 5 to 10 minutes, and whole unstained samples, unmatching detailed studies of viral infection mechanisms will be unlocked. This work describes the design of the beamline and its end-stations, highlighting their compatibility and compliance with biocontainment and decontamination needs.

INTRODUCTION

Since a few years, the Brazilian Center for Research in Energy and Materials (CNPEM) has been granted the opportunity to carry out the Orion Project – introducing Latin America's first maximum biocontainment laboratory, designed for handling and researching the most dangerous and exotic pathogens that pose a high risk of life-threatening diseases [1]. And, remarkably, the campus already hosts four other national labs – namely: the Brazilian Synchrotron Light Laboratory (LNLS), the Brazilian Biosciences National Laboratory (LNBio), the Brazilian Nanotechnology National Laboratory (LNNano), and the Brazilian Bioreneweables National Laboratory (LNBR) – which can be coordinated together to create unmatching scientific capabilities.

Typical biological research of Biosafety Level (BSL) 2, 3 and 4 labs will be expanded with bioimaging capabilities in electron microscopy (EM) and synchrotron techniques. The latter will be a first-of-a-kind worldwide feature, achieved by connecting Orion to end-stations of three beamlines from the 4th-generation light source Sirius [2]. As such, unprecedented engineering and operational challenges are addressed. A paper covering the beamlines and their scientific cases is in preparation. This work is on the design of SIBIPIRUNA (Soft x-ray bio-Imaging Beamline with Partially coherent Illumination for Resolving cellular Ultra-structure in Nanometers), dedicated to single-cell 3D imaging.

BEAMLINE OPTICAL LAYOUT

Cryogenic soft X-ray tomography (cryo-SXT) is a proven absorption-contrast technique capable of imaging subcellular architecture without the need for staining or chemical modification [3–7]. SIBIPIRUNA will be the first to implement biosafety concepts to cope with frozen hydrated cells infected with agents rated up to BSL4. Operating between 300 and 750 eV to take advantage of the so-called water window, it has the optical layout depicted in Fig. 1. The source is a low-field dipole (B2). The primary optics has a cylindrical side-bounce mirror (M1) at 13.5 m, a plane-grating monochromator (PGM) at 27.3 m, and a toroidal side-bounce mirror (M2) at 48 m. The latter produces a collimated beam, creating the chance of two downstream stations with identical optics. The first one, ≈ 50 m, falls still within Sirius experimental hall, allowing for partial integration and technical commissioning well ahead of the delivery of the Orion building. Already implementing the BSL4-compatible beamline instrumentation and operational procedures under development, it will be a functional prototype for validation and debugging, while making a BSL2-rated facility available to the scientific community. The second one, ≈ 110 m, in turn, lies within the Orion premises, with the experimental conditions for BSL3/4 samples.

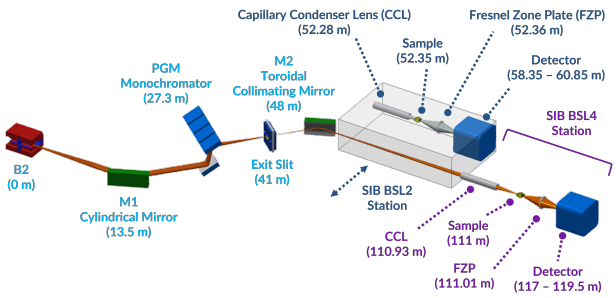

Figure 1: Optical layout of the SIBIPIRUNA beamline.

* renan.geraldes@lnls.br

ISBN: 978-3-95450-263-9 ISSN: 2673-5520 doi: 10.18429/JACoW-MEDSI2025-TUOB02

ACTIVE GRATING COOLING SYSTEM DESIGN FOR SOFT X-RAY MONOCHROMATOR

A. Moyne*, F. Yakhou-Harris, P. Brumund, L. Eybert-Berard, A. Vivo, K. Kummer, N. B. Brookes, D. Coulon, ESRF, Grenoble, France

Abstract

We present an active cooling system for the monochromator gratings of ID32 soft X-ray beamline at the European Synchrotron Radiation Facility (ESRF). The design combines flexible copper braids to minimize mechanical stress in the gratings with active temperature control to accelerate thermal response. Development followed a model-based approach, integrating dynamic Simulink thermal simulations with static finite element analysis. Under variable X-ray beam heat loads, the system maintains grating temperature stability within ±2 mK and reduces thermal settling time from several hours to under 10 min. Interferometric measurements also confirm improved optical surface flatness, with the cooling system contributing less than 50 nrad RMS to slope error. This translates to improved beamline energy resolution from 25 meV to 22 meV at 930 eV photon energy.

INTRODUCTION

The ID32 Soft X-ray Beamline at ESRF consists of two branches: one dedicated to X-ray Absorption Spectroscopy (XAS) and the other to Resonant Inelastic X-ray Scattering (RIXS) studies [1]. Operational since October 2014, the beamline delivers polarized soft X-rays in the 400 eV to 1600 eV energy range. These are selected by a grating monochromator, which is the subject of this paper.

ID32 GRATING MONOCHROMATOR DESIGN

General Design

The ID32 grating monochromator was designed in collaboration between ESRF and BESTEC in 2011, based on the BESSY SX/700 concept [2]. The incoming white X-ray beam is first reflected by a cryogenically cooled pre-mirror, which absorbs most of the X-ray heat load. The deflected beam is then directed onto a water-cooled 200 mm long grating, producing a monochromatic X-ray beam in the 400 eV to 1600 eV range.

The monochromator is equipped with four interchangeable gratings: two for the XMCD branch of the beamline and two for the RIXS branch.

Each grating mirror is mounted on a separate pitch, roll and yaw adjustment support, while the cooling is ensured by a classical passive water-cooling circuit, featuring two side-cooling heat exchangers.

Limitations of Current Passive Grating Cooling System

ID32 users face performance limitations due to the grating assemblies, which rely on a conventional passive water-cooling circuit. The first limitation consists in the energy resolution, which is closely related to the flatness of the grating surface. Surface flatness is primarily influenced by the mechanical configuration of the cooling circuit.

The second limitation relates to the thermal settling time of the grating following variations in the input beam heat load. Energy drifts occur after significant changes to the Insertion Device (ID) settings, which can last up to several hours before the system reaches a steady state again.

These limitations were successfully addressed in a similar case by A. Crisol et al. through a novel active cooling approach featuring flexible heat-conducting foils and Peltier modules [3]. Inspired by this success, the present study explores a slightly different strategy.

ID32 ACTIVE GRATING COOLING SYSTEM DESIGN

Concept

The active grating cooling system designed by ESRF addresses the two above-mentioned limitations. Energy resolution is enhanced by improving the mechanical decoupling between the cooling system and the grating. This is achieved through the use of flexible heat-conducting copper braids between the heat exchangers and the water-cooling circuit, as well as a redesigned clamping mechanism for attaching the heat exchangers to the grating.

In a passive cooling configuration, the use of flexible heat-conducting copper braids would lead to a longer settling time due to the increased thermal resistance between the cooling water and the grating. However, this additional thermal resistance presents an opportunity to operate the heat exchangers in an active manner, as represented in Fig. 1.

In this approach, the heat exchangers not only cool the grating by transferring heat to the water circuit through the copper braids but also provide heating via an electric heater placed on the heat exchanger. This heater can supply heat to the grating, where the thermal resistance of the path remains relatively low, while heat loss to the water circuit is limited by the thermal resistance of the braids.

The electric heater operates within a feedback control loop, using a temperature sensor to regulate the grating temperature at a predefined setpoint. This setpoint is determined as follows: the system is subjected to the maximum input beam heat load, with a minimal yet nonzero contribution

* alban.moyne@esrf.fr

ISBN: 978-3-95450-263-9 ISSN: 2673-5520 doi: 10.18429/JACoW-MEDSI2025-TUOB03

FIRST STEPS INTO THE OPERATION OF THE SAPOTI CRYOGENIC NANOPROBE AT THE CARNAÚBA BEAMLINE AT SIRIUS/LNLS

V. B. Falchetto*, G. G. Basilio, G. O. Brunheira, R. R. Geraldes, L. M. Kofukuda, M. B. Machado, Y. A. Marino, A. C. P. Neto, E. O. Pereira, C. A. Pérez, P. P. R. Proença, F. M. C. da Silva, T.R.S. Soares, A. P. S. Sotero, R. Szostak, V. C. Teixeira, H. C. N. Tolentino
Brazilian Synchrotron Light Laboratory (LNLS), Campinas, SP, Brazil

Abstract

SAPOTI is the second nanoprobe at the CARNAÚBA (Coherent X-Ray Nanoprobe Beamline) beamline at the 4th-generation light source Sirius/LNLS. Working from 2.05 to 15 keV, it relies on simultaneous multi-analytical X-ray techniques (absorption, diffraction, spectroscopy, fluorescence and luminescence) and imaging in 2D and 3D. It has been designed for highly-stable fully-coherent beam sizes from 30 to 120 nm, and monochromatic flux up to 1×10^{11} ph/s/100 mA/0.01%BW after an achromatic KB (Kirkpatrick-Baez) focusing optics. Moreover, a new in-vacuum high-performance cryogenic sample stage has been developed aiming at single-nanometer resolution images. The nanoprobe is now successfully installed and technical commissioning is underway. The focus of this work is two-fold. Firstly, it highlights the system integration results at the beamline, namely: overall thermo-mechanical performance of the KB mirrors and sample stage. And, finally, it showcases the instrument's technical commissioning results, namely: KB alignment and focus stability, and initial fly-scan potential for ptychography and absorption imaging.

INTRODUCTION

Synchrotron scanning X-ray microscopy has evolved into a cornerstone characterization tool across scientific, technological, and engineering fields, apt at bridging the gap between conventional optical and high-resolution electron microscopy [1,2]. The pursuit of enhanced spatial resolution over the past decade has driven the development of numerous nanoprobes, which have pushed the boundaries of techniques like coherent X-ray diffractive imaging and ptychography to sub-5 nm resolution in 3D [3–9]. These advancements make the stability of the beam and the sample the ultimate limiting factors for resolution during the exposure time [10, 11].

SAPOTI, or Scanning Analysis by Ptycho for Tomographic Imaging, is the second nanoprobe to be deployed at the CARNAÚBA beamline at the Sirius light source, located at the Brazilian Synchrotron Light Laboratory (LNLS). Designed for a wide array of simultaneous multi-analytical X-ray techniques-including spectroscopy based on contrasts such as absorption, fluorescence, and luminescence, together with diffraction and coherent scattering imaging, such as Bragg CDI and ptychography-SAPOTI is a capable instrument for 2D and 3D imaging.

* vinicius.falchetto@lnls.br

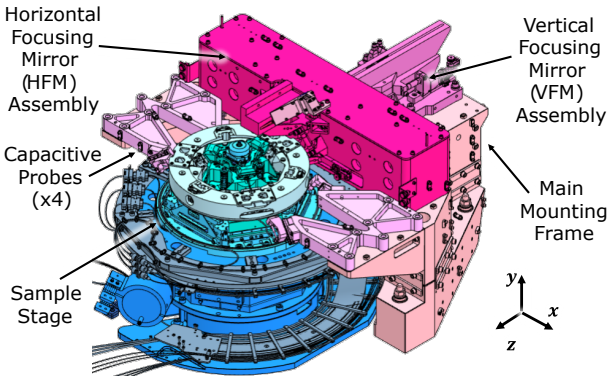

Figure 1: Drawing of the SAPOTI Sample Stage and KB module (see also Ref. [14]).

As detailed in [12, 13], achieving the highest imaging resolution required a tightly integrated mechatronic architecture, driven by the extreme sensitivity of the focusing optics (nanoradian scale) and the nanometer stability demanded by the sample. This work reports the first SAPOTI station results from the modules addressing these requirements—the sample manipulation stage and the KB mirror module Fig. 1. We summarize the system assembly, temperature control, and dynamical stability of these modules, along with the initial imaging results. The design and commissioning of high-performance controllers for nanopositioning scans will be presented in Ref. [15].

SYSTEM INTEGRATION AT THE BEAMLINE

Following the offline commissioning reported in Ref. [14], the station was transported to Sirius, where system integrity and functionality were verified. The mechatronic motion controllers, detector electronics, and advanced trigger system were integrated with EPICS [16] and the Bluesky orchestration environment [17]. Pulse-tube (PT) cryostats for both the loading module and sample manipulator were tested, yielding results consistent with Ref. [14]. Finally, modal tests in the hutch confirmed that the dynamical behaviour of the KB modules and sample manipulator met the required stability specifications [12, 13, 18].

Thermal deformation in synchrotron optics is a well-established research field, particularly for mirrors in 4th-generation light sources such as Sirius [19]. KB mirrors are especially susceptible to errors—such as coma aberration, astigmatism, and focus drift—if thermal expansion is

ISBN: 978-3-95450-263-9 ISSN: 2673-5520 doi: 10.18429/JACoW-MEDSI2025-TUOB04

RECENT ADVANCES IN X-RAY MICROSCOPY INSTRUMENTATION DEVELOPMENTS AT NSLS-II*

E. Nazaretski†, Weihe Xu, D. S. Coburn, H. Yan, Z. Gao, X. Huang, Wei Xu, N. Bouet, J Zhou, M. Ge, W.-K. Lee, Y. Yang, A. M. Kiss, Y. S. Chu
National Synchrotron Light Source II, Brookhaven National Laboratory, Upton, NY, USA

Abstract

X-ray microscopy is a mature characterization tool routinely used to investigate diverse material questions of science, technology, and engineering. The high penetration power of X-rays allows the utilization of different characterization methods and reveals elemental composition, crystalline phases, strain distribution, oxidation states, etc., in macroscopic and microscopic samples. Full-field and scanning X-ray microscopes serve similar scientific purposes but provide technical capabilities that complement each other. In recent years, several X-ray microscopy systems have been designed, constructed, and commissioned at NSLS-II. Below, we provide a brief technical overview of recently designed microscopy instruments. It includes some design details of the Multilayer Laue Lens (MLL) - based nanoprobe optimized for ~10 nm spatial resolution imaging; the zone plate (ZP)-based full-field imaging system capable of 1-minute nano-tomography measurements; and a new Kirkpatrick-Baez (KB)-based scanning microscope designed for ~200 nm spatial resolution experiments.

INTRODUCTION

NSLS-II is a 3 GeV synchrotron facility with a strong emphasis on imaging and microscopy applications. There is a dedicated beamline imaging and microscopy program (IMP) that comprises a few scanning and full-field imaging technique beamlines. The majority of the high-resolution endstation microscopes have been designed and constructed in-house, with technical details for some of them elucidated in the sections below.

MLL-BASED HARD X-RAY SCANNING MICROSCOPE

The 3-ID Hard X-ray Nanoprobe (HXN) beamline enables fluorescence, tomography, differential phase contrast, diffraction, nano-spectroscopy, and ptychography as imaging modalities in 2D/3D, and the photon energy range of 6 to 18 keV. It routinely delivers a focus size of ~10 nm using MLL optics and ~40 nm using ZPs [1-4]. The endstation microscope, shown in Fig. 1, has been designed and constructed in-house and became available to general users around 2015 [5, 6]. A few prototype systems have been commissioned and evaluated for performance prior to finalizing the design of the HXN endstation [7-9]. MLLs were proposed as an alternative to the ZP optics, overcoming the aspect ratio problem, in the hard X-ray regime [10-12]. A pair of linear MLLs is needed to achieve point focusing; therefore, orthogonality between the two MLLs is crucial since any angular misalignment introduces an additional cross-phase term in the wavefront, causing blurring of the focus. Also, placement of individual MLLs along the X-ray beam is important (within the optics depth of focus) since inaccuracies introduce astigmatism. For a ~10 nm point focus, the angular misalignment should be better than 0.01°, and placement along the beam direction should be within ±2 μm [13]. Also, a typical focal length for a 50 μm aperture, ~10 nm resolution lens is less than 5 mm, making it challenging to design such a microscope while ensuring both MLL and ZP compatibility. Therefore, as shown in the lower panel of Fig. 1, two individual modules, i.e., the MLL module and the ZP module, were designed, constructed, and installed inside the vacuum chamber; they can be hot-swapped during the beamtime cycle without any major interruptions to user operation.

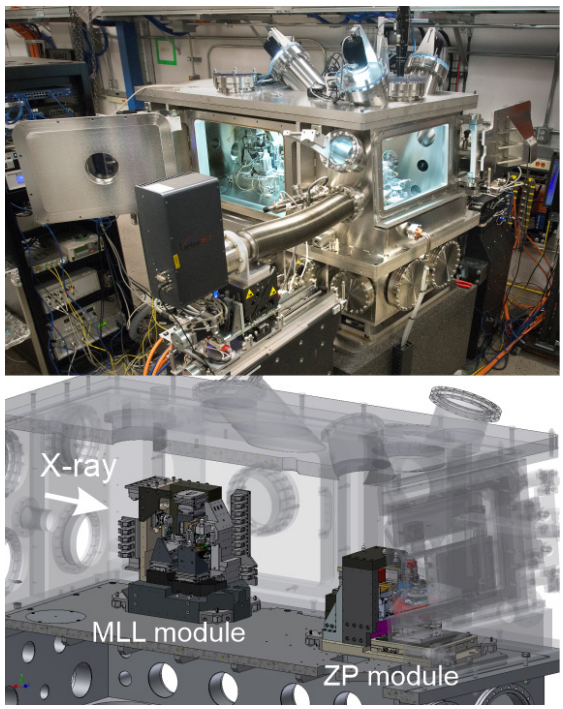

Figure 1: Top panel: a photo of the MLL/ZP microscope installed at 3-ID. Lower panel: upper-level Computer-Aided Design (CAD) model of the MLL and ZP modules arrangement inside the vacuum chamber.

In total, the MLL module comprises 21 rotational and translational degrees of motion and incorporates 9 fiber-optic interferometer channels, which were particularly

* This Work is Not Export Controlled
† enazaretski@bnl.gov

ISBN: 978-3-95450-263-9 ISSN: 2673-5520 doi: 10.18429/JACoW-MEDSI2025-TUOB05

DEVELOPMENT OF A COHERENT DIFFRACTIVE IMAGING ENDSTATION AT THE SPRING-8-II 12XU

Bo-Yi Chen, Yi-Wei Tsai, Ya-Shan Huang, Chao-Chih Chiu, Hsin-Wei Chen, Chi Chan, Jhih-Min Lin, Chun-Yu Chen, Ming-Ying Hsu, Ying-Shuo Tseng, Kang-Ching Chu, Yu-Cheng Shao, Masato Yoshimura, Hiraoka Nozomu, Din-Goa Liu, and Gung-Chian Yin
Experimental Facility Division, National Synchrotron Radiation Research Center, Hsinchu, Taiwan (R. O. C.)

Abstract

The National Synchrotron Radiation Research Center (NSRRC) operates two beamlines, 12B2 and 12XU, at the SPring-8 synchrotron in Japan. With the scheduled for upgrade to SPring-8-II, significant improvements in beam coherence, stability, and brilliance are anticipated. While the Taiwan Photon Source (TPS) and SPring-8-II are both advanced facilities, SPring-8-II provides distinct advantages for high-energy and coherence-demanding applications, offering complementary capabilities to TPS. To harness these improvements, NSRRC is constructing a dedicated Coherent Diffractive Imaging (CDI) endstation at beamline 12XU. Building on successful CDI demonstrations at PETRA III and earlier feasibility studies at SPring-8, the new endstation is located downstream of the inelastic X-ray scattering endstation. Adjustable slits are installed upstream to optimize beam size and intensity, while Kirkpatrick–Baez mirrors are retracted during CDI experiments to preserve coherence. The endstation includes two main subsystems: a zone plate-based X-ray microscope and a detector assembly. The zone plate-based X-ray microscope, mounted on a granite base, integrates modular optics and a nanometer-resolution piezo-driven sample stage with granite or Invar components for thermal stability. A precision linear guideway enables flexible detector positioning over a 1.5 m range, ensuring high-resolution imaging and experimental versatility.

INTRODUCTION

Synchrotron radiation has become a fundamental tool for exploring matter at the nanoscale, driven by advances in fourth-generation light sources that deliver higher beam coherence, stability, and brightness. Among emerging imaging methodologies, Coherent Diffractive Imaging (CDI) stands out for its high-resolution capabilities and reconstructing both amplitude and phase information from diffraction patterns via iterative algorithms. CDI has shown remarkable application in many fields, J. Miao's pioneering work extended crystallography to non-crystalline specimens [1]. More recently, a comprehensive review in Nature showcased how CDI and ptychography have unified microscopy and crystallography, enabling imaging from atomic to centi-meter scales, including 3D atomic defect structures and ultrafast dynamics in quantum and energy materials [2]. CDI's applicability extends across scientific disciplines. In materials science, Bragg CDI (BCDI) has been used to image three-dimensional strain distribution within individual nanocrystals with sub-nanometer accuracy and study how strain affects device performance [3]. Furthermore, CDI has been successfully applied to investigate strain and structural faults in single nanowires [4]. These examples underline CDI's ability to capture fine structural and dynamic details easily. Inspired by these methodological advances and grounded in the feasibility demonstrated at reference facilities, NSRRC is now constructing a CDI endstation on beamline 12XU at SPring-8. This marks a strategic expansion of Taiwan's synchrotron research, leveraging cutting-edge beam quality and instrumentation to advance next-generation imaging science.

CURRENT STATUS OF TESTING CDI ENDSTATION AT SPRING-8 12XU

At the current stage of testing, the CDI endstation is installed downstream of the SPring-8 12XU inelastic X-ray scattering (IXS) endstation, positioned directly behind the IXS detector. The source is 4.5 m long in-vacuum undulator with a magnet period of 32 mm. To accommodate the present parameters of the zone plate, the zone plate-based microscope is mounted on a linear guide rail that allows free translation along the beam axis, thereby enabling fine adjustment of the endstation to its optimal position. The linear rail has a length exceeding 2.5 m, and both the CDI endstation and the downstream detector are supported on granite bases (450 mm x 450 mm x 1065 mm). Once translated to the desired location, the bases are stabilized by lowering Hi-wedge® HWM C-1111 leveling feet, which fill the gap between the granite and the experimental floor and are then securely locked in place to maintain system stability. Since the Hi-wedges only serve to bridge the gap, additional XYZ adjustment stages are mounted on top of the granite bases for fine manual alignment of the endstation and detector modules. These stages provide a travel range of ±8 mm in the horizontal direction and ±10 mm in the vertical direction. During CDI experiments, the upstream IXS endstation, together with the analyzer and the Kirkpatrick–Baez (K–B) mirrors, can be retracted from the X-ray beam path when required, as shown in Fig. 1. This configuration ensures that the CDI setup receives a direct and coherent beam while preserving the operational flexibility of the upstream instrumentation. Under standard operating conditions, the distance between the detector and the sample is approximately 1 m.

ISBN: 978-3-95450-263-9 ISSN: 2673-5520 doi: 10.18429/JACoW-MEDSI2025-TUP01

AIRBOX HOUSING OF THE JUNGFRAU DETECTOR FOR IN VACUUM X-RAY DIAGNOSTICS

A. Schmidt, T. R. Preston, R. Shayduk, S. Göde
European XFEL, Schenefeld, Germany

Abstract

At the European XFEL facility, ultrabright X-ray radiation is employed to investigate phenomena in a variety of sample materials with the highest spatial and temporal resolution. For X-ray detection, the scientific 'Jungfrau' detector is frequently employed, as it matches the parameters of the provided X-ray beams. Originally developed by the Paul Scherrer Institute for in-air use at the SwissFEL, a detector housing has been designed and constructed at European XFEL to meet the requirements of in-vacuum operation at the scientific instruments for high-energy density physics (HED) and material-induced dynamics (MID).

The in-vacuum version of the Jungfrau detector is applied in various specialized diagnostics and methods aimed at resolving atomic lattice structures through X-ray diffraction, observing laser-induced microscopic material changes such as shock-wave dynamics via X-ray imaging and small-angle X-ray scattering, or probing plasma temperatures with inelastic X-ray spectroscopy. To exploit the coherence of the X-rays, the design includes a windowless X-ray photon beam path extending from the source to the sample and detector plane.

This contribution presents the housing design for a single module and showcases fully integrated solutions for selected X-ray diagnostics, incorporating multiple modules to enhance functionality.

DETECTOR HOUSING

The Jungfrau camera [1] is a compact hybrid-pixel detector with a 512 x 1024 sensor format featuring auto-gain switching for high dynamic range measurements and single photon sensitivity. Furthermore, it can record up to 16 frames with currently up to 300 kHz acquisition rate which renders the device well-suited for the X-ray pulse delivery pattern provided by the European XFEL facility to its scientific instruments (Fig. 1).

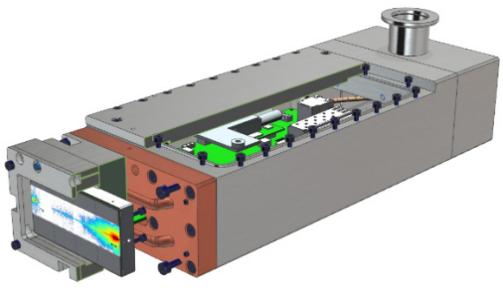

Figure 1: Assembled Jungfrau detector inside the airbox housing (partially cut view).

While other beamlines operate their detectors in an ambient environment, at the HED [2] and MID [3] instruments they must be integrated into the experimental setups accommodated within large vacuum chambers which requires the use of a customized housing. The detector housing assembly, depicted in Fig. 1, satisfies the following development goals: a) window-less sensor directly exposed to vacuum in order to maximize quantum efficiency, minimize scattering background from an entrance window and maintain the coherent properties if the X-ray beam; b) compact and slim housing dimensions to enable the flexible integration into multiple diagnostic setups; c) a nearly gapless modular assembly of two detector housings to double the sensor format to either a 512 x 2048 or 1024 x 1024 pixel matrix, respectively.

Technical Description

The detector key parts consist of a sensor module, referred to as front-end module (FEM), and the printed circuit board (PCB) which features the read-out electronics. While the FEM is designed to operate in vacuum, the PCB must remain at atmospheric condition to allow for convective cooling of the electric components.

The housing design is illustrated via an explosion drawing in Fig 2. It makes use of a vacuum barrier flange attached onto the PCB, mounted against the housing from the inside.

The backend adapter flange allows to mount a standard DN25-KF bellow which accommodates power, data, and trigger cables and support media (water, air/nitrogen). Different version types of this flange point the bellow into different directions. Depending on the vacuum chamber size and the location of the designated chamber feedthrough port the bellow length can be adapted.

Cooling of the detector must be provided to the FEM and to the PCB read-out electronics. Cooling of the PCB is realized via a flow of nitrogen introduced into the airbox housing via a small tube with the bellow acting as a gas outlet. Stable operation of the FEM sensor however requires a temperature stability below 100 mK (milli-degree Celsius). Therefore, a water-cooled system driven by a refrigerator unit is used, which provides sufficient flow to a copper cooling block containing brazed-in copper tubes.

The FEM is assembled to an interface block which keeps the system modular and enables rapid replacement of the sensor during experiments (in case of X-ray damage). Interfaces that are connecting the sensor to the cooling block are contacted with graphite foils (Fig. 2). A sensor cap aims to protect the sensor but also allows to mount experiment specific filter foils in order to block optical light (black Kapton) or attenuate the X-ray signal (thin metal foils).

ISBN: 978-3-95450-263-9 ISSN: 2673-5520 doi: 10.18429/JACoW-MEDSI2025-TUP06

AN OVERVIEW OF THE TIME-RESOLVED CAPABILITIES AND SAMPLE SETUP MODULARITY AT CoSAXS

R. Appio*, B. Ahn, J. L. Da Silva, V. Da Silva, F. Herranz-Trillo, P. Mota-Santiago†, A. E. Terry, T. S. Plivelic, Max IV Laboratory, Lund, Sweden

Abstract

CoSAXS is a multipurpose SAXS instrument located at the 3 GeV ring of MAX IV Laboratory in Sweden. This instrument provides a versatile platform for conducting Small-Angle X-ray scattering (SAXS) experiments on a wide range of research fields. With an extensive pool of sample environments, CoSAXS enables the application of multiple techniques and complex experiments on solid and solution samples.

To accommodate the high demand and facilitate the rapid exchange of sample setups, a standardized mounting system has been implemented, and additive manufacturing techniques are utilized for fast and efficient prototyping and production of customized sample holders. Furthermore, CoSAXS is equipped with advanced sample environments, such as the setup for milliseconds time-resolved SAXS-WAXS experiments in solution (TR-XSS). Among other studies, it has been used in non-reversible protein reactions after laser activation of caged compounds.

OVERVIEW OF CoSAXS CAPABILITIES

CoSAXS is a state-of-the-art multipurpose instrument located at the 3 GeV ring of the MAX IV Laboratory.

A 2 meter long in-vacuum undulator, coupled with a Si (111) HDCM and a Dual KB mirror pair, provides an estimated photon flux of 10^{12} - 10^{13} ph/s. The beam energy can be varied in the range between 4 and 20 keV, with the possibility of changing the focus position, so that the beam dimension at the sample position can vary between $25 \times 15\ \mu m^2$ and $150 \times 150\ \mu m^2$.

The SAXS/WAXS data can be detected and recorded simultaneously using dedicated SAXS and custom L-shaped WAXS detectors installed in a 16 m long vacuum vessel. In addition, a 1-D detector can be mounted on the outside of the vessel.

The detector configuration makes possible the collection of continous data in the q-range between 6×10^{-4} and $3\ Å^{-1}$ [1].

These specifications make CoSAXS a versatile instrument for different kinds of experiment on both solid-state and solution samples.

The pool of sample setups available at CoSAXS includes for example, a multiple capillary holder, a pipetting robot for samples in solution, Linkam heating stages, cells for microfluidics, a rheometer, a stopped flow device, a high magnetic field electromagnet, an ultrasonic levitator, a bi-axial mechanical tester, a setup for combined SAXS with UV–vis and fluorescence spectroscopy (SUrF) [2, 3].

The beamline also includes a specialized time-resolved setup based on laser excitation in the millisecond range. This setup will be discussed in detail in this paper.

Most of the setups are mounted on an x-y stage stack with micrometric precision, for precise alignment and scanning of the sample position, and both beamline and user defined equipment can be mounted.

TIME RESOLVED CAPABILITIES

Time-resolved X-ray solution scattering (TR-XSS) is a technique used to monitor the structural changes in a solution with time, after an initial perturbation and over a variety of time scales.

At CoSAXS, a nanosecond laser with an optical parametric oscillator (OPO) tunable from 675 to 2500 nm (20–140 mJ) and a continuous infrared laser (1470 nm, 50 J energy) are available as triggering for the experiments. These lasers are fiber optically coupled, to transport the light to the sample environment. The fiber optics simplifies the alignment process, guarantees consistent light delivery, significantly reduces the hazards and mitigates the stringent safety requirements typically associated with open beam paths. Other excitation sources, like diode-based monochromatic sources on the UV-VIS-Infrared regime, could be employed in the future.

In one study at CoSAXS, TR-XSS has been exploited to monitor the changes in an enzyme when a caged compound was activated by a nanosecond UV laser pulse. The reaction was monitored up to 50 ms, with a 2 ms temporal resolution [4, 5].

The core of the experimental setup, shown in Fig. 1, revolves around a flow-through cell, designed to accommodate a quartz capillary. Initially, this cell was fabricated from an aluminum block, featuring a precisely machined hole to host 1.5 mm diameter capillaries [6]. However, due to experimental requirements, the demand for greater flexibility in capillary sizes became apparent. To address this, the design was shifted to a 3D-printed capillary block, which offers significant advantages, primarily the ability to rapidly, and cost-effectively, cater for this demand. Given that the system can operate at temperatures ranging from few degrees up to 75 °C, PETG was selected as the ideal material for 3D printing due to its thermal and mechanical resistance.

At the heart of the block lies a central opening. This aperture is where the X-ray beam and the excitation light, perpendicular to each other, converge, allowing them to interact precisely with the same sample volume within the capillary.

* roberto.appio@maxiv.lu.se
† currently at ANSTO, Melbourne, Australia

ISBN: 978-3-95450-263-9 ISSN: 2673-5520 doi: 10.18429/JACoW-MEDSI2025-TUP08

A SAFE AND X-RAY TRANSPARENT ALUMINIUM SAMPLE CELL FOR HIGH PRESSURE AND HIGH TEMPERATURE NANO-DIFFRACTION IMAGING

A-L. Buisson*, P. Brumund, Y. Watier, H. Djazouli, ESRF, Grenoble, France
M-I. Richard, K. Olson, CEA, Grenoble, France

Abstract

The European Synchrotron Radiation Facility beamline ID01 performs Bragg Coherent Diffraction Imaging and X-ray nano-diffraction experiments with in-situ environments. A new sample environment for nanoparticles has been designed and tested. It combines a furnace and a pressurized X-ray-transparent chamber, without the use of beryllium for safety reasons.

The required 180° horizontal and 45° vertical viewing angles necessitate the use of a dome-shaped pressure chamber. Early in the design phase, the thermal effects of the 500 °C furnace on the dome's mechanical properties were identified as critical. A Finite Element Analysis (FEA) study was conducted, accounting for heat sources, gas turbulence, and static pressure.

Aluminium 6082-T6 was chosen for the pressurized dome, providing a safe and easy-to-procure solution. A dome thickness of 0.5 mm provides 80 % X-ray transmission at 33 keV. The sample, a 200 nm-diameter palladium nanoparticle, reaches the super-critical state at 340 °C in a 45 bar hydrogen atmosphere.

Unlike beryllium-based pressure domes, this design uses aluminium, avoiding machining difficulties, procurement issues, and safety hazards.

INTRODUCTION

ID01 at the European Synchrotron Radiation Facility (ESRF) is a nano-diffraction and coherent imaging beamline [1]. Recent in-situ studies of hydrogen insertion in palladium nanoparticles in subatmospheric pressure and up to 550 °C renewed interest in exploring the high pressure region of the palladium-hydrogen phase diagram. Indeed understanding a reaction at a single catalyst particle level is a prerequisite for understanding the behavior of ensembles of particles because of unavoidable dispersion of non-homogeneous samples. Examples of such sample environment include a compact ultrahigh vacuum chamber [2], gas flow cells [3, 4], and liquid environmental X-ray cells [5–8]. Previous Bragg Coherent Diffraction Imaging (BCDI) studies of the Palladium-Hydrogen system have been limited to low pressure (<1 bar relative) and ambient temperatures [9] missing the opportunity to explore new phenomena at more extreme conditions.

The goal was then to upgrade an existing furnace (operating at 900 °C and below 1 bar relative) [4] to a sample cell capable of withstanding high pressures (up to 50 bar) and high temperatures (up to 500 °C) with an x-ray transmission goal of 80 % at 33 keV. The dome-shaped chamber was chosen for its axial-symmetry required for 180° scanning. As illustrated in Fig. 1 the basic design of a sample cell consists of

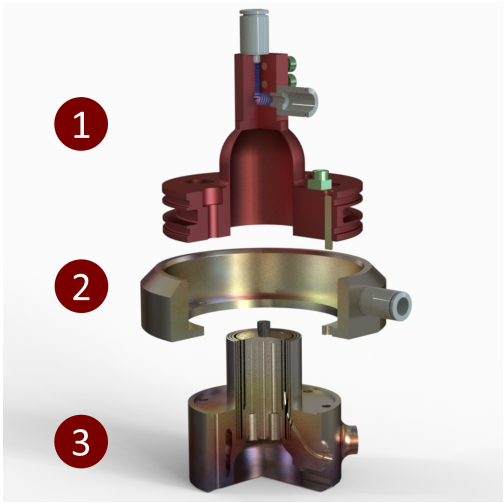

Figure 1: Typical sample cell: (1) Dome chamber, (2) Outer cooling loop, (1) Furnace

1. a removable dome cover that encloses the sample and lets the x-rays pass while permitting rotation around the vertical axis,
2. outer water cooling for the base of the dome a connection to the top of the dome and
3. a heated base (furnace) onto which the sample is mounted with gas inlet and outlet and internal base water cooling loop.

Material choice for dome cell is crucial. While dome cells are often made with beryllium for its high x-rays transmission properties, this material presents significant challenges in terms of procurement and safety due to its toxicity. Ensuring the safety of such pressurized equipment involves validating various steps, including: analytical calculations, Finite Element Analysis (FEA) simulations, water and helium leak tests, outer shape metrology report. Once these steps are validated, the system can be coupled with a furnace and a gas panel, enabling experiments in both static pressure or dynamic flow.

* anne-lise.buisson@esrf.fr

ISBN: 978-3-95450-263-9 ISSN: 2673-5520 doi: 10.18429/JACoW-MEDSI2025-TUP11

COMPACT MULTI-PURPOSE IMAGER FOR THE MATTER IN EXTREME CONDITION END-STATION AT LCLS

N. A. Boiadjieva, E. Galtier, H. Lee, D. Khaghani, G. Dyer, P. McGehee, C. Tsoi-A-Sue, E. Goliger, B. Nagler
SLAC National Accelerator Laboratory, Menlo Park, CA, USA

Abstract

We present the mechanical design of a new imaging system developed at the Matter in Extreme Conditions (MEC) instrument at the Linac Coherent Light Source (LCLS) to improve setup efficiency while maintaining high-quality imaging performance. We designed an in-vacuum setup for imaging the focal spot of the different laser systems we have at MEC as well as the experimental targets themselves. The system integrates high-resolution optics, remote positioning relative to the interaction point and control system. It supports imaging of laser spot sizes ranging from 2 to 600 µm and offers spatial resolutions down to 1 µm. Using kinematic mounting features, we ensure accuracy of the alignment of internal optics and allow for user-friendly modifications when needed.

Multiple magnification and resolution options are supported to cover a wide range of focal conditions. Additionally, the system includes vacuum-compatible, adjustable wavelength filtering and attenuation that maintain optical alignment. Finally, a shutter protects the high-resolution optics from target debris while the whole imager is fully retractable to further clear the target area.

INTRODUCTION

The Matter in Extreme Conditions (MEC) instrument at the Linac Coherent Light Source (LCLS) [1] is designed to investigate a wide range of phenomena in high energy density physics. The experimental requirements are diverse, necessitating imaging of both targets and laser beams across a broad range of spatial scales. For example, the high-energy Nd:glass laser system, typically employed for shock physics [2], produces large focal spots requiring characterization up to 600 µm in diameter. In contrast, the Ti:Sapphire laser, used for studies of warm dense matter [3] and relativistic plasmas [4], demands measurements of spot sizes as small as 2 µm. In addition, accurate imaging of experimental targets is required with varying resolution and field-of-view specifications, along with precise alignment of optical and x-ray beams [5]. These needs must be met within a 2 m-diameter vacuum vessel, where the experimental configuration changes monthly. To address these challenges, a versatile, user-friendly, and geometrically compatible imaging system is essential. The newly commissioned Multi-Purpose Imager (MPI) has been developed to fulfill this role.

The MEC experimental chamber is located about 460 m from the end of the LCLS undulator. The large volume of the chamber provides room for multiple vacuum-compatible spectrometers and scattering diagnostics instruments. The MEC laser beam is routed to the interaction region in multiple configurations. As a result, the MEC end-station is versatile with configurations changed frequently for different experiments, requiring precise, repeatable positioning and alignment.

This paper presents the optomechanical design of a new in-vacuum imaging system aimed at improving experimental set up efficiency while maintaining high-quality / high resolution imaging of the laser spot as well as the targets themselves.

Key Requirements

- A compact retractable package compatible with 0.1 Pa (10^{-5} mbar) experimental target chamber vacuum levels.
- High resolution imaging of the laser focal spot and target for precise positioning.
- Rapid removal and reinstallation with minimum realignment required.
- Support of multiple magnification/resolution options.
- Provide multiple adjustable filters (wavelength and attenuation).

In addition, the instrument needs to include a shutter to protect optics and detectors from debris and accidental full power laser hits

DESIGN

Figure 1 shows the optical layout. The design allows imaging of targets (with the fiber light illuminator) as well as the focused pump laser (spot sizes from ~3 µm to ~500 µm).

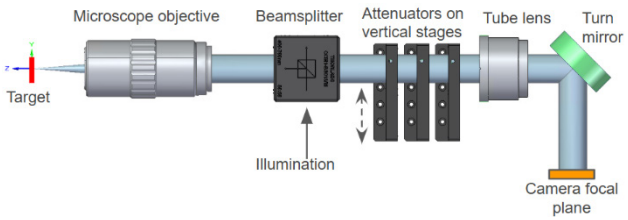

Figure 1: Optical layout.

Layout consists of an infinity-corrected long working distance microscope objective (e.g. Mitutoyo APO) plus a tube lens. The microscope is compatible with 95 mm parfocal length, infinity corrected, visible light microscope objectives with working distance > or = to 15 mm (i.e. Mitutoyo 2x, 5x, 10x and 20x). The filters are placed into the collimated portion of the beam path so that the image location is not affected. Six attenuators are provided allowing attenuation of OD 0 to OD 10 in steps of 0.5.

ISBN: 978-3-95450-263-9 ISSN: 2673-5520 doi: 10.18429/JACoW-MEDSI2025-TUP15

CREATING A MULTI-CAPILLARY FURNACE (MCF)

M. Morrow, D. Butler, L. Keenan, N. Ramanan
Diamond Light Source Ltd, Didcot, United Kingdom

Abstract

The Spectroscopy beamlines at Diamond Light Source regularly have operando/in-situ of X-ray Absorption Fine Structure (XAFS) experiments on catalyst samples. To improve the efficiency of such experiments, a Multi-capillary Furnace (MCF) has been designed to enable the measurement of multiple catalysts in parallel reactions. Subsequent testing has proven that the furnace can have up to four samples at 600 °C without thermal 'cross-talk' and permits samples to be remotely moved into the beam path.

INTRODUCTION

In the existing furnaces at the Spectroscopy beamlines at Diamond Light Source, powder samples are placed inside cylindrical 3mm diameter capillaries, before then being lowered into ceramic furnaces where they are heated for individual catalysis experiments. In these furnaces, only one sample can be loaded at a time. Consequently, replacing the capillaries/samples for the next experiment causes time to be lost during the changeover, reducing beamtime efficiency. The objective therefore was to create a furnace where up to four samples can be placed inside in separate capillary channels, where each sample could be heated and tested independently of each other, whilst allowing remote operation to move between channels to improve efficiency.

OBJECTIVES AND DELIVERABLES

The I18, I20 and B18 beamlines which make up the Spectroscopy group at Diamond Light Source have experimental tables which were already set up with limited space available for the mounting of a furnace. As a result, it was not simply a case of making four separate single capillary assemblies, as the space requirement would have been too large to fit them as opposed to a new Multi-capillary Furnace (MCF).

Catalysis experiments usually involve reactions of catalysts with gases and temperature/pressure. Some of these samples can require long pre-treatment (e.g. activation) before being measured, so having multiple capillaries with independent and stable temperature increase control allows reactions in one sample to continue while another is measured.

The MCF was to be tested and commissioned both offline (e.g. in a separate laboratory) and within the B18 beamline. To assess the suitability of the MCF, acceptance criteria were created to determine whether the MCF fulfils the required functions of simultaneous testing on several samples. The following key acceptance criteria was established as part of the furnace design:

- Temperature at the sample can be controlled from temperatures of at least 600 °C, and independently for each of the four capillaries.
- Temperature stability at the sample within ± 5 °C.
- Temperature 'cross-talk' between the samples within ± 5 °C.

FURNACE CONCEPT DESIGN AND FINITE ELEMENT ANALYSIS (FEA)

The MCF design concept uses kanthal wire heating elements housed in ceramic inside the furnace body as an individual 'box-furnace' unit. This unit is powered by a separate supply with independent temperature control. Individual samples are then located between the heating element and covered by additional ceramics (with apertures for the beam path) to aid heating samples to temperature.

A 'single-cell' prototype of the design (Fig. 1) was developed to determine if the sample could reach 600 °C as required with the proposed design, before being expanded to the MCF. To raise the temperature at the sample, the voltage from the power supply was steadily increased, and the temperature recorded using thermocouple probes placed within 10 mm of the sample position.

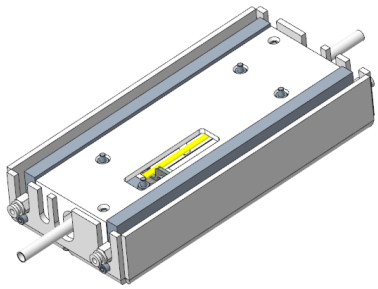

Figure 1: Prototype furnace 'single cell' with 'box-furnace' unit and capillary inside.

The body was made of sheet stainless steel, which allows for the mounting of the furnace units but also is less conductive of heat than other types of metal, with the theory being that the ceramics will contain the heat at the sample in order to keep it at 600 °C whilst ensuring the furnace body does not reach too high a temperature.

The prototype testing showed that the samples could reach temperature, but the 'policeman' thermocouples on the furnace body reached a temperature of ~ 200 °C (too high for safe user contact), and the ceramics cracked due to the temperature increase. Finite Element Analysis (FEA) in Ansys was used to represent the experiment conditions, and results showed large temperature peaks in areas where ceramics got hot and cracks propagated (Fig. 2).

ISBN: 978-3-95450-263-9 ISSN: 2673-5520 doi: 10.18429/JACoW-MEDSI2025-TUP16

CRISTALLINA-Q XFEL DIFFRACTOMETERS

G. Olea, N. Huber, R. Schneider, W. Schülein
HUBER Diffraction GmbH & Co.KG, Rimsting, Germany

Abstract

In a well-known European free-electron laser facility (SwissFEL), a new branch (ARAMIS 3) of the beamline delivers hard X-ray to the CRISTALLINA experimental hutch. CRISTALLINA-Q station inside intends to investigate advanced materials focused on specific quantum materials (QM) structures and properties. Two new dedicated Diffractometers (Dm(s)) have been developed. CrQ-$Dm_{1,2}$ are heavy load precision machines which, through adequate techniques and instruments, under extreme conditions (temp, press, rad), working in tandem are expected to advance the related investigations. CrQ-Dm_1 manipulates a large-size (h = 2.5 m) cryo-magnet (1 t, 5.2 T, -10 mK) and CrQ-Dm_2 a smaller pulse-magnet (0.6 t, 50 T, 30 rate) sample instruments. Both are able to perform most of the investigations in horizontal scattering, but not only. For versatility and flexibility reasons, CrQ-Dm(s) have been conceived with similar configurations, having a high level of compatibility inside and outside, however exhibiting some distinct differences. The kinematic, design, simulations and precision principles applied, together with the challenging aspects and results of tests are presented.

INTRODUCTION

SwisFEL provides a very stable, compact and cost-effective driven by a low-energy and ultra-low emittance beam travelling through short-period undulators [1]. The ARAMIS [2] beamline is operating two experimental stations (ALVIRA, BERNINA). A new branch (ARAMIS 3) or, alternatively CRISTALLINA is currently under completion. Mainly, it delivers ultra-short (sub-femto) pulses (1.77-12.4 keV) X-rays to the dedicated experimental station for condensed matter physics experimental investigations. New instruments here will be focused on quantum phenomena (many body states) analysis.

However, advanced synchrotron investigations require not only improved beam characteristics and/or new modern techniques applied, but dedicated instruments adapted to the specificity of the applications.

A call for interest, including the development of two diffractometers (Dm(s)), working with specific experimental instruments to create extreme sample environmental conditions (magnetism, temperature, pressure) has been released [3]. Mainly, the intention was to effectively use them for manipulating with high precision, two heavy magnets (cryo, pulse), using ultra-fast investigative X-ray diffraction (Df) techniques. A well-known company [4] with the necessary expertise and already acquired experience [5] was in charge with the development.

The associated aspects of the inherent challenging work resulted from specifications (load, precision, environment), together with the kinematics, design solutions, fabrication and last tests for final products are presented here.

CRISTALLINA DMs

Two Dm(s) machines have to alternatively work inside of an experimental station (CRISTALLINA), using the same beamline and accommodating with the use of "diffraction-before-destruction" X-ray techniques. CrQ-Dm_1, manipulating a heavy load cryo-magnet (0.65 t, 5 T, -10 mK) and CrQ-Dm_2 a smaller (pulse) one (0.45 t, 50 T, 30 rate)), holding the sample(s) inside. Dm(s) will be permanently located nearby of the beam (preparation room), to be easily moved/removed from/in the area (and, along the beamline), connected to a fixed rails dock station.

To decrease the beam preparation waiting time, an increased compatibility between the components, and with the third one (Dm-XPP-GPS, BERNINA) have to be assured, guaranteeing easy and fast set-ups/replacements.

The first precision tests (FAT) of the developed products, being already presented [6], a short overview with updates (modeling, SAT) is done here.

Kinematics

The complexity of tasks related to the specificity of work (heavy load, high precision, strong magnetic field), together with additional requirements (efficiency) have led to considering the final kinematics Dm(s) structures (K_i, i = 1, 2), as shown in Fig. 1.

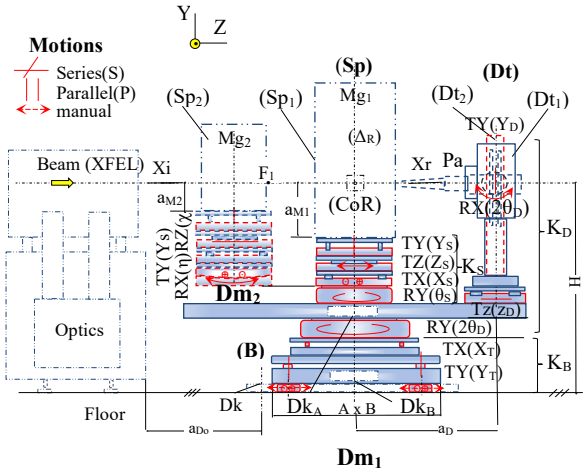

Figure 1: CrQ-Dm(s) kinematics.

($K_{1,2}$) are based on combinations of serial/parallel partial kinematic chains, corresponding to the related components of the machines (K_B, K_D, K_S). Some of them, being actuated by circles (C_i), form the system (machine) manipulator architecture (geometry). The experimental investigations are based on a corelated motions of positioning of two of them (K_S, K_D) relative to the beam. KB supports all structures

ISBN: 978-3-95450-263-9 ISSN: 2673-5520 doi: 10.18429/JACoW-MEDSI2025-TUP17

CXI EXPERIMENTAL STATION AT SOFTIMAX BEAMLINE MAX IV

N. Johansson*, J. Gonzáles, J. Schwenke, E. Malm, MAX IV Laboratory, Lund, Sweden

Abstract

A new Coherent X-ray Imaging (CXI) endstation has been designed and built at SoftiMAX, a soft X-ray spectro-microscopy beamline at MAX IV Laboratory. It features an in-vacuum rotatable detector stage with motorized movement over a 0-500 mm sample-detector distance range. This allows continuous positioning over scattering angles exceeding 120°. For longer distances up to 2 meters, fixed detector positions are supported via detachable vacuum extensions connected to angled ports on the vacuum chamber. This configuration enables a wide range of techniques, including X-ray Photon Correlation Spectroscopy (XPCS), scattering, diffraction and reflection. The internal mechanics are mounted on a granite base, mechanically decoupled from the vacuum chamber to ensure stability. A floor mounted rail system allows the entire endstation to be retracted, enabling quick installation of alternative setups. Final commissioning is expected in autumn 2025.

INTRODUCTION

The CXI experimental station is installed on the second branch of the SoftiMAX, a soft X-ray spectro-microscopy beamline at MAX IV Laboratory, the Swedish national synchrotron facility located in Lund. SoftiMAX operates at the 3 GeV storage ring, which provides exceptionally high average coherent flux due to the ring's low emittance. The CXI branch line uses a Kirkpatrick-Baez (KB) mirror pair to focus the beam to approximately 20 µm at the sample position. The KB mirror mechanics, based on an in-house design developed at MAX IV, are located approximately 2 m upstream from the sample and deflect the beam by 2 degrees both horizontally and vertically.

This endstation is dedicated to X-ray Photon Correlation Spectroscopy (XPCS), as well as diffraction and scattering experiments, and is designed with a very flexible detector geometry.

The experimental setup is housed in a large vacuum chamber designed for good accessibility, accommodating both the sample stages and a custom-built, in-vacuum detector stage. The detector can be continuously positioned within a 0-500 mm range from the sample while rotating across scattering angles exceeding 120°. For larger distances, up to 2 m, the detector can be mounted at discrete positions using detachable vacuum extensions (flight tube) connected to angled ports on the chamber walls.

Figure 1 shows a 3D model view of the CXI endstation assembly with a flight tube connected to one of the chambers angled ports. The design also includes a custom-built trolley to avoid floor collisions with the rail guides.

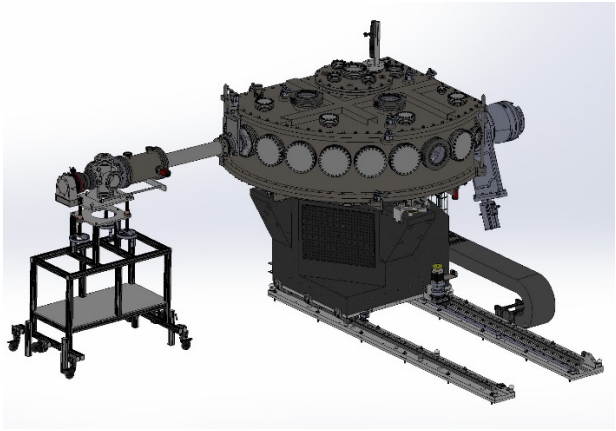

Figure 1: 3D view of the CXI endstation with example of a detachable flight tube on a trolley connected to one of the vacuum chambers angled ports.

The sample positioning system is divided into two subsystems: a coarse alignment stage based on stepper motors offering micron-level resolution and a fine positioning stage using piezo-driven actuators for nanometer-level precision. All internal mechanics are mounted on a granite base that is mechanically decoupled from the vacuum chamber to minimize vibration and drift. Additionally, the entire endstation can be retracted on floor-mounted rails to allow fast installation of alternative equipment or endstations brought by external users.

The following sections describe the design considerations, implementations and performance of each subsystem comprising the CXI endstation: The sample stages, the custom detector stage, the vacuum chamber and the mechanical support.

SAMPLE STAGES

The sample stages of the CXI endstation are designed to provide precise and accurate sample positioning. The sample stages consist of two subsystems: one with submicron resolution using stepper motor stages and a second subsystem with nanometer-level resolution using piezo driven motor stages (see Fig. 2). The sub-micron resolution stack is intended for rough alignment and includes x, y, z and rotation in y degrees of freedom. These stages are motorized using stepper motors and can provide a generous load capacity, ensuring stability and vacuum compatibility.

The nanometer resolution stack is intended for precision positioning and includes x, y, z and rotation in x and z axes degrees of freedom. Piezo motors are used to achieve nanometer resolution. These stages also include appropriate vacuum compatibility. The system includes an adequate general cable management system, with special attention to the cables from the nano-positioning stages, which are accommodated through the stepper motor Y rotation stage.

* niklas.johansson@maxiv.lu.se

ISBN: 978-3-95450-263-9 ISSN: 2673-5520 doi: 10.18429/JACoW-MEDSI2025-TUP18

DESIGN OF A DEDICATED MULTILAYER MONOCHROMATOR FOR ELECTRON BEAM SIZE MEASUREMENTS USING THE HETERODYNE NEAR FIELD SPECKLES (HNFS) TECHNIQUE AT THE ALBA SYNCHROTRON

J. M. Álvarez†, J. García, V. Prósper, A. Rubio, L. Carvajal, M. Llonch, M. Quispe, L. Nikitina, U. Iriso, A. Nosych, J. Moldes, C. Colldelram and N. González
ALBA Synchrotron Light Source, Cerdanyola del Vallès, Spain

Abstract

Within the framework of the ALBA Diagnostics Group's participation in a Future Circular Collider (FCC) collaboration, a dedicated setup for electron beam size measurement based on Heterodyne Near Field Speckles (HNFS) has been developed and installed at ALBA Front End 21 using radiation from a dipole bending magnet. The setup incorporates a high-energy (20–30 keV), high-bandwidth (~1.3%) monochromator, entirely designed in-house, along with the colloid sample environment and the detector system with their corresponding supports. The monochromator features a 300 mm Si substrate with W/B_4C multilayer coating and operates in a vertical Laue reflection geometry. To reduce complexity and for this HNFS-specific application, ultra-high vacuum (UHV) conditions and submicron precision mechanics are not required. The mirror assembly is housed within a standard DN400 CF chamber, mechanically coupled to the chamber itself. This chamber is mounted on a granite-based "skin concept" table, providing two degrees of freedom (vertical translation and tilt) for energy tuning and beam path insertion/retraction. The complete design of the set-up is presented in this paper.

INTRODUCTION

ALBA Beam Physics group in collaboration with CERN and the University of Milano is developing a technique to measure storage ring electron beam size, the so-called Heterodyne Near Field Speckles (HNFS). After first successful measurements using HNFS at ALBA BL11 NCD beamline [1], a dedicated set-up to conduct these measurements has been designed and installed at Fron End 21 (FE21) [2]. Unlike the previous set-up at BL11, FE21 is illuminated by a dipole bending magnet and currently is used by ALBA diagnostics group to conduct beam size measurements using the pinhole technique. This allows direct comparison between both techniques.

The whole set-up has been fully developed at ALBA and consists of a monochromator and a sample and detector table. Both components can be operated to be fully retracted from the x-ray beam path, allowing the alternative use of pinhole diagnostics. A schematic diagram of HNFS set-up integration in FE21 is depicted in Fig. 1.

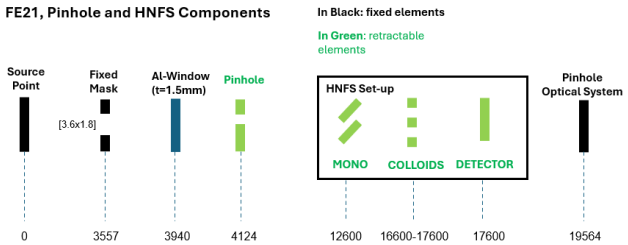

Figure 1: HNFS set-up integration in ALBA FE21 with relative distances from source point.

GENERAL DESCRIPTION

Due to HNFS experimental nature, consisting of x-ray diffracting upon colloid suspension samples, the design of monochromator and sample and detector support is oriented to build simple and cost-effective devices rather than to achieve high end performances in terms of motion accuracy and stability (see Fig. 2).

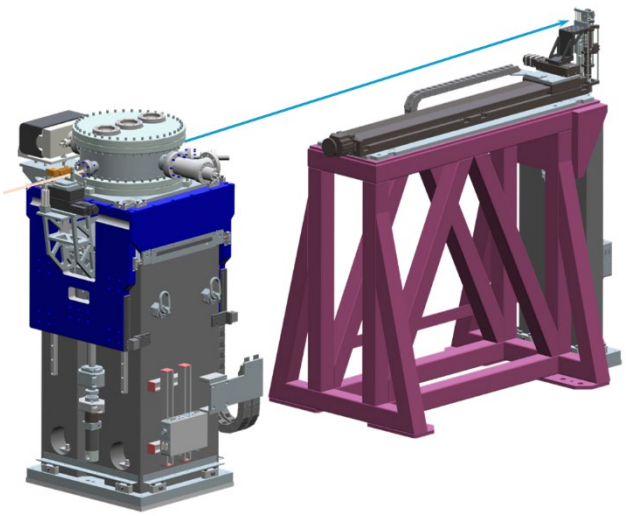

Figure 2: External view of HNFS Monochromator and Detector and Sample table.

† jalvarez@cells.es

ISBN: 978-3-95450-263-9 ISSN: 2673-5520 doi: 10.18429/JACoW-MEDSI2025-TUP20

SCANNING AND TRANSFER OF CRYOGENIC SAMPLES IN THE Bionanoprobe-II INSTRUMENT AT THE ADVANCED PHOTON SOURCE*

Benjamin Davis†, Si Chen, Sunil Bean, Tim Mooney, Kevin Peterson, Tugba Isik, Evan Maxey, Jie Liu, Michael Wojcik, Xiaozhi Zhang, Josh Han, Barry Lai
Advanced Photon Source, Argonne National Laboratory, Lemont, IL, USA

Abstract

A new hard x-ray fluorescence (XRF) nanoprobe instrument called Bionanoprobe-II (BNP-II) has been designed and will be constructed at 2-ID-D of the upgraded Advanced Photon Source. BNP-II will take advantage of the orders-of-magnitude increase in brightness and coherent flux with advanced sample scanning, metrology, cryogenics, and controls. These advancements will enable high-throughput XRF imaging under cryogenic conditions with 10 nm spatial resolution, 2D survey of mm-sized samples, and fast tomography for 3D visualization. BNP-II also introduces a novel robotic sample transfer system that interconnects a cryogenic plasma focused ion beam (cryo-PFIB) milling station alongside the x-ray nanoprobe. The interconnected instruments enable an iterative workflow between x-ray measurements and cryo-PFIB milling and maintains the integrity of vitrified samples by remaining below 110 K even during transfer. Regions of interest can be identified by fast large-area scans, after which the sample geometry can be optimized for nanoscale x-ray imaging and tomography. This work details the engineering advancements required to examine highly complex, multidimensional systems with BNP-II.

INTRODUCTION

The Bionanoprobe-II (BNP-II) at Argonne National Laboratory Advanced Photon Source (ANL APS) Sector 2-ID-D is a hard x-ray fluorescence (XRF) nanoprobe, currently under construction, that will utilize the orders-of-magnitude improvement of brightness and coherent flux of the recently upgraded APS [1]. This next-generation instrument (see Fig. 1) will have sub-10 nm resolution and will enable both fast 2D survey of mm-sized samples and fast XRF tomography for 3D visualization. The instrument is dedicated to studying trace elements in frozen-hydrated biological samples. The samples remain in a frozen-hydrated state from sample preparation stage, during transfer to the beamline, and during data collection.

The first major goal for BNP-II is to achieve 10-100x greater experimental throughput compared to the current instrument's ability [2], meaning substantially larger populations of biological cells are imaged in a shorter time. This faster imaging along with higher resolution requires advanced sample scanning hardware, metrology, and controls development.

The second major goal for BNP-II is to integrate a sample milling station alongside the x-ray nanoprobe. The interconnected instruments enable an iterative workflow between x-ray measurements and sample milling, where regions of interest can be identified by fast large-area scans, after which the sample can be milled down for better nanoprobe access.

The combination of high experimental throughput and micron-level targeted imaging of biological samples establishes BNP-II as a frontier capability in life and soft matter sciences.

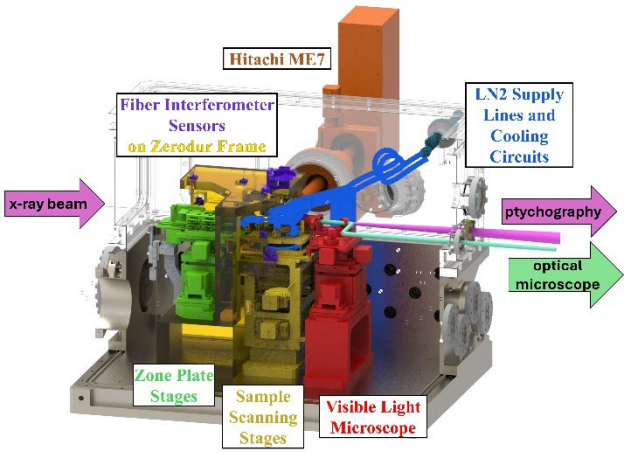

Figure 1. Overview of the BNP-II instrument core

CRYOGENIC SAMPLE TRANSFER

Effective imaging and analysis of biological samples in their 'natural state' requires keeping the samples in a hydrated state and avoiding radiation-induced damage. The integrity of a sample is preserved if it is vitrified and remains below the amorphous-to-crystalline ice transition temperature during transportation, loading, x-ray imaging, and cryo-PFIB milling. Warming of the specimen could cause a phase change and consequent structural and chemical alterations. Three new engineering advancements have been made to prevent such sample damage (see Fig. 2).

Sample Holder, Shuttle, and Dock Systems

BNP-II samples are handled and transported with a hierarchy of interfaces, enabling safe handling at a cryogenic temperature. Samples are fast frozen with liquid nitrogen (LN2) onto either TEM grids or silicon chips with silicon nitride films. The grid or chip is then mounted onto a

* This research used resources of the Advanced Photon Source, a U.S. Department of Energy (DOE) Office of Science User Facility operated for the DOE Office of Science by Argonne National Laboratory under Contract No. DE-AC02-06CH11357. The cryo-PFIB development is supported by U.S. DOE Office of Science Early Career Research Program (ECRP) under Contract No. PRJ1009594.
†bfdavis@anl.gov

ISBN: 978-3-95450-263-9 ISSN: 2673-5520 doi: 10.18429/JACoW-MEDSI2025-TUP22

DESIGNS OF THE FIRST-PHASE BEAMLINES FOR SIAM PHOTON SOURCE-II

C. Euaruksakul†, W. Jenpiyapong, D. Kaewsuwan, B. Pongtippitak, T. Wongpinij
Synchrotron Light Research Institute, Nakhon Ratchasima, Thailand

Abstract

Siam photon source-II (SPS-II) is a new synchrotron facility that is going to be built in Thailand. There are seven beamlines to be constructed together with the new machine. These consist of one soft X-ray beamline, two X-ray absorption beamlines, three X-ray scattering beamlines and one imaging beamline in the lineups. The designs and the selections of insertion devices, front end and beamline components will be presented together with the optical simulation results and the considerations for thermal load management using the combination of front-end components, filters, white/pink beam slits and mirrors along each beamline. New experimental station equipment and the existing equipment from the current Thai synchrotron facility (Siam Photon Source-I) that will be transferred to SPS-II will also be discussed.

INTRODUCTION

Siam Photon Source-II (SPS-II) is a new fourth-generation synchrotron project of Thailand. The 14-cell double-triple bend achromat storage ring of SPS-II can accommodate 21 insertion device beamlines and 7 bending magnet beamlines [1]. The ring circumference is 327.6 m and there are one standard and one middle straight section of each cell with 3.81 and 1.53 m flange-to-flange physical space available for insertion device installations.

There are seven beamlines planned to be installed in the first phase of SPS-II operation. The lineups include: one soft X-ray beamline – High-Resolution Soft X-ray Spectroscopy (HRSXS), two X-ray absorption beamlines – Tender X-ray Absorption Spectroscopy (TXAS) and Hard X-ray Absorption Spectroscopy (HXAS), one imaging beamline – X-ray Micro-Computed Tomography (XMCT), and three X-ray scattering beamlines – Small and Wide Angle X-ray Scattering (SWAXS), High-Resolution X-ray Diffraction/Micromolecular Crystallography (HRXRD/MX) and Grazing Incidence X-ray Diffraction/Total-Reflection X-ray Fluorescence (GIXRD/TRXRF). The energy ranges and the selected insertion devices are listed in Table 1.

BEAMLINE CONCEPTUAL DESIGNS

The main photon sources selected for the first-phase beamlines are in-vacuum undulators (IVU). The period length of 18 mm has been selected as a standard parameter for four beamlines. This period length allows the higher energy photon to be sufficiently produced from the 2.0 m total magnetic length while keeping the energy spectrum discontinuity between the first and third harmonic as small as possible under the constraint that the minimum physical gap is 4.0 mm (defined by the vertical beam stay clear of SPS-II). 23 mm period was selected for TXAS for continuous energy between 1-13 keV. An elliptically polarized undulator with the magnetic period of 58 mm is planned for HRSXS for polarization control, while an in-vacuum wiggler (IVW) with the magnetic period of 50 mm is planned for XMCT that needs high photon energy. Out-vacuum multipole wiggler (MPW) with a magnetic period length of 120 mm (9 periods) is also considered as a cost-effective alternative. The radiation spectra from the selected photon sources are provided in Fig. 1.

Table 1: Beamlines and Insertion Devices of SPS-II

Beamline	Energy (keV)	Insertion device
HRSXS	0.9-2.5	EPU 58 1.6 m
TXAS	1-13	IVU 23 0.9 m
HXAS	6-35	IVU 18 2.0 m
XMCT	10-60	IVW 50 2.0 m
SWAXS	8-20	IVU 18 2.0 m
HRXRD/MX	8-25	IVU 18 2.0 m
GIXRD/TRXRF	8-28	IVU 18 2.0 m

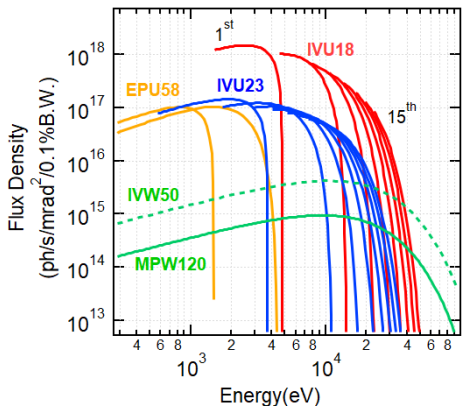

Figure 1: Flux density calculation from the insertion devices of SPS-II.

The conceptual design of the front ends of SPS-II (Fig. 2) is based on the design used at Taiwan Photon Source [2]. The components are standardized for all the seven beamlines. The high heat-load components listed from upstream to downstream are 1) Pre-mask, 2) Fixed Mask, 3) Photon Absorber and 4) X-Y Slits which consist of two motorized L-shape slit blocks. There are two beam positioning monitors (BPMs) placed around 5.5 m away

† chanan@slri.or.th

ISBN: 978-3-95450-263-9 ISSN: 2673-5520 doi: 10.18429/JACoW-MEDSI2025-TUP26

THE MID INSTRUMENT OF EUROPEAN XFEL: 2025 UPGRADES AND EXPERIMENTAL SETUPS

G. Ansaldi †, U. Bösenberg, J.E. Pudell, B. Baranašić, D. Ghoneim, J. Möller, R. Shayduk, A. Zozulya, J. Hallmann, A. Schmidt, L. Oppelt, T. Andersen, A. Rodriguez-Fernandez, A. Madsen
European X-Ray Free-Electron Laser Facility, Schenefeld, Germany

Abstract

In this paper insights are given on some examples of 2025 Upgrades and Experimental Setups at the MID instrument of European XFEL.

The latest design and implementation status of **MID Multi-Purpose Chamber (MPC-2)** project are reported. This represents a set of upgrades and ongoing development of MID instrumentation, as well as the evolution of the current multi-purpose chamber, which has been successfully used at MID since the first experiments in 2019. The aim is to enable new types of scientific experiments and to expand the current capabilities. The MPC-2 project includes an upgrade of the MPC-2 VESSEL and the MPC-2 INTERIOR Upgrade (MPC-2_IU). The latter consists of the following assemblies: Breadboard Assembly, Laser In-coupling 2 (LIC-2), 2-theta Circle.

Another aim of the MPC-2 project is to make operation of experiments easier with better access to sample environments (Pulsed Magnet (PUMA), Cryostat, Fast Solid Sample Scanner (FSSS), Diffractometer, Liquid Injector), and possibilities to install new ancillary equipment included in the MPC-2 INTERIOR Upgrade.

Examples of the most recent EXPERIMENTAL SETUPS are also reported, continuing in the direction of simultaneous multi-detector-use.

MPC-2 VESSEL UPGRADE

A new MID Multi-Purpose Chamber 2 Vessel (MPC-2_V) is required to enable parallel in-coupling of both the optical pump (PP) laser and the X-ray beam. This configuration allows the use of the PP laser in combination with the nano-focusing optics (NaFo). The redesigned vessel supports the use of different wavelengths provided by the PP laser, enabling quick replacement of several laser windows and optics within the new LIC-2 setup during experiments, via large access doors. In Fig.1-3 the most recent concept design status, budgetary quote release candidate, is shown.

Design

During previous MPC operation, we have identified a significant benefit in improving accessibility to the sample interaction point. The design indicated in these paper and poster outlines which existing vessel features - such as feedthrough flanges - are retained, and which are obsolete. Areas where flanges are not required are instead used for significantly increased access ports or doors. The current lid will remain available as a fallback solution.

The MPC-2_V must fulfil several key boundary requirements, including full compatibility with:

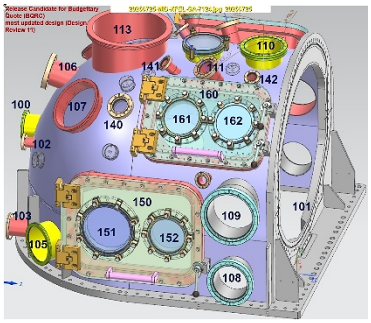

Figure 1: last version of MPC-2 Vessel Upgrade with flange numbering (North side).

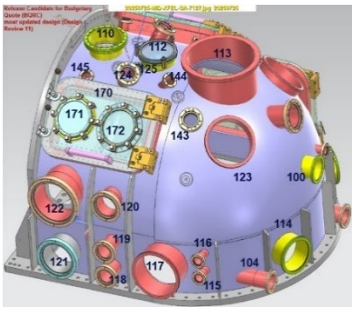

Figure 2: last version of MPC-2 Vessel Upgrade with flange numbering (North side).

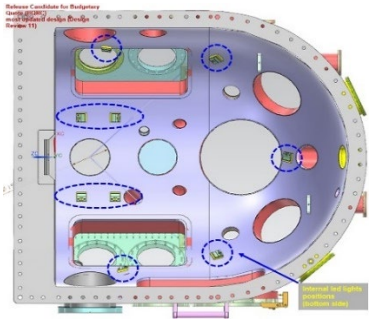

Figure 3: last version of MPC-2 Vessel Upgrade with internal led lights positions (Bottom side).

- The existing lower chamber section onto which it will be mounted, as well as with fixed positions and dimensions for X-ray and PP laser in-coupling.
- The high-vacuum generated with the existing interfaces: chamber base, WAXS window, DN500 gate valve.

† gabriele.ansaldi@xfel.eu, www.xfel.eu

ISBN: 978-3-95450-263-9 ISSN: 2673-5520 doi: 10.18429/JACoW-MEDSI2025-TUP28

MicroMAX BEAM CONDITIONING UNIT*

S. Benedictsson†, N. Al-Habib, M. Al-Najdawi[1], S. An, O. Aurelius, I. Gorgisyan[2], J. Lidon-Simon, M. Milas, S. Scolari, T. Ursby, MAX IV Laboratory, Lund, Sweden
[1]also at Sesame, Allan, Jordan
[2]also at European Spallation Source, Lund, Sweden

Abstract

A new Beam Conditioning Unit (BCU) has been developed for the MixroMAX beamline to condition the beam between the KB mirrors and the sample. It includes two XBPMs, a set of slits, a rotating chopper, a fast shutter and a linear attenuator, all on piezo driven stages. MicroMAX has a close collaboration with the BioMAX beamline, to simplify future work the same fastening rail system, with the same distance from rail to beam was chosen. To protect the XBPMs from oxygen but still allow for some heat transfer through convection, the chamber is filled with a low-pressure helium environment.

INTRODUCTION

MicroMAX is a macromolecular crystallography beamline at MAX IV Laboratory designed for time resolved studies of microcrystals in the temperature range between 90 K and room temperature [1, 2].

For MicroMAX a new Beam Conditioning Unit (BCU) has been developed that will manipulate and monitor the beam upstream of the sample position. The BCU will house a commercial X-ray chopper and provide a suitable environment for operation. A compromise between optimized cooling and minimized friction. The beam entering the BCU can either be focused by the Compound Refravtive lenses (CRL) or deflected and focused by the Kirkpatrik-Baez (KB) mirrors.

SPECIFICATION

The BCU includes two XBPMs, horizontal and vertical slits, alignment mirror, chopper, fast shutter, scintillator screen, and attenuators. It shall work both with standard beam and with a beam deflected horizontally and vertically by 6 mRad by the KB mirrors. All motion shall be motorized according to the specifications in Table 1.

Table 1: Specifications for Internal Parts

	X	Y	Resolution	Repeatability
XBPM 1 and 2	±5 mm	±5 mm	100 nm	100 nm
Slits	±5 mm	±5 mm	100 nm	100 nm
Alignment mirror	-	-	100 nm	100 nm
Chopper	±5 mm	-	-	-
Shutter and screen	-	-	100 nm	100 nm

* Funded by Novo Nordisk Fonden for the MicroMAX project, grant number NNF17CC0030666
† staffan.benedictsson@maxiv.lu.se

The chopper has a magnetically levitating rotor, so there is no conductive cooling through the motion system, therefore the chamber is filled with low pressure Helium that will transfer some heat without creating too much friction and at the same time protect the XBPMs from oxygen.

DESIGN

For general alignment of the chamber and translation between the deflected and straight beam the BCU will be placed on an external stage covering motion in the vertical and transversal axis plus pitch and yaw motion.

One major design choice was to reuse the rail system used in the European Molecular Biology Laboratory (EMBL) developed BCU at the sister beamline BioMAX [3, 4]. All components except the chopper are assembled on platforms on a rail with the same beam height as in the BioMAX BCU to make it possible to swap parts between the two BCU´s if needed. They can be adjusted along the beam, but differently from BioMAX a set of screws are used to give a reference position if a component is taken out for service, see Figs. 1 and 2.

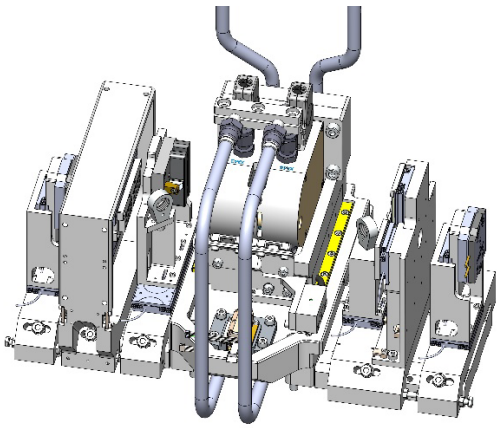

Figure 1: BCU components.

All translations in the BCU are performed by piezo motors and has been selected to fulfil the specifications in Table 1, (see Table 2). The vertical translations for the XBPMs are a high load version to avoid issues experienced at BioMAX. The SLITs are made of four independently controlled tungsten blades originally designed for the NanoMAX beamline. The chopper disc has a step shape to allow for different intervals. To change interval a high load horizontal piezo motor (40 N) is used together with cross roller linear guides. The cooling tubes are long and going around the chopper to allow for more movement and reduce the risk of over bending. The fast shutter and scintillator screen are both on the same horizontal stage, also allowing a passthrough hole in between.

ISBN: 978-3-95450-263-9 ISSN: 2673-5520 doi: 10.18429/JACoW-MEDSI2025-TUP32

HeXI: THE HIGH-ENERGY ELECTRON XTALLOGRAPHY INSTRUMENT

M. Semeraro†, P. Nunes, W. Norman, M. Esnouf, G. Duller, R. Littlewood, A. Siebert
Diamond Light Source Ltd, Harwell Science and Innovation Campus, Didcot, Oxfordshire, UK

Abstract

The High-energy Electron Xtallography Instrument (HeXI), currently under construction at Diamond, is set to expand the range of samples suitable for structure determination via electron diffraction. Funded by the Welcome Trust's "Electrifying Life Sciences" grant and Diamond Light Source, the HeXI project will utilize Mega-electron-volt (MeV) electrons to bridge the crystal size gap between electron and X-ray scattering. This will enable the determination of structures from crystals ranging between 300 nm and 3 μm.

HeXI incorporates a tuneable electron source, adjustable between 100 keV and 1 MeV, along with bespoke collimation and magnetic lenses, capable of achieving the precise optical properties necessary to interrogate nanometre-scale crystals within an in-vacuum sample environment. This first-of-its-kind instrument will combine the unique sensitivity of electrons to structural information with the advanced goniometry developed at Diamond for macromolecular X-ray crystallography to enhance overall data quality.

In this paper, we will explore the design of this 7-meter-long electron beamline and its main challenges.

SCIENCE CASE

Microfocus X-ray beamlines have advanced macromolecular crystallography by enabling studies of smaller crystals, particularly in drug discovery. However, X-ray diffraction (XRD) still requires relatively large samples (3 – 30 μm), limiting access to many biologically and chemically important structures. Electron diffraction (ED) offers a powerful alternative, enabling structure determination from sub-micron crystals [1, 2]. Moreover, high-resolution Coulomb potential maps captured using ED provide direct insights into stereochemistry and charge states which are critical for drug design. ED has resolved structures previously inaccessible to XRD, such as amyloid peptides involved in neurodegenerative disease, and distinguished charges in HIV-1 Gag inhibitor studies where mapping charge distribution was essential to understanding drug efficacy [3, 4].

WHAT IS THE NEED

The HeXI project is designed to explore the potential of using mega-electron volt (MeV) electrons for ED, with the goal of bridging the gap between traditional 3DED and XRD in terms of crystal size and penetration depth. By employing high-energy electrons, HeXI aims to overcome the limitations of low-energy ED systems, which suffer from reduced penetration and increased multiple scattering in thicker samples.

The increased energy of the electron beam will enable the study of larger crystals while preserving the advantages of ED, such as high-resolution Coulomb potential mapping and fast data acquisition. This will significantly expand the conformational landscape accessible to researchers, providing new opportunities for drug design and molecular dynamics simulations.

Once operational, HeXI will become part of the Diamond Light Source user program, offering a unique capability within the biological diffraction portfolio. It will complement existing X-ray and cryo-EM instruments, enable multi-modal structural studies and enhance the facility's ability to support cutting-edge research in structural biology, chemistry, and materials science.

INSTRUMENT DESCRIPTION

General Layout

HeXI, schematically depicted in Fig. 1, is a 7-metre-long instrument housed within a dedicated radiation hutch on the Diamond Experimental Hall floor. The entire beamline, from the electron source to the sample environment and detectors, is contained within this hutch. Operating at 1 MeV, the instrument presents unique challenges in terms of mechanical design, radiation safety, and beamline integration.

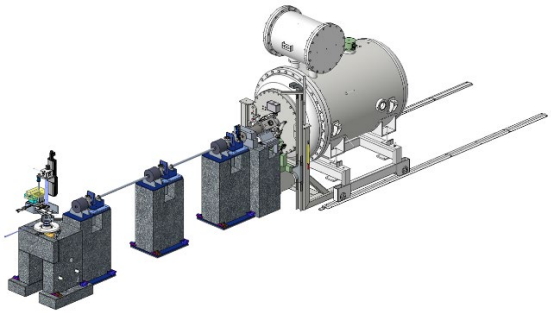

Figure 1: Hexi general layout.

Electron Source

The electron source consists of a commercial LaB_6 emitter coupled to a Singletron accelerator system built by High Voltage Engineering Europa (HVEE) [5].

† Michela.semeraro@diamond.ac.uk

ISBN: 978-3-95450-263-9 ISSN: 2673-5520 doi: 10.18429/JACoW-MEDSI2025-TUP33

HIGH-PRECISION ALIGNMENT OF AN UPGRADED SOFT X-RAY POLARIMETER AT DIAMOND LIGHT SOURCE

Q. Meng, H. Wang†, B. Garvey, M. Hooper, A. Howell, K. Jones, P. Larkin, A. Majhi, A. Malandain, A. Peach, X. Tran, G. Wilkin, D. Winter, K. Sawhney
Diamond Light Source, Didcot, United Kingdom

Abstract

Knowledge of X-ray beam polarisation on a synchrotron beamline is essential, not only for characterising the undulator performance, but also for precise analysis of dichroic and chiral experiments. The upgraded high-precision soft X-ray polarimeter at Diamond Light Source features multiple retarder adjusters to allow precise concentricity and angular alignment to the analyser. An offline alignment procedure has been developed, achieving 69 µm horizontal and 17 µm vertical concentricity alignment, as well as 4 µrad yaw and 9 µrad pitch alignment. Compared to the original version of the instrument, the vertical concentricity alignment improved by 14× and the pitch alignment improved by 18×. The procedure uses a laser diode to mimic the X-ray beam and a hexapod to align the analyser. Concentricity alignment relies on monitoring the intensity as the laser beam is cropped by plane mirrors on the retarder and analyser stages. Angular alignment is achieved by measuring the retarder and analyser rotation vectors using an autocollimator. The improved alignment allows the polarimeter to meet the stringent requirements for complete polarisation measurement above 1 keV.

INTRODUCTION

A polarimeter uses a retarder to introduce phase retardation and an analyser to transmit only one linearly polarised component [1]. The independent rotation of these polarising elements along the beam axis allows polarisation analysis at synchrotron sources to characterise the performance of undulators capable of providing linear and circular polarisations in the soft X-ray region [2]. Highly polarised radiations are utilised in beamlines to perform experiments including X-ray magnetic linear/circular dichroism [3, 4] and X-ray magnetic scattering [5].

Modern soft X-ray polarimeters use multilayer and crystal polarising elements as transmission phase retarders and reflection analysers [6]. At energy above 1 keV, the retarder must be operated at high grazing angle to maximise phase shift [7]. Assuming a sample size of 5 mm and a grazing angle of 10°, the effective sample size is only 870 µm. In addition, the Bragg resonance bandwidth of the polarising elements is very narrow at higher energies [8]. These factors impose a tight tolerance on the concentric and angular alignment between the polarising samples.

The original soft X-ray polarimeter at Diamond Light Source featured a conventional design that lacked alignment adjustability. It had a vertical concentricity offset of 230 µm and a pitch offset of 160 µrad because of mechanical imperfections [9]. These misalignments introduced a modulation of the angle of incidence with a period 2π leading to considerable measurement error when characterising the degree of polarisation of undulators at higher energies. To achieve complete polarisation analysis above 1 keV, the instrument went through a complete redesign to incorporate multiple adjusters on the retarder for concentricity and angular alignments.

Figure 1a shows a render of the upgraded polarimeter. The retarder rotation axis rests on top of a base plate that can be translated as shown in Fig. 1b. Adjusting adjacent pairs of adjustment screws by different amounts also allows for coarse angle alignment. Fine angle alignment can be performed using adjuster screws on top of the retarder rotation axis as shown in Fig. 1c. The rest of this paper introduces an offline alignment procedure developed to improve vertical concentricity alignment 14 times and pitch alignment 18 times compared to the original version of the instrument.

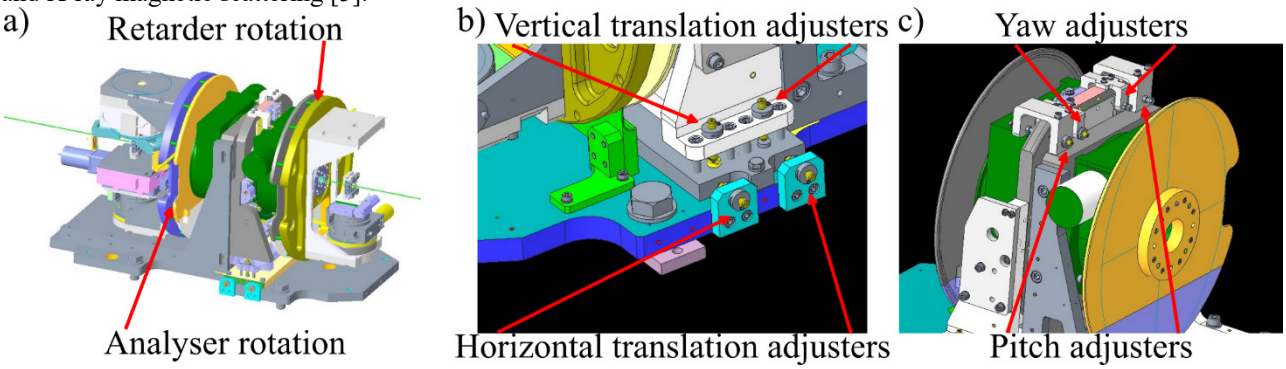

Figure 1: a) The upgraded soft X-ray polarimeter at Diamond. Manual adjusters incorporated on the retarder axis for b) horizontal and vertical translation, and c) yaw and pitch adjustment.

† email address Hongchang.Wang@diamond.ac.uk

ISBN: 978-3-95450-263-9 ISSN: 2673-5520 doi: 10.18429/JACoW-MEDSI2025-TUP39

LATEST PROGRESS ON TWO NEW ALS-U BEAMLINES FOR DIFFRACTION-LIMITED PERFORMANCE*

M. Bergeret†,1 , A. Islegen-Wojdyla[1], S. Morton[1], G. Cutler[1], R. Johnson[1], J. Hervey[1], S. Gleason[1,2], E. Gullikson[1], K. La Fleche[1], A. Allézy[1], R. Armstrong[1], H. Alvarez[1], D. Bryant[1], K. A. Goldberg[1], E. DiMasi‡,1, S. Shah[1], D. Cocco[1], C. Jensen[2], S. Kumar[2]
[1]Lawrence Berkeley National Laboratory, Berkeley, CA, USA
[2]Inprentus, Champaign, IL, USA

Abstract

The Advanced Light Source Upgrade (ALS-U) will increase soft X-ray coherent flux by 100×. We developed two new beamlines, engineered to minimize loss of brightness and utilize the advanced coherence of the light source. Each beamline uses a minimalist optical layout: a cryogenically-cooled silicon M1 mirror, a monochromator with variable-line-spacing gratings, and a final focusing M3 mirror. Optics are designed for Strehl ratio > 0.8 and sub-100 nrad vibration. A piezo-bimorph M3 mirror paired with a wavefront sensor allows for wavefront optimization. Fabrication is underway. New test data include at-wavelength efficiency measurements for blazed gratings, and motion performance of piezo-actuated pitch/roll flexure systems at cryogenic temperatures, granite air-bearing positioners, and monochromators.

THE ALS-U PROJECT

The Advanced Light Source Upgrade (ALS-U) aims to increase the soft X-ray coherent flux by 100× at 1 keV [1] beyond the current ALS capabilities. The new storage ring will operate at 2 GeV with a current of 500 mA. It will deliver an electron beam size and divergence of about 10 µm RMS and 5 µrad RMS to the insertion device beamlines. The ALS-U project selected two beamlines for a complete rebuild.

The COherent Scattering and MICroscopy Beamline (COSMIC) will feature a single branch for coherent imaging. The brightness increase will enable 100× faster experiments, or 3× better spatial resolution, down to ms and nm.

The Microelectronic and Electronic STRucture Observatory (MAESTRO) will feature two branchlines for Angle-Resolved Photoemission Spectroscopy (ARPES). The higher coherent flux will boost the collection efficiency by 10× for better spatial resolution and faster measurements.

They have been engineered to minimize brightness loss and utilize the advanced coherence of the new source.

* This work was supported by the Director, Office of Science, Office of Basic Energy Sciences of the U.S. Department of Energy, under contract No. DE-AC02-05CH11231, and the Laboratory Directed Research and Development Program of Lawrence Berkeley National Laboratory.
† mbergeret@lbl.gov
‡ Present affiliation: Longenecker & Associates, Inc.

BEAMLINE DESIGN APPROACH

The beamline CAD model is shown in Fig. 1. The two beamlines share a simple layout with mutualized designs: a cryogenically-cooled silicon M1 mirror, a variable included angle plane grating monochromator (PGM) with variable-line-spacing (VLS) gratings, and a final-focusing plane-ellipse M3 mirror(s). The ALS-U scope ends at the exit slits and does not include the experimental endstations.

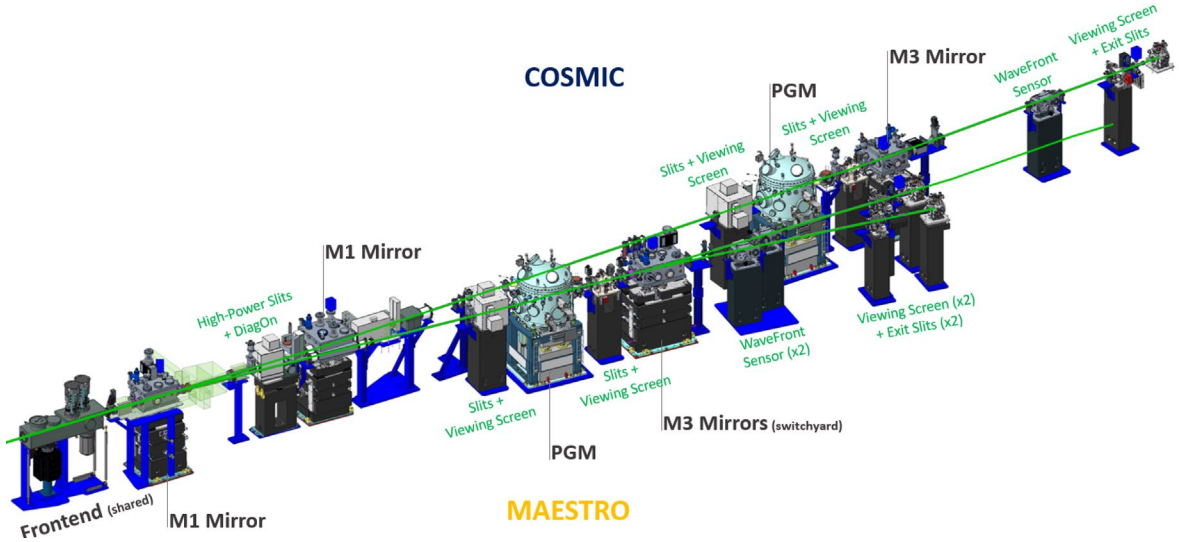

Figure 1: COSMIC and MAESTRO beamline layouts. Each beamline is approximately 30 m long and they share the same frontend. COSMIC has a single branchline, while MAESTRO splits at a M3 mirror switchyard. Optical elements are labelled, and diagnostics are highlighted in green.

ISBN: 978-3-95450-263-9 ISSN: 2673-5520 doi: 10.18429/JACoW-MEDSI2025-TUP41

MECHANICAL DESIGN AND IMPLEMENTATION OF A HIGH HARMONIC GENERATION SOURCE AT THE SXP INSTRUMENT

V. V. Vardanyan[1], P. Grychtol[1], P. Bhardwaj[1], D. Doblas-Jimenez[1], M. Heber[1,2], R. Villanueva Guerrero[1], M. Bueno[1], S. Mitra[1], M. Izquierdo[1]
[1]European X-Ray Free-Electron Laser, Schenefeld, Germany
[2]Deutsches Elektronen-Synchrotron DESY, Hamburg, Germany

Abstract

The first experimental technique implemented at the Soft X-ray Port (SXP) of the European XFEL is femtosecond time-resolved X-ray photoelectron spectroscopy (TR-XPES), enabling studies of ultrafast changes in the electronic, chemical, and atomic structure of materials. It offers femtosecond time resolution and enhanced probing depth via higher electron kinetic energies, enabled by the extended photon energy range from 300 eV to 3 keV. To further expand its capabilities, a laser-based High Harmonic Generation (HHG) source is under development. It will generate extreme ultraviolet (XUV) pulses up to 70 eV using a 1030 nm Ytterbium fiber laser amplifier delivering 200 µJ pulse energy at 334 kHz. This will enable more surface-sensitive measurements, high-fidelity probing of shallow core levels, and valence band mapping with high angular resolution. This contribution presents the mechanical design, key technological developments, implementation, and current status of the HHG source at the SXP instrument of the European XFEL.

INTRODUCTION

The main layout of the SXP Scientific Instrument is shown in Fig. 1. The FEL beam, generated by the SA-SE3 undulator system, is focused using a Kirkpatrick–Baez (KB) X-ray mirror system and guided to the interaction point through the Photon Arrival Monitor (PAM) diagnostic module and the Laser IN-coupling unit (LIN). An Alignment Laser System (ALAS), located upstream of the KB system, enables pre-alignment of all beamline components without the FEL beam [1].

The HHG system is split in two parts: The HHG driving laser and the main HHG system. The former is an Ytterbium fiber laser amplifier (AFS) with a central wavelength of 1030 nm delivering a pulse energy of up to 200 µJ at 334 kHz. The 300 fs long pulses are compressed down to about 40 fs using a Herriot multi-pass cell and then transported to the main HHG unit. The latter will be placed on a support-table of the (PAM) module [2]. The laser pulses interact non-linearly with Ar gas in a cell at high pressure resulting in high harmonics of the fundamental laser frequency [3-5]. The generated HHG photons are separated from the laser beam and guided into to the LIN module via a UHV line. A pair of multilayer mirrors is used to select specific harmonics that are then focused at the interaction point of the TR-XPES experimental station [2]. The FEL and an additional fs optical laser (OL) beam can be colinearly propagated with the HHG beam, allowing to realize different pump-probe schemes beyond the standard OL pump – FEL probe: OL pump – HHG probe, HHG pump – FEL probe, FEL pump – HHG probe.

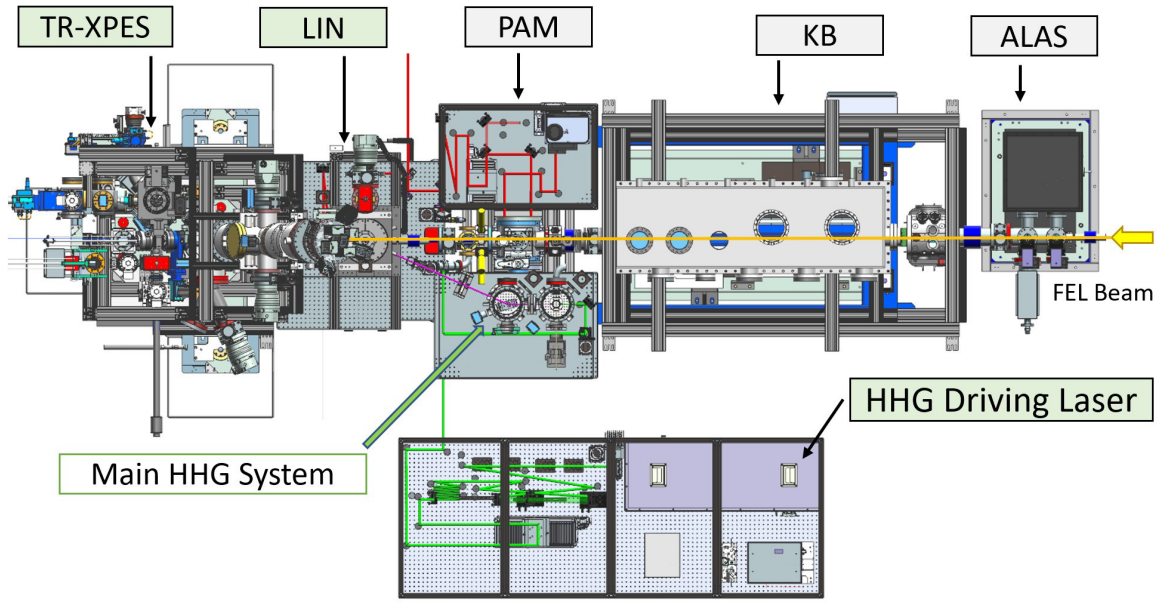

Figure 1: Top view of the SXP instrument, showing all components including the laser-based HHG source. The FEL beam path is indicated in yellow, the laser path in green, and the HHG beam path in purple.

ISBN: 978-3-95450-263-9 ISSN: 2673-5520 doi: 10.18429/JACoW-MEDSI2025-TUP45

NANO-TOMO-PTYCHOGRAPHY 3D-IMAGING ON SWING BEAMLINE

F. Alves†, C. Englom, J. Perez, Y. M. Abiven, F. Berenguer, T. Bizien, A. Gibert, F. Langlois, A. Lestrade
Synchrotron SOLEIL, St Aubin, France

Abstract

In 2018, a new Nanoprobe system which was originally developed in the scope of a collaboration with MAX IV (Sweden), was installed and validated on the SWING beamline (Synchrotron SOLEIL) for 2D-nano-ptychography with an expected imaging resolution of 40 nm. The setup had been designed to be portable and capable of handling multiscale sample-sizes, from the micrometer scale to several hundreds of a micrometer.

This system was then successively upgraded to allow for 2D-imaging resolutions of 20 nm or better, and 3D- nano-tomo-ptychography imaging with spatial resolutions of 50 nm or better. The end-station is composed of: (1) a sample stage with 6 translation and 1 rotation stages, (2) an optical stage comprised of a central stop and a Fresnel zone plate optical (3DOF), (3) an order sorting aperture stage (3DOF). All positioning stages comprise piezo-driven actuators (Piezo Walk or stack), of which synchronized control (with kinematic modelling) is done using the SOLEIL Delta Tau platform. In addition, fibber interferometry feedback was used for image reconstruction purposes. After the last improvements in 2023, imaging results show that the system can resolve 3D- images with a spatial resolution of 31 nm using a teeth sample after 18 h of acquisition.

This contribution will present an overview of the mechanical design concepts and solutions adopted for the Nanoprobe project.

INTRODUCTION

The Nanoprobe Project [1, 2], a four-year collaborative effort between Synchrotron SOLEIL and MAX IV (Sweden), was launched in 2013 with the objective of developing a prototype 3D scanning nanoprobe. Following the project's conclusion in December 2016, a dedicated team based at SOLEIL was established to focus on nanopositioning systems.

In preparation for the upcoming upgrade of the SOLEIL Synchrotron [3] — which will feature a more coherent light source — and in response to increasing user demand, the SWING beamline [4] at Synchrotron SOLEIL has decided to incorporate high-resolution coherent diffractive imaging, specifically ptychography, into its experimental capabilities. As a result, the SWING beamline has defined the following long-term objectives for its nanoprobe end-station:

1. System portability: To ensure flexibility across various experimental setups, any new system must be compact and able to be installed or removed from the beamline within a few hours.
2. Nano-2D-ptychography Achieve imaging resolutions of 20 nm or better, with scan ranges from 10^2 µm to 100^2 µm.
3. Nano-3D-tomo-ptychography: spatial resolution equal to or better than 50 nm, with full-range scans of 10^2 µm up to 100^2 µm.

By the end of 2018, objectives 1 and 2 had been partially achieved, with a newly developed portable nanoprobe end-station successfully performing nano-2D ptychography at a resolution of 40 nm [2].

The focus of the next phase of the project — and the subject of this paper — is to upgrade the nanoprobe end-station to enable even higher-resolution 2D imaging, and to implement and test nano-3D tomographic ptychography on the SWING beamline.

SWING NANOPROBE OVERVIEW

The new end-station can be sectioned up into five main parts: the overall system support structure (including plexiglass cover), the interferometer support structure, an actuated sample stage, an Order-Sorting-Aperture (OSA) stage and a Fresnel-Zone-Plate & Central-Stop Stage (FZP-CS). Figure 1 illustrates the setup, showing each stage and their respective Degrees-of-Freedom (DOF).

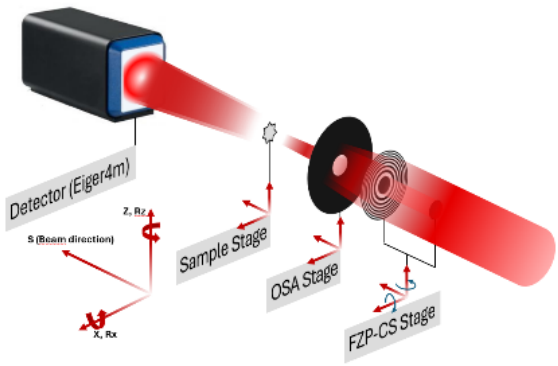

Figure 1: Principal scheme outlining the SXZ-orientation of the Nanoprobe End-Station stages and their respective degrees of freedom.

Metrology Analysis & System Design

A metrology analysis was carried out to identify key parameters for the mechanical design. A high-resolution nano-2D step-scan would, for an example, necessitate differential positional tracking data between the sample and the FZP-CS stage at each step of detector-image-acquisitions. Interferometer position-tracking was consequently

† Filipe.alves@synchrotron-soleil.fr

ISBN: 978-3-95450-263-9 ISSN: 2673-5520 doi: 10.18429/JACoW-MEDSI2025-TUP47

OPTIMIZING SGM BEAMLINE PERFORMANCE: HEXAPOD AND SPECTROSCOPY ENHANCEMENTS

T. M. Pedersen, J. J. Dynes, S. P. LeBlanc, T. Z. Regier*
Canadian Light Source, Saskatoon, Saskatchewan, Canada

Abstract

Recent developments on the spherical grating monochromator (SGM) beamline at the Canadian Light Source (CLS) have significantly enhanced its capabilities, particularly through the integration of a vacuum-compatible Physik Instrumente hexapod (H-811.I2V) and the implementation of Bluesky data acquisition software. These upgrades, along with standardizing sample mounting, have facilitated the transition from traditional x-ray absorption spectroscopy (XAS) measurements to advanced spectromicroscopy techniques. The hexapod allows for sub-micron scale sample manipulation, enabling high-resolution imaging with a 20 mm × 15 mm field of view. Additionally, the modelling of the Kirkpatrick-Baez (KB) mirror system for adaptive focusing has further optimized the beamline's performance, providing a beam spot size of less than 10 μm^2. These developments have not only significantly improved the beamline's capabilities for environmental and catalytic material studies, but also increased the data quality for all routine spectroscopy measurements conducted on the beamline.

SAMPLE MOUNTING

A custom kinematic mount from ThorLabs [1] allows for precise and repeatable positioning of various 3D-printed sample holders. See Figs. 1 and 2.

Figure 1: ThorLabs kinematic mount.

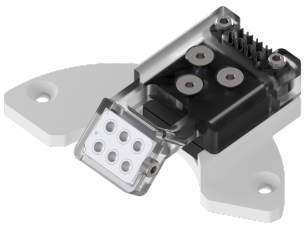

Figure 2: Pellet sample holder.

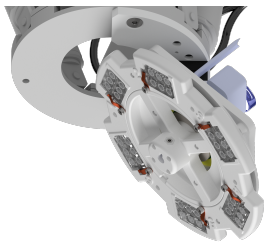

Figure 3: Wheel sample holder.

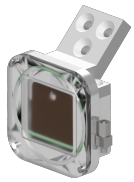

Figure 4: Anaerobic sample holder.

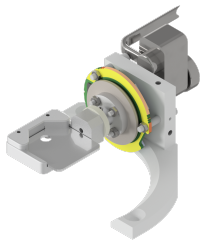

Figure 5: Angular rotary stage.

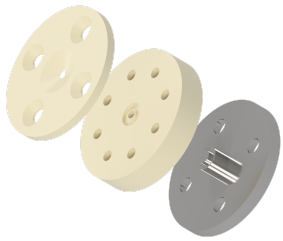

Figure 6: *in-situ* liquid holder.

Figure 3 shows a wheel holder that can accommodate 36-pellet samples without breaking vacuum. An anaerobic holder allows samples to be mounted in an inert atmosphere (Fig. 4). An angular rotary stage (Fig. 5) allows for grazing incidence measurements utilizing a piezo-electric motor with an 18-bit rotary encoder. For battery chemistry development an *in-situ* liquid holder designed for chemical resistivity has been developed in collaboration with a user group in South Korea [2] (Fig. 6).

* Beamline contact: tom.regier@lightsource.ca

ISBN: 978-3-95450-263-9 ISSN: 2673-5520 doi: 10.18429/JACoW-MEDSI2025-TUP48

RAPID BEAMLINE DIAGNOSTICS FOR UPCOMING BESSY II+ SoTeXS BEAMLINE

D. Kraft*, A. Sokolov†, P. Hönicke, M. Noppel, W. Smith, S. Vadilonga, J. Viefhaus,
Helmholtz-Zentrum Berlin für Materialien und Energie GmbH, Berlin, Germany

Abstract

As part of the BESSY II+ upgrade, the new SoTeXS (Soft-to-Tender X-ray Spectroscopy) beamline will enable high-precision, high-throughput studies of battery materials in the 0.5 keV to 5 keV energy range. At the endstation, battery cells with varying material combinations will undergo charging and discharging phases while being exposed to the beam. To ensure that, variations in the measurements are attributable to changes within the cells rather than fluctuations in beam properties, a rapid diagnostics procedure will be implemented. This procedure will monitor beam performance in between the battery measurements. This includes measurement of key parameters such as photon flux, energy resolution, and beam focus. The system combines a retractable ionization chamber for energy resolution measurements and a camera-based setup using OpenCV and ChArUco markers for determining beam spot size and position. These tools allow beam performance monitoring between sample loading cycles and represent an advance over commissioning-only diagnostics on current BESSY II beamlines. This paper presents the technical requirements of the SoTeXS beamline and a selection of potential diagnostic tools.

INTRODUCTION

BESSY II+ is the latest major upgrade to the BESSY II synchrotron light source at Helmholtz-Zentrum Berlin (HZB), developed to meet the growing demands of next-generation research in energy materials [1].

At the core of this upgrade is SoTeXS (Soft to Tender X-ray Spectroscopy), a flagship beamline tailored for operando and in situ battery research. Investigating electrochemical processes in real time requires a stable, high-flux photon source with excellent energy resolution and fast scanning capabilities.

SoTeXS is designed to deliver rapid energy scans in the 0.5 keV to 5 keV range, enabling high-throughput measurements across relevant absorption edges in modern battery chemistries. In collaboration with the National Metrology Institut (Physikalisch-Technische Bundesanstalt - PTB), the beamline also serves as a metrology platform, incorporating rapid beam diagnostics to minimize measurement uncertainty and improve reproducibility.

This combination of advanced spectroscopy and precision metrology makes SoTeXS a central component of the BESSY II+ upgrade. SoTeXS is still in an early stage of the development. The first light is planned for 2029. The following paper will present the current state of the design with the focus on methods to perform rapid beamline diagnostics.

GENERAL DESCRIPTION OF THE BEAMLINE

The optical layout of the SoTeXS beamline, as shown in Fig. 1, is specifically designed to deliver high photon flux and spectral resolution in the tender X-ray regime from 0.5 keV to 5 keV. At the SoTeXS endstation, a dedicated battery-cell storage unit will provide a cyclical flow of samples.

The source of the beamline is a newly developed planar cryogenic permanent magnet undulator [2], optimized for the soft X-ray range, with higher harmonics extending into the tender X-ray range. The emitted radiation is directed onto a toroidal mirror (M1) at an incidence angle of 0.7°. This first mirror provides both horizontal focusing and vertical collimation of the undulator radiation and reflects the light onto the pre-mirror(M2) of the monochromator. The monochromator is equipped with two gratings with line densities of 1200 l·mm^{-1} and 2400 l·mm^{-1}. Depending on the experiment, it is possible to choose between high photon flux and high resolution [3].

To improve reflectivity—and therefore photon flux—in the tender X-ray range, all optics, including mirrors and gratings, are coated with multilayer coatings. Each mirror will carry different coated areas on the same substrate. By moving the mirror normal to the beam, the illuminated region (and therefore the coating) is switched. This approach benefits from experience at ELISA [4].

After the grating, the beam is focused by a cylindrical mirror (M3)—again at an incidence angle of 0.7°- on the exit slit. The slit defines the energy resolution and spatial coherence of the beam delivered to the experiment.

Beyond the slit, the beam is focused onto the sample by a Kirkpatrick–Baez (KB) mirror system, enabling small spot sizes suitable for micro-spectroscopy.

This layout provides the flexibility to perform both fixed-energy and energy-scanning experiments with high spatial and spectral resolution (with emphasis on energy scanning). The beamline is fully compatible with in situ and operando battery setups and incorporates integrated beam-diagnostics infrastructure for rapid monitoring and calibration.

ENABLING TECHNOLOGIES FOR SoTeXS

To meet the scientific needs of the SoTeXS beamline—particularly the operando analysis of modern battery materials—several key technological innovations are being implemented. These are tailored to provide high photon flux, fast

* david.kraft@helmholtz-berlin.de
† andrey.sokolov@helmholtz-berlin.de

ISBN: 978-3-95450-263-9 ISSN: 2673-5520 doi: 10.18429/JACoW-MEDSI2025-TUP50

REMOTE CRYO VALVE ADJUSTER– A NEW DEVICE TO IMPROVE SAFETY AND REDUCE COST

E. Haas, M. Abeykoon, S. LaMarra, J. Trunk, Z. Yin,
NSLS-II, Brookhaven National Laboratory, Upton, NY, USA

Abstract

During the COVID-19 pandemic, non-essential businesses closed or reduced output, prices for products rose, and availability of products needed for research decreased significantly. Many cryogenic gas producers closed or significantly reduced production, causing cryogenic gas prices to rise. In 2022, liquid helium (LHe) cost $12.36; NSLS-II now pays $32.94/liter (as of August 2025). Much effort therefore focused on remote and multi-sample processing capabilities. When staff members were forced to work from home, equipment to facilitate efficient remote research with minimal on-site presence was developed. A prototype remote cryogenic transfer line valve adjuster was then developed that successfully cut LHe consumption to less than half in one week-long series of experiments, but it needed improvement. This paper describes the engineering efforts to develop, improve, and produce working remote cryogenic transfer line valve adjusters to retrofit existing cryogenic transfer lines.

INTRODUCTION

Remote processing capabilities at NSLS-II were developed during the COVID-19 pandemic due to the rising cost and decreased availability of cryogenic gases such as LHe (reference Fig. 1).

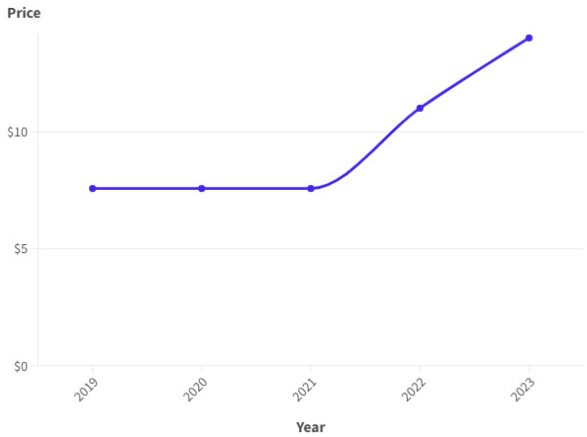

Figure 1: Grade A He price per m^3 (Source: USGS) [1].

At the NSLS-II PDF beamline, a series of week-long experiments using a magnet and cryostat containing samples cooled by an open-loop LHe system consumed three full 100-liter LHe dewars at a FY22 cost of $12.36/liter. The total LHe cost was >$3,700. Although this is just one series of experiments, the total amount of LHe used by NSLS-II in FY22 was 11,620 liters. The cost for this quantity exceeded $140k. As the cost for LHe continued to rise and its' availability continued to decline, three strategies were considered to mitigate this: 1, limit experiments performed requiring cryogens, 2, purchase closed-loop systems that recycle cryogens, 3, develop equipment to efficiently control LHe usage.

All three of these methods were used or initiated in FY22 including the design, production, and testing of a prototype Remote Cryo Valve Adjuster using a stepper motor, internal gears, and a metal housing (reference Fig. 2). The prototype was tested in a similar week-long series of experiments. The result: only one 100-liter dewar of LHe was needed. The LHe cost for this second series of experiments was approximately $1,200, a savings of over $2,500 (excluding labor to fill, transport, and change the additional dewars).

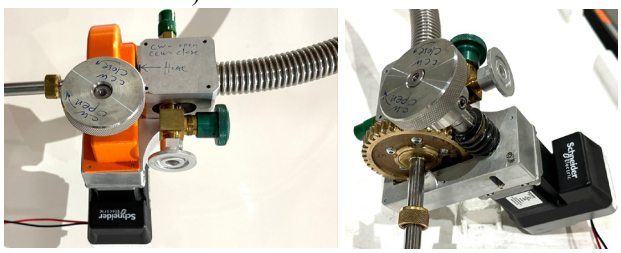

Figure 2: Prototype Remote Cryo Valve Adjuster (a) with, and (b) without the 3D printed plastic gear cover.

Although the first prototype worked well, it was heavy, expensive to produce, and difficult to set up and adjust. It used a NEMA 23 motor that was larger and heavier than needed. An improved, lighter, less expensive, easier to implement remote valve adjuster version was needed.

MATERIAL/PROCESS SELECTION

With the approval of Facilities Improvement Project (FIP) funds, efforts were undertaken to improve the original prototype to minimize weight and cost, then produce three completed devices for other NSLS-II beamlines. A NEMA 17 motor was selected, and the prototype was redesigned using 3D printed materials.

- Stereolithography (SLA) uses a laser to cure liquid resin,
- Fused Deposition Modeling (FDM) builds parts by melting/extruding thermoplastic filaments, and
- Selective Laser Sintering (SLS) uses a laser to fuse powdered polymers.

Both SLS and FDM equipment are available on-site, but SLS equipment was selected due for its' better resin material properties and higher accuracy levels (FDM: 0.20 mm vs. SLA: 0.10 mm). A 4-piece housing was

ISBN: 978-3-95450-263-9 ISSN: 2673-5520 doi: 10.18429/JACoW-MEDSI2025-TUP52

SPring-8 BL12B2 ATTENUATOR DESIGN

Ming-Ying Hsu, Bo-Yi Chen, Tim Lo, Gung-Chian Yin, Chien-Yu Lee
National Synchrotron Radiation Research Center, Hsinchu, Taiwan

Abstract

The light source of the BL12B2 beamline is one of the bending magnets in SPring-8. With this beamline, scientists can conduct experiments in X-ray absorption spectroscopy, high-resolution X-ray scattering, protein crystallography, and micro-beam scattering. SPring-8-II will undergo an upgrade in the next few years.

The attenuator designed for the future upgrade of BL12B2 features nine filters and is cooled by the chamber wall. Each filter carrier can absorb 100 W, and the carrier's maximum temperature remains below 75 °C when the wall temperature is 25 °C. The attenuator also serves as a pumping station, incorporating a 6″ port for both the ion pump and the turbo pump. The attenuator filter is driven by a pneumatic actuator, which positions the filter either in the beam path or in the cooling position. This attenuator was installed in the BL12B2 beamline at SPring-8-II in April 2025.

INTRODUCTION

This study focuses on the design of a new attenuator for the BL12B2 beamline upgrade project at SPring-8-II. The BL12B2 light source is a bending magnet, and its source parameters are summarized in Table 1. The attenuator is located 31.5 m downstream along the beamline. At this position, the beam size is 11.3 µm (horizontal) × 5 µm (vertical), as shown in Fig. 1. The source parameters are listed in Table 2. The beam power is 167 W.

The BL12B2 beam power reaches 167 W when the front-end slit is fully open to 1 mrad. The attenuator consists of nine filter carriers, each capable of absorbing approximately 100 W. This type of attenuator system is already in use at the TPS 31A beamline at NSRRC, with its thermal analysis presented in Refs. [1, 2].

In the present design, the filter carriers move within the chamber via a linear drive, whereas the attenuator used previously at TPS 31A operated using magnetic force.

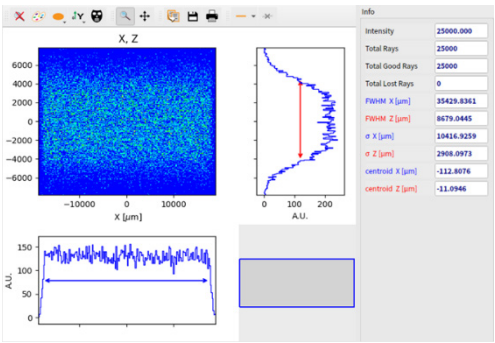

Figure 1: The beam profile at BL12B2 31.5 m.

DESIGN RESULT

The attenuator body is made of 6061 aluminum alloy, which provides high thermal conductivity, as shown in Figs. 2 and 3. The filter carrier is also fabricated from 6061 aluminum alloy. When the filter foil absorbs energy from the light source, the filter carrier effectively dissipates heat and prevents excessive temperature rise.

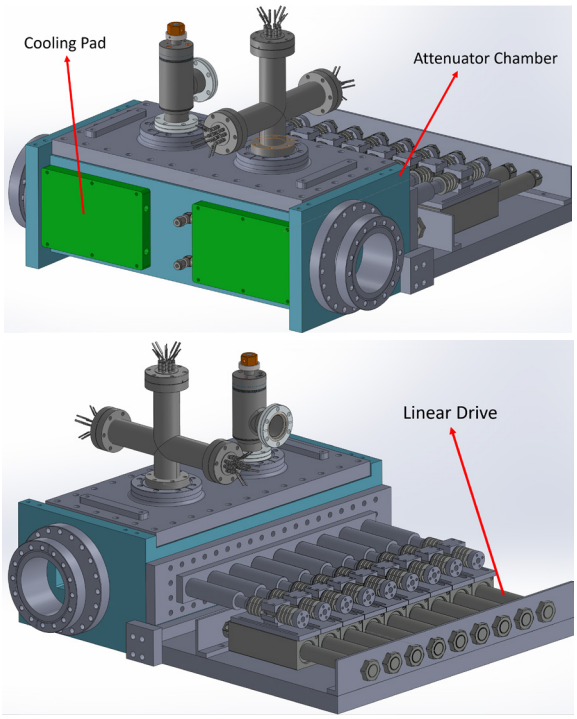

Figure 2: Attenuator chamber system front and back view.

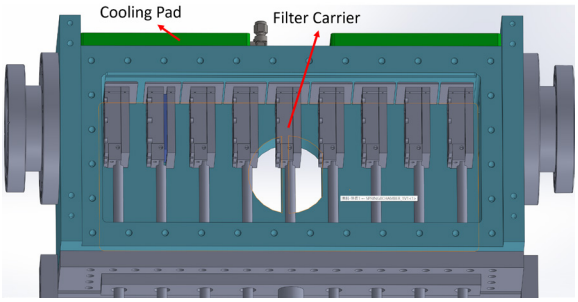

Figure 3: Attenuator chamber inside view and filter carrier.

The filter carrier clips the filter and transfers heat to the copper pad, while the aluminum alloy chamber wall assists in cooling the carrier. On the outside of the chamber, a mini-channel fin water-cooling plate (ATS-CP-1000) is attached. This plate features rectangular mini-channels with a width of approximately 240 µm (ATS, Inc.). At a flow rate of 3.7 L/min (1 gallon/min), the pressure drop is

ISBN: 978-3-95450-263-9 ISSN: 2673-5520 doi: 10.18429/JACoW-MEDSI2025-TUP53

STUDIES FOR A NOVEL GENERATION OF THE BEAM PROFILE MEASUREMENT (BEAM WIRE SCANNER) FOR THE LARGE HADRON COLLIDER (LHC)

W. Andreazza, H. Bursali, N. El Kassem, J. Emery, M. Faure, M. Hamani, C. Pasquino, M. Ramos Garcia, F. Roncarolo, H. Sullivan, R. Veness
CERN, Geneva, Switzerland

Abstract

Aiming for the improvement of the reliability and maintainability of the LHC linear wire scanners, a completely new concept is currently under development. The innovative design will eliminate the use of bellows, feature a more precise and optimized wire positioning system, and incorporate a significantly more robust and resilient mechanical structure. Four next-generation instruments are scheduled for installation in the LHC during Long Shutdown 3, enabling both horizontal and vertical beam profiling for beam 1 and beam 2 with improved accuracy and stability. This paper presents the conceptual study, detailed mechanical design, integration strategy, and the initial experimental tests of the newly developed magnetically driven linear wire scanner.

INTRODUCTION

In the Large Hadron Collider (LHC), Wire Scanners (BWS) play a key role as the reference instrument for machine developments and are used to calibrate other profile measurement devices which provide precise bunch-by-bunch measurements at all energy levels [1].

The scanners currently installed in the LHC were inherited from the Large Electron–Positron (LEP) Collider after its decommissioning, with the original design dating back to the 1980s. In recent years, several reliability issues have required interventions, including:

- Bellow leakage (four cases, most recently in 2023)
- Fork blockage (2015)
- Loss of wire tension (two scanners, 2018)

In 2015, a consolidation project was launched to improve the driving system and the external mechanics. As part of this work, four scanners were upgraded to "hybrid" systems by replacing the legacy motion mechanism with a modern ball screw drive (Fig. 1). These new linear drives were integrated into the standardised LHC Injectors Upgrade (LIU) control system [2].

To date, the in-vacuum mechanics remain unmodified since installation, and are not optimised for positional accuracy and vibration reduction. Furthermore, the continued use of bellows to enable in-vacuum motion has led to ongoing reliability concerns. It was therefore decided to proceed with a complete mechanical redesign as part of a second stage of the consolidation, both to mitigate the need for future interventions and to improve measurement accuracy.

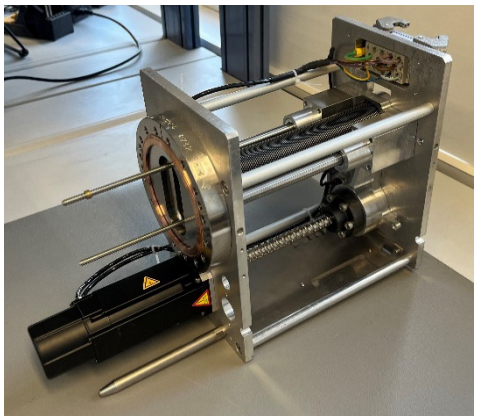

Figure 1: Hybrid linear wire scanner.

The large time span since the legacy design has provided an opportunity to integrate modern materials and motion technologies. This new mechanical overhaul project began in November 2023. A redesigned scanner has since been developed, and the first prototype is now in production for installation during the LHC year-end technical stop (YETS) 2025.

The implementation plan foresees the installation of a prototype during the winter of 2025/26 to validate the design. Full replacement of the eight existing instruments is planned in two stages: the first during Long Shutdown 3 (2026–2030), followed by the second during Operation Run 4 (2030–2033).

This paper presents the conceptual study, detailed mechanical design, integration strategy, and initial experimental tests of a newly developed magnetically driven linear wire scanner.

SYSTEM OVERVIEW

During the conceptual design stage the key constraints and requirements of the scanner were identified:

- The design phase was dedicated to the development of a new instrument compatible with the existing control system and electronics designed for the (BWS) installed in CERN's three circular injectors.
- The design had to comply with the stringent vacuum specifications of the LHC while ensuring high mechanical reliability through a bellows-free architecture.
- A key design driver was impedance optimization, aiming to maintain or improve the overall longitudinal and transverse impedance of the LHC.

ISBN: 978-3-95450-263-9 ISSN: 2673-5520 doi: 10.18429/JACoW-MEDSI2025-TUP56

THE EXTREME CONDITIONS CATALYTIC CELL FOR BL01 AT ALBA

A. Carballedo[†,1], R. Cohen[2], N. González[1], P. C. Heydorn[3], A. Jacquet[4], M. Quispe[1], I. Youssef[1]
[1]ALBA Synchrotron, Cerdanyola del Vallès. Spain
[2]European Molecular Biology Laboratory, Grenoble, France
[3]Instituto de Tecnología Química, Universitat Politècnica de València, València, Spain
[4]École nationale supérieure de techniques avancées Bretagne, Brest, France

Abstract

A new catalytic cell has been developed for the Infrared Spectroscopy and Microscopy (MIRAS-BL01) beamline at the ALBA synchrotron. The aim of this instrument is to study catalytic reactions, crucial for advancing sustainable chemistry by enabling energy-efficient processes and minimizing by-products. Infrared (IR) spectroscopy offers key molecular insights, helping identify active species, understand mechanisms and link structure to activity. It also monitors catalysts in real time, revealing structural changes that affect performance.

The reactor is designed to operate in transmission mode from vacuum conditions to pressures up to 20 bar of different mixtures of gases and within a wide temperature range, covering from cryogenic temperatures up to a maximum of 500°C, while allowing the sample to move vertically few millimetres in order to alternate between exposing it and the background.

Currently in production, the design's key aspects are presented, covering the sample position mechanics, the various FEA calculations performed as well as the necessary auxiliary systems, such as cooling mechanisms and the pressurized gas circuit.

INTRODUCTION

The MIRAS-BL01 is a beamline devoted to Fourier Transform Infrared (FTIR) spectroscopy and microscopy. It consists on a modern synchrotron-based infrared spectrometer and microscope capability covering a wavelength range optimised for investigations from Mid-IR (700-4000 cm^{-1}) to the Far-IR (80-600 cm^{-1}) spectral ranges.

One of the potential research fields in this beamline is the study of catalytic reactions. A preliminary experiment carried out in collaboration with the Instituto de Tecnología Química (ITQ) in Valencia employed a bolometer detector in the far-infrared range and tested different gases under multiple configurations and modes. This cell provided valuable insights that inspired the development of the present design. The following research stage will focus on the development of a transmission-mode approach.

For this reason, a new catalytic cell has been designed for MIRAS aimed at advancing studies in this field.

TECHNICAL SPECIFICATIONS

The specifications that the cell must fulfil are listed below:

- To hold a sample pellet of diameter Ø=13 mm and thickness t=0,025 mm.
- Vertical movement of the sample around 20 mm to be exposed or not to the beam.
- Sample temperature from -196 °C to 500 °C.
- Possibility to work under vacuum (10^{-6} mbar) or accommodate a gas mixture (O2, H2, CO, and an inert gas like Ar) under 20 bar maximum working pressure and under flow mode.
- Easy integration inside the spectrometer (BRUKER Vertex 70).
- Volume of the setup minimized as much as possible.

SYSTEM DESCRIPTION

The proposed catalytic cell solution is shown in Fig 1. This cell consists on three subsystems. The first, called the heat exchanger, is responsible of the sample heating and cooling. The second is the sample stick, which includes the sample holder and the vertical motion mechanism. Finally, the pressure vessel contains the sample at the required pressure. Each of these components is described in detail in the following sections.

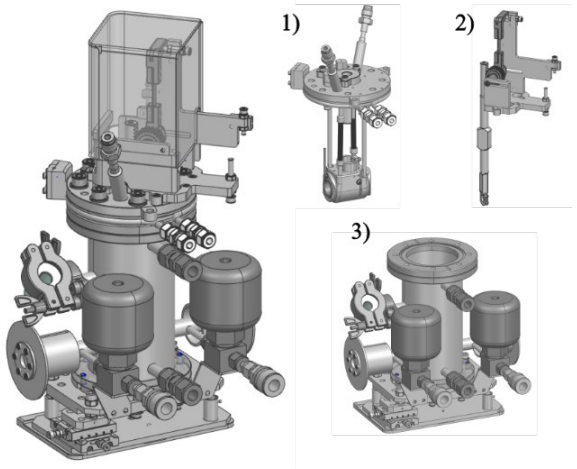

Figure 1: Left: general view of the catalytic cell. Right: 1) Heat exchanger. 2) Sample stick. 3) Pressure vessel.

† acarballedo@cells.es

ISBN: 978-3-95450-263-9 ISSN: 2673-5520 doi: 10.18429/JACoW-MEDSI2025-TUP57

THE MILLISECOND X-RAY FAST SHUTTER FOR BL31 AT ALBA

Antonio Carballedo†, Álvaro Baucells, Javier García-Álvarez, Steven Wohl,
Nilson Bernardo Pereira, Juan Luis Frieiro, Llibert Ribó, Nahikari González, Federico Cova,
Victorien Bouffetier, Alessandra Patera
ALBA Synchrotron, Cerdanyola del Vallès. Spain

Abstract

A new high-speed beam shutter has been developed for the fast x-ray tomography & radioscopy (FAXTOR-BL31) beamline at the ALBA synchrotron, which aims at preventing high dose rate at the sample and provides a synchronization to the acquisition protocol. The non-periodic fast shutter is based on the combination of two tungsten blades each one driven by linear voice coil actuators. The blades synchronization achieves opening and closing times of 10 ms for a monochromatic beam size of H 40 mm x V 12 mm aperture. The design provides flexibility to adjust the aperture dimensions and speed to be able to control the radiation dosage upon the sample, triggered by the image acquisition rate of the detector or timing device. The essential aspects of the design are presented, along with an analysis of the commissioning tests that demonstrate the required performance.

INTRODUCTION

The FAXTOR-BL31 beamline is dedicated to fast X-ray tomography and radioscopy. A portion of its research focuses on the study of biological samples, where it is crucial to ensure precise control over the radiation dose to preserve sample integrity. This necessitates the use of a fast shutter capable of delivering well-defined exposure windows. A key aspect in this particular case lies in the beamline's ability to operate with both white beam and monochromatic configurations, featuring a large beam cross-section of 40 × 15 mm². Blocking such a large beam entirely within a specified time below 10 milliseconds has proven to be particularly demanding, making the selection or development of suitable shutter technology a significant challenge.

TECHNICAL SPECIFICATIONS

Compared to the full beamline capabilities, the technical requirements for the planned research application are narrower in scope and more specifically defined.

The following list represents the most critical constraints considered during the design of the system:

- Monochromatic beam.
- Maximum beam size: 40 × 12 mm².
- Opening/closing time: 10 ms.
- Blade material: Tungsten.
- Minimal blade thickness: 4 mm.
- Beam vertically shutted.

† acarballedo@cells.es

SYSTEM DESCRIPTION

The solution presented is based on the use of voice coil actuators (VCA) [1, 2]. A voice coil operates through the interaction between a magnetic field and a current-carrying coil, generating a linear force proportional to the input current. This technology enables fast and precise motion, with a high force density that provides the large acceleration required to achieve the desired performance. As shown in the Figs. 1 and 2, the system consists of two VCAs, one positioned at the top and the other at the bottom of the shutter. Mounted on each actuator is a 4.5 mm-thick tungsten blade, which is sufficient to fully block the X-ray beam. It is important to note that the system is symmetric, and each blade is slightly offset relative to the other in the beam axis. This offset allows the blades to overlap in the closed position without the risk of collision, ensuring complete beam blockage.

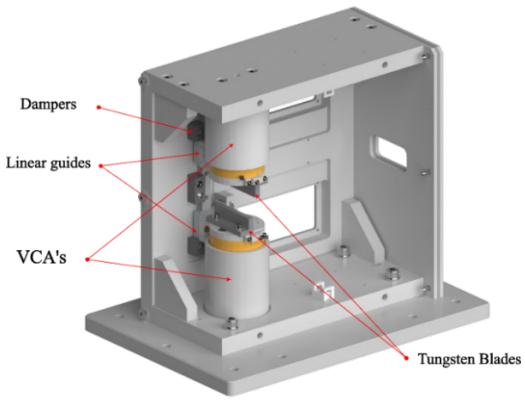

Figure 1: Open view of the shutter.

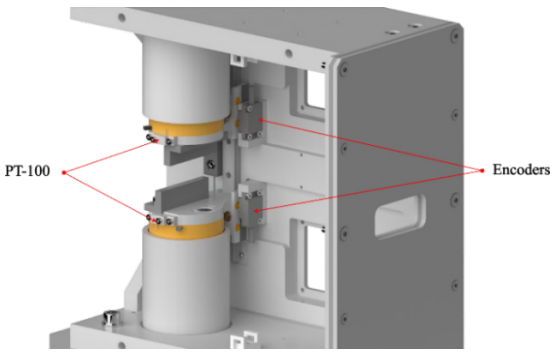

Figure 2: Different sensors provided in the shutter.

The system is equipped with linear guides to ensure accurate linear motion of the blades. In addition, relative encoders are integrated to provide position feedback for each blade. Also, since the blades are mounted directly on the

ISBN: 978-3-95450-263-9 ISSN: 2673-5520 doi: 10.18429/JACoW-MEDSI2025-TUP58

THE NEW ALBA DIFFRACTOMETER FOR MICROFOCUS BEAM MACROMOLECULAR CRYSTALLOGRAPHY EXPERIMENTS AT XAIRA BEAMLINE

N. Gonzalez, D. Garriga, I. Crespo, J. L. Frieiro, N. Pereira, B. Molás, J. Gabadinho, I. Sics, A. Carballedo, C. Colldelram, J. Nicolás, J. Juanhuix
ALBA Synchrotron Light Source, Cerdanyola del Valles, Spain

Abstract

XAIRA, the new microfocus MX beamline at ALBA aims to deliver optimal diffraction images by enclosing the entire end-station in He atmosphere, including the diffractometer and the detector, while keeping the compatibility with standard cryo-crystallography tools and robot. The sub-100 nm SoC diffractometer, based on a unique helium bearing goniometer also compatible with air, has been designed to deliver high quality data from micron-sized crystals from fast oscillation and fixed-target MX experiments while allowing a tight sample-to-detector distance of 70mm. The diffractometer also includes a double on-axis visualization system for sample imaging at sub-micron resolution, a quick retractile collimator and beamstop assembly, a front- and backlight illumination system and a fast in/out YAG:Ce screen system for beam positioning. Here, the overall system design and performance results are presented.

INTRODUCTION

The new BL06-XAIRA microfocus macromolecular crystallography (MX) beamline at the ALBA synchrotron light facility, which has entered into user operation this year, provides a 3.5-14 keV stable, high flux beam which could be focused down to 3×1 μm^2 [1]. The beamline supports single-axis rotation experiments, including helical scans, and fixed-target serial crystallography (SSX).

A key feature of the beamline is a chamber enclosing the whole end station, which allows experiments to be performed either in air or in helium atmosphere, and both at room temperature or under cryogenic conditions. The helium environment not only enables experiments in the low energy range below 6 keV, thus providing optimal conditions for native anomalous experiments, but also benefits the experiments in the whole energy range by eliminating the background from air scattering.

This end station chamber includes the sample environment, diffractometer, cryostream and detector, and it is compatible with automated sample mounting and the standard cryo crystallography sample holders. The components of the diffractometer, an omega axis goniometer and the sample conditioning and monitoring components, are supported over a stable omega XY stage adjusting the whole setup together, see Fig. 1.

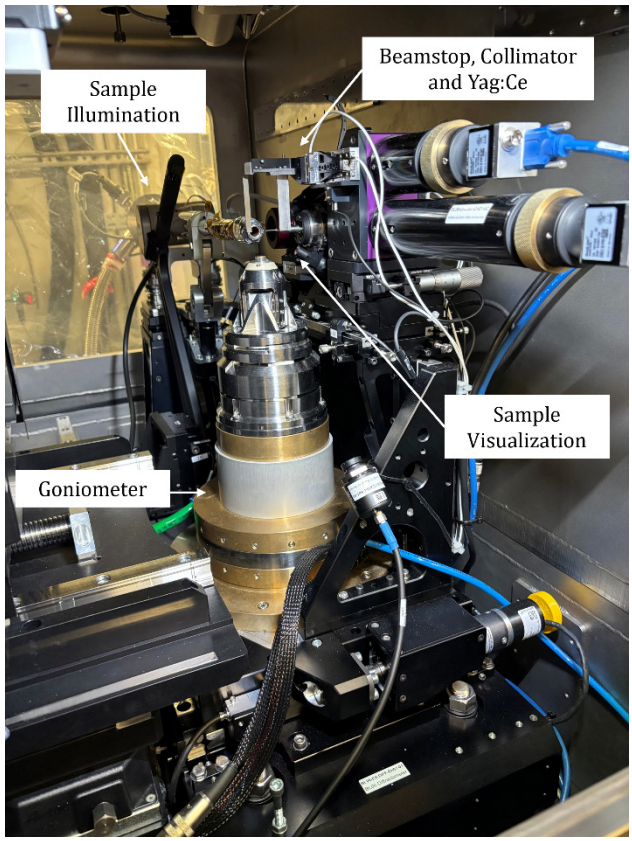

Figure 1: Diffractometer components within the helium chamber.

SYSTEM DESCRIPTION

Goniometer

The central component of the diffractometer is a low friction vertical single-axis goniometer, designed at ALBA to comply with the tight geometrical requirements of the end station and manufactured by Fluid Film Devices Ltd. The goniometer bearing can be fed either by air or He with similar performance. The goniometer is actuated by a direct drive slotless torque motor (Aerotech S-130), which has no cogging torque. The position and speed control loops are closed with a double head ultra-high accuracy rotation analogue encoder (Renishaw REXM20), which meets the requirements in terms of maximum resolution, 0.04 mdeg, and maximum speed, 60 rpm. The goniometer is installed on an in-house designed, 0.1 µm resolution and high stability XY stage, actuated by stepper motors. This stage permits positioning the goniometer axis at the focal

ISBN: 978-3-95450-263-9 ISSN: 2673-5520 doi: 10.18429/JACoW-MEDSI2025-TUP59

THE NEW MICROFOCUS STATION FOR THE NOTOS BEAMLINE AT THE ALBA SYNCHROTRON*

A. Garcia-Herreros†, N. Gonzalez, J. Nicolás, C. Colldelram, C. Marini, E. Villalobos, C. Escudero, L. Aballe
ALBA Synchrotron Light Source, Cerdanyola del Vallès, Spain

Abstract

The NOTOS beamline (BL16) at ALBA synchrotron combines X-ray Absorption Spectroscopy (XAS) and X-ray Diffraction (XRD), operating in the 4.5-30 keV range. Since 2022, it has offered two End Stations (ES): one for metrology and XAS, and another combining XAS and XRD. In this work we present a third Microfocus End Station (μFo-ES) planned to be in operation by the end of 2025. It will provide spot sizes below 10×10 μm² with a flux >$7.3 \cdot 10^{13}$ ph/s/mm², enabling XAS in fluorescence and transmission. It uses the existing beamline optics with the addition of a pair of Kirkpatrick–Baez (KB) mirrors working under high vacuum. The KB positioning system is based on an in-housed developed design and the mirrors will be elliptically bent using ALBA mirror benders with sub-nanometric resolution. High-precision slits included in the μFo-ES will be placed upstream the KB and used for diagnostics and to ensure a correct beam size and collimation. Furthermore, the μFo-ES will integrate a compact sample environment including an ionization chamber, on-axis imaging system, and a fluorescence detector for variable incident angles and small sample to detector distances. To ensure compatibility with downstream ES and prevent photon flux loss, the μFo-ES has been designed to be fully retractable from the beam path.

INTRODUCTION

ALBA is a synchrotron light source facility located near Barcelona, Spain. It currently operates 13 beamlines covering a broad range of scientific applications, with three additional beamlines in various stages of design or construction. Short-term strategic plans include upgrading the facility to a fourth-generation synchrotron source, along with significant enhancements to existing beamlines to support cutting-edge research.

NOTOS is the result from the confluence between the Metrology and Test Beamline proposed for ALBA phase II and the transfer of ESRF's BM25a, devoted to X-ray Absorption Spectroscopy (XAS) and Powder Diffraction (PD). NOTOS beamline operates between 4.5 and 30 keV using a bending magnet as its source. It is a versatile experimental beamline designed for *in situ* and *operando* studies through the combined use of XAS and X-ray Diffraction (XRD). The current setup consists of two experimental End Stations (ES): a multipurpose ES and a PD-XAS ES. The multipurpose ES offers an open-space setup suitable for metrology applications as well as XAS measurements in both fluorescence and transmission modes. On the other hand, the PD-XAS ES is equipped with a two-circle diffractometer, enabling simultaneous XAS (in fluorescence and transmission geometries) and XRD measurements. Additionally, the beamline includes a fully integrated gas handling system with multiple gas lines, flow and pressure control, for a user-friendly operation.

To overcome the current 100×100 μm² spot size limitation on both current ES. a newly developed Microfocus End Station (μFo-ES), placed upstream the multipurpose ES, will be used to increase experimental possibilities by providing beam spot sizes smaller than 10×10 μm² fwhm. Furthermore, to prevent photon flux loss when using the other ES, the μFo-ES has been designed to be fully retractable from the beam path.

END STATION

The μFo-ES is placed downstream a complex set of already working beam conditioning elements and upstream the multipurpose ES (Fig. 1A). Because of the limited available space for the μFo-ES, most of its components must be compact and work in tight spaces. For this reason, the different components of this ES were designed and assembled in-house, even though commercial products with similar functions may be available in the market. The μFo-ES is composed of three main components, in beam path order are: high precision slits, focusing mirrors and a dedicated sample environment. The μFo-ES forms part of InCAEM, a strategic project at ALBA that seeks to enable correlative measurements between synchrotron beamlines and advanced electron microscopy techniques. To meet this objective, every component of the sample environment is designed with a high degree of flexibility and adaptability, ensuring seamless integration of diverse types of samples. A general view of the μFo-ES is presented in Fig. 1B.

High Precision Slits

High-precision tungsten slits are primarily used to control the beam size, as well as for alignment procedures and diagnostic purposes. These compact slits, extending only 65 mm in the direction of the beam, are positioned at the entrance of the main vacuum chamber and are actuated by SMARACT piezo-driven stages (Fig. 2A). To aid in beam alignment, the upstream face of the slits is coated with a fluorescent material that emits visible light upon exposure to the X-ray beam, enabling accurate visualization and tracking of the beam position.

* Work supported by the Spanish MCIN, the Generalitat de Catalunya and NextGeneration EU. (PRTR-C17.I1) From the Recovery and Resilience Mechanism.
† agdeherreros@cells.es

ISBN: 978-3-95450-263-9 ISSN: 2673-5520 doi: 10.18429/JACoW-MEDSI2025-TUP60

THERMAL MODELLING, DESIGN AND EVALUATION OF A CRYOGENIC COOLING SYSTEM FOR A BEAMLINE ENDSTATION

D. Tillin†, S. Beamish, C. Bovo, D. Burn, S. Davies, J. H. Kelly
Diamond Light Source, Harwell Science and Innovation Campus, Didcot, Oxfordshire, UK

Abstract

The accurate estimation of thermal contact conductance (TCC) is a fundamental need towards the optimal design of a cryogenic cooling system for the new flagship beamline CSXID at Diamond Light Source, which utilizes mechanically pressed components of gold-plated copper to form the heat conduction path. To aid development, a study of thermally conducting joints at cryogenic temperatures has been performed combining Mathworks® Simulink and ANSYS Workbench™. To verify and validate the simulation results, an experimental setup will be made to carry out experiments to determine performance of the system, taking into consideration parameters including surface roughness, surface finish, temperature, & clamping force, which all greatly influence TCC.

BACKGROUND

The flagship beamline CSXID at Diamond Light Source is aiming to be a world leader in nano positioning and imaging resolution. The beamline will be used to perform experiments to study the magnetic and electrical properties of materials under certain environmental conditions, using the Quantum Material Imaging (QMI) endstation. Cryogenics is one requirement for this endstation, where the sample environment must be tightly controlled. In addition, the sample must rotate about two axes, have a magnetic field with an adjustable field strength and polarity, and be able to excite the sample with RF signals, all while maintaining position stability in the sub-nanometre range. Here presents a challenge; many systems with small space envelopes which must operate concurrently.

To design a cryogenic system with a high level of confidence, thermal modelling must be performed, which can also aid the development in the early design stage.

REQUIREMENTS

The system's requirements are shown in Table 1.

Table 1: Cryogenic Requirements at the Sample Position

Description	Requirement
Target sample temperature	20 K
Cooldown time after venting	3 hrs
Cooldown time after sample transfer	30 mins
Sample transfer temperature	300 K
Warm-up time	30 mins
Sample position drift during cooling	<10 µm

† david.tillin@diamond.ac.uk

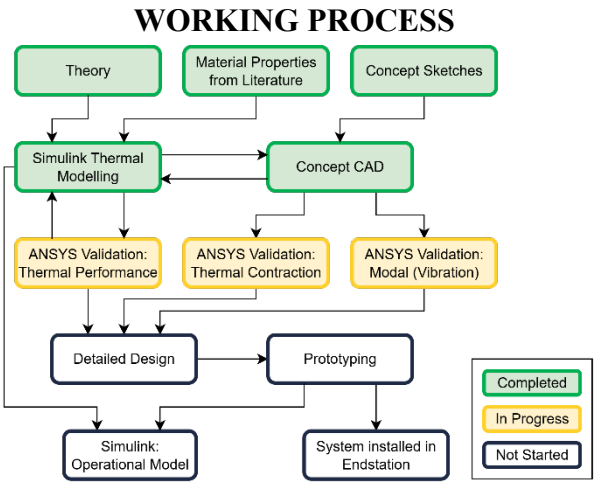

Figure 1: A flowchart showing the working process used to develop the cryogenic system.

Figure 1 shows an outline of the working process behind the development of the cryogenic system. Material properties were taken from literature to generate a model using Simulink in combination with geometrical data from the concept system. This concept is shown in Fig. 2. The Simulink model was then used to rapidly iterate the design. Simulink creates time-resolved models, which allows the prediction of cooldown times and low temperature operations.

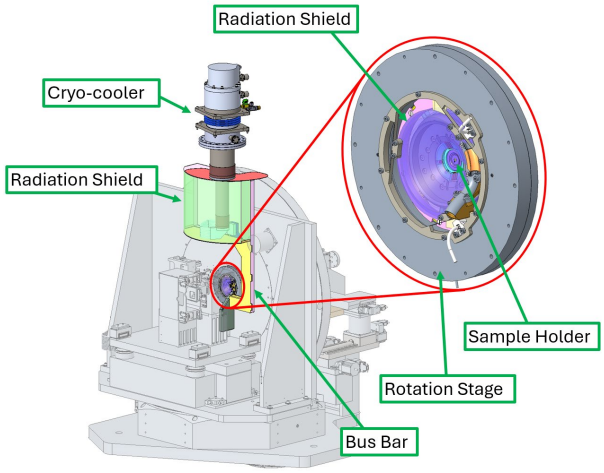

Figure 2: The QMI Endstation concept. The Cryogenic system is highlighted.

Once the design reached a satisfactory level of confidence, an ANSYS steady-state thermal analysis was used to validate the simulated results, to analyse the effects of thermal contraction on positioning, and modal analysis was used to generate expected resonant mode shapes.

ISBN: 978-3-95450-263-9 ISSN: 2673-5520 doi: 10.18429/JACoW-MEDSI2025-TUP64

XBPF DESIGN AND PROTOTYPING

B. Moser*, A. Frassier, R. Larsen, I. Ortega, CERN, Geneva, Switzerland
E. Buchanan, University of Edinburgh, Edinburgh, Scotland

Abstract

The CERN Beam Instrumentation Group has developed a new scintillating fibre beam profile monitor for the secondary beam lines of the CERN North Experimental Area. This innovative monitor employs plastic scintillating fibres, read out with silicon photomultipliers, to provide a cost-effective and efficient solution for beam profile measurement. The design goals for the new monitor included ease and low cost of production, achieving a particle detection efficiency above 95 %, compatibility with beam intensities ranging from 1 to 10^8 particles per second, a spatial resolution of 1 mm, a low material budget, coverage of an active area of 10 cm × 10 cm or 20 cm × 20 cm, operability in a vacuum environment, and equipped with in/out motorisation for retracting the equipment from the beamline. A prototype was tested at the CERN East and North Area facilities, demonstrating excellent performance and validating the design for mass production.

INTRODUCTION

CERN is undertaking a consolidation project of the North Area complex, the largest experimental area at CERN and home to a rich program of fixed-target physics. As part of this effort, the beam instrumentation is also being upgraded. The secondary beamlines are still operating with the original instrumentation, which was designed and installed in the 1970's. Despite their longevity and maintenance, these instruments are now showing signs of degradation due to ageing and radiation exposure, and spare parts are no longer available. At present profile monitoring is done using Multi-Wire Proportional Chambers [1], Delay Wire Chambers [2] and the Filament Scintillator Scanner (FISC) [3]. The detector of choice to replace the existing monitors is the scintillating fibre monitor(XBPF) developed by the Beam Instrumentation(BI) Group [4]. The new detectors are designed for operation in vacuum environments, as the beamlines will be in vacuum wherever possible to improve beam quality, and feature retractable mechanisms to minimize material budget on the line when not in use and extend fibre lifespan. Two types are needed one covering an area of 10 cm × 10 cm cm and another one covering an area of 20 cm × 20 cm. This paper presents the design and validation of the 10 cm × 10 cm prototype, along with ongoing development efforts.

XBPF DETECTOR DESIGN

The overall detector head design has already been implemented in secondary beamlines at CERN [4]. Earlier versions operated in vacuum but were fixed in place, requiring manual intervention for repositioning. The new design introduces an in/out motorisation system that allows the detector to be retracted from the beam, improving operational flexibility. The fibres selected have a thickness of 1 mm and a square cross-section, which enhances detector homogeneity. In practice, 96 fibres are used to match the readout electronics, which have 96 channels. As a result, the actual active area is 9.6 cm × 10 cm. To streamline development, existing vacuum chambers from the FISCs were repurposed, which required adherence to predefined flange and geometry constraints.

In-Out Mechanism

The detector is to be placed in a primary vacuum 10^{-3} mbar environment. A key challenge was minimizing vacuum forces acting on the actuator mechanism. Fibre routing to the readout board required careful consideration of bending radii, requiring a compact actuator footprint. Early concepts involving internal readout boards were discarded due to the need for active cooling in vacuum. The most practical solution for in-out movement was the use of edge-welded bellows. Table 1 summarizes the vacuum forces for available bellow configurations..

Table 1: Vacuum Forces for Different Bellow Sizes

Bellow Size	Vacuum Force
DN100	1121 N
DN150	2287 N
Racetrack 40/130	823 N

The racetrack-shaped bellow was selected for its compact footprint and reduced vacuum force, which eased integration and minimized mechanical stress. A pneumatic actuator was chosen for its simplicity—requiring only ON/OFF control signals—and adjustable force via actuator size or supplied pressure. A 150 mm stroke ensures full beam clearance when retracted. The mechanism is illustrated in Fig. 1.

Detector Head

The detector head comprises three main components:

- Interface flange: Seals the vacuum and connects to the readout board.
- Active area: Interacts with the beam.
- Support structure: Ensures mechanical stability and alignment.

The overall dimension of the support structure inside the vacuum was restricted by the choice of the vacuum bellow. To avoid modifications to the read out board the same fibre pattern was used on the interface flange as on previous XBPFs produced. This meant that we had to start the design

* benjamin.moser@cern.ch

ISBN: 978-3-95450-263-9 ISSN: 2673-5520 doi: 10.18429/JACoW-MEDSI2025-WEOA01

ADDITIVE MANUFACTURE, 3D-PRINTED, METALLIC X-RAY MIRROR FOR SYNCHROTRON AND XFEL FACILITIES

S.G. Alcock†, T. Wearing, S. Beamish, J.H. Kelly, M.B. da Silva, R. Shurvinton, P. Pradhan, K. Sawhney
Diamond Light Source, Didcot, UK

Abstract

We have designed and fabricated the world's first, Additive Manufacture (AM) mirror for X-ray beamlines. For traditional optics, beamline performance is limited by: distortion caused by mechanical clamping; heat-bumps induced by photon-beam illumination; and strain caused by differential thermal expansion when dissimilar materials are cooled. AM enables the creation of intricate internal structures, and the fusion of multiple components into a single piece. The optical substrate, beamline mount, and internal cooling manifold were combined into a monolithic structure. The X-ray mirror was 3D-printed in aluminium alloy AlSi10Mg. Single-point diamond turning created an optical surface, which was coated in ~75 μm of electroless NiP (nickel phosphor), followed by "super-polishing" using chemo-mechanical processing. Optical metrology demonstrates the AM mirror has surface quality comparable to a traditional silicon mirror. The design is virtually immune to clamping deformations, which simplifies beamline installation. AM unlocks exotic internal channel designs, including enhanced cooling performance by turbulent flow, reducing vibrations caused by fluid flow, and conforming to the heat load distribution.

INTRODUCTION

Additive Manufacture is increasingly used for creating novel engineering components and lightweighted optics for space-based astronomy [1] that would be challenging or impossible to create using traditional subtractive methods. We extend this concept to creating a composite X-ray mirror system for synchrotron light and XFEL beamlines.

MANUFACTURING

After design by the Engineering team at Diamond Light Source, based on thermal and mechanical CAD modelling, the mirror was grown using Additive Manufacture (AM) at CA Models, UK (see Fig. 1). This was followed by stress-relieving at 300°C for 2 hours. AlSi10Mg was selected as a cost-effective, and well understood aluminium alloys routinely used for additive manufacturing. One limitation of this alloy is its relatively high thermal expansion coefficient ($20\times10^{-6}\,K^{-1}$). AlSi40Mg promises an improved thermal expansion coefficient of $13\times10^{-6}\,K^{-1}$, which would ease the management of thermal distortion for future optics. However, AM manufacture using this alloy is not-readily commercially available and is still in the materials research phase [2].

After growth and annealing, the surface was diamond-turned at Durham University, UK to create a basic optical finish. It was then coated with a 75 μm layer of NiP since aluminium is unsuitable for super-polishing due to its lower hardness and polycrystalline structure. After coating, the surface quality would be sufficient for infra-red optics, but not for the more demanding specifications for X-ray applications at synchrotron or XFEL facilities.

Super-polishing at Crystal Scientific, UK, improved the micro-roughness and form. Finally, ion beam figuring (IBF) at Diamond [3], reduced the height and slope errors (see Fig. 2).

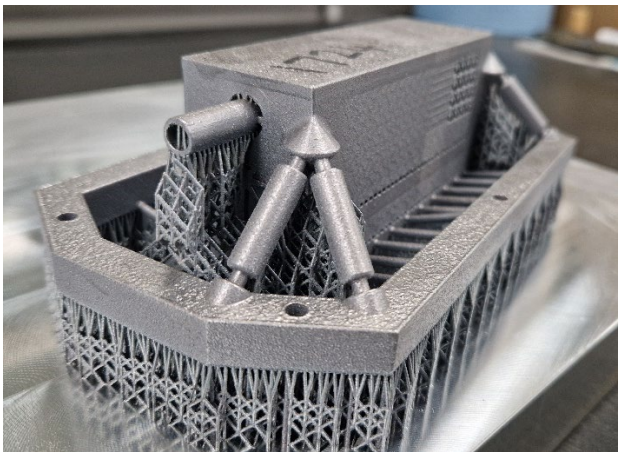

Figure 1: 3D-printed, additive manufactured, X-ray mirror for synchrotron beamlines, combines a high-quality optical surface with novel internal cooling channels and a triple-bipod clamping frame to make beamline installation easier.

METROLOGY

A Bruker GTX micro-interferometer and Zygo HDX Fizeau interferometer were used in the Optics Metrology Lab (OML) at Diamond [4] to measure the micro-roughness, height and slope errors of the mirror at various stages during production (Fig. 3). Metrology data was also used to guide deterministic correction of surface errors using IBF. A further thermal study was undertaken in the OML to observe how the optical surface changes as water was flowed at various temperatures and rates through the internal cooling channels using a portable chiller and pump (Fig. 4).

† simon.alcock@diamond.ac.uk

ISBN: 978-3-95450-263-9 ISSN: 2673-5520 doi: 10.18429/JACoW-MEDSI2025-WEOA02

DESIGNING AND FINE TUNING CRYO-COOLED SILICON MONOCHROMATOR CRYSTALS TO MINIMIZE OPTICAL DISTORTIONS CAUSED BY PHOTON-BEAM HEATING

P. Sanchez Navarro*,[1,2], S. G. Alcock[1], A. Peach[1]
[1]Diamond Light Source Ltd., Didcot, UK
[2]MAX IV Laboratory, Lund, Sweden

Abstract

Slope errors on X-ray optics create distortions in the reflected or diffracted X-ray wavefront and a reduction in energy resolution. This study addresses this challenge by demonstrating a precise and adaptable method for tuning the geometry of liquid nitrogen (LN2)-cooled silicon crystals, with the goal of achieving zero slope errors under specified input power conditions. The findings reveal that an optimal temperature exists, minimizing thermal distortion and slope errors at the X-ray beam footprint. By establishing a straightforward engineering approach to achieve this temperature, the study provides a practical solution for manipulating silicon crystal geometry. This technique ensures minimal slope errors across a broad energy spectrum, enhancing beamline performance and energy resolution. This work overcomes a long-standing limitation in particle accelerator beamlines, where conventional approaches relied on extensive cooling to mitigate thermal effects. The proposed methodology not only improves operational efficiency but also offers a versatile tool for finetuning crystal behaviour in response to varying energy demands.

INTRODUCTION

Crystals with various geometries are used to select the energy bandwidth of intense photon beams from synchrotron and X-ray free-electron laser (XFEL) sources. The performance of monochromator crystals is reduced when diffraction planes are distorted by clamping strain or thermal expansion from heat loads. Slope errors (deviation from the ideal profile) distort the diffracted wavefront and degrade resolution.

Optical quality is a limiting factor for most beamlines, pushing the limits of commercially available solutions. Facilities such as ESRF, SLAC, and Diamond Light Source have shown how thermal deformation in cryogenically cooled silicon crystals impacts double-crystal monochromator performance [1, 2]. With the higher brightness and coherence of new accelerators such as HEPS and Diamond-II, robust optics are needed to manage heat-induced deformation [3].

Promising developments include channel-cut diamond crystals and advanced cooling schemes. Direct-cooling designs are particularly attractive for high-heat-load beamlines with wigglers. Previous tests on an XDS Oxford (formerly FMB Oxford) direct LN2-cooled crystal for the DLS I20 Spectroscopy Beamline confirmed superior performance of Si(111) compared with indirect cooling. However, for Si(311), additional design work was needed to meet the <0.5 µrad slope error requirement across 7–35 keV with zero clamping strain.

METHOD

At approximately –150 °C, silicon's coefficient of thermal expansion (CTE) is zero (see Fig. 1). Cooling further reverses the sign, peaking at –200 °C before returning to zero at –250 °C. Thus, there exists a temperature "sweet spot" where the beam footprint becomes flat, yielding zero slope error (see Fig. 2).

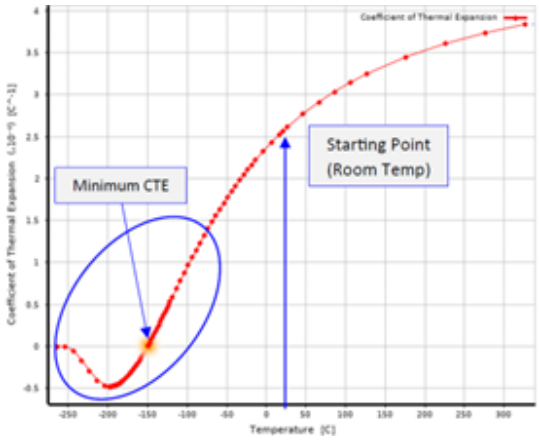

Figure 1: Thermal expansion coefficient of silicon vs. temperature from -250 °C up to 300 °C.

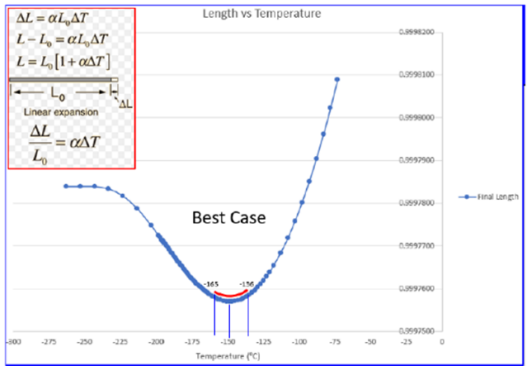

Figure 2: Linear expansion equation for a simple beam using the silicon thermal expansion coefficient chart.

* pablo.sanchez_navarro@maxiv.lu.se

ISBN: 978-3-95450-263-9 ISSN: 2673-5520 doi: 10.18429/JACoW-MEDSI2025-WEOA05

A COMPACT, HIGH THROUGHPUT SVLS SPECTROMETER FOR LCLS-II

Jean-Pierre Torras*, Hengzi Wang, Kristjan Kunnus
SLAC National Accelerator Laboratory, Menlo Park, USA
Joseph Dvorak, Brookhaven National Laboratory, Upton, USA

Abstract

A spherical variable line spacing (SVLS) grating spectrometer has been designed and commissioned for use at the chemRIXS endstation at the Linac Coherent Light Source (LCLS), SLAC National Accelerator Laboratory. We present the design evolution, capabilities, and performance of the SVLS, which was developed to facilitate Resonant Inelastic X-ray Scattering (RIXS) experiments across a broad range of photon energies (250–1200 eV) on the LCLS-II beam. The SVLS spectrometer leverages a spherical grating to achieve simultaneous imaging and spectral dispersion with high energy resolution, while maintaining a compact form factor. A key design feature is its modular architecture consisting of three components: a grating chamber containing the optic and its conditioning units, slits, and a foil; a rotation arm housing the detector; and a vertical stage that drives the detector to its intended diffraction angles. The 36-megapixel scientific complementary metal oxide semiconductor (sCMOS) camera is inclined at a 20° grazing angle to maximize spatial resolution, resulting in a resolving power exceeding 2000 across the relevant photon energy range and offering more than 40× higher throughput compared to existing spectrometers at SLAC.

INTRODUCTION

The Linac Coherent Light Source (LCLS) is a Free Electron Laser (FEL) located on the campus of the SLAC National Accelerator Lab, Menlo Park, CA. LCLS operates in the soft and tender X-ray regimes, 0.25 keV to 5 keV, with the ability to scale into the hard X-ray regime up to 18 keV. In 2023, the LCLS-II beam was turned on, enabling X-ray pulse repetition rates of up to 1 MHz [1]. One of nine operational instruments at LCLS, chemRIXS is optimized for femtosecond resolution pump-probe experiments in the soft X-ray range, from 250 to 1600 eV. Samples are investigated through Resonant Inelastic X-ray Scattering (RIXS) via in-vacuum liquid jet delivery.

To take full advantage of the LCLS-II beam, a new, high-efficiency spectrometer was conceived, designed, and built.

DESIGN CONSTRAINTS AND CONCEPT

The chemRIXS spherical variable line spacing (SVLS) spectrometer was developed to meet several requirements prescribed to achieve significant improvements over the existing VLS spectrometer available to the chemRIXS instrument. At a minimum, the spectrometer must cover an energy range from 250 to 1200 eV, with a resolving power ($\frac{E}{\Delta E}$) of more than 2000 at 930 eV, given a source size of 20 µm FWHM in the dispersion direction. Additionally, the device must be compatible with the existing liquid jet endstation, where optics cannot be installed close to the sample, inside the sample chamber, due to the "dirty" nature of liquid jet delivery. Furthermore, the overall length of the spectrometer, from source to detector, should be minimized to enhance spatial resolution at the detector and promote simplicity of design.

Within these constraints, the primary goal of the new spectrometer was to optimize throughput. Figure 1 shows the basic layout of the SVLS spectrometer. Where a common Hettrick-Underwood (HU) type spectrometer first uses a mirror to focus the beam, and then a planar grating for dispersion [2], the SVLS spectrometer combines both functions into a single optic. Such a layout simplifies the spectrometer design and reduces the required total device length [3].

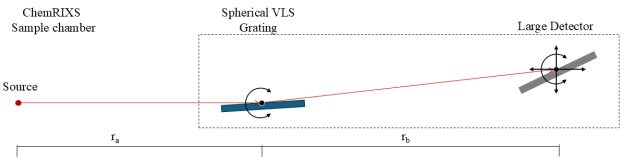

Figure 1: Spectrometer layout concept.

Notably, the SVLS grating is positioned at a minimized distance of $r_a = 600$ mm to the sample, and the detector is inclined at an angle of 20° relative to the incident beam, at $r_b \approx 926$ mm. This incline maximizes the spatial resolution at the detector to less than 10 µm FWHM. To capture the varying diffraction angles, the detector requires both angular positioning and translation in the beam direction.

DESIGN ARCHITECTURE

The SVLS spectrometer is divided into three main components: a grating chamber containing the optic and its conditioning units, a rotation arm housing the detector and a translation stage, and a vertical stage that drives the detector to its intended angular positions. Figure 2 shows the complete spectrometer with the grating chamber on a temporary stand used before installation at the chemRIXS endstation. This architecture provides reliable, quick adjustment of the detector during operation.

Vertical-Rotation Stage

Rotation of the detector relative to the grating is required to maintain focus on the detector at various photon energies and diffraction orders. A vertical motion range of ±50 mm is sufficient to reach the first-order diffraction angle in the 250 - 600 eV range and second and third-order diffraction angles

* jtorras@slac.stanford.edu

ISBN: 978-3-95450-263-9 ISSN: 2673-5520 doi: 10.18429/JACoW-MEDSI2025-WEOB01

COPPER ALLOY ADDITIVE MANUFACTURING FOR SOLEIL II

K. Tavakoli†,[1], Z. Fan[1], A. Mary[1], S. Sharma[2], M. Johanson[2], N. Bechu[1], M. Ribbens[1], F. DePaola[2], V. Leroux[1]
[1]Synchrotron SOLEIL, Saint-Aubin, France
[2]Brookhaven National Laboratory, Upton, NY, USA

Abstract

The Synchrotron SOLEIL is a large-scale research facility in France that provides synchrotron radiation from terahertz to hard X-rays for various scientific applications. To meet the evolving needs of the scientific community and to remain competitive with other European facilities, SOLEIL has planned an upgrade project called SOLEIL II. The project aims to reconstruct the storage ring as a Diffraction Limited Storage Ring (DLSR) with a record low emittance which will enable nanometric resolution.

The mechanical design of this project involves several challenges such as the integration of new magnets, vacuum chambers, insertion devices and beamlines in the existing infrastructure and is mainly based on extensive simulations, prototyping and testing new fabrication methods such as additive manufacturing (AM) to ensure the feasibility, reliability, and performance of several key elements.

This paper presents an overview of the mechanical design R&D and thermomechanical performance verifications on copper alloy parts fabricated in additive manufacturing in the scope of SOLEIL-II project.

INTRODUCTION

Additive manufacturing (AM) is increasingly being considered in the accelerator field to fabricate complex, thermally loaded components such as vacuum absorbers, beam stops, and photon masks. Among the materials under investigation, copper alloys like CuCrZr offer a promising combination of high thermal conductivity and mechanical properties, which are essential for devices exposed to intense synchrotron radiation.

However, components fabricated via AM must be rigorously validated before integration into operational machines, particularly regarding thermal fatigue resistance. In the framework of the SOLEIL II upgrade, a test campaign was launched in collaboration with NSLS-II to study the thermal fatigue lifetime of CuCrZr components manufactured using Direct Metal Laser Sintering (DMLS) method.

SOLEIL II PROJECT

SOLEIL is the French third generation light source operated for users since 2008 with an electron beam emittance of 4 nm·rad at an energy of 2.75 GeV in high intensity (500 mA, multibunch) [1].

The current lattice of the SOLEIL storage ring is composed of 16 modified two-bend achromat cells, 8 of which have short straight sections between the dipoles, altogether giving a total of 24 straight sections. After years of successful operation, a series of feasibility studies were initiated for an upgrade of the storage ring with a significantly lower emittance.

The SOLEIL Upgrade project, known as SOLEIL-II aims to design and build a 2.75 GeV diffraction-limited synchrotron light source preserving the existing infrastructure, 29 beamlines (far-IR to hard X-rays) and the 500 mA uniform filling pattern. The lattice of the new storage ring presented in CDR report [1] is built over a non-standard combination of twelve 7BA cells and eight 4BA cells [2, 3]. Figure 1 shows the arrangement of the magnets in the 7BA cell and the 4BA cell of SOLEIL-II lattice.

The length of the 7BA cell is rather short (~16 m) containing 52 magnets, depending on the lattice version, and including 7 dipoles. This very high density of multipoles increases the problem of compactness and creates implementation difficulties [4].

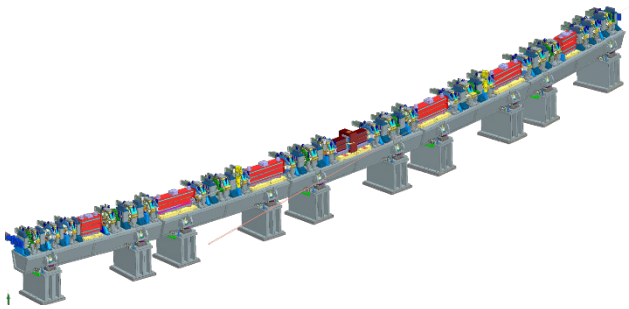

Figure 1: Engineering layout of the 7BA cell type of the new MBA-ARC.

CONTEXT AND MOTIVATION

One of the project's technical challenges is the miniaturization of vacuum chambers (Ø12 mm). Many absorbers and beamline components are expected to undergo high thermal cycling due to their proximity to synchrotron radiation sources like achromat dipoles and insertion devices.

Additive manufacturing (AM) is gaining attention in the accelerator domain for producing complex, thermally stressed components. Among the materials being studied, copper alloys like CuCrZr stand out due to their excellent thermal conductivity and strong mechanical properties, both of which are critical for components operating under intense synchrotron radiation. Additive manufacturing provides the possibility to design and fabricate optimized geometries that would be impossible to achieve using conventional machining [5].

However, the lack of experimental data on thermal fatigue resistance of AM CuCrZr, especially under realistic operating conditions, calls for a dedicated R&D effort. In

† Keihan.tavakoli@synchrotron-soleil.fr

ISBN: 978-3-95450-263-9 ISSN: 2673-5520 doi: 10.18429/JACoW-MEDSI2025-WEOB02

RAPID DEVELOPMENT AND IMPLEMENTATION OF A CUSTOM PHOTON STOP AT THE ADVANCED LIGHT SOURCE: FROM FAILURE ANALYSIS TO PREDICTIVE MAINTENANCE

W. Hutcheson, N. Wenner, G. Cutler, L. Kistulentz, S. Morton, T. Swain
Lawrence Berkeley National Laboratory, Berkeley, USA

Abstract

In June of 2023, the Advanced Light Source (ALS) at Lawrence Berkeley National Laboratory (LBNL) in Berkeley, California, USA, experienced a vacuum interlock event that triggered a beam dump. Upon investigation, technicians discovered a leak in the cooling system of a custom photon stop (PS) in Sector 5 of 12. This paper will detail the event, the temporary restoration of operations, and how a new PS was designed, analyzed, fabricated, assembled, tested, qualified, installed, and commissioned in a 14-week window. The original PS had been in service for over 20 years when failure occurred. During this period, the manufacturing landscape changed significantly, with many specialized capabilities—particularly brazing techniques—becoming unavailable both locally and regionally. Schedule and fabrications constraints strongly drove the design of the replacement PS. Failure analysis of the original PS indicated that corrosion and blocking of coolant channels had led to thermal cycling-induced fatigue cracking in the top surface. A tool for predicting fatigue life of the new PS was developed to estimate remaining cycles to failure, providing operations staff a basis for predictive maintenance and advance warning to prevent unexpected failures in the future.

INTRODUCTION

The photon stop protects three beamlines at the ALS: 5.0.1, 5.0.2, and 5.0.3. These beamlines are used for macromolecular crystallography by the Berkeley Center for Structural Biology. They are fed by a wiggler with a minimum energy of 5,000 eV and a maximum energy of 16,000 eV in operation [1].

Failure of Original Photon Stop

The original PS had been installed and had operated successfully since ~1996. In June of 2023, a failure occurred in the top surface of the PS, close to the area of highest heat flux from the beam. A small crack had formed in the 0.065″ thick faceplate, leading to the leaking of water coolant into the vacuum chamber, which tripped a vacuum interlock and triggered a beam dump, see Fig. 1.

Temporary Restoration of Operations

Upon detection of failure, the PS was immediately removed and temporarily repaired by TIG welding of the Glidcop AL-15 faceplate. This repair allowed the ALS storage ring to remain in operation but required that the gap in the BL5.0 wiggler remain fully open, limiting beam power and preventing the use of all three 5.0 beamlines. A complete repair was planned to coincide with an upcoming ALS summer shutdown.

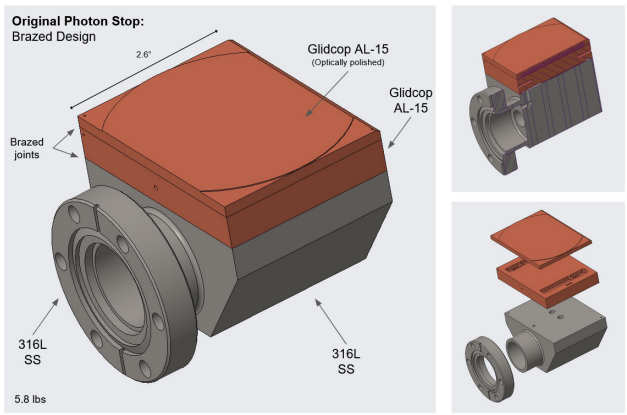

Figure 1: Design of original photon stop. Water coolant follows an anastomosing path through parallel courses of 0.5 mm wide channels below the top face.

DEVELOPMENT OF NEW PHOTON STOP

A replacement PS was developed to replace the temporarily repaired unit such that the beamline could be run at full power. The requirements were to block all radiation from the beamline and absorb and dissipate related power (~11.3 kW) while maintaining safe temperatures and stresses during operation. The original PS served as an IR mirror for a since-decommissioned beamline, and this was no longer a requirement, obviating related requirements for dimensional stability and optical surface quality. The minimum intended lifetime of the PS was ~3 years, leading up to an intended replacement of the entire ALS storage ring.

Schedule and Fabrication Constraints

Aggressive schedule constraints generated additional fabrication constraints, and these strongly drove the design of the new PS. While the original PS had a brazed design, it was determined early on that the timeline did not allow for the long lead-times brazing would require, particularly as on-site and regional machine shops no longer supported the kinds of complex brazing that were required. A wide range of alternative designs were investigated. For example, designs with incidence angles of 15° were investigated. These had the advantage of decreased maximum heat fluxes (15.9 W/mm^2 compared to 30.6 W/mm^2), but fitment concerns and concerns related to excessive pressure drop in the significantly longer coolant channels precluded their further development. Ultimately, a design similar to that of the original PS was chosen, the

ISBN: 978-3-95450-263-9 ISSN: 2673-5520 doi: 10.18429/JACoW-MEDSI2025-WEOB03

CRYOGENIC RADIOMETRY: A NEW ABSORBER FOR X-RAYS UP TO 150 KeV

O. Marinos†,1,2, J.M. Vogt[1]
[1]Canadian Light Source, Saskatoon, Canada
[2]University of Saskatchewan, Saskatoon, Canada

Abstract

The accurate measurement of radiant power is essential for the calibration of X-ray detectors, such as silicon photodiodes. Cryogenic electrical substitution radiometers (ESRs) perform high accuracy and absolute measurements of radiant power. Material and geometry of the absorber in an ESR are chosen to maximize the absorption in the energy range of interest, while providing a high thermal response and a short time constant. The highest energy design previously reported allowed the measurement of X-rays up to 60 keV. In this work we present a new absorber developed at the Canadian Light Source for energies from 25 keV to 150 keV. Monte Carlo simulations led to a design with an absorption > 99% in the entire energy range considering all losses due to fluorescence and scattering. Measurements have been successfully performed at the Biomedical Imaging and Therapy (BMIT) beamline (05ID-2), which has a 3.7 T wiggler source and provides X-ray energies up to 140 keV.

INTRODUCTION

Cryogenic temperatures (typically around 4 K) provide the chance to measure low power beams by the physical principle of reducing the heat capacity of materials to very low values so a low power monochromatic incident beam absorbed by this material can provide a noticeable temperature variation that would be otherwise negligible at ambient temperatures. At this temperature, heat capacity and thermal noise of materials such as copper and gold dramatically reduce, enabling sensitivity and stability not possible to achieve at room temperature [1-3]. In this way, for achieving the highest-accuracy measurements of radiant power across the X-ray spectrum, the cryogenic absorber should be made to provide the highest possible absorption of the incident radiation power, so we can equate this incident X-ray radiant power (with precisely controlled electrical heating), directly to SI electrical units with minimal uncertainties. These features can be obtained by a combination of the appropriate material and geometrical design. In this way, ESRs function as absolute thermal detectors.

For high energies some material become transparent, e.g., copper at >30 keV, which makes them inefficient and inaccurate. In literature [1-3] can be found that, to overcome these limitations, researchers at PTB (Physikalisch-Technische Bundesanstalt) have designed a gold absorber with a thin copper shell for applications up to 60 keV. In this case Monte Carlo simulations were performed using Geant4 claiming a near-unity absorption with uncertainties well below 0.2%. Experimental measurements were performed at BESSY II using cavity absorbers of 500–550 µm gold base and ~80–90 µm copper shell. Authors claim standard uncertainties of less than 0.2–0.3% for 50 eV–60 keV photons

This work intends to push the limits forward by presenting a new absorber design able to be used up to 150 keV. For our design the same Monte Carlo approach is considered, but instead of Geant4, the FLUKA code is used. Simulation results show absorption levels > 99%.

DESIGN

The core concept involves the direct measurement of beam power, which can be used later to calculate the photon flux through the relationship:

$$P_{beam} = N * F * E. \quad (1)$$

Here P_{beam} is the beam power in J/s, N is the number of photons/s, F is the conversion factor $1.6*10^{-19}$ J/eV and E is the photon energy in eV.

Considering we are working with power levels in the range of microwatts (µW), reducing the heat capacity of the material is important so we can achieve noticeable temperature variations that can be accurately measured and controlled. As well, the highest absorption of the beam is required, as well as thermal isolation. For cryogenic conditions gold becomes a very good option. Its specific heat capacity drops from 0.129 J/g·K at room temperature to 0.00016 J/g·K at 4 K [4]. This is a reduction of 99.9%.

In a similar way, Gold also has good X-ray properties, particularly due to its high atomic number and known K- and L-edge behaviour which provides high absorption levels for a wide range of photon energies. In order to maximize X-ray absorption, the final geometric shape of the absorber was determined through iterative simulations and modelling. A conical geometry was adopted for the absorber, which provided the largest absorption of the beam considering all the possible interactions for the range analyzed, i.e., photoelectric absorption, Compton scattering, etc. As presented in Table 1, Monte Carlo simulations using the FLUKA code confirmed the absorber's efficiency across various energies. The design performs absorption levels > 99% for energies up to 150 keV, which means minimal loss with highest accuracy. Figure 1 shows some settings of the simulation.

The absorber is expected to remain at the same temperature when the beam is on and off. To achieve this condition an electrical resistor is attached to the absorber to compensate for the beam power when the beam is off, so the

† Omar.Marinos@lightsource.ca

ISBN: 978-3-95450-263-9 ISSN: 2673-5520 doi: 10.18429/JACoW-MEDSI2025-WEOB04

CBXFEL DESIGN, PRODUCTION, ASSEMBLY, TESTING AND INSTALLATION STATUS

X. Permanyer[†,1], M. D. Balcazar[1], G. Lanza[1], A. Halavanau[1], Z. Huang[1], P. Liu[1], A. Montironi[1], H. Wang[1], D. Zhu[1], J. Anton, A. Bernhard[2], M. Golebiowski[2], S. Mashrafi[2], D. Shu[2], Y. Shvyd'ko[2], M. White[2]
[1]SLAC National Accelerator Laboratory, Menlo Park, CA, USA
[2]Argonne National Laboratory, Lemont, IL, USA

Abstract

Use of a cavity-based X-ray free electron laser (CBXFEL) is potentially a way to dramatically improve the stability and coherence of existing XFELs. CBXFEL consists of a low-emittance electron source, a magnet system with several undulators and chicanes, and an X-Ray cavity. The X-Ray cavity stores and circulates X-ray pulses for repeated FEL interactions with electron pulses until the FEL reaches saturation. The CBXFEL is expected to operate using 9.831 keV photons from LCLS, using synthetic diamonds as cavity Bragg mirrors. The LCLS copper linac will deliver two electron bunches 624 RF buckets apart, resulting in a total X-ray cavity length of 65500.87 mm. The final X-ray cavity design, assembly, and installation status will be presented in this paper.

INTRODUCTION

The mechanical system for the rectangular x-ray cavity at LCLS-II consists of four diamond crystals. The first two of these crystals (C4 and C1) reflect the X-ray pulse into (C4) and out (C1) of the undulator line when operating the FEL with the x-ray cavity in CBXFEL mode. These optics need to be inserted on the undulator axis and are accompanied by additional x-ray and electron beam diagnostics (X42, X42, X11, X10, BODs) [1-3].

Crystals C2 and C3 reflect the X-ray pulse in and out of the return line.

The mechanical system also includes five diagnostic stations (Stations C, D, E, F and G) and a vacuum pipe system as the cavity X-ray return path. The X-ray diagnostic stations C, D and E are located in the return path and its extension line. Station F is located in the electron beam downstream of crystal C4 of Station B. Station G is located in the LCLS-II experimental station [4].

To keep the optics from intercepting the electron beam in CBXFEL mode, the diamonds and diagnostics are located within 4-dipole electron bunch-delay chicanes that enclose the 7 undulator sections. The electron bunch chicanes divert the electron beam around the inserted optics and must create a beam orbit and deflection in order to maintain the undulator Beam Containment System requirements. The chicane will displace the electron beam by at least 3.914 mm from the undulator axis at the longitudinal location of the diamond insertion [3].

Figure 1 shows a schematic of the CBXFEL cavity with stations A, B, C, D, E and F. Table 1 shows the location of the stations in the SLAC LTU Coordinate system [5].

The return line, shown in Fig. 2, must comply with SLAC's vacuum requirement for LCLS level 2 vacuum. Partial pressure from the sum of all peaks >44 AMU has to be $<1\text{x}10^{-11}$ Torr. Maximum single-peak partial pressure for >44 AMU has to be $<5\text{x}10^{-12}$ Torr. The return line comprises 12 ion pumps 75 l/s, 4 pairs of Pirani and Cold Cathode gauges. A new cable tray has been installed in the tunnel to provide signal and power cables to CBXFEL.

Table 1: CBXFEL Coordinates of the Main Components

Station	Z Location [m]	X Location [m]
C1-C2 axis	548.116240	N/A
C3-C4 axis	516.015803	N/A
C1-C4 axis	N/A	-1.25
C2-C3 axis	N/A	-1.90
Station C	546.298572	-1.90
Station D	530.138572	-1.90
Station E	515.249803	-1.90
Station F	517.87823	-1.25

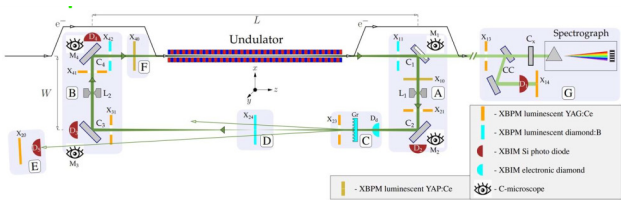

Figure 1: Layout of the x-ray diagnostic design.

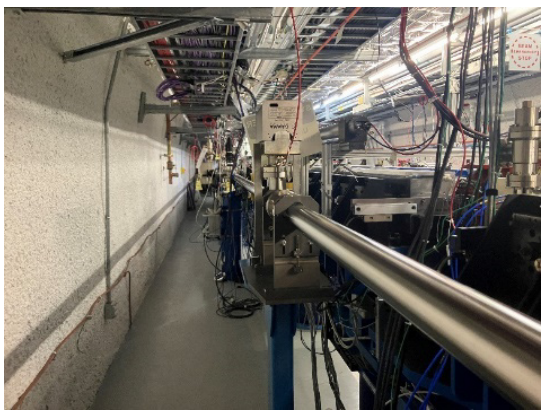

Figure 2:View of the return, with the new cable tray installed on top of CBXFEL.

† xavip@slac.stanford.edu

ISBN: 978-3-95450-263-9 ISSN: 2673-5520 doi: 10.18429/JACoW-MEDSI2025-WEOC01

DEVELOPMENT OF MAGNET PROTOTYPE FOR SIAM PHOTON SOURCE II

S. Prawanta, P. Sunwong, T. Leetha, P. Numanoy, P. Pruekthaisong, M. Sroison
N. Thiabsi, P. Chaithaweep, P. Klysubun
Synchrotron Light Research Institute, Nakhon Ratchasima, Thailand

Abstract

The Siam Photon Source II (SPS-II) is Thailand's next-generation 3 GeV synchrotron light source, designed to deliver high-brightness radiation for scientific and industrial use. Its storage ring, comprising 14 Double Triple Bend Achromat (DTBA) cells and targeting a natural beam emittance below 1 nm·rad, requires numerous high-precision magnets with strict mechanical and magnetic specifications. This work presents the development of magnet prototypes, covering the full design process including magnet type and material selection, yoke and pole geometry optimization, and magnetic field simulation with OPERA 3D considering saturation and permeability. Mechanical design involved core and coil material selection as well as structural, thermal, and vibrational analyses using AutoCAD, SolidWorks, and ANSYS to ensure mechanical integrity. Prototypes were fabricated using high-precision machining and vacuum pressure impregnation (VPI) for coil insulation, then tested for dimensional accuracy and magnetic field performance. This marks Thailand's first domestically developed magnet prototype, realized through collaboration with local industry, laying a solid foundation for the SPS-II project.

INTRODUCTION

The Siam Photon Source II is a fourth-generation synchrotron light source currently under development in Thailand [1]. The facility consists of a 150 MeV linear accelerator, a 3 GeV booster synchrotron, and a 3 GeV storage ring with a circumference of 327.6 m, as presented in Fig. 1. The storage ring comprises 14 Double Triple Bend Achromat (DTBA) cells and is designed to achieve a natural beam emittance below 1 nm·rad, providing high brightness at an RF frequency of 496.654 MHz with a beam current of 300 mA. The stability of the electron beam and the quality of the synchrotron light depend on the overall performance of the storage ring. The magnets, which control the trajectory and focusing of the electron beam, must possess accurate magnetic field characteristics and be installed and aligned with high precision.

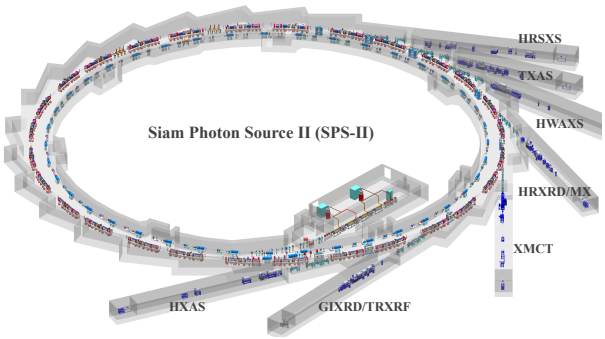

Figure 1: Overview of the SPS-II accelerator complex.

The development of a magnet prototype for the storage ring was carried out to produce a magnet with the required mechanical properties and precise magnetic field characteristics in accordance with its functional specifications. Key processes included magnetic design, mechanical design, electrical design, and prototype fabrication, serving as preliminary steps before entering full-scale production.

MAGNET DESIGN & ENGINEERING

The DTBA cell of the storage ring consists of various types of magnets, including dipole, quadrupole, dipole-quadrupole, sextupole, octupole, steering, and fast corrector magnets, as shown in Fig. 2 [2 - 4]. It can be seen that the magnets are mounted on three upstream girders and another three downstream girders.

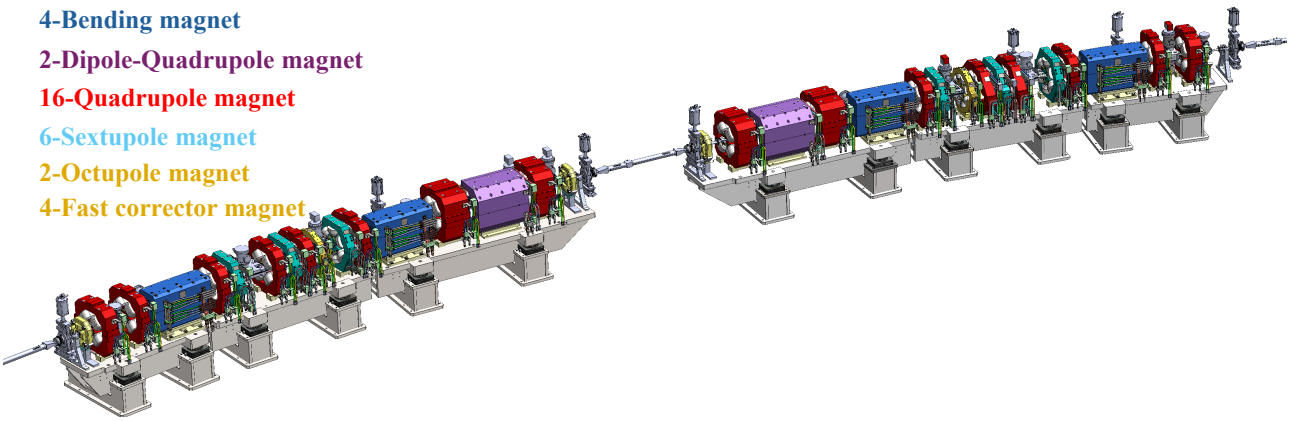

Figure 2: Double-Triple Bend Achromat (DTBA) cell of the storage ring.

ISBN: 978-3-95450-263-9 ISSN: 2673-5520 doi: 10.18429/JACoW-MEDSI2025-WEOC03

COMPLEX BEND VACUUM CHAMBER FOR NSLS-II UPGRADE

M. Seegitz[1], R. Todd[1], A. Khan[1], D. Hidas[1], M. Ferreira[2],
P. Palecek[1], S. Sharma[1], T. Shaftan[1], V. Smaluk[1]
[1]Brookhaven National Laboratory, Upton, NY, USA
[2]ESS, Lund, Sweden

Abstract

While the NSLS-II synchrotron is a third-generation light source offering outstanding brightness and flux, a robust R&D program is underway to upgrade the facility to a fourth-generation, or beyond, capability. Inherent in the so-called complex-bend magnet and lattice designs are significant limitations on the beam channel and exit slot apertures of the vacuum chamber. These restrictions, along with the need for the vacuum chamber to be mechanically aligned and decoupled from the magnets, present unique challenges. For our chamber, the selected solution is not novel: it utilizes an aluminum split clamshell design, a proven approach used in many machines, past and present. The adaptation of this design, combined with precision machining and welding, is expected to provide the most cost-effective solution. Geometric and resistive-wall impedance considerations, along with structural and thermal modeling, will be presented, as well as dynamic pressure simulations generated using SynRad+ and MolFlow+ modeling codes. With ongoing changes in lattice and magnet parameters, a systematic, iterative approach to vacuum design has been implemented and will also be discussed.

INTRODUCTION

NSLS-II is based on the well-established double-bend achromat lattice (Fig. 1). Commissioned with first light in 2014, it was the last synchrotron constructed using this lattice type. Since then, new and upgraded synchrotrons have adopted various forms of multi-bend achromats to reduce horizontal emittance.

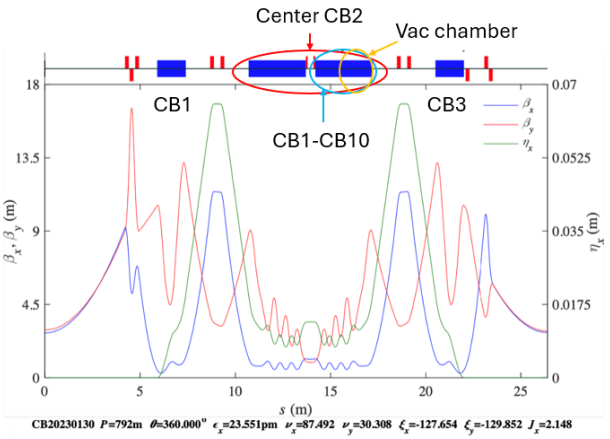

Figure 1: TCBA lattice showing central bending region CB2 of interest.

The goal of NSLS-II-U is to select a lattice with world-leading emittance and brightness. To achieve this, lattice designs based on the complex-bend principle are being investigated [1]. One promising candidate is the triple complex-bend achromat (TCBA), which incorporates three bending regions per cell [2]. The central bending region forms the basis of this prototype effort, as it imposes the most stringent constraints on magnet and vacuum chamber design due to its reduced aperture requirements.

MECHANICAL DESIGN

The vacuum chamber design was required to meet several key criteria: it needed to accommodate two different PMQ geometries (focusing and defocusing), maintain adequate clearance between the chamber and magnets along its entire length, and achieve an average base pressure below 1×10^{-9} Torr. Additionally, it was necessary to provide a smooth, continuous internal beam aperture of Ø11 mm, incorporate an exit slot for beam extraction, and structurally withstand the forces associated with vacuum conditions (Fig. 2).

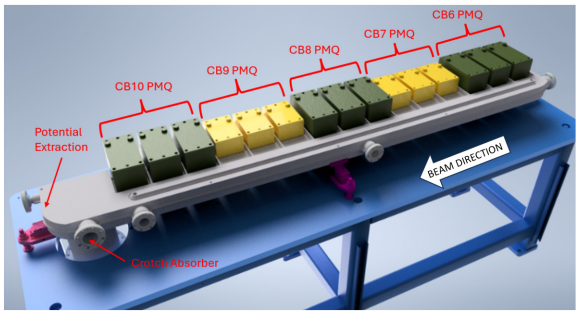

Figure 2: Arrangement of complex-bend PMQs with vacuum chamber (defocusing magnets shown in green, focusing magnets in yellow).

Based on the vertical emittance angle (Fig. 3), a vertical exit slot height of 3.5 mm was determined to be sufficient for extracting the bending magnet fan over a length of approximately 2 meters.

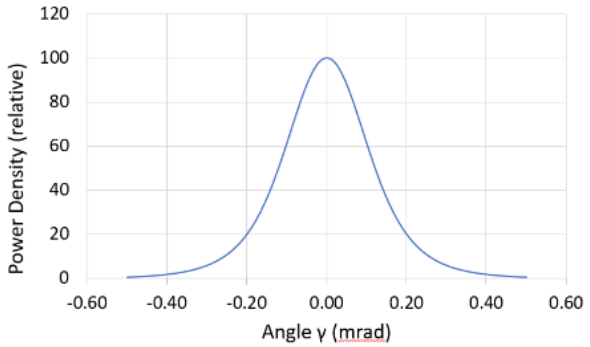

Figure 3: Approximate vertical dipole power density vs Angle.

ISBN: 978-3-95450-263-9 ISSN: 2673-5520 doi: 10.18429/JACoW-MEDSI2025-WEOC04

EXPERIENCE WITH A BUNCH LENGTHENING CAVITY AT THE APS*

J. Fuerst†, T. Berenc, M. Kelly, S. MacDonald, U. Wienands
Argonne National Laboratory, Lemont, USA

Abstract

The Advanced Photon Source Upgrade (APS-U) at Argonne National Laboratory (ANL) provides hard x-ray photon beams at 6 GeV with a brightness 500 times greater than the original machine. A bunch lengthening cavity is used to decrease the effects of Touschek scattering (on beam lifetime) and intrabeam scattering (on beam emittance). The superconducting RF (SRF) cavity operates at 2 K in a passive, i.e. beam-driven mode at the 4th harmonic (1408 MHz) of the main RF system. A helium cryoplant provides 2 K refrigeration for the SRF cavity.

CAVITY AND CRYOMODULE DESIGN

In 2014 a concept was developed for a superconducting higher harmonic cavity (HHC) for the APS-U storage ring. The design, assembly, and testing of the device were conducted in the ANL Physics Division [1]. Scope includes:

- A single 1.4 GHz elliptical-cell SRF cavity.
- A low-level RF (LLRF) system to provide RF diagnostics and control cavity amplitude via a slow tuner.
- A cryomodule to support the SRF cavity and associated RF, cryogenic, and beam vacuum subsystems.
- A liquid helium refrigerator providing up to 50 W of cooling power at 2.1 K.
- Height and width consistent with tunnel dimensions.
- Overall cryomodule length not to exceed half of an APS-U 5-meter straight section.

Cavity and Cryomodule

Figure 1 shows the completed SRF cavity/liquid helium (LHe) tank assembly. Symmetrically placed variable couplers (ports shown on the right side) have not proven necessary in operation. The bellows on the left provides a flexible element in the LHe tank for cavity tuning.

Figure 1: LHe tank containing SRF cavity.

* Work supported by the U.S. Department of Energy, Office of Science, under Contract No. DE-AC02-06CH11357
† fuerst@anl.gov

Figure 2: Cryomodule lid with suspended cold mass.

The cold mass assembly is suspended from the lid of the module (see Fig. 2). The angled end-walls of the lower vessel (see Fig. 3 below) allow the lid assembly, including vacuum gate valves at each end, to be lowered into the vessel. The valve actuators emerge through the openings in the ends and seal against the inside walls of the openings.

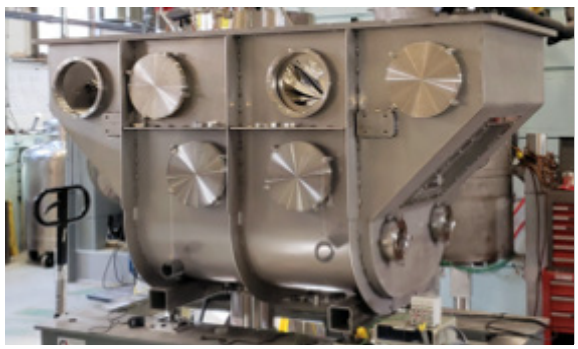

Figure 3: Cryomodule lower vacuum vessel.

RF Systems

Figure 4 provides an overview of the main RF systems and the HHC. The electron beam induces voltage in the HHC to lengthen the beam bunches while the main 352 MHz systems replenish beam energy which is lost to synchrotron radiation. The HHC field (see detuning curve, Fig. 5) depends on beam current, external Q, and amount of detuning. Cavity parameters are listed in Table 1.

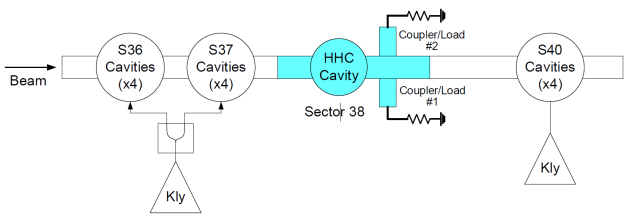

Figure 4: Main and harmonic RF systems.

ISBN: 978-3-95450-263-9 ISSN: 2673-5520 doi: 10.18429/JACoW-MEDSI2025-WEOC05

RESULTS FROM THE ALS-U STORAGE RING ALIGNMENT SYSTEM PROTOTYPE*

R. Miller†, R. Johnson, H. Zhu, C. Hernikl, K. Ray, S. Nguyen, F. Matichard, E. Lizotte
Lawrence Berkeley National Laboratory, Berkeley, CA, USA

Abstract

ALS-U stability and alignment requirements coupled with tight space constraints present in the existing ALS prompted a new design for the storage ring support and alignment system. A prototype has been built and tested with alignment accuracy results in the 30 micron range and stability results in the 35 nm range. The new design overcomes distinct ergonomic challenges and reliability failures of earlier hardware iterations. The prototype has also been tested to an alignment time requirement needed to minimize dark time--the phase of the program where storage ring alignment occurs. This paper presents the innovative solutions implemented for the alignment system prototype to address the unique problems of ALS-U.

ALIGNMENT SYSTEM DESIGN

Background and Architecture

We previously tested the baseline design of the alignment system along with vibration stability, thermal performance and other subsystem prototype tests [1]. However, the baseline design experienced mechanical failures of roller bearings on two separate occasions so we built and tested a new alignment system. In the new design, the raft is supported on three sets of spherical bearings on Airloc load levelers in a symmetric configuration during alignment. The load levelers are mounted on a plinth which is bolted to an embedded plate in the ALS concrete floor. These load levelers are topped with custom 954-bronze (conforming to ASTM B505) bushings coated in Molykote G-0010 (a mineral-oil-based grease thickened by a di-urea system) to provide a low friction surface resistant to stick-slip behavior.

Once the raft is aligned, an M20 stud that penetrates through the center of each load leveler is torqued to 134 Nm for a preload of approximately 48 kN. For enhanced vibration stability, two additional load levelers are implemented with non-lubricated 954-bronze bushings. These have the additional benefit of providing a higher friction joint to lock the rafts in place for long-term positional stability. An overview of the alignment system design is shown in Figure 1 and the entire SR raft assembly prototype is shown in Figure 2. Figure 3 is a top view of the plinth showing details the bushing configuration.

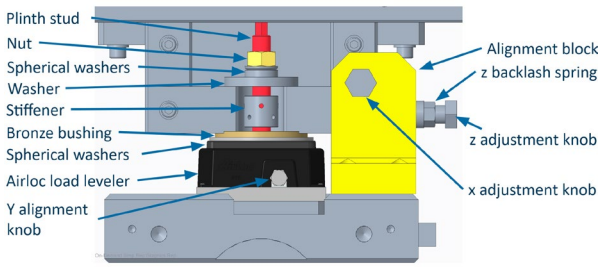

Figure 1: Alignment system CAD model.

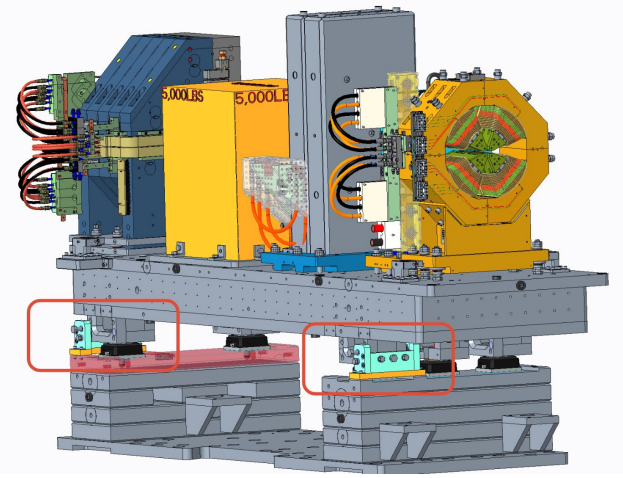

Figure 2: SR raft assembly prototype CAD model.

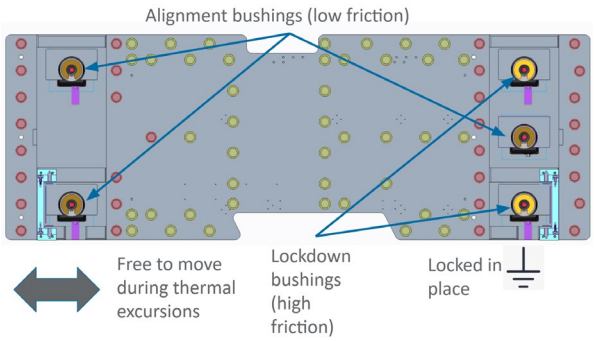

Figure 3: Bushing configuration.

Adjustment Mechanisms

Adjustments are made in 6 degrees of freedom (6-DOF) using 4 alignment screws in the x-direction, 2 alignment screws in the z-direction and 3 adjustable load levelers in the y-direction. Extra-fine M20 screws with a 1.5 mm pitch are used to adjust in the x- and z-directions, leading to 42 µm translation per 10 degree turn of the screw. The load leveler uses a sliding-wedge system to raise or tilt the raft with a 10 degree rotation of its adjustment screw, leading

* Work supported by the Director, Office of Science, Office of Basic Energy Sciences, of the U.S. Department of Energy under Contract No. DE-AC02-05CH11231
† RyanMiller@lbl.gov

ISBN: 978-3-95450-263-9 ISSN: 2673-5520 doi: 10.18429/JACoW-MEDSI2025-WEP01

A CONCEPT IMPROVEMENT DESIGN OF THE GIRDER ADJUSTMENT SYSTEM FOR TPS STORAGE RING

T. C. Tseng†, W. Y. Lai, H. S. Wang, K. H. Hsu, C. S. Huang, D. G. Huang, C.-J. Lin, C. K. Kuan
National Synchrotron Radiation Research Center, Hsinchu, Taiwan

Abstract

The girder adjustment system of TPS storage ring can fine adjust each girder in 6 axes with 6 kinematic mounting motorized cam movers. The installation of the TPS had demonstrated this design. However, this design is freely mounted with gravity and the 1st natural frequency is less than 30Hz even with supplement side locking system. Moreover, the motor controller restricts the beginning power output and sometimes the girder will fall down when the electromagnetic motor brake is released.

A concept improvement design is thus introduced to modify these situations. In this design, a worm gearbox addition can raise the reduction ratio to prevent the falling and inverse kinematic mounting movers with strong springs not only firmly lack the girder to raise the natural frequency but also preserve the motorized algorithm. This paper describes the design in detail.

INTRODUCTION

Taiwan Photon Source (TPS) was finished installation at 2014 and reach the design spec (500mA) at the end of 2015. The girder system for the TPS storage ring is of an auto-tuning design in order to align the girders precisely and quickly with less manpower. Each girder can be fine adjusted in 6 axes with 6 motorized cam movers of kinematic mounting design on 3 pedestals. With sensors between each girder, there are 72 girders to make up a whole ring auto-alignment girder system [1-5]. There had 3 auto-tunings been performed before commissioning. In the design spec, the1st natural frequency more than 30 Hz of the girder system was requested. But after installed with all the components, it can be measured to about 24~25 Hz and 26~28 Hz with the side locking systems.

After a few years operation, the tunnel was found some local settlement areas form yearly survey works as shown in the Fig. 1. So two locally girder system adjustments were performed in 2020 & 2021 to correct this situation [6]. However, the motor controller restricts the beginning power output and sometimes the girder will fall down to the hard stop when the electro-magnetic motor brake is released.

Recently, the study of TPS upgrade was initialized after the 3rd beamline construction is nearly finished. A concept improvement girder design is thus introduced to modify the weak situations found. If the formal study begins, a prototype may be setup with the existing backup girder system in the laboratory.

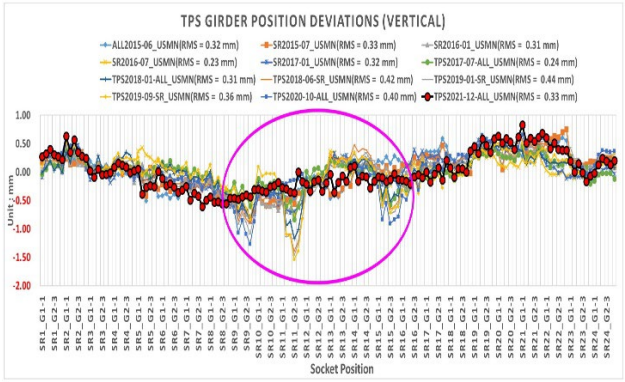

Figure 1: TPS girder position deviation from 2015~2021.

GIRDER SYSTEM DESIGN

The single girder system of the TPS storage ring is shown as in the Fig. 2. This design is freely mounted with gravity and the 1st natural frequency is less than 30 Hz even with supplement electrical side locking system. An improvement design is introduced as in the Fig. 3.

In this design, the cam movers and transfer unit housings will be installed upside down. There are mold springs inside the 3 pedestals. These mold springs not only support the total weight of girder system (16 tons) but also will be suppressed with the movers with another 12~16 tons when adjustment.

The girder system will be strongly and fully kinematically clamped with the cam movers and the mold springs. The hard stopper and locking system in the original design will be no longer need and the 1st natural frequency is expected to be raised at least √2 times to more than 36 Hz. A detailed components design and simulation will be performed when the formal study is assigned.

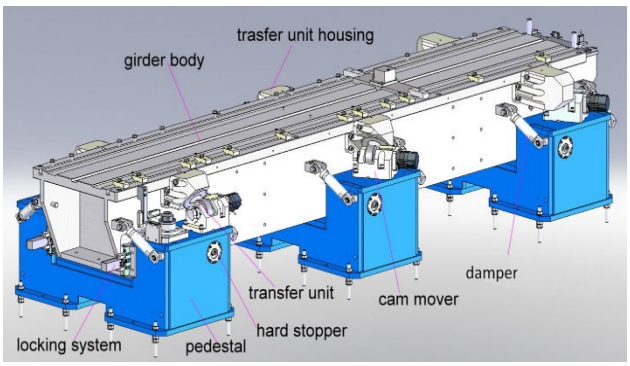

Figure 2: A single girder system of the TPS storage ring.

†tctseng@nsrrc.org.tw

ISBN: 978-3-95450-263-9 ISSN: 2673-5520 doi: 10.18429/JACoW-MEDSI2025-WEP02

AS-BUILT FRONT ENDS FOR THE ADVANCED PHOTON SOURCE MBA UPGRADE*

Y. Jaski[1], F. Westferro[1], S. Oprondek[1], M. Erdmann[2], T. Clute[1], M. Ramanathan[1]
[1]Argonne National Laboratory, Lemont, IL, USA
[2]Laurance Berkeley National Laboratory, Berkeley, CA, USA

Abstract

The Advanced Photon Source (APS) upgrade from double-bend achromats (DBA) to multi-bend achromats (MBA) lattice is completed. All storage ring components and front ends were installed between April 2023 to April 2024 and fully commissioned. Some major changes have been made on front ends since preliminary design that was published in MEDSI'18 proceedings. The changes are a) Incorporated a Burn-Through-Mask (BTM) as the first fixed mask for all Insertion Device (ID) front ends; b) Removed clearing magnet from all front ends; c) Replaced beryllium window with diamond window in High Heat Load Front End (HHLFE). This paper presents the as-built version of HHLFE and Canted Front End (CFE).

INTRODUCE BURN THROUGH MASK

The APSU front ends functional requirement documents require all ID front ends to have sufficiently large inlet aperture (called front end acceptance) to accept all missteered beam given off by storage ring regardless of the storage ring beam dynamics. This acceptance is specified as ±1.67 mrad horizontal and ±0.67 mrad vertical. The required acceptance is the same for all ID front ends independent of whether it is HHLFE or CFE. This specification is very different from the original APS front end acceptance which depends on the type of front ends (single beam vs canted beam) and derived from storage ring beam dynamics. The First Fixed Mask (FM1) in original APS single beam front ends has the inlet aperture of 38 mm (H) × 26 mm (V) which is not large enough for the new APSU HHLFE. The FM1 which is located at 16.7 m needs to have an aperture at least 56 mm (H) × 22 mm (V) plus the half beam size. There is no space in front end to add an additional mask upstream of FM1, so the burn through mask (BTM) concept was developed. Before we can explain how BTM works, we need to explain how the storage ring beam position is monitored. Storage ring vacuum chamber and absorber are only able to withstand the heat load from dipole beam and not from undulator beam. To protect storage ring components from undulator beam strikes, there are two RF beam position monitors at each end of the straight section serving as Beam Position Limit Detector (BPLD). Based on APS operational experience, the BPLD is set at ±1.5 mm for horizontal and ±1.0 mm for vertical. These numbers already contain a 0.5 mm error margin. When electron beam position is out of that limit, the stored beam will be dumped to protect storage ring components. For front end BTM, when beam is within the BPLD limit, beam will just pass through the BTM aperture to reach FM2. If the BPLD is off or malfunctioning, the beam can burn through the front face of the BTM. There are air vent slots behind the mask face that cover the entire beam striking region defined by the maximum beam missteering defined by the storage ring aperture. The breach of the air vent will trigger the Storage Ring Valve (SRV) to close and dump the storage ring beam. The schematic of how the BTM works is shown in Fig. 1. Since the beam passing through the BTM can be fully captured by FM2, the FM1 no longer performs a function and is removed.

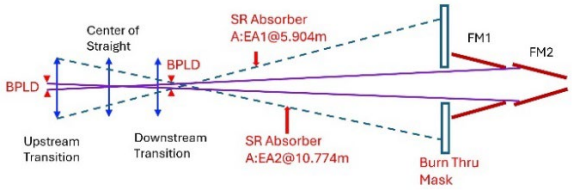

Figure 1: Schematic of missteering, BPLD and BTM.

HIGH HEAT LOAD FRONT END

The layout of the new HHLFE is shown in Fig. 2. The apertures of key components are shown in Table 1.

Table 1: HHLFE Aperture Table for APSU MBA

Components	Aperture H×V (mm)
Low Power Photon Shutter (LPPS)	130×40 shutter blade size
BTM	40.6×35.2 (inlet)/ 26×20.6 (out)
FM2	27.7×22 (inlet)/ 9×12 (outlet)
Lead Collimator	19.5×19.5 (optical)
	26×26 (shielding)
GRID-XBPM	15.3×50 (inlet)/ 1.6×50 (outlet)
FM3	16×48 (inlet)/ 3.6×6 (outlet)
Photon Shutter	10×48 (inlet)/ 5×48 (outlet)
	at open
Safety Shutter	72×20 (optical/shielding)
Wall Collimator	27×17 (optical)
	37×26 (shielding)
Exit Mask	12×48 (inlet)/ 2×1 (outlet)
Diamond window	5.5 dia. 0.2 mm thick
Exit Collimator	5×5 (optical/shielding)

* Work supported by the U.S. DOE Office of Science-Basic Energy Sciences, under Contract No. DE-AC02-06CH11357

ISBN: 978-3-95450-263-9 ISSN: 2673-5520 doi: 10.18429/JACoW-MEDSI2025-WEP04

COLLABORATIVE DESIGN WITH AN INTEGRATED CAD MODEL IN THE PETRA IV PROJECT

M. Diercks, B. List, C. Kula, P.-O. Petersen, M. Hüning, L. Hagge
Deutsches Elektronen-Synchrotron (DESY), Hamburg, Germany

Abstract

The PETRA IV project involves the refurbishment of the 2.3 km PETRA accelerator to accommodate almost 40 beamlines. It also includes the conversion and construction of numerous buildings, including a large experimental hall, with first light planned for 2032.

To support planning and design with a model-based approach, a comprehensive, integrated CAD model has been set up. The model comprises civil infrastructure, the accelerator, beamlines, and infrastructure systems. Serving as a single source of truth, it supports a diverse project team, including civil and mechanical engineers, beamline scientists, and other stakeholders, each with different technical backgrounds and needs.

The fully integrated CAD model is tied to systems engineering processes like requirements management, and supports collaboration across disciplines. Multiple levels of abstraction, a structured hierarchy, and explicit modelling of interfaces help bridge communication gaps. They also reduce redundant work and minimise design errors, all critical for efficient design in collaboration.

INTRODUCTION

A CAD model can serve more than as a design tool in accelerator development. It can also support project processes and create a shared understanding of the project. For the model to become the working basis of all design activities, it must be developed as a comprehensive integration model. Such a model provides the context for the work of all stakeholders. It forms the communication basis for collaborative design. In the PETRA IV project at DESY, fundamental methods have been applied to ensure the model is comprehensive and to enable it to support project tasks such as review processes.

METHODS

Comprehensive CAD Model

A comprehensive CAD integration has been established at DESY as part of the PETRA IV project. This model includes all project-relevant buildings and tunnel systems (comprising approximately 80 buildings) as well as the entire machine equipment along the 2.3 km storage ring and its pre-accelerator complex, represented in different configurations (current state and target design). In addition, the model incorporates user systems, experimental installations and technical infrastructure, including supply routes, escape paths and transport routes. It serves as a single source of truth and provides all stakeholders involved in construction and design processes with a complete and reliable geometric context.

Structure

The model is hierarchically structured with levels designated (from top to bottom) complex, facility, area, unit and component, adapted from the physical hierarchy of the ISA-106 standard [3]. On the “complex” level, the model comprises buildings, accelerator, photon science complex, technology complex and campus. Major facilities are individual buildings, accelerators, the photon science experimental halls. This CAD structure is aligned with the project structure in order to facilitate design processes such as functional and requirements analysis, verification, and reviews. A correspondence to the work package structure ensures that responsibilities are clear. The data integration also includes attaching technical documentation, which is linked to the CAD data and project structure. Together with the modularisation and abstraction principles described below, the structure enables navigation from the overall PETRA IV programme down to the smallest components such as individual fasteners (Fig. 1).

Modularisation

In the PETRA IV integration model, the system is organised into clearly defined modules, each representing a physically bounded and functionally self-contained unit with explicit interfaces to its environment. Modularity is applied consistently across all design levels, from large-scale structures such as accelerator arc to technical subsystems like local media supplies or beamline optics. Even non-technical zones, such as transport corridors or safety areas, are treated as modules to support coordinated planning. This modular approach enables structured integration and facilitates parallel development throughout the entire PETRA program.

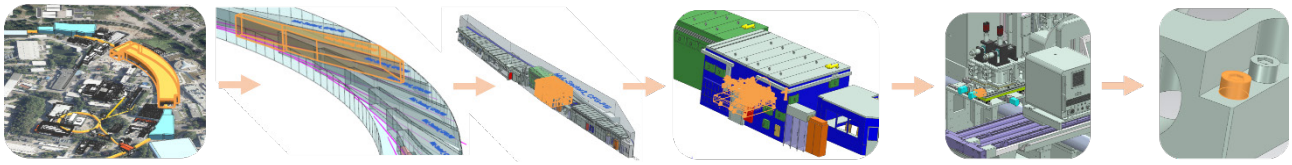

Figure 1: CAD structure allows vertical navigation from the entire program to every individual part.

ISBN: 978-3-95450-263-9 ISSN: 2673-5520 doi: 10.18429/JACoW-MEDSI2025-WEP05

SYSTEMATIC REDUCTION OF LATTICE COMPLEXITY THROUGH VARIANT MINIMIZATION

M. Diercks, B. List, C. Kula, M. Hüning, L. Hagge
Deutsches Elektronen-Synchrotron (DESY), Hamburg, Germany

Abstract

The design of an accelerator system requires translating the lattice into an engineering design model from which the machine can be built, fulfilling the requirements of beam dynamics and from mechanical engineering. To achieve this in an efficient manner, a systematic and manageable iterative design process has been established, which ensures consistency between the lattice and the mechanical model and enables a fast translation of the calculated lattice into a CAD model with correctly placed components within one day through the use of newly developed automation tools.

An analysis process of the lattice, a highly modular CAD structure focused on maximal reuse, and strategic variant management together minimize the number of variants necessary. As a result, design, manufacturing and logistics efforts are significantly reduced.

This approach establishes a fundamental toolkit. It ensures the traceable integration of physics and engineering requirements throughout the system design process of PETRA IV, the planned next-generation synchrotron light source at DESY.

INTRODUCTION

The lattice is the central specification of an accelerator. It results from beam optics calculations and defines the required physical properties and performance. The lattice describes all beam-influencing components and specifies their exact positions along the beamline. To allow the physical design of the accelerator, a main focus is the transfer of the lattice specification into a geometrical model. This transfer has two contributions. The first is validity, achieved through automated integration of the lattice into a consistent 3D geometry model. The second is optimization, enabled by the structuring and analysis of variant diversity. This forms the basis for iterative design improvements, in which a alignment of requirements between physical and engineering design is enabled.

In the PETRA IV project at DESY, this methodology allows the transfer of more than 4,000 beamline components into a 3D CAD environment. These are positioned precisely along the 2.3 km storage ring. The resulting geometrical representation provides the foundation for the design of dependent technical systems like support structures, alignment systems, vacuum chambers, and diagnostics.

The layout of a storage ring is highly repetitive and consists of arcs and straight sections, which are composed of cells and girders. Variants occur through local differences like variations in insertion devices or sections for injection or extraction.

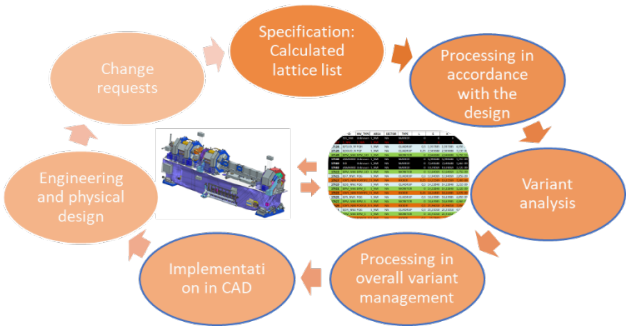

Figure 1: Iterative process for implementing a lattice specification into CAD. After the lattice list is provided by beam physics, it is adjusted for CAD implementation. The lattice is then analysed for variants and changes compared to the previous version. Variant changes are managed in the variant management system, which also tracks variants of all associated technical systems. All changes are transferred into CAD (as in section 'Automation and Black-White-Box principle'). Engineering design drives the further development of technical systems, generating requirements that are incorporated into a new lattice version. Contributions from CAD integration are highlighted in blue.

OBJECTIVES

A main objective is to provide a geometrically precise representation of the accelerator lattice as the foundation for the physical design.

A workflow is established that ensures efficiency, reliability, and traceability in the transfer of the lattice into the engineering model. The same process maintains alignment between physics and engineering through controlled feedback and iteration (Fig. 1).

A structured variant management is introduced to reduce complexity and improve quality. This approach enhances the overall overview, reduces design effort and supports manufacturing and logistical planning from the earliest design stages.

METHODS

Multiple methods are applied:

- Structured data organization is implemented. A hierarchy organizes the information and forms the basis for analysis.
- Modularity is introduced to encapsulate technical details. Modules are logical design elements and serve as the foundation for variant management.
- A girder assembly is established as the physical assembly unit.

ISBN: 978-3-95450-263-9 ISSN: 2673-5520 doi: 10.18429/JACoW-MEDSI2025-WEP06

COMPACT PERMANENT MAGNETS FOR SMALL BORE ACCELERATORS

C. Huschke†, A. Allézy, R. Schlueter
Lawrence Berkeley National Laboratory, Berkeley, CA, USA

Abstract

In synchrotron light sources, electromagnets are used to bend and accelerate electron beams. In 4th generation sources, the electron beam can fit in smaller bore accelerators, allowing the use of permanents magnets, which have many advantages over electromagnets. This paper focuses on the mechanical design, fabrication and testing of two compact permanent magnet systems. The first is a dipole-quadrupole magnet assembly, providing a 1 T dipole + 50 T/m quadrupole field to steer the electron. The second is an assembly to adjust a set of tuner and corrector permanent magnets. Regardless of the magnetic forces involved, the tuner magnets can rotate simultaneously and provide a ±1 T/m quadrupole field for in situ quadrupole focusing strength adjustments, while corrector magnets can be oriented into a prescribed configuration to compensate for small field errors. Prototypes for the dipole-quadrupole, tuner and corrector holders were manufactured and tested, validating the conceptual design.

INTRODUCTION

The Berkeley Center for Magnet Technology (BCMT) group at Lawrence Berkeley National Laboratory (LBNL) is investigating permanent magnets as an alternative to commonly used electromagnets for small bore accelerator lattices, like 4th generation light sources.

Unlike electromagnets, permanent magnet alternatives are significantly smaller and do not require electricity nor a cooling system to operate. Choosing permanent magnets as an alternative comes with challenges though. First, it is known that the strength of a permanent magnet can be affected by environmental changes, like high temperatures and radiation exposure [1]. Second, the assembly process of rare earth magnets can be difficult since they strongly interact with ferromagnetic objects in proximity. Third, magnetic field errors introduced during the fabrication process may be difficult to correct.

Dipole and quadrupole permanent magnet systems have been studied as alternatives to electromagnets at other accelerator facilities [2, 3], where this paper focuses on the mechanical design, fabrication and testing of a stronger compact permanent magnet system: comprised of a combined function dipole-quadrupole (DQ) and a corrector-tuner (CT) assembly. The latter two challenges of permanent magnets mentioned above are the focus this paper will address.

† chuschke@lbl.gov

DIPOLE-QUADRUPOLE

Mechanical Design

A combined function DQ assembly is comprised of eleven wedge shape neodymium rare earth permanent magnets, designed to provide the magnetic strength required to steer the electrons. Each magnet is magnetized across the width of the wedge, and the magnetic arrangement resembles a Halbach array (Fig. 1). Additionally, the field orientation and strength of each magnet is verified with a Helmholtz Coil [4] before assembly.

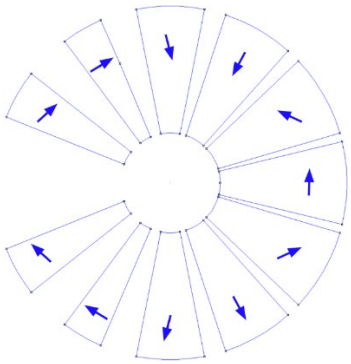

Figure 1: Individual magnetic field direction for DQ assembly.

The functional features of a DQ assembly are shown in Fig. 2. The set screws and guard plates secure the magnets within their respective pockets, whereas the hinge is designed to open and close the assembly to be easily inserted or removed from around a vacuum chamber.

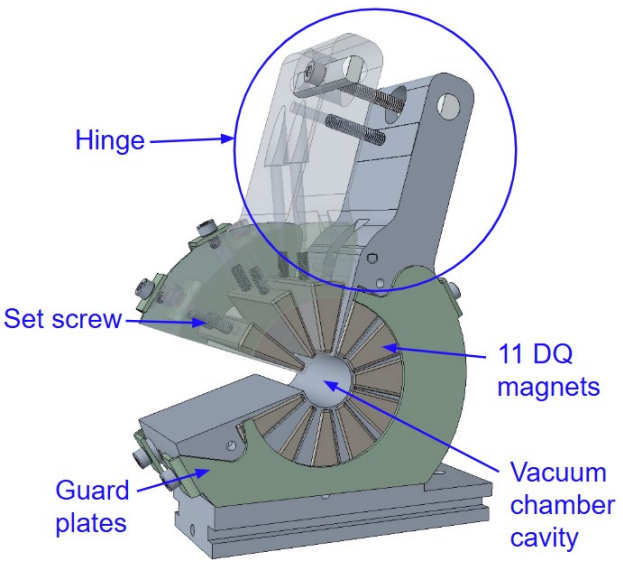

Figure 2: CAD model of DQ assembly showing functional features.

ISBN: 978-3-95450-263-9 ISSN: 2673-5520 doi: 10.18429/JACoW-MEDSI2025-WEP12

DESIGN AND DEVELOPMENT OF THE BEAM COLLIMATORS FOR CiADS *

Haihua Niu†,1,2, Hanjie Cai[1,2], Huan Jia[1,2], Fengfeng Wang[1,2], Yuanshuai Qin[1], Yuxuan Huang[1], Wenwen Shuai[1,2], Yajun Zheng[1,2], Yongxiang Pan[1,2]
[1] Institute of Modern Physics, Lanzhou, China
[2] University of Chinese Academy of Sciences, Beijing, China

Abstract

The China initiative Accelerator Driven System (CiADS) consists of a 350 m-long linac, a spallation target, a sub-critical reactor and several experimental terminals. The linac will provide protons at the energy of 500 MeV with 2.5 MW power. In order to keep the uncontrolled beam loss along the beam transport line before entering the target and the reactor less than 1 W/m, a two-stage collimation system with 2+1 periodic structure has been designed for the linac and target coupling section of CiADS. The detailed design of the beam collimation system is presented, including material selection, structural design, thermal performance analysis, radiation shielding optimization, and remote maintenance. Key technical issues which affect the collimation equipment development are also introduced.

INTRODUCTION

In particle accelerators, beam loss management is one of the core challenges for ensuring the efficient and stable operation of the accelerators. In high-energy particle accelerators, the collimator is a key component for managing beam loss. It is mainly used for beam collimation, impurity removal and equipment protection. Its performance directly affects the operational efficiency of the accelerators, the service life of the equipment, and radiation safety [1-5]. However, the current technology still faces the following major bottlenecks: thermal damage to materials caused by high heat load and energy deposition, insufficient cooling efficiency, irradiation damage, high positioning accuracy requirements, stability and ultra-high vacuum performance requirements, as well as remote operation and maintenance of collimators during equipment failures or equipment upgrade processes. The detailed design of the beam collimation system is presented, including material selection, structural design, thermal performance analysis, radiation shielding optimization, and remote maintenance. Key technical issues which affect the collimation equipment development are also introduced.

CONCEPTUAL DESIGN

The China initiative Accelerator Driven System (CiADS) consists of a 350 m-long linac, a spallation target, a sub-critical reactor and several experimental terminals. The linac will provide protons at the energy of 500 MeV with 2.5 MW power [6]. In order to keep the uncontrolled beam loss along the beam transport line before entering the target and the reactor less than 1 W/m, a two-stage collimation system with 2+1 periodic structure has been designed for the linac and target coupling section of CiADS. Considering high-energy proton scattering and forward secondary particles, the first two periods include a primary collimator and a secondary collimator, while in the third period, only one secondary collimator is arranged to collect the scattered particles at the end. The beam scraping block of the primary collimator needs to be remotely synchronized for high-precision adjustment. In addition, considering the ultra-high vacuum and high stability requirements of the accelerator equipment, the main technical specifications are shown in Table 1.

Table 1: Main Specifications of the CiADS Primary Collimator

Movement Range [mm]	Adjustment precision [mm]	Vacuum leakage rate [Pa·m^3·s^{-1}]	Limiting vacuum [Pa]
2～40	＜0.1	＜1×10^{-9}	＜1×10^{-6}

The Overall Scheme Design and Key Equipment Design

According to the physical requirements, the length of a single period of the first two periods is 6.16 meters, including the primary collimator, the secondary collimator, and the local shielding, as shown in Fig. 1.

According to the physical requirements, the primary collimator adopts four independently adjustable thick beam scraping blocks, with one pair in the horizontal direction and another in the vertical direction. Considering the strength of the material, thermal conductivity, beam stop ability, irradiation damage performance, etc., the material of the beam scraping block is selected as tungsten [7-8]. The size of the beam scraping block in the horizontal direction is 80 mm×50 mm×170 mm; the size of the beam scraping block in the vertical direction is 80 mm×50 mm ×180 mm. Taking into account the physical properties of the tungsten block and its welding performance with oxygen-free copper, the beam scraping block is divided into multiple tungsten sheets, which are welded to the oxygen-free copper transition layer to form a tungsten-copper composite part, and then connected with other components. To ensure a good heat exchange effect, the cooling of the beam scraping block assembly is carried out by water cooling.

* Work supported by Young Scientists Fund of National Natural Science Foundation of China (Grant No. 12305169).
† niuhh@impcas.ac.cn

ISBN: 978-3-95450-263-9 ISSN: 2673-5520 doi: 10.18429/JACoW-MEDSI2025-WEP13

DESIGN AND IMPLEMENTATION OF AN IN-VACUUM MAGNETIC FIELD MEASUREMENT SYSTEM FOR THE TPS NONLINEAR IN-VACUUM KICKER

C. S. Yang†, F. Y. Lin, Y. L. Chu, C. K. Yang , C. K Chan, C. C. Chang,
H. Chen, C. S. Fann, J. C. Jan and T. Y Chung
National Synchrotron Radiation Research Center, Taiwan, ROC

Abstract

The Taiwan Photon Source (TPS) storage ring utilizes a conventional four-kicker bump off-axis injection scheme, which may induce beam perturbations during the injection process. To enhance beam stability and enable reliable top-up operation, a novel Nonlinear In-Vacuum Kicker has been developed. This device is engineered to produce zero magnetic field components in both the horizontal (Bx) and vertical (By) directions at the beam center, while generating a peak By field at the injection point. This magnetic field configuration enables transparent injection with minimal disruption to the stored beam.

To precisely characterize the magnetic field distribution of the NIK and eliminate arcing issues encountered during atmospheric measurements, a vacuum-compatible magnetic field measurement system has been designed and implemented. The system enables accurate field mapping across various excitation currents. This paper presents the system's mechanical design, fabrication process, and initial experimental validation results.

INTRODUCTION

The National Synchrotron Radiation Research Center (NSRRC) is advancing an innovative injection scheme for the TPS that incorporates a nonlinear injection kicker. Unlike conventional implementations used at facilities such as MAX IV, BESSY II, and Sirius which operate out-of-vacuum, the TPS adopts a novel in-vacuum nonlinear injection kicker design [1]. Consequently, we have named it the Nonlinear In-vacuum Kicker (NIK). This configuration is expected to improve injection performance while minimizing interference with the stored beam.

However, during initial magnetic field measurements under atmospheric conditions, electrical arcing was observed due to the system's high-voltage characteristics. To address this issue and improve operational safety and reliability, a vacuum-compatible magnetic field measurement system was developed. The system was designed based on the NIK magnet structure, specifically optimized to prevent electrical discharge in high-voltage environments. The magnet features a magnetic length of 0.36 m and a racetrack-shaped aperture of 68 mm (horizontal) by 8 mm (vertical). With a nominal current of 1588 A, the peak field reaches 895 Gauss, yielding an integrated field of 32,127 Gauss · cm. The printed circuit board (PCB) coil used for signal detection has a total length of 0.75 m, allowing high-resolution measurement of the magnetic field profile.

MECHANICAL DESIGN

To facilitate the development of the NIK at TPS, a dedicated magnetic field measurement system was designed and constructed. This system utilizes a PCB coil to measure the integrated magnetic field, as illustrated in Fig. 1. Optimized for vacuum operation, it features high-precision PCB translation capabilities, allowing for a motion range of ±20 mm along the X-axis and ±2 mm along the Y-axis. The motion stages are equipped with precision actuators, enabling a positioning resolution of up to 10 µm. These specifications fulfill the spatial resolution requirements essential for accurate magnetic field profiling, making the system well-suited for evaluating complex nonlinear magnetic field structures.

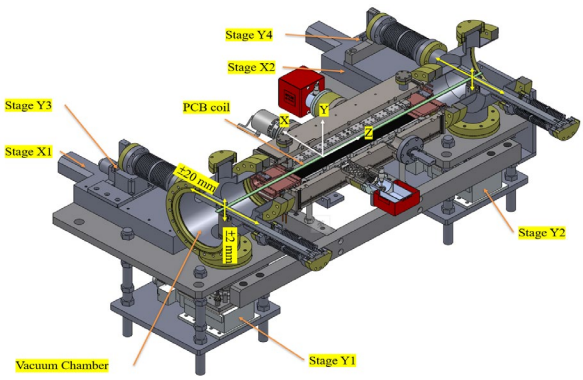

Figure 1: Vacuum magnetic field measurement system with PCB coil on X–Y stages for the NIK at TPS.

In designing the vacuum chamber, special attention was given to evaluating the mechanical stability and positional behaviour of the structure under both atmospheric and vacuum conditions, ensuring consistent operational reliability and motion accuracy across varying pressure environments.

During system operation, vacuum-induced compression and tension in the bellows generate non-uniform reaction forces on the motion platform Y3 andY4, particularly during transitions between these two states. This mechanical imbalance leads to platform instability, causing the PCB coil to experience undesirable vibrations or sudden jumps a phenomenon especially noticeable when the PCB is positioned near X = 0 mm, where the platform is most sensitive to force fluctuations.

† yangzs@nsrrc.org.tw

ISBN: 978-3-95450-263-9 ISSN: 2673-5520 doi: 10.18429/JACoW-MEDSI2025-WEP14

DESIGN AND IMPLEMENTATION OF AN OPTICAL DIAGNOSTIC BEAMLINE AT THE BESSY II INJECTION LINE

P. Ahmels*, T. Atkinson, S. Wiese, Helmholtz-Zentrum Berlin, Berlin, Germany

Abstract

In order to improve the present LINAC injection line diagnostic system at BESSY II, a non-destructive source point imaging system is being developed. This paper presents the conceptual design, including technical requirements, simulation results, and expectations for the optical transport line and mechanical integration. The design aims to ensure beam quality during operation using synchrotron radiation emitted from the dipole magnet. The primary components of this beamline are a CCD camera and a lens system. To enable precise positioning, the optical system is equipped with a motorized linear feed through. The entire setup is designed to operate under high vacuum conditions. A basic, fixed focal length setup is initially employed to experimentally validate the simulation results, using the same CCD camera as in the final beamline setup.

MOTIVATION

To maintain and improve the injection process of the third-generation synchrotron radiation source BESSY II [1], accurate beam size measurements on exit of the linear accelerator (LINAC) are essential. Until now these measurements have mainly relied on retractable Fluorescent screens (FOMs), which are inherently destructive due to directly imaging the electrons. A non-destructive solution involves a short beamline equipped with a camera and lens system to observe synchrotron radiation.

A fixed implemented system of this kind has already been installed as shown in Fig. 1, which allows no further adjustments during machine operation. Furthermore the system lacks sufficient position accuracy and has not been fully characterized. To improve the setup it is necessary to develop a mechanical solution that allows for precise, under operational condition adjustments of the lens position and a fully characterized optical response.

LabVIEW [2] is used to process the image shown on the CCD camera as shown in Fig. 2. Such an image is readily available in the control room for live monitoring as part of the essential high-end diagnostic. The post processing in LabVIEW includes Gaussian fit of the beam intensity profile for beam position and size within the region of interest.

INITIAL DESIGN AND GENERAL REQUIREMENTS

The objective is to implement a motorized and characterized lens system with integrated Prosilica GT 1920 camera [3] for non-destructive source point imaging.

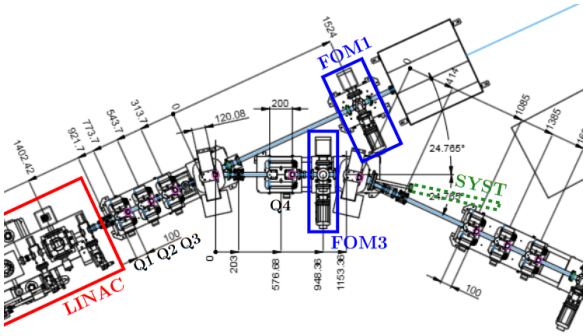

Figure 1: Technical drawing of the injection line at BESSY II with marked LINAC, FOMs and placement of new optics. Dimensions in mm.

Given the fixed lens system placement a few preconditions are already established: pipe diameter of 25.4 mm, minimal distance between lens and source of 1.3 m, non-magnetic steel 316L, focal length of 200 mm and possible implementation of a vacuum system.

For a straightforward implementation a common design is chosen: motorized paired bellows moving a lens horizontal.

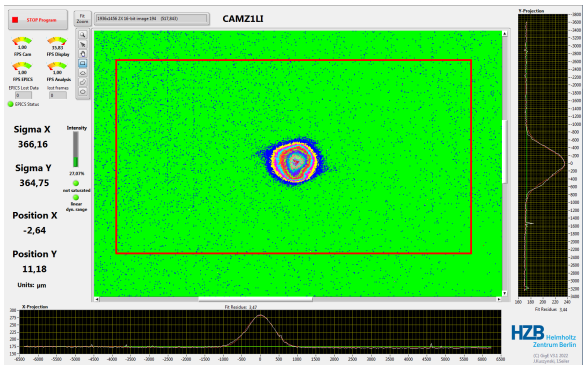

Figure 2: Typical image analysis of the present fixed lens source point system. Image taken after LINAC optimisation.

To calculate the stroke length and maximal distance between lens-source the electron beam and the emerging photon beam was simulated as documented in the following sections. The simulations resulted in maximal length of 1.6 m and stroke length of 50 mm. Given that the following setup has been designed Fig. 3.

SIMULATING ELECTRON BEAM

The beam emittance on exit of the LINAC was found through the common quadrupole scan method [4] before LINAC optimisation using Q3 and FOM1 (Fig. 1). The

* pauline.ahmels@helmholtz-berlin.de

ISBN: 978-3-95450-263-9 ISSN: 2673-5520 doi: 10.18429/JACoW-MEDSI2025-WEP15

DESIGN AND IMPLEMENTATION OF A PARALLEL LINKAGE MECHANISM WITH SPRING ASSEMBLY FOR MAGNETIC FORCE COMPENSATION IN INSERTION DEVICES

C. K. Kuan, W. Y. Lai, K. H. Hsu, C. J. Lin, C. S. Huang, D. G. Huang,
H. C. Ho, T. C. Tseng, Y. C. Liu
National Synchrotron Radiation Research Center, Hsinchu, Taiwan

Abstract

This study presents the design and fabrication of a mechanical compensation system aimed at neutralizing the magnetic attraction forces inherent in insertion devices (IDs) used in synchrotron radiation facilities. In long IDs, such as those measuring 4 meters in length, multiple compensation modules, typically four, are required to maintain structural stability and magnetic field uniformity. In this work, a single compensation module was designed, fabricated, and installed on a test platform to verify the feasibility and mechanical performance of the proposed mechanism.

The system integrates a parallel linkage mechanism with a spring assembly consisting of twelve coil springs. The parallel linkage ensures synchronized and stable movement of the magnetic arrays with minimal structural deformation, while the spring assembly provides a counteracting force that balances the increasing magnetic attraction as the ID gap narrows. Although the mechanism was not installed on a working ID, test results demonstrate its effectiveness in reducing structural load and maintaining precise displacement control under simulated magnetic force conditions. This confirms the concept's viability and its potential for improving operational efficiency and safety in future ID applications.

INTRODUCTION

Insertion devices (IDs), such as undulators and wigglers, are essential components in synchrotron radiation facilities. These devices consist of opposing arrays of permanent magnets that generate highly periodic magnetic fields. By varying the gap between the magnet arrays, the spectral characteristics and intensity of the emitted synchrotron radiation can be finely controlled. However, a major challenge arises from the strong magnetic attraction forces that act between the two arrays, particularly when the gap is reduced. These forces increase nonlinearly as the gap narrows, posing significant mechanical challenges to the gap adjustment and support systems. Excessive magnetic forces can lead to structural deformation of the support beams, introduce positioning errors, and impose high loads on actuators, ultimately compromising beam quality and system reliability.

To mitigate these effects, various magnetic force compensation strategies have been implemented, including counterweights, hydraulic systems, magnetic force dynamic compensation, and spring-based mechanisms [1-4].

This study proposes a novel approach that integrates a parallel linkage mechanism with a spring assembly to provide passive compensation for the magnetic attraction forces in IDs. The parallel linkage ensures synchronized and vertically constrained motion of the magnetic arrays, thereby minimizing parasitic forces and improving motion precision. The spring assembly, composed of twelve coil springs, is designed to produce a counteracting force that closely follows the nonlinear increase of magnetic attraction as the gap decreases.

For long IDs (e.g., 4 meters in length), multiple compensation modules, typically four, are required to evenly support the structure and minimize deformation. In this work, a single compensation module was designed, fabricated, and installed on a test platform to evaluate the feasibility and performance of the proposed mechanism under simulated conditions. Although the system was not mounted on an actual ID, the experimental results confirm the design's effectiveness in compensating large magnetic forces and maintaining precise gap displacement. This work serves as a proof-of-concept and provides a solid foundation for future integration of such systems into operational insertion devices.

MAGNETIC FORCE IN INSERTION DEVICES

Insertion devices (IDs) utilize arrays of high-strength permanent magnets to generate periodic magnetic fields essential for producing synchrotron radiation. As the magnetic gap between the upper and lower magnet arrays decreases, the magnetic attraction force increases dramatically—often reaching several tons in large-scale systems. This substantial magnetic force poses a significant mechanical challenge, particularly in maintaining precise gap control and minimizing structural deformation.

In practice, the total magnetic attraction force increases linearly with the length of the ID, as each additional magnet segment contributes cumulatively to the overall force. For example, a 4-meter-long ID typically requires compensation for several tons of magnetic loading. The compensation system proposed in this study is designed such that each individual module can counteract up to 1.5 tons of magnetic force. Consequently, for a 4-meter-long ID, four compensation modules are strategically distributed along the device to ensure uniform load sharing and to minimize deflection of the beam supporting the magnet arrays.

The magnetic force F between permanent magnet arrays can be accurately approximated by an exponential function [5] of the form:

ISBN: 978-3-95450-263-9 ISSN: 2673-5520 doi: 10.18429/JACoW-MEDSI2025-WEP16

MECHANICAL DESIGN OF THE IN-VACUUM TAPERED UNDULATOR AT TAIWAN PHOTON SOURCE

W. Y. Lai, K. H. Hsu, C. K. Kuan
National Synchrotron Radiation Research Center, Hsinchu, Taiwan

Abstract

Synchrotron light sources commonly provide users with two types of insertion devices for experiments in biology, medicine, and other fields: in-vacuum undulators (IUs), which have short period lengths and are used for medium-energy photon generation, and cryogenic permanent magnet undulators (CPMUs), which are designed for higher-energy photons. The strong magnetic fields generated by these devices exert significant forces on the magnets, resulting in structural deformation that can degrade the magnetic field quality. This paper presents the design and measurement methods of an in-vacuum tapered undulator, analyzes both simulation and experimental results of its structural deformation, and demonstrates how a flexible structure can be employed to achieve nonlinear magnetic force compensation, thereby improving overall system performance.

INTRODUTION

The in-vacuum tapered undulator (IUT) is a critical device in third-generation synchrotron light sources for generating hard X-rays[1,2]. To achieve hard X-ray production, a smaller undulator gap is required, which significantly increases the magnetic force. This force acts on the undulator's frame and crossbeams, leading to considerable structural deformation. Even after precise calibration, such deformations can cause subtle positional shifts in the magnets, resulting in variations in the magnetic field as the gap size changes. To address this, it is essential to design a rigid frame and crossbeam structure capable of limiting deformation to less than 10 μm under load. In addition to ensuring structural rigidity, this paper also presents the mechanical design of the in-vacuum tapered undulator and introduces a newly implemented flexure mechanism for compensating magnetic forces.

Requirements

The IUT mechanical system must meet six essential functional requirements:

- Travel Range:
  The opening/closing motion must exceed 35 mm to accommodate energy tuning and magnets installation, with a usable magnet gap range of 5 mm to over 40 mm.
- Tilt Range:
  In addition to vertical movement, the IUT requires tilt adjustment functionality. The required tilt angle adjustment range must exceed ±0.5 mrad.
- Resolution:
  The magnet gap must be adjustable with a resolution finer than 1 μm to meet the needs of magnetic field measurements and future beamline energy tuning.
- Deformation Tolerance:
  The crossbeam must withstand a uniform load of 50 kN, with deformation under 5 μm. Additionally, the main frame of the undulator should ensure that crossbeam rotation under a 50 kN load is less than 0.1 mrad.
- Weight Limitation:
  The total weight of the undulator system must be less than 13 metric tons, accounting for a 15-ton crane capacity minus 2 tons for the magnet and vacuum chamber.
- Space Constraints:
  Each crossbeam should be 2 meters long to accommodate the magnet array. The overall system height must be under 2.5 meters, and the distance from the electron beam center to the aisle-side structure must be less than 1 meter.

Based on the above requirements, the IUT system must include two magnet-supporting crossbeams capable of both angular adjustment and opening/closing operations. Each 2-meter-long crossbeam must withstand a 50 kN load with deformation less than 10 μm. The design adopts a dual rectangular shaped crossbeam configuration to support the magnetic force. Each crossbeam is equipped with a rotational axis to enable tilting. Thus, at least two independent motion systems are required: one for opening/closing the beam and another for adjusting the beam angle, as illustrated in Fig. 1.

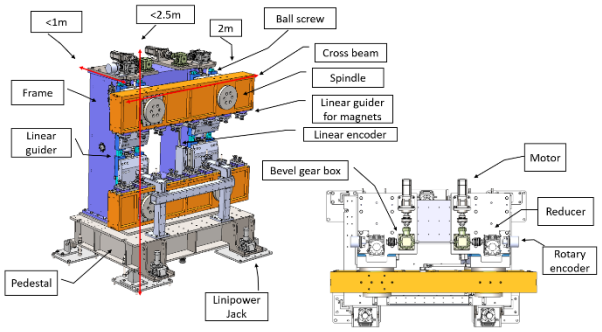

Figure 1: IUT Structure diagram.

Mechanism Design

The two primary deformation regions of the insertion device (ID) magnet are the cross beams that suspend the magnets and the main supporting frame that controls the opening and closing of these beams. The magnetic forces act on the magnet array beams, causing deformation that affects

ISBN: 978-3-95450-263-9 ISSN: 2673-5520 doi: 10.18429/JACoW-MEDSI2025-WEP17

DESIGN OF A DAMPING WIGGLER AT SPring-8-II AS A HIGH-ENERGY X-RAY SOURCE

K. Tsubota†,[1], H. Ohashi[1,2], S. Shimizu[1], S. Takahashi[1,2], T. Tanaka[1,2]
[1]Japan Synchrotron Radiation Research Institute, Hyogo, Japan
[2]RIKEN SPring-8 Center, Hyogo, Japan

Abstract

A damping wiggler (DW) system was designed for the upcoming SPring-8-II, with the dual purpose of reducing the emittance of electron beam and providing high-energy X-rays. The proposed system consists of three DW units (2.6 m length, 20 mm gap, 160 mm period) to be installed in one of the four long straight sections (LSSs). The total radiation power of the three DWs is 75 kW, while the optimization of mask aperture suppresses the absorbed power by the crotch absorber (CA) to 0.63 kW. The photon flux through the front-end slit (FES) with a width of 20 mm and a height of 3 mm was estimated to be 1.1×10^{14} photons/s/0.1% bandwidth (b.w.) at 100 keV and 1.2×10^{13} photons/s/0.1% b.w. at 200 keV. Thermal analyses of Cu-CrZr masks confirmed surface temperatures below 250 °C with sufficient safety margins. The proposed DW design offers high-energy flux comparable to that of the current SPring-8 while satisfying high heat load constraints. The installation is scheduled during the extended shutdown period for the upgrade to SPring-8-II.

INTRODUCTION

The SPring-8-II upgrade project aims to reconstruct the storage ring to realize the fourth-generation synchrotron radiation facility. Introducing a multi-bend achromatic (MBA) lattice and lowering the beam energy from 8 GeV to 6 GeV will significantly reduce the natural emittance, thereby improving brilliance and horizontal coherence [1-3]. However, the reduction in electron energy also decreases the high-energy X-ray flux, which is indispensable for advanced scientific applications such as high-energy imaging.

A DW has the potential to enhance radiation damping, thereby reducing emittance, while also functioning as a broadband, high-energy photon source. It has been shown at several synchrotron facilities, including NSLS-II and PETRA III, that damping wigglers can significantly reduce the emittance [4, 5], and they have also been employed as photon sources [6]. This dual role makes it a promising solution for maintaining high-energy performance in SPring-8-II. However, the significant radiation power requires careful thermal management in the front end and optical components. This paper reports the parameter optimization of the DW system, the evaluation of heat load distribution, and the expected photon flux for high-energy applications.

DAMPING WIGGLER DESIGN

SPring-8-II has four LSSs, each approximately 30 m long. One of these is under consideration for use as the DW section. This LSS consists of five drift spaces, each allocated for the installation of DWs, masks, and related devices. The design objectives were defined as follows:

- Maximize the high-energy photon flux and radiation damping
- Minimize the absorbed power at the CA below 1 kW
- Keep the DW mask thermal load manageable

To achieve these objectives, the following parameters were optimized:

- Number of DW units, gap and period length
- Aperture sizes and positions of the DW masks

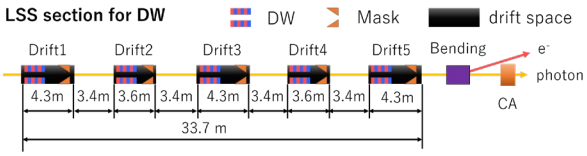

Figure 1: Schematic layout of the LSS section for DW.

Design Objectives

Figure 1 shows the schematic layout of the LSS section, indicating that DWs and masks can only be installed in the drift spaces. The masks prevent excessive heat loads from being imposing on downstream components and beam ducts by radiation emitted from upstream DWs. The CA is primarily designed to absorb bending-magnet radiation and is not intended to intercept that from the DWs. Therefore, the DW heat load has been carefully optimized to ensure that the heat loads on the CA remain within its acceptable capacity. While the heat loads can be reduced by narrowing the mask apertures in the drift spaces, they must remain wide enough to avoid any adverse effects on the electron beam. Figure 2 shows the minimum mask apertures in the horizontal and vertical directions at each drift space. These were evaluated based on the relevant boundary conditions in the SPring-8-II storage ring.

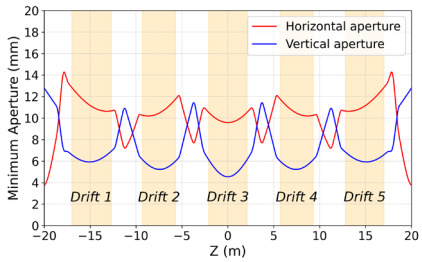

Figure 2: Minimum mask apertures in the horizontal (red) and vertical (blue) directions at each drift space.

† tsubota@spring8.or.jp

ISBN: 978-3-95450-263-9 ISSN: 2673-5520 doi: 10.18429/JACoW-MEDSI2025-WEP22

FABRICATION CHALLENGES AND LESSONS LEARNED IN PROTOTYPING SPS-II STRAIGHT SECTION VACUUM CHAMBERS

T. Phimsen†,[1], S. Boonsuya[1], S. Chitthaisong[1], O. Seegauncha[1], S. Sumklang[1], J. Sukain[1], W. Woranut[1], K. Trongklang[1], O. Utke[1], P. Sudmuang[1], G.Y. Hsiung[2]
[1] Synchrotron Light Research Institute, Nakhon Ratchasima, Thailand
[2]National Synchrotron Radiation Research Center, Hsinchu, Taiwan

Abstract

The development of a manufacturing plan for the aluminum straight section vacuum chambers of the Siam Photon Source-II (SPS-II) was undertaken through a multi-stage prototyping program. This work began with the successful reduction of the internal surface roughness (Ra) of domestically produced aluminum extrusions from approximately 19.9 µm to below 0.42 µm by polishing the extrusion die. A dedicated prototype was then used to validate fundamental Ultra-High Vacuum (UHV) processes, confirming the integrity of in-house Tungsten Inert Gas (TIG) welding and establishing a baseline for the chemical cleaning procedure via Photon Stimulated Desorption (PSD) measurements, which showed the cleaning provided an acceptable baseline but requires further optimization. Subsequent full-scale fabrication trials revealed critical lessons. An initial build without a fixture resulted in both significant deformations, confirming the need for mechanical support, and contaminated welds, highlighting the importance of meticulous in-process cleaning. A second trial with a first-generation fixture solved the deformation but caused weld penetration due to obstructed tool access. This iterative development process successfully identified the key challenges of fabrication and has resulted in a de-risked manufacturing methodology, based on an optimized cleaning protocol and a purpose-built fixture, for the final production chambers.

INTRODUCTION

The Siam Photon Source-II (SPS-II), a 3 GeV 4th generation light source under development at the Synchrotron Light Research Institute (SLRI) in Thailand [1], requires a reliable ultra-high vacuum (UHV) system to meet its high-brightness performance goals. Built from aluminum alloys, the system's chambers must meet stringent requirements for UHV pressure, geometric tolerance, and low surface impedance [2, 3]. The manufacturing of these chambers involves mastering core technologies like UHV cleaning and precision welding, with component complexity varying significantly. The intricate arc chambers pose the greatest challenge. Consequently, our development strategy began with the more fundamental straight section chambers, using their simpler geometry as the ideal starting point to establish and validate baseline fabrication processes before tackling more complex components [4].

This paper presents the results and key lessons learned from this foundational work. We report on the validation of our UHV cleaning process via a Photon Stimulated Desorption (PSD) test chamber, followed by the iterative development of our fabrication technology. This was accomplished through a series of prototypes that revealed successive challenges: first, in welding quality and the need for fixturing with an elliptical chamber, and subsequently, in the nuances of proper fixture design during a trial with a circular chamber.

PROTOTYPING AND PROCESS DEVELOPMENT

Aluminum Extrusion

A key project goal was to establish a domestic capability for producing high-quality aluminum vacuum profiles for the standard 16 mm x 40 mm elliptical beam duct. Initial trials resulted in a high average surface roughness (Ra) of approximately 19.9 µm. Polishing the extrusion die resolved this issue. As shown in Fig. 1, this single modification dramatically reduced the internal Ra to less than 0.42 µm, providing an excellent starting material for subsequent fabrication.

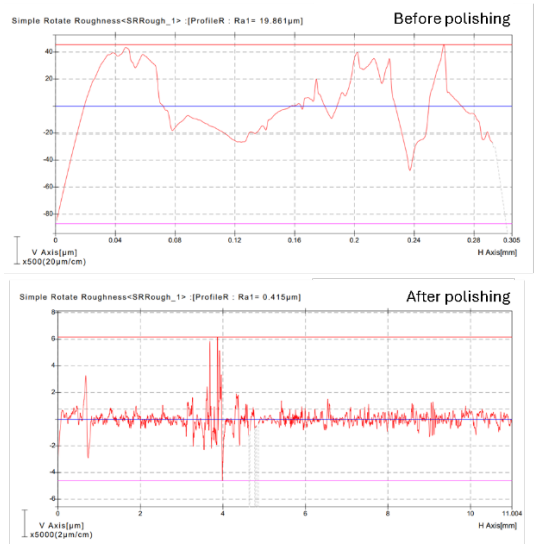

Figure 1: Comparison of the internal surface roughness of the aluminum extrusion before (top) and after (bottom) polishing the die. The initial average roughness (Ra) of about 19.9 µm was dramatically reduced to less than 0.42 µm.

To resolve this, the extrusion die was removed and meticulously polished to create a much smoother forming surface. This single modification resulted in a dramatic improvement in quality, as shown in the comparison in Fig. 1.

† thanapong@slri.or.th

ISBN: 978-3-95450-263-9 ISSN: 2673-5520 doi: 10.18429/JACoW-MEDSI2025-WEP23

DESIGN OF HIGH STABILITY MIRROR SYSTEMS FOR HALF

Shuaikang Jiang†, Zimeng Wang, Jie Chen, Yang Peng, Zhanglang Xu, Shen Wei, Qiuping Wang, Xuewei Du, National Synchrotron Radiation Laboratory, USTC, Hefei, Anhui, China

Abstract

Hefei Advanced Light Source (HALF) is a diffraction-limited light source in the soft X-ray range. It provides a powerful tool for nano-focusing, ultra-high spectral-resolution power and coherent diffraction imaging experiments. To fully utilize the source characteristics, optical mirrors and their manipulators require high accuracy and stability. At present 10 beamlines are in the process of construction, dozens of mirrors with different shapes, sizes, and working conditions are used to achieve high-fidelity transmission, collimation and focusing. They can be divided into three categories: the mirror with water cooling to absorb high heat load; the mirror without water cooling; and the bendable mirrors. In this paper, the standard manipulator for different kind of mirror with high stability is proposed. A universal mirror system with a three-point support structure is developed to hold different manipulators and provide fine-tuning for height, roll, and yaw adjustment. The mirror system and the manipulator design are given in this paper, and the preliminary test results are presented.

INTRODUCTION

As a diffraction-limited light source in the soft X-ray range, the Hefei Advanced Light Facility (HALF) has the advantages of low emittance, high resolution (both spatial and energy), high brightness, and high coherence. Ten beamlines are under construction in phase I, and the mirrors can be divided into three categories: the mirror with water cooling to absorb high heat loads, the mirror without water cooling, and the bendable mirrors. A batch of mirror systems are required to satisfy the mirror clamping and bending, adjustment with high stability.

From the aspects of stable support and alignment, high-precision mirror clamping and mirror surface shape acquisition, high-precision adjustment, system thermal management [1-3], several standard manipulators for different kind of mirror with high stability are designed, and a universal mirror system with a three-point support structure is developed, as shown in Fig. 1.

THE UNIVERSAL MIRROR SYSTEM

The universal mirror system is designed to accommodate mirrors with a length of 300 - 600 mm. Three sets of wedge stages are installed on the top granite to support the manipulator inside the vacuum vessel and provide three degrees of freedom along Tx, Ry and Rz.

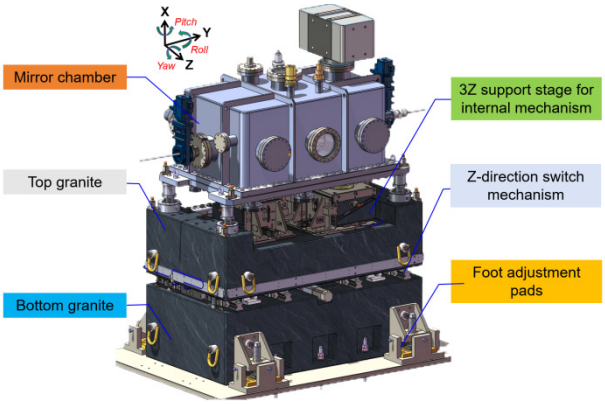

Figure 1: The standardized mirror system for HALF.

Most of the mirrors in Phase I need the degrees of freedom along Tz to satisfy the requirements about aligning with the photon beam and moving in and out of the optical path. A switching mechanism is inserted between the top granite and bottom granite, providing the freedom in the Tz direction. Four manual adjustment pads are installed on the bottom granite for pre-alignment. The mirror system's dimensions and the characteristic parameters for electric adjustment are summarized in Table 1.

Table 1: Overall Specifications of a Mirror System

Specification		Value
Overall dimensions (L×W×H)		1.35×1.34×1.92 [m]
Internal volume (L×W×H)		0.8×0.6×0.35 [m]
Vacuum requirements		6×10^{-8}Pa
DOF	**Resolution**	**Range**
Tx	0.5 μm	±10 mm
Tz	0.5 μm	±10 mm
Ry	0.5 μrad	±5 mrad
Rz	0.5 μrad	±5 mrad
Rx	0.1 μrad	±1mrad

The universal mirror system provides all the necessary degrees of freedom needed for the mirror, except Rx, which is used for precision optical adjustment. Therefore, the manipulator in-vacuum only needs to cope with mirror clamping and precision Rx (pitch) adjustment, greatly simplifying the mechanical design and ensuring high system stability. The manipulators for water-cooled and non-cooled mirrors, the mirror bender with manipulator can be integrated onto the standardized designed flexible decoupling components in the vacuum vessel, as shown in Fig. 2. Details about the different types of manipulators, and preliminary test results of wedge stages are given in the following sections.

† jiangshuaikang@mail.ustc.edu.cn

ISBN: 978-3-95450-263-9 ISSN: 2673-5520 doi: 10.18429/JACoW-MEDSI2025-WEP25

DEVELOPMENT OF PERMANENT MAGNETS REPLACING ELECTROMAGNETS AT NSRRC

J. C. Jan†, Y. L. Chu, Y. Y. Hsu, C. S. Yang, T. Y. Chung
National Synchrotron Radiation Research Center, Hsinchu, Taiwan

Abstract

Integrating permanent magnets as substitutes for large electromagnets offers advantages such as energy savings, space efficiency, and low maintenance. An electromagnetic dipole magnet on the TPS transfer line is proposed to be replaced by a permanent magnet. This permanent magnet will be hybridized with an electrical coil to allow fine tuning of the magnetic field. Additionally, an NMR system is integrated into the magnet to monitor long-term field variations. The magnetic circuit design for the 1m-long permanent magnet has been preliminarily completed. Currently, the prototype-1 magnet with 150 mm employs adhesive technology to bond small magnetic blocks into larger ones. The magnetic field strength and uniformity of prototype-1 meet the design specifications. NiFe material has also been used for temperature compensation. During the development process, some assembly procedures and mechanical designs were revised. The prototype-2 is currently in production. This paper presents the magnetic circuit design, the mechanism design, the magnet prototype and the field measurement result of the permanent dipole magnet.

INTRODUCTION

The Taiwan Photon Source (TPS) is a third-generation synchrotron radiation accelerator operating at an electron energy of 3 GeV and a beam current of 500 mA. In achieve of energy savings and technology upgrades, the substitution of large dipole electromagnets with permanent magnet is under development [1, 2]. A schematic comparison between the current electromagnet and the proposed PM is shown in Fig. 1(a). A prototype-1 permanent magnet was designed and fabricated, as shown in Fig. 1(b).

The integral field and excitation current of the existing electromagnet are 0.8929 T·m and 407.65 A, respectively. To meet the performance criteria, the integral field uniformity $\Delta IB_y(x)/IB_y(0)$ must be better than 0.1% within the ±25 mm good field region (G.F.R.). The outer plate (OP) and correction coil are integrated into the permanent magnet, enabling magnetic field strength tuning during laboratory mapping with OP adjustments and during operational use via the coil.

The permanent magnet (PM) blocks are composed of Sm_2Co_{17}, while the pole and yoke are made of DT4E iron. The specifications (measured) properties of the large PM blocks are: (i) residual magnetism B_r > 1.08 T (1.0801 T measured), (ii) intrinsic coercivity iH_c > 1591 kA/m (1888 kA/m measured), and (iii) total flux deviation $\Delta\phi_{p\text{-}p}/\phi_{avg}$ < 1.5% (measured at 1.39% for the large PM and 1.06% for the small PM). The dimension tolerances of the PM blocks are 120±0.1 × 50±0.05 × 50±0.05 mm³ and 50±0.02 × 30±0.02 × 30±0.02 mm³, and all measured results meet the required specifications.

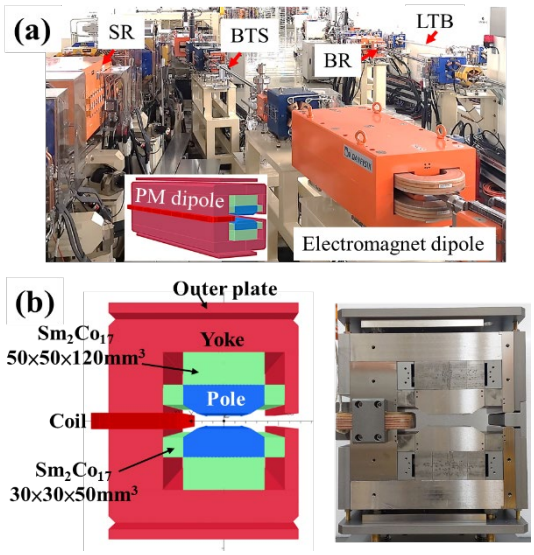

Figure 1: (a) Electromagnet and permanent-magnet dipole, and (b) prototype-1 permanent magnet.

MAGNET BLOCK BONDING AND FIELD IMPACT ASSESSMENT

To reduce manufacturing costs, smaller Sm_2Co_{17} blocks are bonded together to form larger PM blocks. Figure 2 (a) illustrates the PM block bonding procedure. Dimensional errors typically occur at the bonding interface between blocks A and B, primarily due to challenges caused by the repulsive force during bonding. Figure 2 (b) shows a bonded PM block with dimensions of 120 × 50 × 50 mm³. The resulting dimensional tolerances are within ±0.05 mm for the short edge and ±0.1 mm for the long/bonding edge.

Due to the large mass of the PM block, 2.5 kg per piece, a custom fluxmeter was developed to measure its magnetic flux using a precision integrator. A coil with an inner diameter of 300 mm and 100 turns passes through the fixed PM block and is connected to the integrator. The fluxmeter's integrator outputs the maximum integrated voltage in volt-seconds (V·s), which is proportional to the total flux of the PM block. The measurement repeatability of the fluxmeter is characterized by a standard deviation (STDEV) of 0.005% and a maximum peak-to-peak deviation of 0.1%. Flux distribution results for large and small PM blocks are presented in Fig. 3(a) and (b), respectively. For the larger blocks, the flux variation is 1.74% across all 50 blocks and 1.39% among 40 selected blocks. For the smaller blocks,

† janjc@nsrrc.org.tw

ISBN: 978-3-95450-263-9 ISSN: 2673-5520 doi: 10.18429/JACoW-MEDSI2025-WEP26

DEVELOPMENT OF RADIAL MAGIC FINGER DESIGN FOR PERMANENT MAGNET QUADRUPOLE

T. Brookbank, S. Brooks, O. Chubar, F. DePaola, M. Musardo, P. N'Gotta, S. Sharma
NSLS-II, Brookhaven National Laboratory, Upton, NY, USA

Abstract

Permanent magnets (PM) have been widely used in synchrotron light sources for insertion devices and recently for the accelerator multipole magnets. The NSLS-II accelerator upgrade is based on the complex bend lattice that will use combined function permanent magnet-based dipole-Quadrupole (PMQ). The Halbach type design is considered for the PMQs. To achieve the required field quality with the Halbach PMQ, a field harmonic correction method based on assembly of small PM blocks called "Magic fingers" (MF) is developed. This paper presents the radial MF magnetic and mechanical design, the prototype and the correction results.

INTRODUCTION

The Halbach magnet design composed with PM segment can generate a strong multipolar magnetic field with a compact structure suitable for new generation of light sources. The future complex bend lattice, envisioned for NSLSII upgrade, requires combined function dipole-quadrupole magnets with a field strength of 130 T/m and 0.5 T for the quadrupole and dipole component, respectively. The magnetic field quality describing the deviation from the ideal field, is defined as the part of unwanted multipoles (harmonics), and specified at 10 units (the field main multipole component is normalized at 10000 units).

A Halbach PMQ prototype, using 16 PM wedges, was designed and built to achieve the combined function magnet. The magnetic simulation predicts a field harmonic error larger than 100 units for the real magnet due to tolerances of the PM characteristics (remanence, magnetization angle) and wedge assembly and geometrical errors. The magnetic measurement of the in-house PMQ prototype confirmed this prediction with a field error of 137 units [1, 2]. This report presents the design and prototyping of the MF system and the field correction of the PMQ prototype with MF that achieves a field quality close to 10 units.

MAGNETIC DESIGN

The Magic Finger field correction method is based on an assembly of small rectangular PM blocks placed at the longitudinal extremity of the PMQ magnet. The MF assembly generates an additional field with harmonics of the opposite sign to cancel the field harmonics of the magnet. To generate the required arbitrary correction field, the radial magnetization direction (up or down) and the radial length of the MF assembly are controlled. The PMQ and MF model are built with RADIA to simulate the magnetic field (Fig. 1) [3].

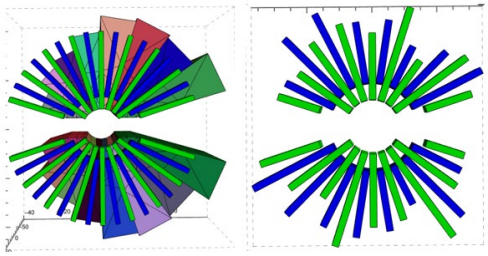

Figure 1: Halbach PMQ with MF correction.

The discrete MF rectangular PM block is a 2x2 mm^2 section and 15 mm longitudinal length. Two layers of PM stack (green, blue) are arranged to fully use the space. The harmonics correction capability of the MF is estimated using a statistical approach based on the generation of several random sets of MF assembly with random radial length and random magnetization direction. The generated harmonics strength is presented in Table 1.

Table 1: Maximum Harmonics Strength

Harmonic order	3	4	5	6	7	8
Strength [units]	215	75	21.5	10.5	3.8	0.5

The generated harmonics strength ranges from 215 units for the first order harmonic (n=3, sextupole), to lower value below 1 unit for the higher order (n≥8). This result gives the maximum strength for each harmonic when the MF assembly generates mainly a particular harmonic order.

Another simulation is performed with 1000 random MF assembly, and the harmonics root square sum (RSS) is calculated to estimate the MF correction capability. The results shown in Fig. 2, give an estimate of the MF correction capability of 150 units RMS, that is higher than the specified 100 units PMQ errors after assembly [1].

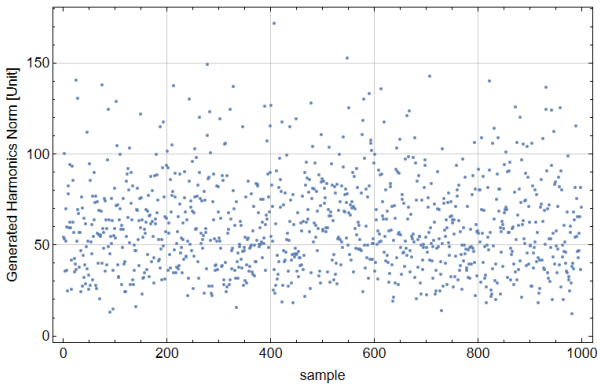

Figure 2: RSS of harmonics generated by 1000 random MF assembly.

ISBN: 978-3-95450-263-9 ISSN: 2673-5520 doi: 10.18429/JACoW-MEDSI2025-WEP28

DOUBLE CRYSTAL BENT LAUE MONOCHROMATOR: MODELLING AND MEASUREMENTS UP TO 150 KeV

O. Marinos†,1,2, S. Gasilov[3], D. Chapman[1,2]
[1]Canadian Light Source, Saskatoon, Canada
[2]University of Saskatchewan, Saskatoon, Canada
[3] Helmholtz-Zentrum Hereon, Geesthacht, Germany

Abstract

A main application of Laue diffraction in thick bent crystals is on developing high energy/high power monochromators for synchrotron sources. Whereas most of the studies mainly focuses on modelling and simulation of ideal shapes, e.g., cylindrical deformation, this preliminary work aims to study a wider picture including mechanical and optical measurements performed on 2 mm thickness double bent Laue crystal monochromator currently used at the Biomedical Imaging and Therapy (BMIT) 05ID-2 beamline at the Canadian Light Source (CLS). Initial measurements are compared to simulations from tools such as ANSYS and XRT ray-tracing based on Tagaki-Taupin equations. We infer real deformed crystal is far from ideal cylindrical shape and we found the diffracted beam intensity raised 12X due to deformation using an incident white beam. Also, photon flux measurements were performed using a cryogenic radiometer. Measurements have been performed at both the 05ID-2 (3.7 T wiggler) and the 05B1-1 (1.35 T bending magnet) beamlines with diverse energies between 25 keV and 150 keV. Thus, considering the scarcity of experimental data, this work becomes relevant as it presents some measurements of a real bent Laue monochromator and compares it to simulations.

INTRODUCTION

At synchrotron facilities, as in many other applications, the need for monochromatic beam is required. This can be obtained from Bragg or Laue geometries. Each of them with pros and cons. For the Laue case, a very well-known configuration is the Double Crystal Laue Monochromator (DCLM), which has become a high-precision optical device commonly used in synchrotron beamlines for monochromatic X-ray production. Its operation is based in the Laue configuration, i.e., two aligned crystals (usually silicon) diffract an X-ray beam as goes through them (transmission). Better thermal resilience, a higher photon flux and an improved beam stability are some of the advantages of this configuration, which makes it well suited for high energy beams applications (insertion devices).

A technique to increase the diffracted beam intensity from an incident white beam is to bend the crystals, i.e., increase the deformations of the crystal planes to produce a wider range of Bragg angles that widen usable reflection bandwidth. The quality of the final output beam (non-dispersive, divergence, spatial coherence, etc.) will depend on the quality of the crystal deformation, i.e., a homogeneous strain provides a homogeneous deformation of the crystal planes and produce a more symmetrical bandwidth of the beam. At synchrotron applications, the small source-size and the beam divergence require optimal alignment and bending of the crystal to ensure regular energy-angle distribution (DuMond diagrams) and energy resolution [1].

Thus, considering the relative extensive use of DCLMs at various synchrotron facilities (e.g., Australian Synchrotron [2], PETRA III [3], ESRF [4], etc.), the lack of a final theory of bent Laue diffraction, and the current simulation tools developed for perfect conditions (e.g., XRT code [5] provides ray-tracing simulations assuming a perfect cylindrical deformation), it becomes convenient to study the performance of the DCLM setup (and some available predictive tools) with the intention to improve its design and operation. The present work intends to be a starting point towards this direction.

DESIGN

The DCLM used at the BMIT-ID beamline (05ID-2) consists of two (111) 2 mm thickness silicon crystal with an asymmetric cut of 15° mounted in Laue transmission configuration (see Figure 1). The X-ray source consists of a Wiggler (26 periods, 48 mm length) that can generate a field of up to 3.7 T and is located at 44.5 m from the DCLM. Its main purpose is to produce "monochromatic" beams of specific energies to be used in synchrotron-based imaging. Both, the upstream and downstream crystals, have benders to generate deflection in the crystals with the main purpose of increasing the photon flux and improve the signal-to-noise ratio (SNR).

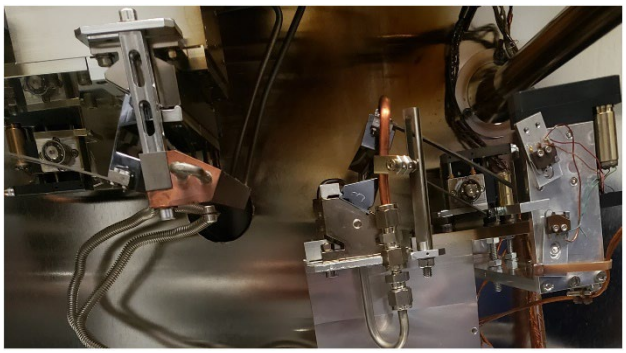

Figure 1: Picture of the interior of the DCLM used at the BMIT-ID beamline of the Canadian Light Source.

The main purpose to produce a curvature in the crystal is to maximize the bandwidth (photon flux) by slightly altering the angle dispersion of the lattice planes around a

† Omar.Marinos@lightsource.ca, omar.marinos@usask.ca

ISBN: 978-3-95450-263-9 ISSN: 2673-5520 doi: 10.18429/JACoW-MEDSI2025-WEP29

Elettra 2.0 DISCRETE STORAGE RING PHOTON ABSORBERS

G. Scrimali†, Elettra Sincrotrone Trieste S.C.p.A., Trieste, Italy

Abstract

The Elettra 2.0 project is upgrading the Elettra synchrotron radiation facility to 4th generation standards. This paper presents the overall photon absorption strategy adopted in the design, which includes both distributed and localized absorption of emitted photons, focusing on discrete photon absorbers and their geometrical configurations within the storage ring. All discrete photon absorbers will be manufactured entirely from Copper-Chromium-Zirconium alloy (CW106C or CuCr1Zr). The components will be produced using wire electrical discharge machining (EDM) for the main geometries, supplemented by conventional milling, with the integration of the flange knife-edge into the absorber geometry without the need for brazing. Two main absorber families are introduced: transversal photon absorbers, designed to protect vacuum chambers near bending magnets and to serve as initial beam-shaping elements, and axial photon absorbers, which function as transitions between different chamber geometries and protect sensitive components, such as RF contact bellows. The paper also presents the current production status and includes photographs of the first manufactured units.

INTRODUCTION

The Elettra 2.0 project is upgrading the Elettra storage ring to diffraction-limited, fourth-generation synchrotron radiation facilities standards. To contain the emittance, the twelve-fold, double-bend achromat (2BA) will be updated to a symmetric six-bend achromat (S6BA) installed in the same existing tunnel, therefore highly increasing the device density and space occupied by the magnets [1]. In this new configuration, because of the often-limited separation between the emitted photons and the electron beam path, the photon absorption strategy is based on a combination of distributed and localized absorbers. This paper presents the design solutions developed for the discrete absorbers to meet the requirements of the Elettra 2.0 storage ring.

GENERAL CHARACTERISTICS

The discrete photon absorbers for the Elettra 2.0 storage ring will all be manufactured in CW106C copper alloy (UNS C18150, or CuCr1Zr). This material offers good mechanical properties while still maintaining a high thermal conductivity [2]. Another key attribute of CW106C is its ability to machine functional flanges directly from solid stock [3, 4], enabling the production of vacuum-tight designs without the need for brazing or welding. All absorbers have integrated flanges in their design.

The active geometries involved in the interactions with photons are designed to be fabricated through Wire Electrical Discharge Machining (W-EDM), chosen for its capability to produce complex shapes with high tolerances, superior surface finish, minimal burrs formations and negligible post processing. In addition, all absorbers feature cut-outs matching the Elettra 2.0 vacuum chamber profile, to minimize the impact on the storage ring impedance budget.

Two main absorber types are employed, distinguished by their geometries and roles: transversal and axial photon absorbers. A detailed analysis of both types follows in the subsequent sections.

TRANSVERSAL PHOTON ABSORBERS

Transversal absorbers handle the majority of storage ring power dissipation, absorbing two-thirds of the bending magnet output and withstanding the primary load from insertion devices, thus ensuring beam compatibility with beamlines beam-transport chambers. Positioned at the ends of the bending magnet vacuum chambers, they feature CF63-compatible, turning-focused geometries. Each absorber incorporates one or two K-type thermocouples in 192 mm long, Ø6 mm stainless steel sheaths, enabling the sensing tip to be positioned near the maximum temperature areas. Integrated cooling circuits, assembled with straight fittings to avoid welding, and dedicated reflection shields complete the design.

Almost all transversal photon absorbers are designed to have a minimum of ±2 mm acceptance of beam deflections, keeping maximum temperatures below 280°C, while receiving powers close to 3 kW and power densities of more than 540 W/mm^2 at normal incidence.

These absorbers build on previous work [5], adapting established design principles to Elettra 2.0 sources requirements [1]. The resulting configurations can be then grouped into three families: toothed, holed, and hybrid.

Toothed Photon Absorbers

Toothed photon absorbers (Fig. 1) are associated to bending magnets without insertion devices, representing thus the strict majority. They are characterized by a one-sided toothed geometry with an open top, a configuration that simplifies machining and manufacturing. Dedicated reflection shields are included to prevent reflected photons from hitting the stainless-steel walls of their hosting chamber. The teeth are optimized to withstand the high spatial power densities imposed by the short source-to-absorber distance, which at a minimum of 0.40 m results in more than 640 W/mm² at 90° incidence

Slotted versions of toothed absorbers are dedicated to bending magnets beamlines, featuring a cut-out to let photons through. Near the cut, the teeth sequence is optimized to prevent thin regions or problematic reflections using a transition tooth, as can be seen in Fig. 2.

† giulio.scrimali@elettra.eu

ISBN: 978-3-95450-263-9 ISSN: 2673-5520 doi: 10.18429/JACoW-MEDSI2025-WEP31

FLANGE APERTURE GAP RF CONTACT GASKET FOR Elettra 2.0 STORAGE RING

I. Mrak†, G. Scrimali, S. Cleva, Elettra-Sincrotrone Trieste, Trieste, Italy

Abstract

The fourth-generation X-ray source Elettra 2.0, currently under development, aims to significantly enhance the brilliance and coherence of the emitted light, with high currents and ultra-low emittances as design goals. Fourth generation machines have tight constraints in terms of beam coupling impedance, requiring that the flanged connections along the beam orbit contributes as less as possible to the storage ring impedance budget, either by reducing the flange aperture gaps ideally to zero (zero-gap flanges connections), or by properly shielding the cavities generated (RF contact fingers). Space constraints of Elettra 2.0 limit the usage of conventional RF contact fingers, and the storage ring includes components where zero-gap flanges connections cannot be applied. This paper presents a compact RF contact gasket designed to work within the constraints of Elettra 2.0 chambers, inside the cavity created by the coupling of two CF40 flanges. The geometry is presented, along with its characterization with finite element modelling and RF impedance calculations. A presentation of prototypes is also included.

INTRODUCTION

Elettra operates for users since 1994, being the first third generation light source for soft X-rays in Europe. After 32 years of operation, the facility is going through a massive upgrade to the fourth-generation light source Elettra 2.0. The existing 12-fold two-bend achromat lattice of Elettra will be replaced with a modern 12-fold symmetric six-bend enhanced achromat lattice (S6BA-E), while keeping the same storage ring circumference (259.2 m). The new lattice will reduce the horizontal emittance by approximately 50 times, increasing X-ray brilliance and coherence by more than two orders of magnitude [1].

To achieve such performances, an important factor to consider is the electron beam stability. The stored beam, interacting with its environment, generates electromagnetic fields (known as wake fields), which act back on the beam itself. Those interactions are quantified in terms of impedance and can generate instabilities and deteriorate both beam lifetime and quality [2, 3]. Each component along the electron beam orbit contributes to the total impedance of the machine. In the design phase, the goal is to reduce the total impedance of the machine as much as possible, to be within the impedance budget which ensures beam stability.

To minimise the beam coupling impedance of flanged connections, the gap between flanges has to be reduced as much as possible, ideally to zero by using zero-gap gaskets, avoiding the creation of any cavity between the flange surfaces. Elettra 2.0 will mainly use zero-gap flanged connections by means of flat seals with the chamber profiles embedded in the gasket design. Though, a few components (mainly valves) are unable to be adapted to the flat, zero-gap design, requiring a different solution. This paper presents a CF-flanges-compatible, compact, alternative solution to zero-gap gasket for the rhomboidal profile chambers, that is used in Elettra 2.0 in all the cases where conventional zero-gap approaches [4, 5] cannot be implemented because of space constraints.

RF CONTACT GASKET DESIGN

The proposed solution is the usage of a compact contact RF gasket in addition to the standard CF vacuum gasket. Elettra 2.0 flanges are modified DN40CF-F, (ISO 3669:2020), where the rhomboidal chamber profile has been integrated in the geometry. Previous work on their impedance contribution [3] referred to them as "spigot flange lip" (SFL). As previously analysed, two closed SFL flanges generate a cavity between their respective inner lips and the CF gasket (Fig. 1), leaving a "gap", whose definition is the distance between two connected SFL flanges measured between the frontal surfaces of their inner lips. In order to shield this cavity, the RF gasket is mounted on frontal surface of the lip. The outer edge of the lip is used for the gasket positioning and keeps the gasket in place during assembly.

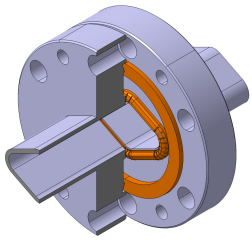

Figure 1: The CF40 flanged connection of rhomboidal chamber.

The gasket has a rhomboidal shape, which follows the chamber profile (Fig. 2) and has cuts along its surface that are used to pump vacuum in the generated cavity.

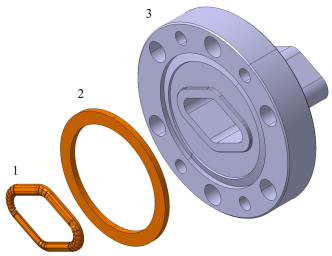

Figure 2: the RF contact gasket (1), the CF vacuum gasket (2), the SFL CF40 flange (3).

The cross-section of the RF gasket is shown in Fig. 3. The RF gasket is made by stamping process in annealed

† igor.mrak@elettra.eu

ISBN: 978-3-95450-263-9 ISSN: 2673-5520 doi: 10.18429/JACoW-MEDSI2025-WEP32

IMPROVING THE SPUTTERED TITANIUM FILM FOR THE NIK CERAMIC CHAMBER IN TPS

C.S. Huang, B.Y. Chen, Y.C. Liu, W.Y. Lai, C.J. Lin, T.C. Tseng, C.K. Kuan
National Synchrotron Radiation Research Center, Hsinchu, Taiwan, R.O.C.

Abstract

The development of the Nonlinear In-vacuum Kicker (NIK) is one of the key projects of the Taiwan Photon Source (TPS). Efficient conduction of the image current generated by the stored beam requires the deposition of a highly conductive titanium thin film on the inner surface of the NIK ceramic chamber. Based on tests involving the sputtering of a 5.5 μm titanium film onto a 34 cm × 6 cm ceramic substrate, the uniformity of the titanium film was controlled within 5%. The adhesion strength between the titanium film and the ceramic substrate reached 60 MPa, and the electrical resistivity was measured at 7.2 × 10^{-5} Ω·cm. This paper presents a detailed overview of the coating system, experimental methodology, and test results.

INTRODUCTION

The development and manufacturing of the Nonlinear In-vacuum Kicker are intended to enhance the electron beam injection efficiency, as compared to the four injection kickers currently used in the TPS. Using DC magnetron sputtering technology, a 5.5 μm titanium film is deposited on two ceramic substrates sized 34 cm x 6 cm and installed inside the NIK vacuum chamber. It is used to conduct the image current of the stored beam and reduce the waveform attenuation of the pulsed magnetic field induced by eddy currents [1, 2].

The main principle of sputtering is to use the target material as the cathode and the substrate as the anode. Glow discharge is generated by introducing a working gas in a vacuum environment and applying a DC or AC voltage between two electrodes. Positive ions in the plasma are drawn to the target material by the negative voltage on the cathode, causing surface bombardment. Atoms from the target material gain kinetic energy and escape the target surface into the plasma zone. Finally, the atoms diffuse onto the substrate and form a thin film. This technology is widely applied in the production of optical films, metal coatings, ceramic films, and various other applications [3-5].

To meet the requirements of the NIK ceramic chamber, the uniformity of the titanium film must be maintained within 5%. Therefore, the sputtering system was upgraded to improve the uniformity of film deposition on large-area substrates. After testing, the titanium film has achieved the required thickness and uniformity, with good adhesion and electrical resistivity. The detailed results are as follows.

EXPERIMENTAL

The sputtering system used in this report has a total length of 4.36 meters, with a maximum component size of 1.2 meters in length and 0.10 meters in height, as shown in Fig. 1. It is equipped with two magnetic sputtering sources, which are vertically mounted in front of the substrate. During the coating process, the substrate is fixed on a moving platform that is driven in a reciprocating motion by a stepper motor.

Figure 1: The sputtering system.

To meet the requirements of the Nonlinear In-vacuum Kicker, two ceramic substrates, each measuring 34 cm × 6 cm, needed to be coated with a 5.5 μm thick titanium film with a uniformity of 5%. Therefore, an 80 cm × 6 cm support was first fabricated to mount five sets of glass substrates for thickness testing and ceramic substrates for adhesion and electrical resistivity evaluations, as shown in Fig. 2. In the early stage of the titanium coating process, only one sputtering gun was used. However, to shorten the processing time, two sputtering guns were used simultaneously for the titanium coating, which effectively reduced the overall process time.

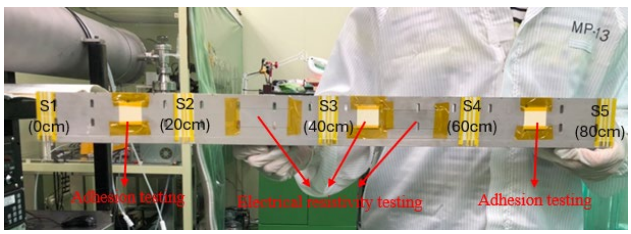

Figure 2: Coating test for 80 x 6 cm support.

The parameters of the titanium coating process involved the use of two 3-inch titanium targets with a purity of 99.999%, each mounted on a separate sputtering gun. Argon (99.999%) was introduced as the process gas, with the process pressure set at 3 mTorr. A DC power of 120 W was applied to generate plasma in a vacuum environment. This report will describe the process improvements made to complete the coating of two ceramic substrates for use in NIK ceramic chamber.

ISBN: 978-3-95450-263-9 ISSN: 2673-5520 doi: 10.18429/JACoW-MEDSI2025-WEP40

MAX IV PHOTOINJECTOR GUN

L. Roslund*, J. Andersson, H. Duarte, D. Kumbaro, R. Svärd, MAX IV Laboratory, Lund, Sweden

Abstract

This paper presents the latest photoinjector gun developed for the Short Pulse Facility (SPF) at MAX IV. The focus is on the mechanical design, which has been optimized around a simulated RF internal volume to ensure high performance and precision. Key areas of investigation include RF tuning strategies, thermal management via integrated internal cooling channels, and the challenges encountered during manufacturing and assembly, along with the corresponding engineering solutions. Design enhancements introduced throughout development are highlighted to provide insights into technical progress and practical experience. Potential future improvements are also discussed, targeting further optimization of performance, efficiency, and long-term operational reliability.

INTRODUCTION

The MAX IV linac [1] has two different electron sources. A thermionic RF gun used for injection to storage rings, and a photo-cathode RF gun for production of electrons for the Short Pulse Facility (SPF) [2] and the possible future soft x-ray free electron laser SXL [3]. To increase the performance of the linac pre-injector a new photoinjector gun has been under development during some years with the goal of reaching 100 Hz repetition rate. Tuning, conditioning and tests is being performed in our gun test facility [4]. The gun is powered by a pulsed klystron and a laser system [5].

THE INTERNAL VOLUME

The volume (see Fig. 1) consist of two cells, the rear cell houses the cathode from where electrons are released and the front cell has all connections. The connections are RF input from the top with a symmetry reflector in the bottom, two small exits on the side where RF is monitored, the opening to the rear cell and the ejection port of the gun. Simulations has initially been performed in COMSOL and later in CST.

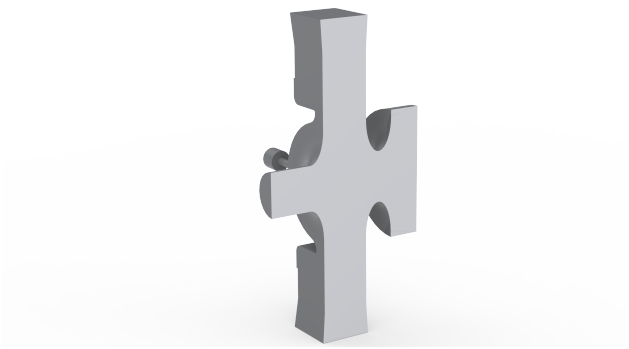

Figure 1: Internal volume of photoinjector gun.

THE GUN DESIGN

The design (see Fig. 2) has focused on three main goals apart from respecting the inner volume. Cooling performance, manufacturability, and tolerance chains. In order to realize the internal volume multiple bodies has to be merged together as it is not manufacturable with enough precision and surface finish as one body. To keep the tolerance chain down, both cells is manufactured in one body with an iris wall separating them. This means that all of the most important dimensions is maintained by this body. Completing the closing of the volume is the lid with the ejection hole. It mainly have to have the profile of the exit and be centred on the main body which makes the tolerance chain simple and with a minimum of dependants. To these two bodies which is made of OFHC copper all flanges is attached. LIL flanges on the top and bottom is tapered to bridge the change in aperture in the waveguides to the aperture in the gun. A DN 40 CF flange is connecting the to the accelerator and on the sides DN 16 CF flanges allows monitoring with antennas and on the rear a DN 100 CF allows the mounting of the cathode.

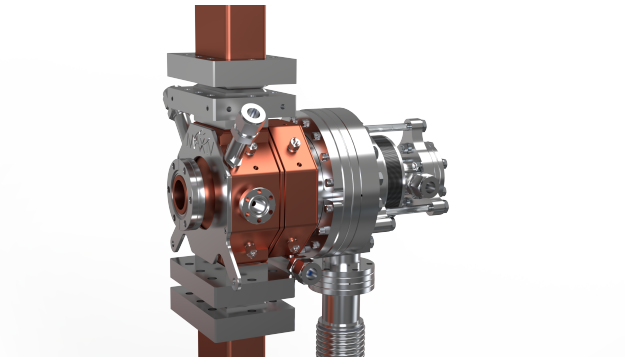

Figure 2: Photoinjector gun with cathode clamp and waveguides connected.

COOLING PERFORMANCE

The cooling is focused in-between the cells and at the end of the cells with a circular or semi circular flow at these locations. Holes bridge the three sections which is machined from outside and then they receive caps that are brazed on. Water connections is brazed on the side of the gun with two inlets placed at the rear bottom underneath the cathode and the exits at the front top of the gun on each side of the waveguide entrance (see Fig. 3). With the gun running with a repetition rate at 100 Hz a flow of 4 l/s on each of the total three circuits with a water temperature of 25 °C is required to keep the temperature between 45 °C and 55 °C in the gun body (see Fig. 4).

* linus.roslund@maxiv.lu.se

ISBN: 978-3-95450-263-9 ISSN: 2673-5520 doi: 10.18429/JACoW-MEDSI2025-WEP42

MECHANICAL DESIGN AND DEVELOPMENT STATUS OF A SUPERCONDUCTING WAVELENGTH SHIFTER FOR SIRIUS

G. R. de Oliveira†, W. E. Ricardo, P. Souza, T. Jasso, G. Pilon,
M. Rocha, I. Cavassani, P. Martins
Brazilian Center for Research in Energy and Materials, Campinas, Brazil

Abstract

A cryogen-free Superconducting Wavelength Shifter (SWLS) designed to generate a peak magnetic field of 6.6 T, operating at 5 K, is currently under development for an upcoming hard X-ray beamline of Sirius, the Brazilian synchrotron fourth-generation light source. This work presents an overview of the mechanical development of several key subsystems of the SWLS. It includes the design and fabrication of the clamps for both lateral and central coils, the development of all thermal components responsible for coupling the cold mass to the cryostat cooling stages, and the construction of the base frame that supports the SWLS cold mass. Additionally, the implementation and testing of Kevlar wires used to suspend the base frame are described. The design of the vacuum chamber through which the beam will pass is also presented, along with the tolerance analysis to ensure the 0.5 mm gap between the coils and the vacuum chamber is maintained. The project also considers the reuse of some parts from a decommissioned Superconducting Wiggler previously operated at UVX. This article summarizes the ongoing mechanical design and development of the SWLS project.

INTRODUCTION

Sirius, the Brazilian 4th generation synchrotron particle accelerator, is set to receive a new beamline of high-energy X-rays. The insertion device that will operate this beamline is a cryogen-free 6.6 T Superconducting Wavelength Shifter (SWLS) [1]. To ensure conformity with Sirius optics specifications, the SWLS design must incorporate a high-field region measuring 30 mm in width, a magnetic gap of 7 mm, and Holmium poles, which are known for their high flux concentration properties at low temperatures [2]. Consequently, the operating temperature is maintained below 5 K.

Meeting the necessary specifications for the source of this beamline is a significant challenge in many areas, such as manufacturing, assembly, and thermal conditions.

This study presents an overview of the mechanical design of the SWLS and the progress of the final manufacturing and assembly steps.

MAGNET COILS

The NbTi coils of SWLS are refrigerated by clamps in aluminum, because of the difference in thermal expansion coefficients, which causes the components to move closer together. This effect makes the clamps contract more and press against the coils [3].

The magnetic structure is composed of two lateral coils and one central coil. In both cases, the strategy employed to develop the clamps involved the as-built construction of the coils in a CMM by generating a dense point cloud (approximately one point every 0.5 mm). This information was then processed using CAD to design a surface very close to the coil at the aluminum clamp.

An interference analysis of the coil and clamp was performed using the 3D model and the point cloud, by best-fitting them (Fig. 1). For the central coils, the interference target was set to 0 mm, because their clamps are bipartite. For the lateral coils, the target was set to 0,075 mm, due to the assembly method, which considers heating for thermal expansion.

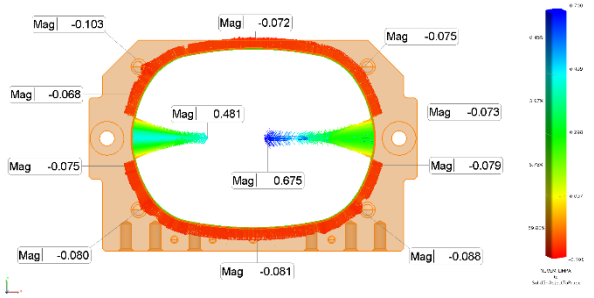

Figure 1: Interference analysis of a lateral coil/clamp.

To ensure that the central coil and clamps are in contact with the magnetic carbon steel yoke, a fixed clamp is placed in vertical contact against the bipartite clamp and is bolted under the yoke. Its parallel responsibility is to apply pressure to the bipartite clamp against the coil, using M8 bolts and Belleville washers (Fig. 2). The bolts were tightened to a torque of 6 N·m, using a set of Belleville washers, resulting in 70% deformation.

This approach guarantees that the coil, the clamp, and the yoke maintain optimal contact, safeguarding the system functionality and the thermal specifications. Both coils were tested in a vertical cryostat, and have achieved simulation results.

†gustavo.rovigatti@cnpem.br

ISBN: 978-3-95450-263-9 ISSN: 2673-5520 doi: 10.18429/JACoW-MEDSI2025-WEP44

MECHANICAL DESIGN OF HIGH HEAT LOAD FRONT-END FOR IVU BEAMLINE AT KOREA-4GSR*

Jongha Park†, Hyung-seok Choi, Young-duck Yun, Sungnam Kim, Jehan Kim, Ki-jeong Kim
Pohang Accelerator Laboratory, Pohang, Republic of Korea

Abstract

The Korea-4GSR, to be built in Ochang, South Korea by 2030, is a new 4th generation synchrotron radiation facility. It is designed with an electron beam energy of 4 GeV, a stored electron beam current of 400 mA, and an emittance of 62 pm·rad. In Phase I, 10 beamlines will be constructed, five of which will use the IVU24 undulator. When the undulator gap is set to 5 mm, the X-ray source has a total power of 17.95 kW and peak power density of 165 kW/mrad².

The High Heat Load Front-End(HHLFE) system is designed to absorb up to 17 kW of heat using a fixed mask and a movable mask, ensuring that only the central cone is transmitted to the beamline optical devices. The main materials are GlidCop or CuCrZr, selected for their high thermal conductivity, and the cooling channels are designed with a rectangular cross-section to maximize the heat exchange area for efficient thermal management. In addition, tungsten is applied to precisely shape and effectively absorb the X-ray beam.

The structural design of the heat-absorbing devices was determined based on thermal analysis results. This presentation introduces the structural and mechanical design details of the HHLFE.

INTRODUCTION

The front-ends are the sections tangential to the storage ring. Most of the front-end components are housed inside the storage ring tunnel enclosure. The synchrotron beam extracted from the storage ring must pass through the front ends first. In the Korea-4GSR Phase I, there are a total of 28 straight sections, of which there are 21 beam ports except for 3 RF cavities, 1 Injection, 3 Harmonic cavities, and are capable of extracting a synchrotron beam. As shown in Fig. 1. Each sector consists of an ID and a BM beam port. A Layout of both ID and BM front ends of the Korea-4GSR for one sector is shown in installation view (Fig. 2).

Required Front-end Types

The Korea-4GSR Phase I requires four types of front ends: (The name of Front-End was determined by referring to the APS Report. [1])

- IVU Front-End (IVUFE) for one In-vacuum undulator of period length 20, 22, 24.
- EPU Front-End (EPUFE) for one in Elliptically polarizing undulator of period length 78, 98.
- Canted Front-End (CANTEDFE) for two undulators of IVU24 and EPU78.
- Bending Magnet Front-End (BMFE) for bending magnet source.

Beamline Location

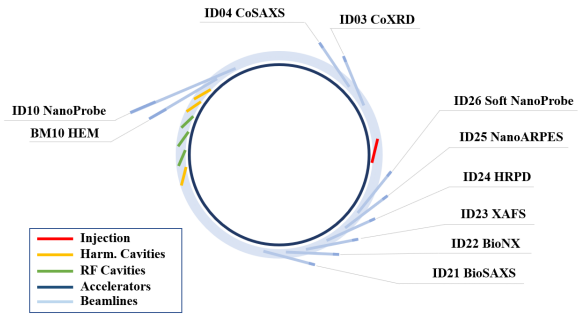

Figure 1: Beamline location in Phase I.

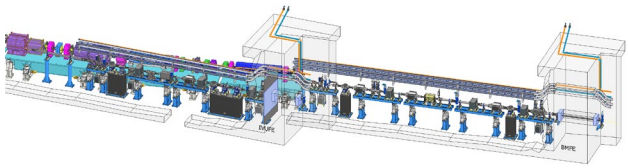

Figure 2: Installation view of IVUFE and BMFE.

Heat-load from IVU24

The IVU, EPU, Canted types Front-Ends are designed based on IVU24 with maximum power. The maximum output of IVU24 was applied when the 4 GeV, 400 mA storage ring operated in an in-vacuum undulator at 5 mm gap. Therefore, for the most severe scenario, the front-end must be able to absorb a total power and peak power density shown in Table 1.

Table 1: Heat Load of In-vacuum Undulator

Type of IVU24	IVUFE
Total Power	17.95 kW
Power density	165.5 kW/mrad²
White beam divergence	0.279 mrad, 0.128 mrad
Central cone divergence	0.01293 mrad, 0.01265 mrad

Total Power Distribution of IVU24

The divergence of white beam using spectra simulation shows distributed total power where movable mask's location (Fig. 3). And the movable mask is designed to absorb partial power as shown in Fig. 4.

* This research was supported in part by the Korean Government(MSIT: Ministry of Science and ICT) (No. RS-2022-00155836, Multipurpose Synchrotron Radiation Construction Project) and also supported by Pohang Accelerator Laboratory (PAL). PAL is supported by Korean Government(MSIT) and POSTECH.
† jonas81@postech.ac.kr

ISBN: 978-3-95450-263-9 ISSN: 2673-5520 doi: 10.18429/JACoW-MEDSI2025-WEP45

MECHANICAL DESIGN OF THE DIAMOND-II INJECTION STRIPLINES

V. Zhiltsov*, A. F. D. Morgan, A. Lueangaramwong, A. Amiri, I. P. S. Martin, L. Bobb, M. P. Cox, N. Warner, R. Fielder, R. Grant, T. Lockwood, W. Tizzano
Diamond Light Source, Didcot, UK

Abstract

Transparent injection is a key goal of the upgrade of Diamond Light Source to a fourth-generation synchrotron, Diamond-II. This work presents the mechanical design of the Diamond-II K01 straight, which includes three pairs of injection stripline modules, and highlights the following aspects of the design: the general layout (covering the location of the modules, vacuum pumping, and protection from synchrotron radiation); detailed design and assembly of the stripline modules; lessons learned from the testing of the stripline prototype on the existing machine. The general layout ensures that the modules are optimally positioned to maximize efficiency and minimize interference from synchrotron radiation. The detailed design and assembly process involved rigorous testing and refinement to ensure that each component met the high standards required for operation in a high-energy environment. Lessons learned from the prototype testing provided valuable insights into potential improvements and adjustments needed for the final design, ensuring that the system will perform reliably under operational conditions.

K01 STRAIGHT LAYOUT

The mechanical layout of the Diamond-II [1, 2] K01 straight was driven by the need to integrate a sufficient number of stripline pairs within a tightly constrained space of ≈2.6 m. The design also had to ensure effective radiation shielding, maintain vacuum performance, and implement smooth aperture transitions with taper ratios between 1:5 and 1:10 to minimize impedance and beam disturbance.

The downstream end of the straight section provided a clear starting point for the layout, offering favorable phase advance and available space for effective injection. The first module was positioned at this location, and subsequent components were added progressively upstream. This reverse design approach helped optimise space usage and simplify integration with surrounding systems.

To shield the striplines from synchrotron radiation originating from the upstream DQ dipole, custom absorbers were designed. Their tips were positioned as close as possible to the beam stay-clear envelope, typically around 0.38 mm. As the beam stay-clear dimensions vary significantly along the beam path, especially in the horizontal plane with excursions up to 2.3 mm, each absorber was individually tailored in length and shape to match its specific location.

Initial modelling was simplified using two-dimensional ray tracing and basic component geometries. A clearance of 2 mm between the stripline blades and the radiation fan was initially targeted as optimal.

The original concept featured two modules, each containing four stripline pairs with a 14 mm diameter aperture. However, this configuration could not be adequately shielded from radiation. To address this, the design was revised to shorter modules with two stripline pairs each. A notch was introduced in the stripline blade to remove material exposed to the radiation fan, reducing the risk of damage and improving long-term reliability. After several iterations, the final configuration was selected: three modules, each containing two stripline pairs with a 3 mm diameter notch and a 16.2 mm aperture. This solution met both radiation protection requirements and power supply constraints [3].

In the final layout, illustrated in Fig. 1, the targeted 2 mm clearance between the stripline blades and the radiation fan was achieved for all stripline pairs except the second pair of the first module, where only 1.74 mm was possible due to spatial constraints.

A Synrad simulation that accounts for various missteering scenarios did not reveal any issues related to synchrotron radiation. RF heating and the combined thermal impact are yet to be assessed. If finite element analysis indicates that this is problematic, widening the notch could be considered. Given the strongly non-linear distribution of the heat load, even small increases in notch width would significantly reduce the total power deposited on the stripline.

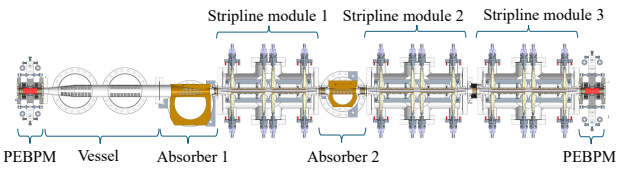

Figure 1: K01 straight layout.

DESIGN OVERVIEW

Diamond-II Stripline Kicker Types

Diamond-II will require two types of stripline kickers during normal operation [3]:

- Feedback kickers for the transverse multi-bunch feedback system
- Injection stripline kickers for transparent injection

While both types share a similar electrical design, they differ in vacuum layout, orientation (vertical vs horizontal), and most notably in voltage requirements.

The feedback kicker is expected to operate with a maximum peak voltage of 100 V, whereas the injection kicker is

* vitalii.zhiltsov@diamond.ac.uk

ISBN: 978-3-95450-263-9 ISSN: 2673-5520 doi: 10.18429/JACoW-MEDSI2025-WEP46

MECHANICAL ENGINEERING DESIGN OF THE DIAMOND-II INJECTION SYSTEMS

W. Tizzano*, S. R. Ahamad, C. Bailey, M. P. Cox, D. Grenville, T. Lockwood, I. P. S. Martin, A. Shahveh, V. Zhiltsov, Diamond Light Source, Didcot, UK

Abstract

This work presents the mechanical engineering design of the Diamond-II injector, which includes a new low-emittance booster with combined function magnets, modifications to the existing transfer lines and a novel storage ring injection scheme. The latter features two alternative schemes: the first scheme is based on a traditional four-kicker closed bump paired with a novel in-vacuum thin septum, combined with an in-air permanent magnet thick septum. This arrangement will be used for commissioning and initial fill of the ring; the second scheme, used for top-up during user operation, aims to deliver transparent injection and it is based on innovative stripline kickers.

INTRODUCTION

The Diamond-II Programme, to deliver to the scientific community the benefits detailed in its science case, will have at its core a new Storage Ring (SR) based on a Modified Hybrid 6-Bend Achromat (M-H6BA) [1–3].

To achieve high injection efficiency into the new low-emittance SR, as well as transparent top-up, a new booster and a new injection scheme are needed [4]. The remainder of this paper will describe the mechanical engineering design of the various injection systems, the technical challenges faced and the solutions identified.

BOOSTER

The main reasons to replace the booster are the fact that its extraction energy has to match that of the new SR (3.5 GeV, up from 3.0 GeV), and that, to inject efficiently into the proposed M-H6BA lattice, a booster ring emittance below 20-30 nm rad and a bunch length below ≈40 ps rms are required [4].

A booster with a lattice satisfying the requirements above based on Theoretical Minimum Emittance (TME) was proposed, however this design was later superseded by one based on combined-function magnets which both reduced their number and relaxed the required field parameters [2, 4–6]. Table 1 shows a comparison between some of the existing booster parameters and its Diamond-II replacement.

Table 1: Booster Parameters at Extraction [4]

Parameter	Existing Booster	New Booster
Energy Range	0.1-3.0 GeV	0.1-3.5 GeV
# Cells	22	36
Circumference	158.4 m	163.8 m
Emittance	134.4 nm rad	17.7 nm rad
Nat. Bunch Length	99.3 ps	38.7 ps

General Layout

Figure 1 shows a schematic representation of the general layout of the Diamond-II booster. The existing Personnel Safety System (PSS) zones will be retained, but the fences will need to be modified to accommodate the new booster. The booster will be divided into four sectors by vacuum gate valves to facilitate installation and maintenance and connections to the corresponding Computer and Instrumentation Areas (CIAs). The straight sections between the racetrack arcs include the components below [3]:

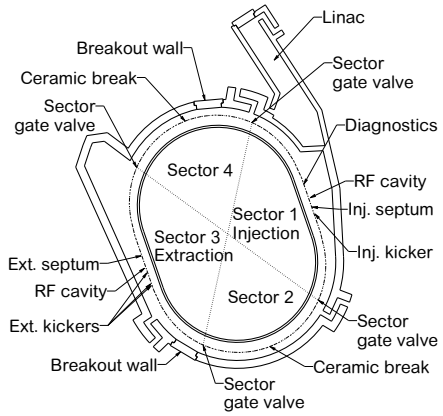

Figure 1: Diamond-II booster general layout.

- **RF cavities:** the existing pair of five-cell cavities will be relocated and reused, however the tapers at each extremity have been redesigned to match the aperture of the surrounding components.
- **Septum magnets:** Whilst the injection septum will be based on the existing design, the extraction septum will use the same design of the SR injection septum described in the "Injection into the Storage Ring" section.
- **Kicker magnets:** four custom-designed in-vacuum kickers will be used, one for injection and three for extraction. They have a modular design where the main magnet module is identical to reduce cost and the end modules have different apertures to match the surrounding components.
- **Additional diagnostics:** other than the BPMs distributed around the ring, additional diagnostics included in the straights include two screens, current monitor, striplines and DC Current Transformer (DCCT).

* walter.tizzano@diamond.ac.uk

ISBN: 978-3-95450-263-9 ISSN: 2673-5520 doi: 10.18429/JACoW-MEDSI2025-WEP47

MECHANICAL EVALUATION AND CAD MODELLING FOR MAX 4U: MAX IV STORAGE RING UPGRADE

K. Åhnberg†, E. Al-Dmour, Å. Andersson, A. M. Carboneres, M. Grabski, P. F. Tavares
MAX IV Laboratory, Lund, Sweden

Abstract

MAX 4U is an upgrade project of the MAX IV 3 GeV storage ring, to be realized by the early 2030's in Lund, Sweden. The goal of the upgrade is to reduce the horizontal electron beam emittance to below 100 pm·rad. A new magnet lattice will be used to achieve this goal. Many different scenarios for different lattices are evaluated from the mechanical engineering aspect to serve as input for the final lattice choice. In this paper, we describe the method used to build CAD-models for the evaluation work and how the components are affected, both mechanical and thermal loads on the vacuum system from the new synchrotron radiation power.

INTRODUCTION

The work on the lattice design and the engineering design for MAX 4U [1] is progressing in parallel. Several lattice configurations have been studied, and components have been investigated to match the modified beam dynamics requirements.

MAX 4U goals and boundary conditions:

- Electron beam emittance ≲ 100 pm·rad
- Electron beam energy: 3 GeV
- Keep shielding wall
- Keep light source positions
- Keep injector and accumulation capability
- Limited dark period
- Cost-effective
- Realizable until the early part of the next decade

As defined by the project boundary conditions, the overall layout with shielding walls, source positions, injector and energy of the MAX 4U storage ring will correspond to the existing MAX IV 3 GeV ring [2].

The MAX 4U ring is divided into 20 cells, with each arc section measuring 21.6 m and each straight section 4.5 m in length. The machine is designed to operate at 3 GeV with a beam current of 500 mA. The magnet layout and apertures follow the 7-Bend Achromat (7BA) scheme implemented at MAX IV and take advantage of the closed magnet block design concept. A summary of the main storage ring parameters is provided in Table 1.

Table 1: MAX 4U 3 GeV Storage Ring Main Parameters

Parameter	Value
Energy	3 GeV
Design Beam Current	500 mA
Horizontal bare emittance	<100 pm·rad
Circumference	528 m
Number of achromats	20
Straight section length	4.5 m

LATTICE

One of the main changes to the MAX 4U is the introduction of reversed bends. The orbit change in a single dipole can be 9 mm in the most extreme case and for a full achromat the change in orbit can be up to 64 mm in the center of the middle magnet block (U3).

Key Considerations

The following aspects has been considered during the mechanical integration for MAX 4U

- Orbit displacement: comparison with the MAX IV standard lattice to reveal shift of the beam path.
- Power deposition: stronger dipole fields, reverse bends and distance to source increase radiated power and power density.
- Critical component shielding: Beam position monitors (BPM), bellow's, Radio frequency (RF) fingers must be protected from direct radiation exposure.
- Cooling requirements: new exposed regions to the photon beam may require improved cooling provisions.

In the evaluation work several lattices has been considered. Two types have been selected for MAX 4U to be presented in the Conceptual Design Report (CDR).

Absolute Requirement (AR) Lattice

The AR lattice type is a new orbit which fulfils all goals and boundary conditions of MAX 4U. This is cost effective with limited dark period and efficient reuse of many components.

Stretched Goal (SG) Lattice

The SG lattice aims for a lower emittance than AR and assumes a deeper intervention with more vacuum chambers and magnets replaced. Still keeping all goals and boundary conditions.

RAY TRACING

Orbit trajectories and vacuum chamber walls is represented as spline-driven geometries (Fig. 1) in SolidWorks CAD. Beam path coordinates are imported from the lattice files provided by accelerator physics group, enabling a direct comparison between the reference MAX IV orbit and new MAX 4U orbits. This allows a fast evaluation of each proposed lattice for feedback to other work packages within MAX 4U project. With checking the start and end of the bends the irradiated areas are identified.

† karl.ahnberg@maxiv.lu.se

ISBN: 978-3-95450-263-9 ISSN: 2673-5520 doi: 10.18429/JACoW-MEDSI2025-WEP49

MECHANICAL SYSTEM OF THE DOUBLE-PERIOD UNDULATOR PROTOTYPE FOR SHINE

S. W. Xiang, T. T. Zhen†, S. D. Zhou, Y. Y. Lei, J. Yang, W. Zhang,
Z. Q. Jiang, Y. Zhu, H. X. Deng
Shanghai Advanced Research Institute, Chinese Academy of Sciences, Shanghai, China

Abstract

The Shanghai High repetition rate XFEL and Extreme light facility (SHINE) is under construction and aims at generating X-rays between 0.4 and 25 keV with three FEL beamlines at repetition rates of up to 1 MHz. The three FEL beamlines of the SHINE are referred to as the FEL-I, FEL-II, and FEL-III. Shanghai Advanced Research Institute (SARI) will manufacture 14 double-period undulators for the FEL-II. The double-period undulator is equipped with two rows of magnetic array of different period lengths on the same girder, and magnetic force compensation is achieved by translating the upper and lower magnetic array with a certain longitudinal offset. A double-period undulator prototype has been developed by SARI. This paper describes the design, simulation, and measurement results of mechanical system.

INTRODUCTION

FEL-II is the most versatile of the three FEL beamlines for SHINE [1-3], including SASE, self-seeding, EEHG, polarization control, and several advanced FEL modes [4]. The radiation undulator used for the EEHG operation is mainly the double-period undulator with working period length 55 mm and 75 mm respectively. The relatively lower harmonics operation depends on U75 with lower beam energy and while U55 is mainly used for the higher harmonics. Working mode can be switched online.

MECHANICAL SYSTEM DESIGN

The mechanical system is composed of a base plate, a L-shape frame, steel girders, aluminum girders, main drive units, frame switching mechanism, girder switching mechanisms, and alignment jacks, as illustrated in Fig. 1. The main function of the mechanical system is to support and drive the upper and lower girders with magnetic array to move symmetrically relative to the beam center. Gap drive repeatability can achieve less than 1μm with four independent precision drive units and absolute linear encoders.

The frame is a welded steel structure supported by a set of six jacks for leveling and alignment. To ensure beam center height of 1.3 m and space for the frame switching mechanism, a wedge mechanism is used for height direction adjustment. This not only compresses the height dimension, but also achieves high adjustment resolution and stability, as illustrated in Fig. 2.

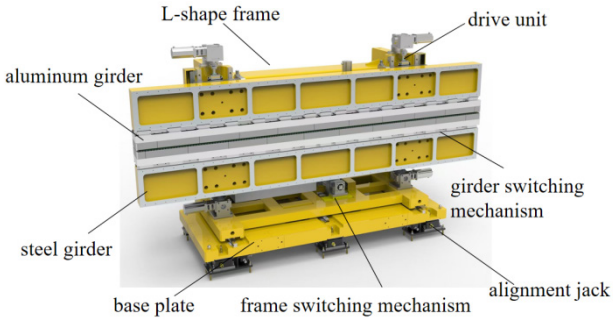

Figure 1: SHINE double-period undulator prototype mechanical system.

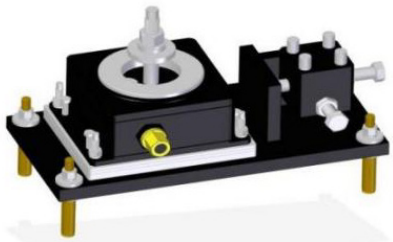

Figure 2: Jacks for leveling and alignment.

To minimize the bending moment caused by magnetic force, it is necessary to shorten the distance between the center of the magnetic array. Considering the influence of the magnetic field generated by the parallel magnetic array, it is necessary to ensure that the distance should not less than 100 mm according to physical analysis, as illustrated in Fig. 3. The frame switching mechanism is mounted on the base plate, and can switching working mode online through its lead screw and linear guide rails. The three rows of linear guide rails are beneficial for reducing frame deformation and improving smooth motion.

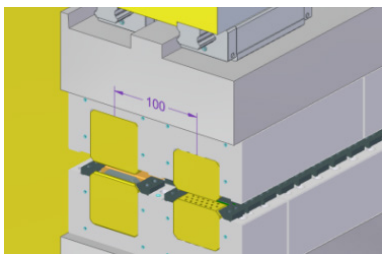

Figure 3: The magnetic array of U55 and U75 mounted on the aluminum girders.

If the magnetic array has no longitudinal offset, the magnetic force on the girder is the sum of the two undulators, which is about 117.3 kN in the Y direction. If the upper and lower magnetic array has a certain longitudinal

† zhentt@sari.ac.cn

ISBN: 978-3-95450-263-9 ISSN: 2673-5520 doi: 10.18429/JACoW-MEDSI2025-WEP50

MOCKUP ASSEMBLY OF AN SRF MODULE: SPACEFRAME AS TOOLING AND STRUCTURAL SUPPORT FOR HIGHLY HOM-DAMPED CAVITIES

N. Wunderer*,[1], F. Pflocksch†,[1], D. Böhlick[1], V. Dürr[1], A. Frahm[1], F. Glöckner[1], J. Knobloch[1,2], N. Ohm[1], H. Plötz[1], K. Schemmel[1], M. Schuster[1], A. Velez[1,3], S. Wiese[1], D. Wolk[1]
[1]Helmholtz-Zentrum Berlin, Berlin, Germany
[2]University of Siegen, Siegen, Germany
[3]Technical University Dortmund, Dortmund, Germany

Abstract

To support the elliptical VSR cavities featuring five protruding waveguides, a spaceframe was engineered to serve a dual purpose: providing structural support and functioning as tooling during assembly. This spaceframe facilitates cavity rotation in the cleanroom, simplifying the installation of HOM loads and fundamental power coupler components. Designed specifically for the particular cavity geometry, the spaceframe has a diameter of 1.5 m and provides axial and radial support for the cavity, along with its ancillaries, magnetic and thermal shields, and piping. A mockup assembly was conducted to evaluate the design's functionality, assessing key aspects such as rotation and railing performance, cavity support and alignment, and the mountability and stability of ancillary components.

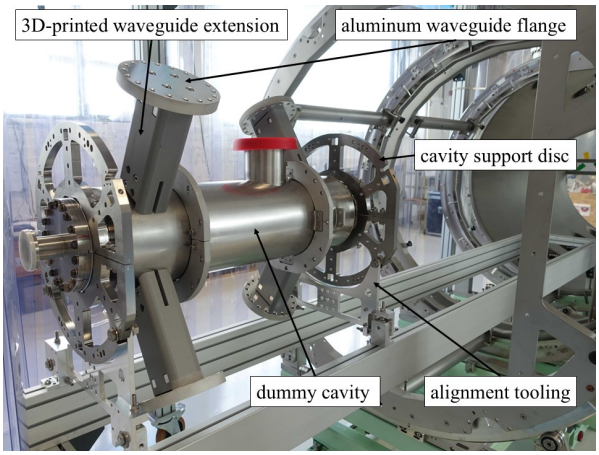

Figure 1: Dummy cavity on the installation table during alignment before installation into the spaceframe.

INTRODUCTION

The variable storage ring (VSR) project has aimed at providing long and short pulses in the BESSY II storage ring using a beating scheme achieved by installing two pairs of cavities – at 1.5 GHz and at 1.75 GHz [1]. To demonstrate the feasibility of all required components and processes, the VSR DEMO module was designed. This module houses two 1.5 GHz superconducting RF (SRF) cavities with fundamental power couplers. The module design is described with a focus on the installation process in the following. For further information on the mechanical aspects of the module design please see Ref. [2]; for the cold string components, see Refs. [3] and [4]; and for the cavity, see Ref. [5].

MODULE DESIGN CONCEPT

Many elements of the VSR DEMO cold string are somewhat peculiar and present challenges during installation and operation. The most demanding components are the 1.5 GHz SRF cavities with five protruding waveguides, each terminated by a higher order mode (HOM) load at room temperature. These cavities are supported by a modular spaceframe, segmented per cavity and connected after completing the cold string assembly. Unlike the ESS monolithic frame (cf. [6]), this segmented design allows the spaceframe to serve as part of the tooling during HOM load installation.

To support the five waveguides per cavity, the spaceframe requires a 1.5 m diameter, presenting a unique design challenge. A spaceframe design was favoured over other design approaches (as compiled in Ref. [7] and cf. Ref. [8]) to maximize the position stability of the cold string during cool-down. Additionally, the spaceframe and ancillaries are designed such, that the cavity can be rotated in steps of 60° for convenient and clean HOM installation. This mounting procedure is considered the safest approach to prevent particulate contamination of the cavity. Here, the spaceframe serves as part of the tooling. And at a later stage it also supports additional subsystems, including thermal and magnetic shields, helium piping, and interconnecting cold string elements such as bellows. The frame's C-shape (rather than circular) provides necessary access for coupler installation.

Once cold string and cold mass are assembled into the frame, this assembly is railed into the module. The module features ten rollers supporting the railing on the frame. When in position, support pins convert sliding bearings into fixed bearings.

Coupler warm part installation requires reaching from outside of the module into the cold mass down to the coupler cold part attached to the cavity. This installation will be performed without module doors to allow visual inspection.

INSTALLATION PROCEDURE

Installation of the cavity into the frame begins by transferring a cavity from its transportation frame onto a table with support discs, allowing sliding and alignment (cf. Fig. 1). The support discs also align the cavities in the spaceframe.

* nora.wunderer@helmholtz-berlin.de
† fabian.pflocksch@helmholtz-berlin.de

ISBN: 978-3-95450-263-9 ISSN: 2673-5520 doi: 10.18429/JACoW-MEDSI2025-WEP55

PROGRESSION OF THE DEVELOPMENT OF A FOUR-CRYSTAL MONOCHROMATOR FOR PETRA IV

J. Raabe†, J. Rauß, D. Weschke, W. Roseker, M. Sprung, O. Seeck
DESY Deutsches Elektronen Synchrotron, Hamburg, Germany

Abstract

The development of a four-crystal monochromator (4CM) represents a crucial step in advancing beamline instrumentation for PETRA IV, DESY's upcoming ultralow-emittance synchrotron source. Designed to fulfil the stringent requirements of fourth generation light sources, the 4CM as a low power device should provide an exceptionally stable possibility to adjust energy resolution, high order suppression and coherence properties while preserving the wave front quality of monochromatized beams. The poster presents the ongoing development of 4CM designed specifically for PETRA IV. Two different beamlines will be discussed and compared. This approach focuses on optimizing the crystal arrangement, vibration control and precise alignment to achieve excellent energy resolution and intensity. Utilizing silicon crystals in a channel-cut configuration, the monochromator ensures high mechanical stiffness and robust control, enabling stable operation over a wide energy range. In addition, the engineering challenges and solutions encountered during the design phase, including thermal management and mechanical stability, are outlined.

INTRODUCTION

With the further development of PETRA III to PETRA IV, nanometre-sized X-ray beams will be available with high intensity, high energy resolution, improved brilliance and unprecedent coherence properties of the X-ray beams [1].

The monochromator prepares the X-ray beam for the experiments. Many different techniques and methods will be offered at the beamlines, so that the requirements are based on different criteria. But despite all differences, what they all have in common is that the beam properties and wave front should be preserved.

A four-crystal monochromator enables the X-ray beam to be guided in the direction of the incident beam, which offers many advantages for operation. Particularly advantageous for beamlines is that the energy can be adjusted and the outgoing beam remains in the same position without having to move a crystal or readjust the sample. There is the opportunity to use a four-crystal monochromator for higher harmonic suppression as well, allowing for a high-resolution mode or maximising the coherence contrast.

An analysis of the PETRA IV beamline conceptional designs was carried out in respect to needs of a 4CM. Detailed requirements were collected by means of a beamline application survey. The results are not unambiguous and it emerged that the demands differ considerably depending on the experiment and method. For the first attempt of a prototype, the requirements were simplified in order to minimise and facilitate error management. Two beamlines that actually require a 4CM due to their experimental application were selected and compared in Table 1.

The Beamline PB24 for High Energy Diffraction and Scattering Tomography is requesting a 4CM in order to be able to realise measurements with monochromatic beams at different bandwidths at the same beam and sample position: a) a high photon flux mode (without 4CM) and b) a high energy resolution mode (with 4CM).

The Coherence Application Beamline PB69 will utilise a 4CM to maximise the achievable coherence contrast by employing high index reflections of Silicon crystals to reduce the energy bandwidth and increase the longitudinal coherence length.

Table 1: Comparison of two 4CM-requesting Beamlines

	Beamline PB24 High Energy Diffraction and Scattering Tomography	**Beamline PB69 Coherence Application Beamline**
h, k, l	220	220/440
Energy (keV)	40–100	7–25
Travel range (°)	1.85–4.7	7–27.5/15–38
Deflecting plane	horizontal	Vertical
Scan	No scan	Step scan
Distance to sample (m)	5–15	50
Retractable	Yes	Yes

DESIGN APPROACH

A comprehensive market research [2 - 7] revealed the pros and cons of various design approaches for 4CM. The concept for the 4CM is developed on the basis of requests from the PETRA IV beamline conceptional designs and considering findings from developments at other synchrotron radiation sources.

Challenging problems are the small Darwin widths of high index reflections especially at high energies, the need to ensure the parallelism of the crystal surfaces during scanning and the synchronisation of the Bragg axes. All studies aimed at improving stability were strongly considered as the stability requirements are very strict. To reach the stability requirements, it will be necessary to consider

† jana.raabe@desy.de

ISBN: 978-3-95450-263-9 ISSN: 2673-5520 doi: 10.18429/JACoW-MEDSI2025-WEP58

STRUCTURAL DESIGN OF THE INJECTION AND EXTRACTION ELECTROSTATIC SEPTUM OF PREF*

Yongxiang Pan†,1,2,3, Yajun Zheng1,2,3, Yongbin Lang1, Lu Zhang1, Xiaowei Xu1, Haijiao Lu1, Yan Cong1,2, Jingjing Zhang1, Haihua Niu1,2, Wenjun Chen1,2, Zeen Yao3
[1]Institute of Modern Physics, Chinese Academy of Sciences, Lanzhou, China
[2]University of Chinese Academy of Sciences, Beijing, China
[3]Lanzhou University, Lanzhou, China

Abstract

Proton Radiation Effects Facility (PREF), which is a dedicated accelerator generating 10-60 MeV proton beams for studying and testing the displacement damage effect, has been completed and is in operation in China. To achieve a compact and cost-effective synchrotron (circumference of 18 m), the electrostatic septum was developed with the requirement of providing uniform and continuously adjustable high field strength under limited space and extremely high voltage, while also meeting the performance and ultra-high vacuum demands of the structure. Lab tests confirm the design's superior compliance with physical requirements, and two years of operation demonstrate the devices' high stability and long-term reliability.

INTRODUCTION

Displacement damage effect [1] is known to cause performance degradation and functional failures in electronic components. The experimental evaluation of the displacement damage effect on electronic components by proton beam irradiation is an important approach to solving a series of key problems in the field of device space applications. The PREF (Proton Radiation Effects Facility), as China's first 60 MeV proton space science and technology experimental research accelerator for testing the displacement damage effect, has been designed and constructed by IMP (Institute of Modern Physics, Chinese Academy of Sciences).

The accelerator complex is composed of an Electron Cyclotron Resonance Ion Source (ECRIS), a linac injector, a compact synchrotron, and two irradiation terminals [2]. A schematic layout of the entire complex is shown in Fig. 1.

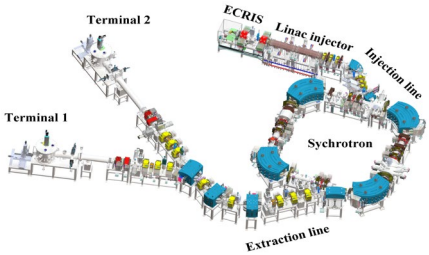

Figure 1: Overall layout of the accelerator complex.

Due to the specific operational requirements of the PREF facility and the growing trend toward accelerator miniaturization, the performance demands for accelerator components are becoming increasingly stringent.

As a core element for beam injection and extraction in synchrotrons, the electrostatic septum must provide a steady and easily adjustable electric field, even in very small spaces and at very high voltages. Furthermore, it must satisfy rigorous mechanical performance criteria and ultra-high vacuum compatibility. The development of such a device is essential for reducing the overall circumference of synchrotrons, which in turn lowers construction costs and enhances market competitiveness. The overall layout of the synchrotron complex is shown in Fig. 2.

Figure 2: Overall layout of the synchrotron.

DESIGN REQUIREMENTS

The physical parameters for the injection and extraction septum in the synchrotron were proposed by the physical designer, with the basic parameters shown in Table 1.

Table 1: Parameters of PREF Electrostatic Septum

Parameters	Injection	Extraction
Maximum voltage[kV]	85.0	130.0
Maximum field[kV • cm^{-1}]	30.46	84.5
Effective length[mm]	200	580
Bending radius[m]	3.4	25
Aperture size[mm^2]	23x30	15x30
Vacuum chamber size[mm]	450	450

DESIGN RESULTS

The electrostatic septum was required to deliver uniform fields of 30.46 kV/cm (injection) and 84.5 kV/cm (extraction) under an ultra-high vacuum of 1×10^{-8} Pa·m^3/s in the maximum gap of 23 mm and 15 mm, respectively. In order to avoid local discharge phenomena during the operation of the septum [3], based on existing design experience, the

* Work supported by the National Key R & D Program of China (Grant No. 2019Y313 FA0405400)
† panyongxiang@impcas.ac.cn

ISBN: 978-3-95450-263-9 ISSN: 2673-5520 doi: 10.18429/JACoW-MEDSI2025-WEP60

SURVEY AND ALIGNMENT OF BEAMLINES FOR ADVANCED PHOTON SOURCE UPGRADE

Altaf Khan, Jonathan Knopp, Mark Erdmann, Oliver Schmidt
Advanced Photon Source, Argonne National Lab, Lemont, United States

Abstract

As part of the Advanced Photon Source Upgrade (APS-U) Project, all 72 beamlines needed to undergo alignment to the new storage ring installation. Prior to beginning the alignment efforts, beamline geometry files were created to identify the location of components with respect to the beam source. For new beamline installations, the remaining process was simpler. New components were fiducialized in a lab, along with their support tables. Tables were then installed and aligned to the beamline geometry configuration and a final report was generated for approval. However, for existing beamlines, the process was more intricate. Fiducial records dating back to 1996 were used to generate fiducial files. However, some information was lost over the years. In response, new techniques were implemented to fiducialize components missing records in-situ to avoid removing components from the beamline. Existing component positions were measured with respect to the new source, then realigned. A report of pre-alignment and a report of realignment were generated for approval. All beamlines have undergone realignment in the course of one year and successfully gone through commissioning process.

MOTIVATION

As part of the Advanced Photon Source Upgrade (APS-U) project, 9 feature beamlines were built and 15 major enhancements. Additionally, all Bending Magnet (BM) beamlines were shifted laterally and longitudinally due to the new storage ring lattice. The original scope of work did not include realigning Insertion Device (ID) beamlines that were not upgraded. However, during the installation of the new APS-U storage ring, it was discovered that the original APS was not a perfect circle. Therefore, the question arose if the storage ring should be installed to match the existing positions of the beamlines or installed as designed and realign all of the beamlines. Ultimately, it was decided that all beamlines would be realigned so as to not sacrifice any performance of the storage ring.

METHODS

Storage Ring and Beamlines

The APS-U storage ring was aligned using a dense network of monuments and laser trackers as seen in Fig. 1. Each component was precisely aligned to within 100 microns of its nominal position. Once this network was finalized, it was expanded to the experimental floor to include the beamline sectors. Using the same network for storage ring and beamlines proved useful as beamline component positions could be measured with respect to the front end.

To align beamline components, a combination of laser trackers, portable Coordinate measuring machine (CMM) arms, and traditional optical equipment were used. The process for new beamlines versus existing beamlines were similar with some unique challenges.

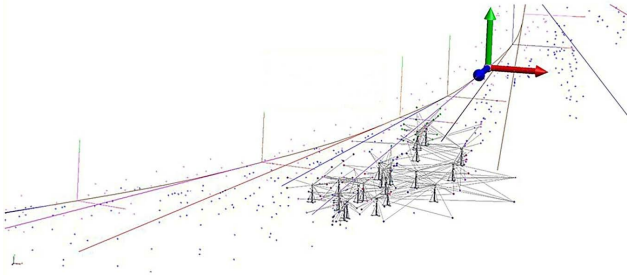

Figure 1: Screenshot of survey network inside the storage ring created using a series of laser trackers.

Aligning New Beamlines

To align new beamlines, the first step was for survey engineers to meet with beamline staff and engineers to review raytraces and component reference tables (CRT) which define the position of the component with respect to the source. The meetings were necessary as the documents were not necessarily consistent between beamline teams. The positions of the components were then placed in a metrology software package, Spatial Analyzer (SA), which incorporated data from the storage ring lattice and the beamline source. In addition to the positions, X, Y, Z, rotation angles about each axis could also be included.

Once the geometry file was created in SA, new components were fiducialized using portable CMM arms and optical scopes. External fiducials were used that could be measured by both CMM arms and laser trackers. Multiple components sharing a table were aligned with respect to each other and the table was fiducialized as well. Once the beamline components and tables were roughly installed, a laser tracker system was located using the beamline network and components were installed using the external fiducials. In the case of tables, the tables were aligned and then individual components were verified and adjusted if needed. It was important to verify the components as components can move once adjacent components are connected such as bellows and gate valves. Alignment of new beamlines averaged about 2 weeks of effort due to the enhanced capabilities of laser trackers over traditional optical methods.

As part of the upgrade, a new report format, as seen in Fig. 2, was created which showed the nominal position of

ISBN: 978-3-95450-263-9 ISSN: 2673-5520 doi: 10.18429/JACoW-MEDSI2025-WEP62

THE GIRDER SYSTEM PROTOTYPE FOR ALBA II STORAGE RING*

J. Boyer†, L. Ribó Mor, N. Gonzalez, B. de Abreu Francisco, P. Salmeron Roma, C. Colldelram
ALBA Synchrotron, Barcelona, Spain.

Abstract

ALBA Synchrotron is upgrading its accelerator to a diffraction-limited storage ring, achieving a twenty-fold emittance reduction. The upgrade, planned before the decade's end, will maximize use of existing infrastructure, such as the tunnel, while replacing components like magnets, vacuum chambers, and girders. This paper outlines the design status of the new girder system needed to support the expanded magnet array of the Alba II lattice, which more than doubles in number. Key design requirements include 50 µm positioning accuracy between adjacent magnets, allowing repositioning due to long-term slab deformation, vibrational stability of mounted components, and modular construction for reduced installation time. Each of the 16 arcs is divided into preassembled modules to ease assembly, transport, and final installation. A dedicated project was launched to build ALBA II prototypes. Two girders are currently under construction and expected to be tested by year-end.

FROM ALBA TO ALBA II

ALBA storage ring is composed by 264 magnets, which are distributed in 16 cells in an array of 2 girders (GI) of 6 meters for each cell, in a circumference of 268.8 m. ALBA II proposed layout is composed by 720 magnets (MA), in the same arc length of 12.8 m and circumference as current ALBA storage ring [1], meaning that the compactness ratio of the element on top of the girder has increased by a factor of 2. In Fig. 1 is represented an overall distribution of one sector for the current and new storage ring, where the reduction of free space can be appreciated.

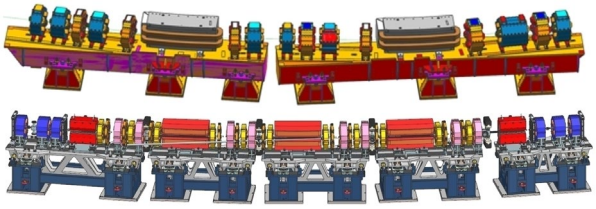

Figure 1: Magnetic distribution of ALBA (top) and ALBA II cell layout (bottom).

The ALBA II upgrade aims to transform ALBA into a fourth-generation, diffraction-limited storage ring, reducing emittance by at least a factor of twenty. This demands tighter tolerances for positioning girders and components, along with high stability requirements [1], as shown in Table 1.

Table 1: Sizes Comparison

Dimension	ALBA	ALBA II
Compactness grade	49%	80%
Vacuum chamber size	28x56 mm	18 mm
Dynamic aperture	50 mm	6 mm

ALBA II GIRDER PROTOTYPES

Two girder prototypes and a granite plinth were designed for manufacturing and will be available at ALBA for testing by Q4 2025, as part of the ALBA01 prototype project under the Next GenEU framework [2]. The prototypes were mechanically developed with all components for the new SR, in sync with the lattice design [3], keeping both aligned.

Originally developed for the 6BA lattice, the prototypes differ in several aspects from current 5BA requirements [3]. Based on slab movement study results [4], automatic height adjustment was considered unnecessary. The design was swiftly adapted and remains fully functional for testing all elements required to evaluate the optimal construction concept. Updated requirements are shown in Table 2.

Table 2: Requirements for the Girders

Specification	Value	Comments
Length	2 to 3 m	Limited by weight
Top surface height	1000 mm	Beam height 1.4 m
Width	1200 mm	Limited by tunnel
MA positioning Tol.	50 µm	GI to GI magnets
Eigenmodes	>50 Hz	By design
XY range	+/-3 mm	Manual
XY resolution	20 µm	Manual
Z range	+/-5 mm	Manual
Z resolution	5 µm	Manual
Assembly weight	<12 Tn	Module GI+MA

In Fig. 2 is shown all prototypes considered to build: two different geometries in welded steel for the top frame, two units of the same design of welded steel for the plinth and an extra one plinth of granite, along with several and redundant mechanics for positioning.

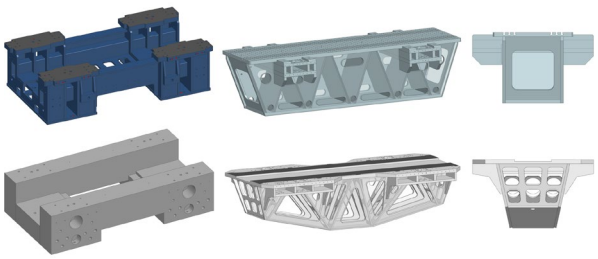

Figure 2: Girder prototypes components.

* Work supported by the Spanish MCIN and Catalan Government, and co-funded by the European Union – NextGenerationEU project ICTS-MRR-2021-02-CELLS from the Recovery and Resilience Mechanism.

† jboyer@cells.es

ISBN: 978-3-95450-263-9 ISSN: 2673-5520 doi: 10.18429/JACoW-MEDSI2025-WEP64

THERMAL FATIGUE TESTS ON CuCrZr PHOTON SHUTTERS*

S. Sharma†, F. DePaola, R. Faussete, J. Grandy, M. Johanson, R. Todd, G. Wang
NSLS-II, Brookhaven National Laboratory, Upton, NY, USA

Abstract

The CuCrZr alloy has emerged as a preferred material for thermal absorbers in synchrotron light sources, balancing mechanical strength, thermal conductivity, and cost-effectiveness. However, thermal fatigue design criteria for CuCrZr components under high-intensity X-ray beam exposure are not well established. This gap exists due to a lack of experimental data from test specimens subjected to several thousand cycles of localized high temperatures exceeding 300 °C. To address this gap, thermal fatigue tests were conducted on three CuCrZr photon shutters at the NSLS-II instrumentation front end. The experimental setup, receiving an X-ray beam from an undulator, provided a peak power density ranging from 19.95 W/mm² to 38.80 W/mm² on the photon shutters' surfaces. Within the beam footprints, calculated peak temperatures ranged from 326.8 °C to 416.5 °C. This paper presents the experimental setup, the test results, and finite element analyses of the thermomechanical response of the photon shutters. Based on both experimental and analytical findings, thermal design guidelines are proposed for CuCrZr absorbers, masks, and photon shutters.

INTRODUCTION

Precipitation hardened CuCrZr (solution annealed, water-quenched and aged) has an excellent combination of high thermal conductivity and high mechanical strength in terms of yield strength, fracture toughness and fatigue life. It compares favorably with other copper alloys in retaining mechanical strength at an elevated temperature of up to 350°C [1, 2]. The thermal fatigue performance of CuCrZr has been investigated in detail [3, 4] for plasma-facing divertors of the ITER project.

A new design of high-heat-load photon absorbers was proposed [5] wherein Conflat flanges were integrated in the main bodies made from CuCrZr. However, despite increasing adoption of CuCrZr photon absorbers in the light sources worldwide [6-9], the design criteria for the absorbers are inconsistent [6, 10] due to a lack of applicable experimental data.

This paper presents experimental and FE analysis results for 3 NSLS-II photon shutters fabricated from conventional precipitation-hardened CuCrZr. The experimental setup for thermal cycling was like those used previously for Glidcop® [11, 12].

EXPERIMENTAL SETUP

The thermal fatigue experiments on CuCrZr photon shutters were carried out on a test station built at the end of the instrumentation front end (IFE) of NSLS-II (Fig. 1), downstream of a fixed mask and a pair of L-shaped slits. The main components of the test station — namely, the sample photon shutter, pneumatic thruster, X-ray flag and IR sensor viewport — are depicted in Fig. 1.

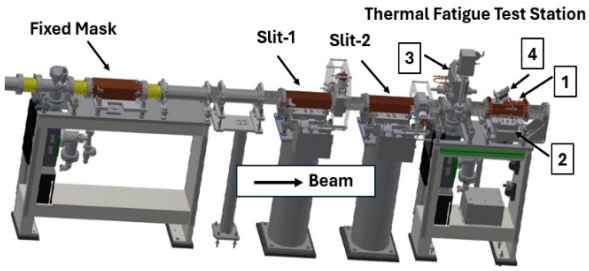

Figure 1: Thermal fatigue test station in the IFE, (1) sample photon shutter, (2) pneumatic thruster, (3) X-ray flag, and (4) IR sensor viewport.

The X-ray source for the IFE is an undulator, U68, with the following characteristics: period = 68 mm, effective length = 3.468 m, and deflection parameter = 4.567. Figure 2 shows horizontal and vertical distributions of the power density with their origins at the center of the beam footprint. The maximum power density at the origin is 38.80 W/mm² and the total integrated power is 5.12 kW at beam current of 500 mA.

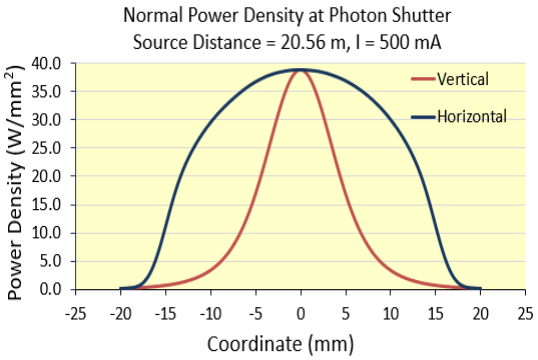

Figure 2: U68 power density distributions at a source distance of 20.56 m and beam current of 500 mA.

For thermal cycling, the photon shutter is moved up and down by the pneumatic thruster with travel time of ~100 ms, stroke of 40 mm, and dwell time of 30 seconds.

Three CuCrZr photon shutters, PS1, PS2 and PS3, were thermally cycled. PS1 (Fig. 3, left) is based on the conventional NSLS-II photon shutter design, except that the angle of beam interception is 40º (Fig. 3, right) as compared to ~ 3º normally to compensate for the lower power density of U68. The two beam footprints corresponding to the pneumatic actuator's up and down positions are depicted in yellow rectangles.

† sharma@bnl.gov * Not Export Controlled

ISBN: 978-3-95450-263-9 ISSN: 2673-5520 doi: 10.18429/JACoW-MEDSI2025-WEP65

THERMAL STABILITY OF THE DIAMOND STORAGE RING

E. Rippin†, Diamond Light Source, Didcot, UK

Abstract

This presentation explores the thermal stability of the Diamond storage ring, highlighting significant air temperature variations both spatially and temporally. To monitor component temperatures, 34 Pt1000 temperature sensors have been installed across three girders within the same cell. Observations indicate a 0.5°C increase in girder temperature during machine startup, primarily due to a rise in magnet temperature of up to 2.5°C when powered, while beam presence has minimal impact on machine temperature. This data has been instrumental in informing the development and analysis models for Diamond-II. Additionally, sensors installed on two Diamond EBPM columns provide targeted analysis to enhance Diamond-II beam stability.

INTRODUCTION

To maximise both electron and x-ray beam stability at Diamond, it is necessary to control the temperature within the storage ring. This is achieved by splitting the storage ring into ten zones, each with its own air handling unit (AHU) and control air temperature sensor.

Temperature variation within the machine will lead to thermal expansion of components and the support structure, and non-homogenous variation throughout the machine could lead to components moving relative to the beam, or to each other, leading to warping of the overall structure. This can cause unwanted movement of the beam, or false indications of beam movement leading to unnecessary interventions.

In 2023, 264 air temperature sensors were installed around the Diamond storage ring, to monitor the air temperature stability, and effectiveness of the AHU system. This found larger variations in temperature than expected – both on a local scale, and across the whole machine. As the Diamond girders have a significant thermal mass, their temperature may lag behind and potentially remain more stable than the surrounding air. Therefore, temperature monitoring of the Diamond machine was implemented using surface temperature sensors, to assess the impact of the air temperature variation on the machine itself.

SETUP

Cell 22 was selected as the location for the additional temperature monitoring as a 'worst case' due to the temperature variations observed within the cell. Throughout a run, the air temperature fluctuates by approximately 0.25°C with a period of 50 minutes, with occasional step changes of around 0.2°C. The average air temperature in cell 22 over a 24-hour period of normal machine operation is shown in Fig. 1.

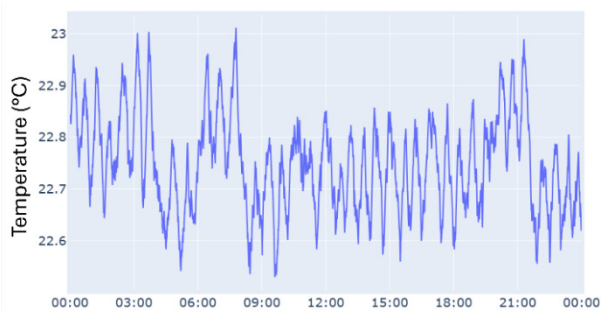

Figure 1: Average air temperature in Diamond cell 22 over a 24-hour period.

Class A, 2 wire, Pt1000 sensors have been used. These have a stated tolerance of ±0.15C at 0°C [1], and from testing a standard deviation of 0.034°C to 0.039°C across 21-24°C. The majority of the sensors are self-adhesive, silicone patch style sensors, applied directly to the machine surface. There are also bolt style sensors, with the Pt1000 element embedded within an M6 bolt, for installation in the storage ring floor. For this a hole was drilled directly into the concrete floor and a metal insert installed, into which the bolts are fit. Both sensor styles are shown in Fig. 2.

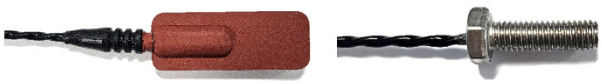

Figure 2: Images of sensors used – slicone patch surface sensor (left), M6 bolt in sensor (right).

A total of 34 sensors were installed, split across the three girders that make up the cell. 6 sensors were installed on each main girder body, 3 equally spaced along the top surface, and 3 in corresponding locations towards the bottom of the girder, allowing for the detection of any temperature gradient over the height of the girder. 3 sensors have been installed on magnet yokes per girder, 1 on the magnet furthest upstream, 1 on the furthest downstream, and 1 located at the approximate midpoint of the girder. A further 3 bolt sensors have been installed into the concrete floor below girders 1 and 2, equally spaced along the length, and only 1 below girder 3 due to connection constraints. The sensor positions shown on girder 3, in Fig. 3, are representative of the layout for all three girders. Across the cell, 6 of the magnet sensors are located on quadrupoles, 2 on sextupoles, and 1 on a dipole.

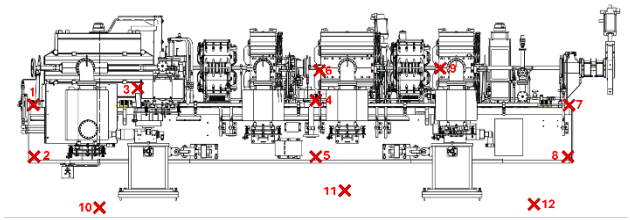

Figure 3: Sensor positions on girder 3.

† ella.rippin@diamond.ac.uk

ISBN: 978-3-95450-263-9 ISSN: 2673-5520 doi: 10.18429/JACoW-MEDSI2025-WEP68

DEVELOPMENT OF A CIRCULAR FLEXURE BENDER FOR A LONG, ELLIPTICAL BENT X-RAY MIRROR

Z. Y. Ren†, N. Wang, J. H. Zhang, Y. M. He, N. X. Tian, J. H. Chen, S. Xue, W. Q. Zhu
Shanghai Advanced Research Institute, Chinese Academy of Sciences, Shanghai, China

Abstract

Mechanical benders are classical instruments for shaping X-ray mirror surfaces with high precision. A circular flexure bender has been developed at SSRF (Shanghai Synchrotron Radiation Facility) for a 1200 mm-long hard X-ray mirror with an effective optical length of 1000 mm. Elliptical bending in the tangential direction is achieved using two actuators equipped with high-precision load cells, transmitting torque through circular flexure hinges at both ends of the mirror. The mirror is oriented to reflect vertically and faces upward, requiring consideration of gravitational deformation. Slope profilometry measurements using a Long Trace Profiler (LTP) indicate a total slope error of 0.45 μrad RMS, with mechanical error compensating gravity limited to 70 nrad. A liquid-metal-bath water cooling method is integrated to manage thermal loads. Finite element analysis (FEA) is conducted to evaluate thermally induced deformation, calculated at 0.2 μrad RMS and corrected to 33 nrad, and to optimize the flexure hinge design. The developed system provides stable, high-precision elliptical bending for long X-ray mirrors and is well adapted for advanced synchrotron radiation beamlines.

INTRODUCTION

In synchrotron radiation beamlines, mirror systems are indispensable optical elements, responsible for beam distribution, collimation, and focusing, ultimately transmitting the beam stably to the experimental station. For the focusing mirror system, to meet the beam focusing requirement, it is necessary to adjust the surface shape of the mirror to the targeted surface shape, typically circular, elliptical, or parabolic [1].

As synchrotron radiation sources advance with lower emittance and higher brightness, performance demands on mirrors become increasingly stringent. In this context, elliptical focusing, with its unique advantages, is regarded as an ideal focusing mode in synchrotron radiation beamlines. By placing the light source point and the imaging point at the two foci of the ellipse respectively, it can effectively reduce the transmission error of the beamline and significantly improve the focusing quality [2].

Mechanical bending remains the most widely adopted strategy for achieving the required mirror surface profiles in synchrotron radiation optics. Such benders provide precise and tuneable curvature control, enabling mirrors to be shaped to the desired optical figure for beamline applications [3–5]. This capability is essential for optimizing focusing performance and ensuring that the optical response meets the increasingly stringent requirements of synchrotron radiation light sources.

† renzy@sari.ac.cn

In this work, a circular flexure bender was developed at the Shanghai Synchrotron Radiation Facility (SSRF) for a 1200 mm-long hard X-ray elliptical mirror at a superbend magnet beamline. Elliptical bending is achieved via two high-precision actuators with load cells for accurate and reproducible control. Mirror characterization with a Long Trace Profiler (LTP) yielded a total slope error of 0.45 μrad RMS, with the bender itself introducing only 70 nrad RMS after gravity compensation.

To manage operational heat loads, a liquid–metal cooling system was integrated. Finite Element Analysis (FEA) showed thermally induced deformation of 0.2 μrad RMS, which can be corrected to 33 nrad RMS by the bending mechanism. The FEA is also utilized to optimize the flexure hinge design, enhancing the overall stability and precision of the system. The developed mirror system provides stable, high-precision elliptical bending for long X-ray mirrors, making it ideal for advanced synchrotron radiation beamlines.

WORKING CONDITIONS AND ANALYSIS

The focusing mirror system presented in this paper is designed for a superbend magnet beamline. It adopts an upward-reflecting configuration to focus the beam emitted from the superbend source. The parameters of the mirror and the corresponding elliptical focusing configuration are summarized in Table 1.

Table 1: Mirror and Elliptical Surface Parameters

Parameter	Value
Dimension of the mirror[mm^3]	1200 × 90 × 50
Tangential effective range [mm]	1000
Sagittal radius [mm]	45.5
Incidence angle [mrad]	3.5
Object distance [m]	13
Image distance [m]	5000

Given that the tangential effective range of the mirror extends to 1000 mm, the mirror dimensions are specified as 1200 mm × 90 mm × 50 mm to provide sufficient optical coverage. To achieve focusing in the sagittal direction, the mirror surface is designed with a sagittal radius of curvature of 45.5 mm.

The elliptical tangential figure is generated by a conventional mechanical bender applying different moments at the two mirror ends. Accurate realization of this figure necessitates evaluation of surface figure error contributions, which include: intrinsic surface error of the mirror, the approximation error associated with the bending mechanism,

ISBN: 978-3-95450-263-9 ISSN: 2673-5520 doi: 10.18429/JACoW-MEDSI2025-WEP71

REMOVAL AND INSTALLATION PLANS FOR THE SOLEIL II UPGRADE

G. Baranton†, C. De Olivera, F. Trias, N. Bechu, A. Carcy
Synchrotron SOLEIL, Saint-Aubin, France

Abstract

The SOLEIL synchrotron, which has been open to the scientific community since 2008, will benefit from an upgrade aimed at improving the brilliance, coherence, and flux of the X-ray beam delivered. This will make it possible to follow biological processes or the functioning of devices operating at sub-millisecond timescales at nanometric resolution, while sharply reducing the detection limit for trace elements. The accelerators (booster and storage ring) will be completely renewed, within the existing tunnels. In addition, six beamlines will be relocated to other places in the experiment hall. An 18-month "dark period" is planned to bring the removal and installation program for SOLEIL II accelerators to a successful conclusion. This article presents the strategic plans being developed for dismantling the current accelerators, installing the upgraded components of the new accelerators (girders, magnets, vacuum chambers, electrical and fluid servitudes), and move the six beamlines (radiation protection hutches and equipment). Prioritizing a cost-effective and time-efficient approach, we began planning by focusing on optimizing spaces and equipment movement necessary for the upgrade process.

INTRODUCTION

The removal of the accelerators, booster, and storage ring presents several significant challenges and constraints that must be carefully managed to ensure both efficiency and safety. First, the dismantling process must be carried out as quickly as possible, requiring work in shifts across different areas. This necessitates the deployment of at least four teams of authorized crane operators, five days a week.

Simultaneous handling with two cranes demands rigorous coactivity management and the use of five designated unloading zones to streamline operations and prevent bottlenecks. Since two cranes cannot operate at a distance less than 13.5 meters from each other, a minimum of two closed cells must separate any two open cells during dismantling. Safety protocols further mandate that no workers are permitted in adjacent closed cells while slabs are being handled. The handling of heavy loads on slabs follows a specific safety protocol, and certain beamline hutches must be evacuated whenever cranes are operating overhead. Continuous rotation of evacuations from the unloading areas to the disassembly building, using forklifts and trailers, is essential to maintain workflow. Finally, ensuring safe circulation on site for all users remains a priority throughout the dismantling process.

SPACE REQUIREMENT

We first assessed the spatial requirements in order to optimize the available areas on our site (Fig. 1). As a result, we plan to modify four existing buildings: Buildings T2 and T3 will be primarily dedicated to the storage of magnets and girders from the storage ring. Building T5 will be used for magnetic measurement and subsequently for the assembly of girders with the measured magnets. The alignment group specified a thermal stability requirement of ±0.1 °C to ensure the precise correlative alignment of the magnets on the matching section girders.

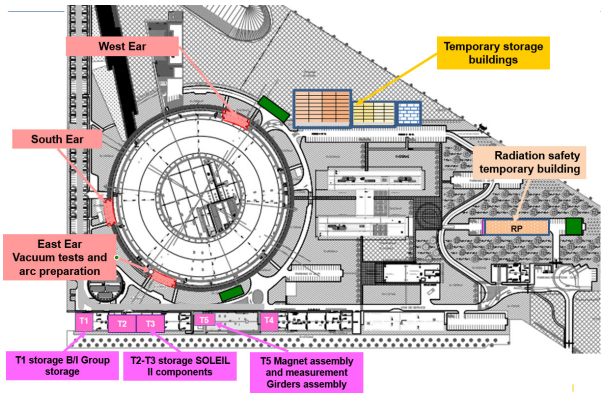

Figure 1: Synchrotron SOLEIL buildings.

We will construct three temporary buildings for storage, radiation safety measurements, and use by external companies. Additionally, we will create a new 210 m² extension in the synchrotron building, referred to as the "East Ear" (Fig. 2). This space will be dedicated to the assembly, NEG activation, and vacuum testing of the new 20 arc vacuum strings, which are 9 meters and 16 meters long.

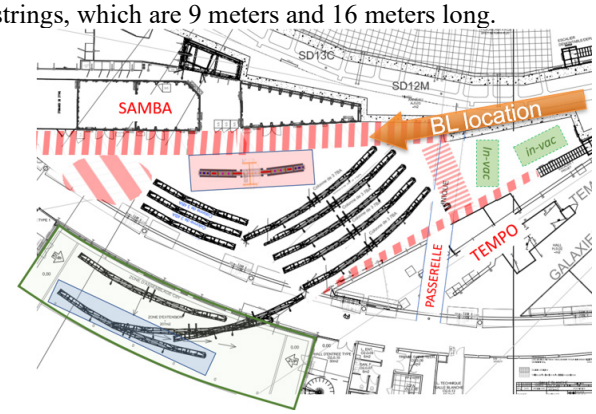

Figure 2: East Ear and “Tempo” area for vacuum strings and Mock-up.

A special trolley will be designed to evacuate the arc vacuum strings for storage in the experimental hall, specifically in the "Tempo" area. This zone will also house the mock-up until shutdown (Fig. 7), and we will need to share the space with the construction of the new beamline (Fig. 8) [1].

† gil.baranton@synchrotron-soleil.fr

ISBN: 978-3-95450-263-9 ISSN: 2673-5520 doi: 10.18429/JACoW-MEDSI2025-THOA02

PARAMETRIC DESIGN AND OPTIMIZATION OF SOLEIL II VACUUM CHAMBER THERMAL PROPERTIES

Z. Fan†, M. Ribbens, K. Tavakoli, T. Souské, V. Leroux, C. Herbeaux
Synchrotron SOLEIL, Saint-Aubin, France

Abstract

In the context of the upgrade to SOLEIL II, a 4th-generation synchrotron, the use of Multi-Bend Achromat lattices significantly reduces natural emittance but requires smaller vacuum chambers (12–16 mm), leading to higher power density on chamber walls with limited cooling space. In some cases, there is no room for crotch absorbers, and chambers must fit between magnet poles with less than 1 mm clearance. These constraints demand high thermo-mechanical stability, making design highly challenging and it is often difficult to identify the most efficient direction for further optimization.

This paper presents a parametric thermal analysis and optimization method for SOLEIL II vacuum chambers. Simulations are conducted using ANSYS DesignXplorer, with key parameters identified through sensitivity analysis of their impact on thermal performance. The heat-flux map, imported from Synrad+, provides precise power distribution. From multiple parameter combinations, a predictive temperature map (response surface) is generated, enabling estimation of thermal behaviour without lengthy simulations. An optimized parameter set is proposed to streamline the design while ensuring performance.

INTRODUCTION

The design of the SOLEIL II vacuum chamber (VC) represents a complex, multi-criteria, and highly constrained engineering problem [1, 2]. It must simultaneously satisfy strict geometric requirements while controlling maximum temperature, mechanical stress, and structural deformation. Determining the optimal design strategy is particularly challenging because modifying a single parameter can have multiple effects, making traditional trial-and-error approaches both inefficient and time-consuming.

To accurately represent the thermal environment, we employed realistic power distributions of synchrotron radiation obtained from Synrad+ [3]. These distributions are highly non-uniform and exhibit localized hotspots. Neglecting this non-uniformity by assuming a uniform heat load would fail to account for these critical local effects. However, simulations that account for realistic heat loads are computationally demanding.

To overcome these challenges, a systematic parametric study combined with an optimization approach is essential. DesignXplorer [4] was selected for this purpose due to its full integration within ANSYS Workbench, its efficiency in handling medium-sized parametric studies, and its ability to provide a robust compromise between solution accuracy and computational cost. This methodology enables the identification of the most effective design modifications while minimizing unnecessary iterations and computational effort.

PARAMETER CHOICE AND BOUNDARY CONDITIONS

As a representative case, we studied a vacuum chamber passing through a long dipole magnet. A key design requirement is to keep the external surface temperature below 40 °C, in order to minimize thermal impact on the magnet. As stress and strain are closely coupled with temperature, the only output objective chosen here is the temperature to speed optimization. Efficient cooling is essential.

The chamber is cooled via water channels located on both the beam-facing side, where power deposition occurs, and on the opposite (inner) side. To optimize the thermal performance of the system, seven key design parameters were identified (see Fig. 1) as potentially influencing the maximum external temperature:

- Cooling channel width on the power deposition side (P1-power) and the opposite side (P1-inner): defines the contact surface between the cooling water and the vacuum chamber. In this study, the width varies from 4 to 12 mm.
- Cooling channel depth (P2-inner and P2-power): defines the distance between the cooling water and the inner chamber surface. A minimum thickness of 3 mm is imposed to ensure vacuum tightness. Depth can vary from 3 to 7 mm.
- Vacuum chamber wall thickness (P3): ranging from 2 to 5 mm.
- Material thermal conductivity (P4): represented by the choice of chamber material. Different copper alloys such as CuCrZr and OFS (Oxygen-Free Silver-Copper) are considered, as they offer different balances between conductivity and mechanical strength. Conductivity varies from 300 to 400 $W \cdot m^{-1} \cdot K^{-1}$ depending on the copper alloy selected.
- Convection film coefficient h (P5), which governs heat transfer efficiency. The coefficient varies between 9,000 and 15,000 $W \cdot m^{-2} \cdot K^{-1}$, depending on the hydraulic diameter of the cooling channel and the water flow rate.

† Zhengxuan.fan@synchrotron-soleil.fr

ISBN: 978-3-95450-263-9 ISSN: 2673-5520 doi: 10.18429/JACoW-MEDSI2025-THOB03

CHALLENGES AND OPTIMIZATION OF Mu2e PROTON TARGET DESIGN WITH RADIATIVE COOLING*

Z. Liu†,1, G. Annala[1], M. Bloomer[2], A. Edmonds[3], M. Hedges[1], K. Lynch[1], A. Makovec[1], J. Miller[4], F. Pellemoine[1], J. Popp[3], J. Williams[1], K. Yonehara[1]
[1]Fermi National Accelerator Laboratory, Batavia, IL, USA
[2]Emory University, Atlanta, GA, USA
[3]York College / CUNY, Jamaica, NY, USA
[4]Boston University, Boston, MA, USA

Abstract

The Mu2e experiment at Fermilab will search for the charged lepton flavour violating process of coherent neutrinoless muon-to-electron conversion in the presence of an aluminum nucleus. The muons are produced by an 8 GeV proton beam from the Fermilab Booster striking a production target to create hadrons that decay to muons. The production target design space is strongly constrained by a required one-year operating lifetime and the need for radiative cooling in a vacuum. Uncertainties in the lifetime of the existing baseline design – a monolithic, segmented tungsten (WL10) target – are large, particularly due to unknown effects of radiation damage at the very high proton fluences expected in the experiment. We have begun evaluating a new design utilizing Inconel 718. Here, we present an engineering analysis of a prototype modular design. specifically thermal management, structural stability, fatigue lifetime, and fabrication changes. The results approve a promising new target design for the Mu2e experiment.

INTRODUCTION

The Mu2e experiment at Fermilab, will search for the coherent neutrinoless conversion of muons to electrons in aluminium [1]. An 8 GeV proton beam from Fermilab Booster strikes the production target to produce particles, mostly pions, that decay to muons for the experiment. Further details on the Mu2e experiment design, motivation, and proposed run plan can be found in Ref. [1].

The production target design is fundamental to the success of Mu2e experiment as the source of the muon beam. The existing production target design, codenamed "Hayman", shown in the top-left of Fig. 1, is made from tungsten, a high Z material, to maximize production while the geometry is designed to minimize reabsorption. The Hayman target is 220 mm long with its core of 6 mm in diameter and four fins to increase surface for radiation cooling. The target support structure consists of a ring with six spokes that attach to end-rings affixed to the monolithic target. The whole assembly of the ring and the target shall be removed for change through a remote handling system (RHS), no more than once per year.

*This manuscript has been authored by Fermi Research Alliance, LLC under Contract No. DE-AC02-07CH11359 with the U.S. Department of Energy, Office of Science, Office of High Energy Physics.
† zunping@fnal.gov

Radiation damage to the production target is a key factor in ensuring lifetime requirements. Radiation damage changes physical properties of the material, including mechanical strength and thermal conductivity. The degree of radiation damage is often quantified with displacements per atom (dpa) at lattice level. As dpa increases, the material's ability to manage heat and absorb shock decreases, accelerating degradation and failure. Unfortunately, recent application of tungsten in highly irradiated conditions has shown that it's possibly harmfully susceptible to radiation damage [2]. For a tungsten target subjected to the 8 GeV proton beam at Mu2e for one year of running, preliminary simulation studies, using FLUKA [3, 4] show dpa levels approximately an order of magnitude above operational limits found in the literature [5], suggesting alternative target material considerations are warranted.

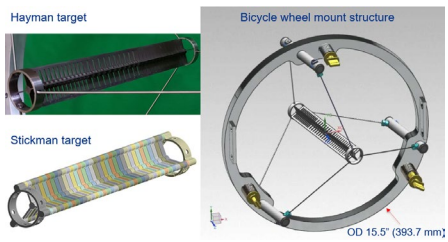

Figure 1: Mu2e production targets and mount structure.

Recently, a G4Beamline [6] simulation of muon production per proton on target (POT) shows that the muon production does not increase linearly with target density but does so with the nuclear interaction length [7]. This motivates investigation into previously unconsidered materials with available data on high levels of radiation damage. Nickel-based Inconel is one such option for an alternative material for the Mu2e target [8].

Inconel 600 was used in the Fermilab Antiproton Source [9], but there is no record of Post Irradiation Examinations (PIE) on this target. Recently a solution-annealed Inconel 718 proton beam window at the Spallation Neutron Source at Oak Ridge National Laboratory was reported with observation of an increase in ductility, rather than embrittlement, under 10 dpa of proton irradiation [10]. Preliminary physics analysis estimates a peak of 10 dpa in an Inconel 718 target in one-year of proton beam irradiation for Mu2e. In addition, Inconel 718 has high emissivity, up to 0.9 of hemispherical total emissivity [11], which suits radiation cooling as a requirement for the design. These motivate the design of an Inconel 718 target design, codenamed "Stickman" as shown in bottom left of Fig. 1.

ISBN: 978-3-95450-263-9 ISSN: 2673-5520 doi: 10.18429/JACoW-MEDSI2025-THOB04

FROM SIMULATION TO MEASUREMENT: ENHANCING FE SIMULATION FOR PETRA IV AND EuXFEL GIRDERS

Daniel Thoden*, Normann Koldrack†
Deutsches Elektronen-Synchrotron DESY, Hamburg, Germany

Abstract

Finite element models are widely used to raise eigenfrequencies of accelerator magnet girders. However, beam stability also depends on the coupling of mode shapes to mounted components and on structural damping, which are rarely characterized at full scale. We present the study of two girders at DESY: a topology optimized cast iron PETRA IV girder and an ultra high performance concrete EuXFEL streaker girder. Both structures were tested in suspended and supported configurations to separate material damping from effects introduced by the supports and to validate the simulations. Eigenfrequencies were identified from averaged FFT spectra up to 500 Hz, and damping ratios were obtained by narrowband filtering around each mode, Hilbert envelope extraction, and exponential decay fitting. Measured damping levels are consistent with literature values for cast iron and for ultra high performance concrete and reveal a clear influence of support design on dynamic behaviour. The results provide validated parameters for system level simulations and support future girder optimization that targets damping and mode shape coupling in addition to high eigenfrequencies in PETRA IV and EuXFEL.

INTRODUCTION

Finite element analyses are widely used to obtain highly accurate results when investigating monolithic components such as girders for accelerator systems. To ensure stable beam operation, the dynamic behaviour of these components is simulated and optimized during the design process. During this optimization, not only the eigenfrequencies of the girder itself are relevant, but also the effects on the components mounted on top of it, most importantly the magnets. Knowledge of eigenfrequencies alone is therefore not sufficient for girder optimization, since not all modes influence the components in the same way, and some may not affect them at all.

While finite element simulations help to identify and avoid critical resonances, they do not provide information on how much of the vibrational energy is dissipated within the structure and how much remains to influence the beam. Addressing this limitation requires both advanced calculation methods and reliable input parameters for the simulations. At DESY, several accelerators with different requirements for girders have led to a variety of designs over the years. For the development of future girders for XFEL and PETRA IV (PIV), particular attention is being given not only to increasing eigenfrequencies but also to understanding damping behaviour and the impact of mode shapes on beam stability. This study therefore investigates girder properties with a focus on material choice and support configurations.

PETRA IV Topologically Optimized Girder

Magnet girders in particle accelerators have traditionally been constructed from welded steel and, in some cases, supplemented with iron or cast concrete substructures [1]. In contrast, the PIV project will mark the first instance where girders are fully cast and shaped through topology optimization. This development represents a significant departure from conventional design paradigms.

To fully exploit the potential of topology optimization, all relevant boundary conditions must be modeled as realistically as possible. In the present case this includes the position and weight of the magnets and other mounted components, together with the interfaces that connect the girder to the ground. The latter is realized through wedge movers, which provide precise alignment and load transfer, and must therefore be incorporated into the optimization process.

To validate the feasibility of this approach, a demonstrator girder was produced. It was topology optimized based on assumptions regarding load distribution, boundary conditions, and structural response. The physical prototype now serves to confirm these assumptions and to further refine the numerical models.

The demonstrator has approximate dimensions of 5 × 1 × 1 m, a total weight of 5 t, and is manufactured from cast iron of grade EN-GJS-600-3U (Fig. 1). It is designed to support a total payload of 7 t.

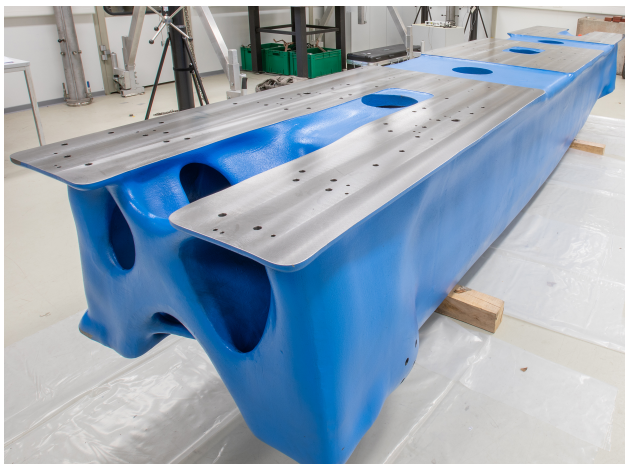

Figure 1: PETRA IV Demonstrator Girder.

A central challenge lies in determining the damping properties of the girder and quantifying the influence of the wedge

* Daniel.Thoden@desy.de
† Normann.Koldrack@desy.de

ISBN: 978-3-95450-263-9 ISSN: 2673-5520 doi: 10.18429/JACoW-MEDSI2025-THOB05

DESIGN OF SLS 2.0 BPM BLOCK SUPPORT STRUCTURE WITH DAMPING MECHANISM

Xinyu Wang, Romain Ganter, Boris Keil, Maximilian Wurm
PSI Center for Accelerator Science and Engineering, Villigen, Switzerland

Abstract

The positional stability of SLS 2.0 beam position monitors (BPM) is crucial for effective fast orbit feedback and beam stability. This work presents the thermal and mechanical optimization of the BPM support structure, which incorporates a dedicated damping mechanism to minimize vibrational and thermal-induced displacements.

INTRODUCTION

The SLS 2.0 upgrade progressed rapidly in 2025. Following an intensive 15-month "dark time", the first stored beam was achieved on 23 January. By April, the nominal current of 400 mA was reached, and eight beamlines have been successfully commissioned. The second phase of beamline commissioning and full user operations is scheduled for 2026.

The electron channel of SLS 2.0 storage ring has an octagonal shape, which facilitates the integration of four equally spaced beam position monitors (BPMs). The beam pipe is typically made of NEG-coated copper with an aperture of 18 mm. The BPM chamber, however, are made of stainless steel due to the corrector magnets. This chamber has a thickness of 0.5 mm, with its inner surface copper-coated to reduce impedance [1].

The BPM electronics are designed to meet a precision of 50 nm RMS position noise [2]. Thermal and mechanical stability of BPM blocks is essential for achieving the accurate beam position measurement and overall beam stability.

MECHANICAL DESIGN

The mechanical supports of the BPM blocks are designed as a sandwich structure, consisting of two steel plates bonded to a stiff balsa wood core using viscoelastic adhesive. In the upper part of the BPM support, a water-cooled copper alloy block (CuCrZr) is integrated to reduce the beam-induced temperature variations, as shown in Fig. 1.

Damping Design

Viscoelastic materials can effectively suppress vibrations in accelerator design through damping mechanism, as demonstrated in [3, 4]. In mass transportation systems, flexible bonding has long been established for joining dissimilar materials and for reducing vibrations in buses and high-speed trains [5, 6]. A thick adhesive layer, typically a few millimeters, combined with its gap-filling capacity, allows compensation for tolerances between joined parts. The one-component adhesive, which cures with atmospheric moisture into a durable elastomer, is also easy to apply.

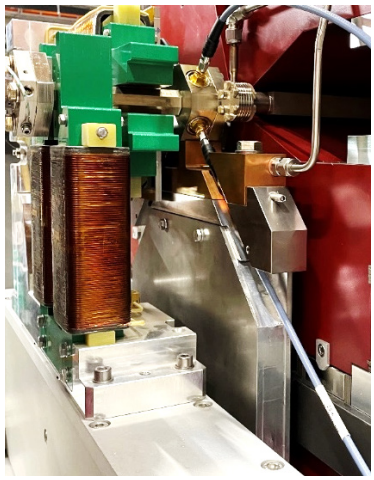

Figure 1: BPM chamber, corrector magnets in green.

The end-grain balsa wood exhibits good damping behaviour and is selected as core material due to its high rigidity, as well as thermal and dimensional stability compared to many polymer foams. The grain is oriented perpendicular to the plate surface, which allows efficient load transfer between the face layers. The higher shear stiffness is oriented in the desired thickness direction. The open cell ends absorb adhesive readily, making it easy to prepare for bonding.

Vibration Tests

To select the adhesive type and optimize the bonding layer thickness, dedicated vibration tests were performed. The BMP support was tested on a mock-up girder. A series of random vibration measurements and modal tests were performed to evaluate adhesive materials, including a one-component flexible adhesive and a two-component epoxy adhesive.

The test setup includes a BPM chamber with the BPM support mounted on a mock-up girder (Fig. 2). Vibrations on the top of the BPM are measured and compared with vibrations on the girder. In this test configuration, the highest vibrations in the longitudinal direction on the BPM (red) and on the girder (black) are shown in Fig. 3, comparing a basic support with two plates to another support with a balsa wood core bonded between the two plates.

With the sandwich design, the first peak frequency shifted from 25 Hz to 39 Hz, while the RMS amplitude decreases from 284 nm to 41 nm (Table 1), corresponding to a sevenfold reduction. The RMS amplitude amplification ratio from the girder to the BPM was 16 for the stainless-steel support, reduced to only 2 for the sandwich support. The vibration reduction is attributed to the increased stiffness and higher eigenfrequencies, and more importantly, to the added damping.

ISBN: 978-3-95450-263-9 ISSN: 2673-5520 doi: 10.18429/JACoW-MEDSI2025-THOC01

PROGRESS IN THE ENGINEERING DESIGN AND INSTALLATION OF THE HIAF PROJECT*

Yajun Zheng†,1,2,3, Jiancheng Yang[1], Yaqing Yang[1], Yongxiang Pan[1,2,3], Haihua Niu[1], Haijiao Lu[1], Xiaowei Xu[1], Lu Zhang[1], Yongbin Lang[1], Wenjun Chen[1], Zeen Yao[3]
[1] Institute of Modern Physics, Chinese Academy of Sciences, Lanzhou, China
[2] University of Chinese Academy of Sciences, Beijing, China
[3] Lanzhou University, Lanzhou, China

Abstract

The High Intensity heavy-ion Accelerator Facility (HIAF) is a state-of-the-art accelerator complex currently under construction at the Institute of Modern Physics (IMP) on the Huizhou campus in China. This facility aims to provide an internationally competitive platform for cutting-edge research in nuclear physics, atomic physics, and applied heavy-ion beam technologies. The 2-kilometer-long beamline, installed in an underground tunnel 12.7 meters below the surface, incorporates over 6,000 large-scale devices, 5 million components, and 1 million meters of pipelines. To address the complex multidisciplinary coordination challenges across subsystems and stakeholders, we developed cross-domain collaborative design strategies and a Building Information Modeling (BIM)-based lifecycle management platform. This platform encompasses architecture, accelerator systems, auxiliary facilities, and decommissioning processes, providing comprehensive digital support for the facility's lifecycle engineering. The full installation of the Booster Ring (BRing), Spectrometer Ring (SRing), and beamline components was completed within 8 months, with integrated commissioning currently underway. The construction is expected to conclude in 7 years, with the facility anticipated to be commissioned by late 2025.

INTRODUCTION

The High Intensity heavy-ion Accelerator Facility (HIAF), as one of the key infrastructure projects during the 12th Five-Year Plan period identified by The Medium-and Long-Term Plan for the Construction of Major National Science and Technology Infrastructure (2012-2030). As part of the Chinese Academy of Sciences (CAS), with the Institute of Modern Physics (IMP) serving as the administrative entity. HIAF was officially approved by the National Development and Reform Commission of China in December 2015 following rigorous evaluations. After the assessment of technical feasibility, construction of HIAF started up on December 23, 2018 [1-2]. The facility comprises main components: the accelerator system, the terminal experiment system and civil engineering supporting facilities. The accelerator system includes a superconducting electron cyclotron resonance ion source (SECR), a superconducting ion linear accelerator (iLinac), a Booster Ring (BRing), and beam transmission lines connecting these subsystems. The terminal experiment system consists of Low Energy Nuclear Structure Spectrometer, Intensive Ion Beams Irradiation Terminal, High Energy Fragment Separator (HFRS), External Target Terminal, Spectrometer Ring (SRing) for High-precision Experiments, High Energy Multi-disciplinary Terminal, and High Energy Density Physics Terminal. Civil engineering supporting facilities encompass construction, cooling water, ventilation, electricity and other infrastructures to ensure the smooth operation of HIAF. Figure 1 illustrates the integrated layout of the accelerator complex and its tunnel, the key components clearly labelled on the diagram.

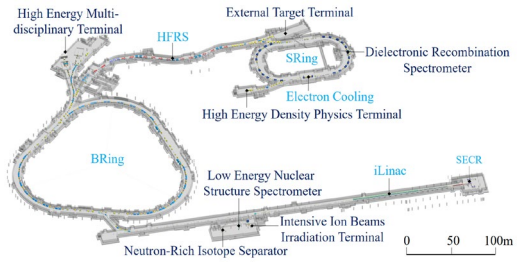

Figure 1: Schematic layout of the accelerator complex and its tunnel.

MECHANICAL DESIGN CHALLENGE

The HIAF facility is equipped with a 2-kilometer beamline located within an underground tunnel at a depth of 12.7 meters below ground level, auxiliary facilities are situated in above-ground buildings that cover a campus area of approximately 0.33 km². As shown in Table 1 the facility's performance limits, including vacuum levels, auxiliary system parameters and mechanical specifications [3]. The mechanical design of HIAF inherently complex, confronts several challenges, such as its massive scale, extensive equipment, densely packed pipelines, structural intricacy, multi-system integration requirements, ultra-high vacuum requirements, and stringent installation precision.

DESIGN METHODS

HIAF represents a pioneering facility constructed on a primordial place without any pre-existing infrastructure [2], which poses significant challenges to the engineering construction. Due to its advantages in collaboration, visualization, simulation, optimization, cost efficiency, and shared data creation, Building Information

*Work supported by the National Development and Reform Commission, China
† zhengyj@impcas.ac.cn

ISBN: 978-3-95450-263-9 ISSN: 2673-5520 doi: 10.18429/JACoW-MEDSI2025-THOC04

DESIGN OF ALIGNMENT NETWORK FOR THE SIAM PHOTON SOURCE II

J. Saetiaw†, S. Prawanta, K. Rittaprom, P. Pruekthaisong,
P. Rattanawichai, S. Srichan, P. Klysubun
Synchrotron Light Research Institute, Nakhon Ratchasima, Thailand

Abstract

The development of the 3 GeV synchrotron light source in Thailand represents a major advancement in national scientific infrastructure, aiming to provide high-brightness synchrotron radiation for broad scientific and industrial applications. The installation of core accelerator systems, including magnet systems, vacuum systems, and girder systems, requires micrometre-level precision to ensure long-term stability. This study introduces a newly designed alignment network system focused on minimizing measurement uncertainty to meet the tight positioning tolerances of the electron storage ring. Simulations and analyses were performed using Spatial Analyzer software and the Unified Spatial Metrology Network (USMN), integrated with high-precision laser trackers. The resulting network achieves sub-millimetres accuracy within specified tolerances, supporting precise component installation. This work enhances the capabilities of Thailand in reference network design for high-precision systems and offers an adaptable framework for future advanced technology applications.

INTRODUCTION

The alignment of the electron storage ring in the SPS-II project must meet stringent precision requirements. All magnet and vacuum components are continuously mounted on girders along the 327.6 m circumference of the ring (see Fig. 1), Maintaining beam stability and ensuring the accelerator operates according to its design specifications require installation tolerances to be controlled at the micrometre level [1, 2]. The process is supported by Spatial Analyzer software, which provides capabilities for coordinate adjustment and uncertainty evaluation. A hierarchical alignment strategy is adopted, beginning with global girder positioning and followed by fine alignment of individual components. This stepwise approach minimizes error accumulation, ensures long-term operational stability, and is reinforced by continuous monitoring and re-adjustment to maintain precision throughout the facility's lifetime [3].

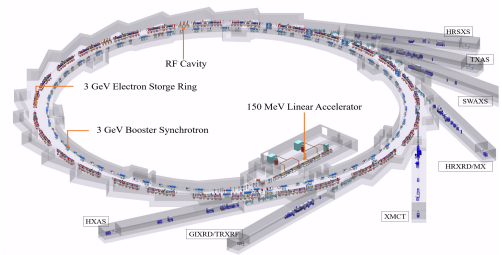

Figure 1: Overview of the SPS-II accelerators complex.

NETWORK ARCHITECTURE

A site-wide reference network has been established and structured into three levels: the Ground Control Network, the Primary Survey Network, and the Alignment Network. The Ground Control Network, based on GNSS benchmarks anchored into bedrock, defines the overall coordinate reference system with an accuracy of ±3 mm horizontally and ±2 mm vertically. Once the building floor is completed, the Primary Survey Network is installed to support the layout of shielding walls, providing ±3 mm horizontal and ±0.2 mm vertical accuracy. This network forms the basis for the Alignment Network (see Fig. 2), which guides the installation of accelerator components with a higher precision of ±0.05 mm in both directions. Target bases mounted on walls and floors enable the use of high-precision instruments for accurate magnet alignment within the specified tolerances.

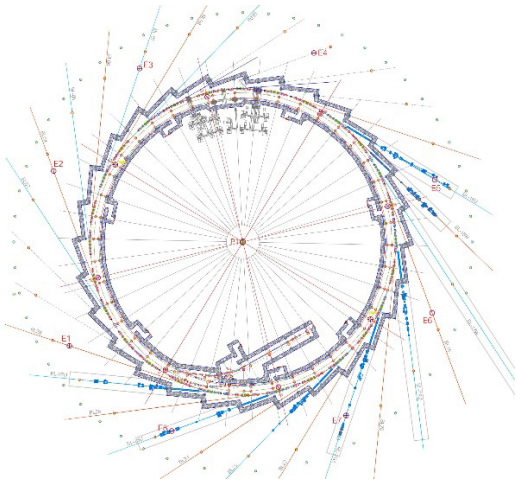

Figure 2: The layout of alignment network.

MEASUREMENT WORKFLOW

The survey network was designed and simulated in Spatial Analyzer (SA) with spacings of 6.139 m, 7.599 m, and 9.382 m, ensuring a balanced distribution of observation points and meeting accuracy requirements for both global and local alignment. The measurement process followed a systematic procedure using the free station method with laser trackers and other high-precision instruments. Setups were placed at multiple locations and viewing angles (see Fig. 3), and measurements were performed in looped sequences to increase redundancy and reliability. All data were then processed for network adjustment, quality evaluation, and computation of optimal coordinates for subsequent alignment tasks.

† jullada@slri.or.th

ISBN: 978-3-95450-263-9 ISSN: 2673-5520 doi: 10.18429/JACoW-MEDSI2025-THOC06

LAYOUT OF ALBA II ACCELERATOR

L. Ribó†, N. González, F. Fernández, J. C. Giraldo, P. Salmerón, J. Boyer, R. Parise, F. Pérez
ALBA Synchrotron Light Source, Cerdanyola del Vallès, Spain

Abstract

ALBA Synchrotron Light Source will be upgraded into a diffraction limited machine by the replacement of the storage ring, which implies the reduction of the emittance by at least a factor of twenty. Compactness ratio of the magnetic elements has increased by a factor of 2. The new lattice has been designed with two big constrains. Firstly, keeping the same orbit length allows us to preserve the actual injector. Secondly, the medium and short straights will be collinear with respect to ALBA current layout to avoid moving the present Insertion Devices Beamlines. The bending magnet beamlines must be repositioned on the new machine. Magnetic array, vacuum chambers and girders are positioned with respect to the main orbit under tight clearances, that's why envelope studies of those clearances will have to be performed for the 3 subsystems. Easiness of assembling and installation of the different subsystems of the machine has to be considered also as a design requirement, in order to minimize the installation time. A mock-up of one sector is being prepared for this reason. The upgrade will be executed before the end of the decade and will be profiting at maximum all existing ALBA infrastructures, in particular the building.

INTRODUCTION AND GEOMETRICAL CONSTRAINTS

Low Emittance Alba II storage ring is composed by about 720 magnets distributed in 16 arcs. As a first constraint, it is requested the orbit length to be the same as it is in the actual ALBA machine [1], this means 268.800 mm. Apart from that, the straight sections between the arcs where the insertion device (ID) beamlines are already located have to be colinear with the actual orbit, in order to keep these beamlines position as they are now. With respect to the accelerator, linac and booster are not upgraded, but the booster to storage ring transfer line will be redefined.

Another geometrical constraint for fitting the new storage ring is the existing infrastructure. Tunnel walls, roof and the primary cooling circuits will be the same.

The position of the ID front ends centrelines is kept but for two bending magnet actual beamlines a new optimal extraction point has to be found in a way that the optical layout of the beamlines changes minimally.

The full storage ring is composed by 4 quarters, each quarter composed by 4 arcs, and 5 straights, two long, two short and one medium. Medium and short straights are collinear with the ALBA storage ring, not as the long straight which will offset radially with respect the actual beam path.

LATTICE CELL

The lattice cell is under optimization. At the moment, is composed by 3 dipoles, 2 permanent magnet dipoles. 8 anti-bending quadrupoles, 6 pure quadrupoles, 11 sextupoles, 11 octupoles and 4 correctors fitted in an arc length of 12.800 mm. Additionally, each arc will have 8 to 10 beam position monitors. the tolerances for positioning the magnets and the girder will need to be tighter corresponding to a low emittance new machine, where the emittance is reduced by a factor of 20 [2]. The arc is represented in the next picture (Fig. 1) as a simplified scheme, where the dipoles and the 8 anti-bending quadrupoles are represented. The sextupoles, pure quadrupoles, octupoles and correctors are not represented on the figure but they are distributed evenly between the magnets.

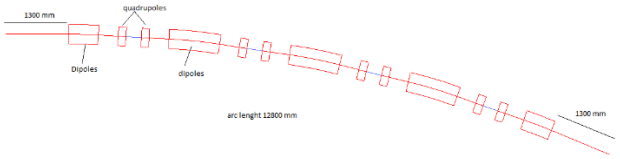

Figure 1: Schematic representation of the lattice arc.

MECHANICAL DESIGN OF THE CELL

Optimization of the lattice is being nowadays a continuous task, that is already converging into the most optimal solution in terms of emittance and beam life time. Due to the project planning, mechanical design cannot wait until the lattice distribution is frozen, that's why an updateable 3D model has been created to implement all the modifications in the most optimal way. Basically, the storage ring arcs are modeled in 4 subassemblies, where magnetic array, vacuum system, girders, Insertion devices, diagnostics and RF systems as others are restricted with respect to a fixed wireframe that follows the beam. This beam wireframe is the master reference for the remaining components of the storage ring, and it is built having the lattice geometrical model as an input. In this way, each time there is a lattice upgrade, the wireframe can be updated and all the components are automatically repositioned

Figure 2 shows an example of the wireframe beam path where all the coordinate axis are located to be the reference when positioning the magnets. After that, the girders and vacuum system are added, as can be seen in Fig. 3, where the compactness of the system can be appreciated

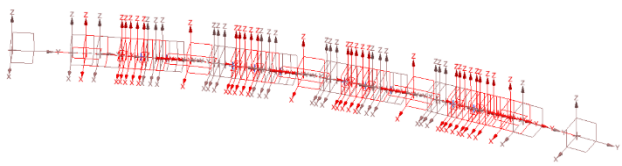

Figure 2: Wireframe beam path with magnets references.

† lribo@cells.es

ISBN: 978-3-95450-263-9 ISSN: 2673-5520 doi: 10.18429/JACoW-MEDSI2025-THOD01

A LASER TRACKING SYSTEM FOR SAMPLE POSITIONING

F. Villar[†,1], J. Bonnefoy[1], J. M. Clement[1], T. Dehaeze[1], S. Ducourtieux[2], D. Fiole[1], J. Fluegge[3], J.L. Frieiro[4], P. Got[1], K. Kiefer[5], P. Marion[1]
[1]ESRF, Grenoble, France
[2]Synchrotron SOLEIL, Saint Aubin, France
[3]PTB, Braunschweig, Germany
[4]ALBA, Barcelona, Spain
[5]HZB, Berlin, Germany

Abstract

ESRF, PTB, ALBA, SOLEIL and HZB have compared commercial fibered interferometers to characterize their non-linearities. Three different products have been compared and results show that periodic errors span from 50 nm down to below 1 nm.

After that, the ESRF has built a position measuring system capable of tracking the position of a target that moves in a plane along 3 degrees of freedom (DoF): two ±2.5 mm translations and one ±20 degrees rotation. Results obtained on a prototype system show that measurement repeatability is below 10 nm.

INTRODUCTION

In the frame of the LEAPS-Innov pilot project funded by the European Union, ESRF together with ALBA, SOLEIL, PTB and HZB have developed a position measuring system based on fibered laser interferometers and beam steering mirrors that track the position of the object to be measured using a closed loop control system. The overall objective is to measure the position of objects moving in a plane along three degrees of freedom (two translations and one vertical rotation), with a typical range of a few millimetres and a few tens of degrees and with a repeatability of 10 nanometres. This system could typically be used for measuring sample position in experimental stations.

The project was divided in two parts, the first one being dedicated to the characterization by project partners of periodic non linearities of commercially available fibered interferometers. The second part was devoted to the design and construction of a three axes prototype system at ESRF.

This paper presents the results of the interferometers characterization, the design of the mechanical, optical and control systems used to implement this prototype and the experimental results obtained.

FIBERED INTERFEROMETERS

In recent years, fibered laser interferometers have become commercially available. Owing to their compactness, ease of installation and alignment, vacuum compatibility, radiation resistance, nanometric resolution and affordable cost, they have been used in many high-precision synchrotron instruments to measure position variation of samples, X-rays diffraction crystal, X-rays focusing elements…

However, despite these qualities, these interferometers may suffer from periodic non-linearities that impair their measurement performance [1]. In certain circumstances, these errors can reach several tens of nanometres with a period of half the wavelength of the laser used (1530 nm in this work). When used to calculate the angular position of crystals in Double Crystal Monochromators from two laser beams spaced 100 mm apart, these non-linearities generate angular errors of several hundreds of nanoradians, which makes them unsuitable for the latest instruments requiring errors below 30 nrad, see Refs. [2, 3].

To characterize these errors, PTB, ALBA, SOLEIL and ESRF have compared fibered interferometers sold by three different companies with measurement references at their laboratories. The figure 1 shows the different setups built for this purpose. The measurement references vary among laboratory, from a capacitive sensor (ESRF, SOLEIL), to a strain gauge (ALBA) or homemade interferometer (PTB). Capacitive sensors and strain gauges may also exhibit non-linear errors, but their typical periods are several orders of magnitude larger (e.g., 50 µm approximately) than those of the tested commercial interferometers. By limiting the comparison to a range of a few micrometres, we can consider the measurement reference to be purely linear.

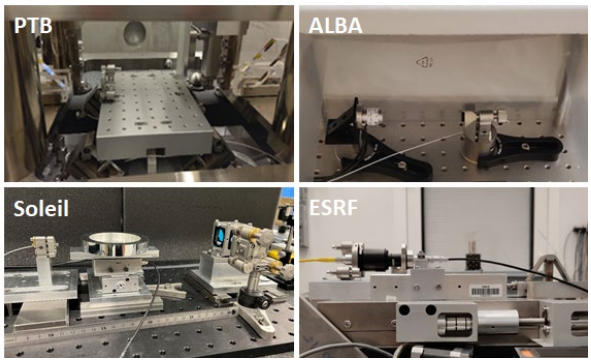

Figure 1: comparison setup used at partner's laboratories.

Figure 2 shows results obtained at PTB over a 5 µm displacement performed at 10 µm/s. The first fibered interferometer (in blue) exhibits peak to peak errors below 1 nm, the second one (in green) errors around 10 nm, and the third one (in orange) errors around 50 nm. A frequency analysis shows that the main period of these errors is equal to half the laser wavelength, i.e., 765 nm approximately.

Due to space constraints in this document, measurement results obtained at ESRF, ALBA, and SOLEIL are not shown, but their conclusions are identical to those obtained at PTB.

† villar@esrf.fr

ISBN: 978-3-95450-263-9 ISSN: 2673-5520 doi: 10.18429/JACoW-MEDSI2025-THOD03

ENABLING HIGH-PRECISION NANO-POSITIONING FOR BEAMLINES: THE PRECISION METROLOGY LAB AT DIAMOND LIGHT SOURCE

Q. Meng†,[1], B. Mullan[1], S. G. Alcock[1], R. Ince[1,2], H. Patel[1], K. Sawhney[1]
[1]Diamond Light Source, Didcot, UK
[2]National Physical Laboratory, Teddington, UK

Abstract

The Precision Metrology Laboratory (PML) at Diamond Light Source provides an ultra-stable environment and specialist instrumentation to perform micro- and nano-scale dimensional metrology to support beamline operation. The lab enclosure is actively stabilised to 10 mK RMS in temperature and 0.5 %RH RMS in humidity. Under these conditions, sub-nm displacements have been measured using capacitive sensor and linear interferometers, and sub-nrad angles have been measured using autocollimator and angle interferometers. Such measurement capabilities are required to characterise and enhance the performance of positioning systems for samples, optics, and detectors on the beamlines. This philosophy has frequently helped to identify faults prior to installation, including misalignments, parasitic motion errors, and controller issues, thereby saving a significant amount of X-ray commissioning time. Increasingly, the PML is involved in prototyping new beamline components that are beyond the production limits of commercial suppliers. Metrology data is routinely used to guide Engineering design decisions, following mechatronics principle.

PRECISION METROLOGY LAB

Diamond Light Source (Diamond) is the UK's national facility for generating and utilising ultra-intense synchrotron radiation. The facility is preparing for the Diamond-II project, which combines a major machine upgrade with new flagship beamlines, and a comprehensive series of upgrades to optics, detectors, sample environments, and computing for existing beamlines [1].

Accurate nano-positioning of samples, diagnostics, and X-ray optics is crucial for beamline operation at all synchrotron light and XFEL facilities. To achieve reliable nano-positioning requires stages capable of making accurate, reproducible and traceable motions on the nanometre and nanoradian level, and suitable instruments and environments to measure these extremely small motions.

The Precision Metrology Laboratory (PML), operated by the Optics & Metrology group, provides an ultra-stable environment for nano-metrology at Diamond. The lab is equipped with a range of metrology instruments shown in Fig 1. The PML team provides a valued service to help specify, procure, assemble, install, and commission major beamline components, thereby improving the scientific output of Diamond.

ENVIRONMENTAL STABILITY OF PML

The PML has an area of ~100 m^2 and is built on the Experimental Hall floor at Diamond. This stable concrete floor slab is supported by approximately 1500 concrete piles anchored into the chalk bedrock 15 meters below the surface. There are four experimental stations in the PML which can simultaneously accommodate multiple metrology projects. Two, passively damped, pneumatic, optical tables attenuate floor vibration when floated. A granite table grouted to the floor, which behaves rigidly up to 100 Hz, provides a stable base for the most demanding tests. This is surrounded by a protective enclosure (4 × 2.6 x 2.7 m^3) which reduces air turbulence, stray-light levels,

Figure 1: The Precision Metrology Laboratory provides an ultra-stable environment for micro- and nano-scale metrology characterisation of beamline motion stages using commercial and in-house-developed instrumentation.

† edward.meng@diamond.ac.uk

ISBN: 978-3-95450-263-9 ISSN: 2673-5520 doi: 10.18429/JACoW-MEDSI2025-THOD04

TRACEABLE SUB-NANOMETRE INTERFEROMETRY TO IMPROVE NANOPOSITIONING AT SYNCHROTRON AND XFEL BEAMLINES

S.G. Alcock†,1, R. Ince[1,2], Q. Meng[1], H. Patel[1], A. Yacoot[2], K. Sawhney[1]
[1] Diamond Light Source, Didcot, UK
[2] National Physical Laboratory, Teddington, UK

Abstract

Coupled with faster detectors, X-ray optic upgrades, new flagship beamlines, and advanced data pipelines, the new low emittance Diamond-II source will benefit a wide range of scientific communities. Smaller, brighter, X-ray beams enable sample scanning systems to progress from slow, step-based motion to rapid, freeform dynamic trajectories. Metrology feedback devices, such as interferometers or capacitive displacement sensors, are increasingly used for real-time monitoring and correction of parasitic errors of micro- and nano-positioning stages. Beamlines are often noisy environments, with mechanical, acoustic and electrical disturbances, and temperature or humidity fluctuations. To provide accurate, closed-loop feedback for nano-positioning stages, metrology instruments need to be calibrated and optimised to nullify errors caused by variations on the beamline. We demonstrate the importance of characterising nano-positioning stages in the ultra-stable environment of the Precision Metrology Lab using a traceable, linear interferometer. Lessons learnt are applied to compensate for environmental changes in "real-world" beamline conditions to achieve sub-nm nano-positioning.

INTRODUCTION

Smaller, brighter, X-ray beams generated by 4th generation synchrotron light and XFEL sources require nano-positioning stages and mechatronic solutions capable of providing high-resolution, multi-axis motion of samples, X-ray beam diagnostics, and optics. Increased photon flux and faster detectors also enable sophisticated dynamic scanning of beamline components, progressing from slow, discrete steps to rapid, freeform continuous "on-the-fly" trajectories. High-speed synchronisation and triggering of multiple beamline components are increasingly common.

Nano-positioning devices typically include embedded positional or angular sensors, such as encoders or capacitive displacement sensors, to provide "real time" feedback inputs for active, closed-loop control of stages. However, for multi-axis, stacked systems used by many beamline applications, cumulative parasitic errors, thermal expansion, and backlash of the various components can lead to substantial unwanted and unexpected variations at the point of interest (typically the sample under test). To solve these issues, additional metrology sensors are used to close the "measurement loop". This concept includes contributions to the overall error caused by the instrument and target, support structures, and optical path variations [1]. This strategy is increasingly used for demanding beamline applications at Diamond Light Source. A recent example is the end-station for the new CSXID (I17) flagship beamline, currently under construction, as part of the Diamond-II facility upgrade [2]. Multiple interferometers will be employed for closed-loop feedback control of sample position and orientation relative to the zone plate and order-sorting aperture. Motion with six-degrees of freedom is required, with incremental displacements < 10 nm, and stability < 1 nm (1 to 1000 Hz). However, if the metrology devices providing feedback are not accurate, or are subject to drifts caused by environmental variations, they will erroneously command errors in the beamline positioning stages, leading to misalignments and a reduction in scientific data quality. This motivates the study of external factors which influence interferometers, and how such effects can be mitigated to provide enhanced beamline performance.

† Email address simon.alcock@diamond.ac.uk

DIMENSIONAL METROLOGY

Precision Metrology

The Precision Metrology Lab (PML) at Diamond provides an ultra-stable environment and specialist instrumentation and expertise to characterise the linear, angular, and vibrational performance of beamline motion stages. Since 2013, the Optics & Metrology group have conducted acceptance testing of commercial motion systems, helped to diagnose and solve faults, and assisted with beamline installation and commissioning. Examples include: measuring linearity, repeatability, hysteresis, vibrations, and parasitic errors of stages for samples, monochromators and X-ray mirrors; dynamic changes in performance or misalignment between components during motion or cooling; parallelism and orthogonality between optics; and hardware and software fault diagnosis for motion controllers. The PML team also work closely with scientists and engineers to develop novel, state-of-the-art hardware for beamlines.

Stability

The PML is actively stabilised in temperature to <0.13 °C peak-to-valley (PV) and humidity to <4%RH PV. A large granite block grouted to the Experimental Hall floor, and anti-vibration platforms reduce seismic noise for test apparatus. Further enhancements are provided by passive thermal enclosures around critical experiments, which also reduce acoustic noise and air turbulence. This provides an "idealised" environment to characterise the ultimate performance of any motion stage. It also enables quantification of the effects likely to be present in the "real

ISBN: 978-3-95450-263-9 ISSN: 2673-5520 doi: 10.18429/JACoW-MEDSI2025-THP06

AN ULTRA-STABLE, 3-AXIS GONIOMETER FOR PRECISE ANGULAR ROTATIONS FOR OPTICAL METROLOGY OF X-RAY MIRRORS

S.G. Alcock†, M. Bazan da Silva, A. Evangelista, A. Howell, J. Kelly, A. Male, I-T. Nistea, G. Preece, N. Rubies
Diamond Light Source, Harwell Science and Innovation Campus, Didcot, UK

Abstract

Deterministic polishing of X-ray mirrors for synchrotron light and XFEL sources requires metrology instruments capable of accurately measuring optics with slope errors < 50 nrad RMS and height errors < 1 nm peak-to-valley. To improve the performance of the Diamond-VeNOM slope profiler, we have developed an ultra-stable, 3-axis rotation stage to orient the mirror under test. The goniometer employs a spherical air-bearing, actuated by three piezo-walkers via flexure struts. This combination provides high stiffness, zero friction, and minimal parasitic errors. Linear interferometers provide positional feedback to the piezo actuators for fast, closed-loop control of 3D angles. Temperature controllers and forced air stabilisation minimise thermal drifts. FEA and dynamic modelling optimised all components via mechatronic principles. The goniometer can accommodate X-ray mirrors up to 500 mm long and 10 kg in mass. It has an angular range of ± 10 mrad in 3 orthogonal directions, a minimal incremental step of < 100 nrad, and thermal drift of ~ 100 nrad over 30 minutes. Shielding of heat sources reduces air turbulence for probing autocollimators or laser beams. The system is controllable via EPICS to enable dynamical synchronisation with other motion stages and detectors.

INTRODUCTION

For the Diamond-II upgrade, many beamlines require enhanced quality X-ray optics to achieve diffraction-limited performance. Deterministic polishing techniques, such as ion beam figuring [1], demand accurate optical metrology data to guide the correction tool to improve the surface form of X-ray mirrors and achieve slope errors < 50 nrad RMS and height errors < 1 nm peak-to-valley (PV). An R&D program is in progress to enhance the functionality and accuracy of all instruments in the Optics Metrology Lab (OML) at Diamond, including the Diamond-VeNOM slope profiler [2]. This includes the development of an ultra-stable, 3-axis goniometer to precisely orientate and stabilise the X-ray mirror under test relative to the Diamond-VeNOM's autocollimators [3]. Motorised alignment also enables the optic to be measured under various angles of incidence, after which algorithms can extract systematic measurement errors and improve accuracy [4, 5].

EXPERIMENTAL

Design Specifications

The brief was to design, build, and commission a motorised goniometer capable of rotating an X-ray mirror about three orthogonal axes. Acceptance criteria included:

- Support mirrors < 500 mm long and < 10 kg
- Angular range of each axis: ± 10 mrad
- Minimal incremental angle step < 500 nrad
- Ultra-stable, with minimal vibrations
- Repeatable rotations, with minimal backlash
- Thermal drift < 100 nrad over 30 minutes

Commercial solutions were considered, including high-performance hexapods, but rejected due to financial constraints and performance limitations. Prototype tests also demonstrated that the device must not cause mechanical, acoustic, or thermal disturbances to the nearby environment since the metrology instruments are extremely sensitive to turbulent air flows and refractive index changes. Mechanical and thermal finite element analysis (FEA) studies were performed to investigate various design options and predict dynamic performance via mechatronic principles [6]. Mechanical time and frequency domain stability was predicted using a Reduced Order Model extracted from a modal analysis simulation using ANSYS Workbench™, in combination with vibration data from accelerometers. Prototype tests and lessons learned from previous projects were utilised by the Engineering and Controls teams to inform the choice of actuators, bearings, flexures, and interferometers for the final design.

Hardware Implementation

The 3D goniometer (Fig. 1) employs a spherical air-bearing (Speciality Components Inc), actuated by 3 piezo-walkers (PiezoMotor®) via custom titanium flexure struts. Three linear interferometers (Attocube IDS3010), monitoring the position of corresponding retroreflectors mounted on the optic platform, provide dimensional feedback for fast, closed-loop control and stabilisation of 3D rotations (Fig. 2). The combination of air-bearing, piezo-walkers, and flexure struts provide high stiffness, zero friction, and minimal parasitic rotations or translations.

† Email address simon.alcock@diamond.ac.uk

ISBN: 978-3-95450-263-9 ISSN: 2673-5520 doi: 10.18429/JACoW-MEDSI2025-THP07

APPLICATION OF AI INTELLIGENT CONTROL IN UTILITY SYSTEMS

Z. D. Tsai†, C. S. Chen
National Synchrotron Radiation Research Center, Hsinchu, Taiwan

Abstract

At the Taiwan Photon Source (TPS), several studies on energy savings and utility system optimization are currently underway, with AI solutions being actively explored for laboratory applications. The proper operation of the cooling tower and chilled water system plays a crucial role in energy conservation. Through AI-based analysis, we can clearly observe the impact of ambient wet-bulb temperature on system power consumption. Furthermore, system efficiency is enhanced by optimizing temperature setpoints, controlling pump flow rate, and managing the on/off scheduling or frequency modulation of facility operations. In this study, a model is constructed to verify the practical impact on power consumption. The analysis demonstrates that these mechanisms can effectively improve overall energy performance.

INTRODUCTION

The use of artificial intelligence (AI) in optimizing utility systems has gained widespread traction, especially in large-scale facilities where chilled water systems and cooling towers account for a significant portion of energy consumption. AI-based intelligent control strategies enable predictive, adaptive, and real-time optimization, offering clear advantages over conventional rule-based methods. Numerous studies have shown that AI-driven control can significantly improve both energy efficiency and system reliability in central cooling applications [1]. In critical environments such as hospitals, advanced optimization methods have achieved meaningful energy savings by dynamically adjusting operating parameters in response to changing load and ambient conditions [2]. Similar successes have been seen in industrial applications. For instance, machine learning combined with particle swarm optimization has enabled real-time control of multi-cell evaporative cooling towers, effectively reducing power usage [3]. In complex systems with heterogeneous parallel chillers, neural network-based frameworks have coordinated chiller and cooling tower operations to minimize overall energy use [4]. Additionally, deep reinforcement learning approaches have shown strong potential in balancing energy efficiency with operational constraints, especially under variable environmental and load conditions [5].

Building on these advancements, this study investigates the application of AI-based intelligent control in the utility systems at the Taiwan Photon Source (TPS). The focus is on analyzing the relationship between ambient wet-bulb temperature and system performance, and on optimizing key operational parameters—such as temperature setpoints, pump flow rates, and scheduling—to validate the potential for significant energy savings and enhanced operational stability under real-world conditions.

† zdtsai@nsrrc.org.tw

MODEL CREATION OF COOLING TOWER AND CHILLED WATER SYSTEM

To enhance the operational efficiency of large-scale cooling and chilled water systems, a comprehensive data-driven modeling framework was established. Real-time monitoring was deployed across all major equipment, including chilled water pumps, cooling water pumps, chillers, and cooling towers, to collect high-resolution operational and performance data. Each equipment unit was assigned independent operating parameters, enabling flexible and optimal control through dynamic adjustment strategies tailored to varying load conditions. Power consumption sensors were routinely inspected and calibrated to ensure the accuracy, consistency, and reliability of the collected data.

System-level efficiency was assessed by analyzing the effects of varying operational parameters under different environmental and load scenarios to determine the most energy-efficient operating conditions. To model these complex interdependencies, machine learning techniques were employed to capture nonlinear relationships between equipment behavior and external factors such as weather, occupancy load, and seasonal variations. These models provided predictive insight for energy demand forecasting and early fault detection. Iterative testing and hyperparameter tuning were performed to maximize model accuracy and robustness, thereby offering reliable decision support for system control and energy management.

Among various modeling techniques, Recurrent Neural Networks (RNNs) were selected due to their ability to process sequential and time-series data generated from sensors. Unlike traditional feedforward neural networks, RNNs maintain an internal state that preserves temporal context, making them well-suited for scenarios where prior states influence current outcomes. To further enhance learning capacity and long-term dependency handling, we adopted the Long Short-Term Memory (LSTM) architecture—a variant of RNNs that introduces memory cells and gating mechanisms (input, forget, and output gates). These structures enable the model to retain relevant information over extended time periods and discard irrelevant signals, thereby mitigating vanishing gradient issues and enhancing stability during training. The LSTM model demonstrated high predictive accuracy in forecasting energy demand, allowing precise estimation of future power consumption patterns based on historical operational data. By incorporating external variables such as weather conditions and diurnal cycles, the model provided reliable forecasts that informed optimal resource allocation and adaptive control strategies.

To identify the primary factors influencing system energy consumption, we selected eight key input variables

ISBN: 978-3-95450-263-9 ISSN: 2673-5520 doi: 10.18429/JACoW-MEDSI2025-THP09

A VIBRATION CONTROL METHOD FOR LINEAR ACCELERATOR*

Z. Lei, R. Deng†, F. Gao, H. Deng, L. Yin, T. Zhen, Y Liu, Z. Jiang
Shanghai Advanced Research Institute, Chinese Academy of Sciences, Shanghai, China

Abstract

The beam orbit or effective emittance is correlated with the mechanical vibrations of quadrupole magnets. To mitigate the impact of vibrations on beam orbit stability, active vibration isolation platforms can be employed to enhance the stability of magnets and other components. This paper presents an active vibration isolation system based on the inverse piezoelectric effect, combined with a feedforward control algorithm to improve the positional stability of the magnets. This vibration isolation system has been deployed in batches in the SHINE project. Test results demonstrate that the active vibration isolation system achieves over 50% displacement attenuation, facilitating beam tuning and indicating that this control strategy holds significant potential for broader application in linear accelerator construction.

INTRODUCTION

Shanghai High Repetition rate X-ray Free Electron Laser and Extreme Light Facility (SHINE), currently under construction, stands as one of the world's most efficient and advanced user facilities based on free-electron laser technology [1, 2]. The superconducting linac is built from cryomodules, each operating at 1.3 GHz and measuring approximately 12 meters in length. A typical module incorporates eight TESLA-type 9-cell superconducting cavities, along with couplers, tuners, beam position monitors (BPM), and a superconducting quadrupole magnet at one end. To meet the sub-micron beam stability specifications of the superconducting accelerator and to suppress cavity frequency detuning induced by mechanical vibration, the allowable position jitter is generally constrained to within 10% of the beam size [3]. In particular, engineering specifications require that the vibration amplitude of certain quadrupole magnets perpendicular to the beam direction remain below 0.2 μm within the frequency range of 1–100 Hz.

The SHINE facility is located near the Shanghai Synchrotron Radiation Facility (SSRF). A comparative analysis of ground vibration levels at major light source sites worldwide, conducted by DESY, showed that the vibration levels at the SSRF campus are significantly higher than those at other comparable facilities [4]. Therefore, the development of an active vibration isolation platform suitable for large-scale accelerator applications is of great practical importance for the SHINE project.

* Work supported by the CAS Project for Young Scientists in Basic Research (YSBR-042), the National Natural Science Foundation of China (12125508, 11935020), Program of Shanghai Academic/Technology Research Leader (21XD1404100) and Shanghai Pilot Program for Basic Research – Chinese Academy of Sciences, Shanghai Branch (JCYJ-SHFY-2021-010).

† email address dengrb@sari.ac.cn

DESIGN OF THE ACTIVE VIBRATION CONTROL STRATEGY

The active vibration platform based on piezoelectric ceramics achieves precise vibration isolation through real-time monitoring and counter-phase cancellation. Its core working principle consists of three key steps: Firstly, Vibration Sensing, High-sensitivity sensors detect vibration signals in real time and convert mechanical vibrations into electrical signals. Secondly, Signal Processing & Control, A control algorithm analyzes vibration characteristics and generates an inverse-phase control signal with matched amplitude to counteract disturbances. Thirdly, Piezoelectric Ceramic Actuation, The control signal drives piezoelectric actuators to rapidly deform, generating opposing forces to cancel vibrations. The inverse piezoelectric effect enables precise conversion of electrical energy into mechanical motion.

EXPERIMENTAL RESULTS

The active vibration isolation platform developed based on the control strategy introduced above has been installed in the undulator section of the SHINE facility. It provides active vibration attenuation for quadrupole magnets requiring high positional stability, as shown in Fig. 1. In the undulator section of the SHINE facility, the vibration tolerance for quadrupole magnets is 200 nm.

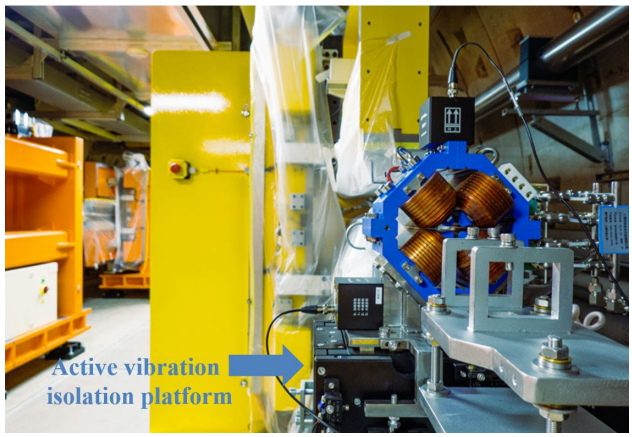

Figure 1: Test bench.

Figure 2 presents the measured vibration results over a continuous 48-hour period in the tunnel, demonstrating that this active vibration isolation platform meets the specified physical performance requirements.

ISBN: 978-3-95450-263-9 ISSN: 2673-5520 doi: 10.18429/JACoW-MEDSI2025-THP10

BEAM-INDUCED HEATING ON THE SECTOR GATE VALVE IN THE SPring-8-II STORAGE RING

H. Ota[†,1], K. Tamura[1,2], M. Oishi[1,2], M. Shoji[1,2], Y. Taniuchi[1], Y. Ueda[1], T. Masuda[1], H. Dewa[1], M. Masaki[1], S. Takano[1,2], T. Watanabe[1,2]
[1] Japan Synchrotron Radiation Research Institute (JASRI), Sayo, Japan
[2] RIKEN SPring-8 Center (RSC), Sayo, Japan

Abstract

SPring-8-II is an upgrade project toward the 4th generation synchrotron light source to provide hard X-ray with nearly two orders of magnitude higher brilliance compared to the current SPring-8. Low electron beam emittance less than 100 pm· rad for the high brilliance requires high gradient multi-pole magnets with a small bore radius and vacuum chambers with a narrow aperture.

Strong beam wake field due to the narrow aperture increases vacuum chamber heating, so its evaluation and countermeasures are an important issue. In particular, the heating of the sector gate valve (SGV) with RF shield structure should be evaluated to see if a water cooling is necessary. In this study, we report the results of simulations using the Finite Element Analysis (FEA) code ANSYS to evaluate temperature rising at the SGV for SPring-8-II due to beam-induced heating and to determine whether forced cooling is necessary.

INTRODUCTION

Synchrotron radiation-based research has become indispensable in diverse fields such as materials science, life science, and condensed matter physics. As these research fields rapidly advance, the demands on the light source are also becoming more stringent. Consequently, upgrades of synchrotron light source facilities are underway worldwide. SPring-8-II [1] has also been officially funded in FY2024 and started the project.

In SPring-8-II, the electron beam emittance will be significantly reduced from the current 2400 pm·rad to less than 100 pm·rad. Achieving this requires high gradient multipole magnets with a small bore radius and vacuum chambers with a narrow aperture. The SPring-8-II vacuum chamber has a rhombic cross-section with a distance of 26.16 mm between parallel inner surfaces [2]. The vacuum chamber with the narrow aperture poses challenges such as tighter manufacturing and installation tolerances and lower pumping conductance compared with the current SPring-8. In addition, the narrow aperture increases vacuum chamber heating due to strong beam wake fields.

Among various components, evaluating the temperature rise of the SGV is of particular importance due to its specific internal structure. The SGV contains an RF shield structure to reduce coupling impedance. This RF shield must deform during opening and closing operations and is therefore constructed from a very thin leaf spring structure with a thickness of 0.127 mm. Consequently, its long-term operational reliability is crucial; its opening and closing performance must not be compromised by the cyclic heating from beam wake fields over the facility's operational lifetime of more than 20 years. Therefore, in this study, we have simulated the temperature rise of the entire SGV, including its RF shield, using the FEA code ANSYS. Based on the results, we report on an evaluation of the structural reliability of the SGV during user operation and the necessity of a forced cooling system.

SIMULATION METHOD

For the SGV, an all-metal gate valve from VAT, known for its high reliability and proven performance, will be installed in the SPring-8-II [3]. This valve incorporates an internal RF shield structure. As shown in Fig. 1, the electron beam passes through the center of the rhombic aperture during ring operation. As previously mentioned, strong beam wake fields are generated as the beam passes; therefore, the SGV is equipped with an RF shield to pro-

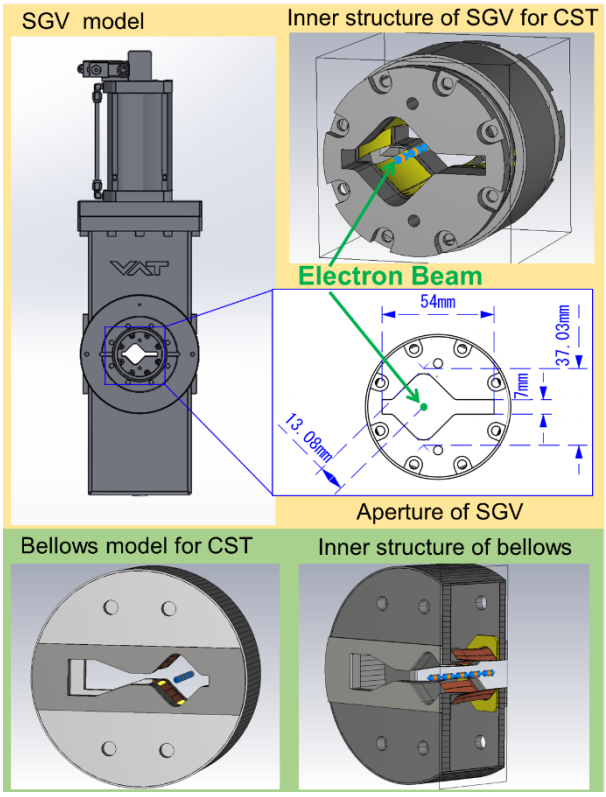

Figure 1: 3D model of SPring-8-II SGV with RF shield structure and bellows with RF finger structure.

† hiroshi.ota@spring8.or.jp

ISBN: 978-3-95450-263-9 ISSN: 2673-5520 doi: 10.18429/JACoW-MEDSI2025-THP14

COMMISSIONING OF THE APS-UPGRADE STORAGE RING VACUUM SYSTEM

J. Carter, Argonne National Laboratory, Lemont, IL, USA

Abstract

The APS-Upgrade Project (APS-U) built a new 1100-meter circumference 6 GeV storage ring within the original APS tunnel. APS-U's new storage ring vacuum system is a complex assembly of over 2500 custom vacuum chambers. The vacuum pumping system is a hybrid combination of NEG-coated vacuum chambers, ion pumps, and uncoated chambers with NEG strip pumping. APS-U began operations in April 2024 and by early 2025 has successfully commissioned the vacuum system to achieve low UHV operating pressures which helped the machine reach key performance parameters and allows for reliable delivery of beam to the users with minimal downtime. The commissioning performance of the machine indicates the NEG coated chambers are performing reliably even with a relatively minimal bakeout and activation. This presentation will share results and analysis of the vacuum system commissioning.

INTRODUCTION

The Advanced Photon Source (APS) in Lemont, Illinois recently completed a major upgrade, replacing the original storage ring with a 6 GeV, 200 mA multi-bend achromat lattice. The new storage ring design features a natural emittance of 42 pm-rad, enabling production of x-rays up to 500 times brighter than the original APS. The storage ring is 1.1 km in circumference and contains 40 sectors.

The APS-U's storage ring vacuum system design [1] contains primarily thin-walled 22 mm inner diameter aperture vacuum chambers, see Figure 1, passing through narrow magnet pole gaps. The design target for the vacuum system was to achieve a 2 nTorr average pressure during 200 mA operations, or a ratio of 1E-11 Torr / mA, by 1000 A*hrs of conditioning time. Low pressures ensure sufficient beam lifetimes can be maintained to deliver reliable beam to the users.

Each sector contains over 60 unique vacuum components including vacuum chambers, absorbers, and beam position monitor (BPM) chambers with rf-lined bellows and the full storage ring vacuum system contains over 2500 vacuum components. The vacuum system contains a hybrid of pumping elements to pump down the conductance limited apertures including NEG-coated chambers, chambers with NEG-strip pumping, and ion pumps backed by NEG cartridges. NEG coated vacuum chambers comprise approximately 50% of the length of the new APS storage ring vacuum system. Each sector contains 2 cold cathode (CC) gauges (1 in the arc and 1 in the straight section) and at least 10 ion pumps (typically 9 in the arcs and 1 in the straight section with additional ion pumps in special Zone F straight sections).

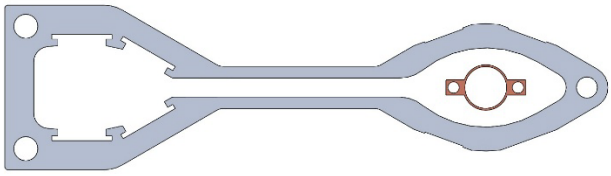

Figure 1: Cross section comparison of previous 300 mm wide APS vacuum chamber to APS-U's new 22 mm ID chamber.

The previous APS was shut down in April 2023 to begin storage ring removal and replacement. Each sector is comprised of 5 magnet-vacuum modules in the arc section and a straight section. The magnet-vacuum modules and straight sections were pre-assembled prior to the shutdown and the 200 modules and straight sections were assembled in tunnel during the following year. The vacuum assemblies within each module were connected by a BPM with flexible bellows and each arc and straight section can be isolated by rf-lined gate valves. Each arc section and straight section was baked prior to start up at a temperature of 130 C for 24 hours. The bakeout temperature was limited to reduce risk of overheating aluminum vacuum chambers and to avoid creating leaks across the new complex assembly. The bakeout was sufficient to purge gases but may have only partially activated the NEG coatings.

Assembly and bakeout of the upgraded storage ring were completed in February 2024 and commissioning approval was granted in April 2024 [2]. In this paper we present the storage ring vacuum system commissioning results as of the completion of the new APS's 4th run in August 2025.

STORAGE RING VACUUM SYSTEM COMMISSIONING

The new APS began commissioning in April 2024 and quickly ramped up to higher currents, see Figure 2. The APS sustained runs operating over 50 mA by July 2024, 100 mA by October 2024, and the designed current of 200 mA by February 2025. In August 2025 the 4th run cycle of APS was completed with the APS surpassing 810 A*hrs of accumulated conditioning time.

Figure 3 highlights the decay of APS operating pressures as measured at cold cathode gauges in Sectors 1 through 4. The pressure response is as expected with a linear response to the rise and falls of beam current. Following high initial pressures at start up the pressures continue to reduce with accumulated conditioning time allowing for further ramp up of beam current.

A full activation of the NEG-coated chambers at higher temperatures may have led to lower pressures however the sufficient vacuum performance indicates the vacuum system is benefiting from low PSD yield rates of non-activated

ISBN: 978-3-95450-263-9 ISSN: 2673-5520 doi: 10.18429/JACoW-MEDSI2025-THP15

COMPARISON OF FEA SIMULATIONS AND EXPERIMENTAL DATA FOR A NEW GERMANIUM DETECTOR FOR X-RAY SPECTROSCOPY AT SYNCHROTRON FACILITIES

M. Quispe†, J.J. Casas, C. Colldelram, L. Nikitina, G. Peña
ALBA – CELLS Synchrotron, Cerdanyola del Vallès, Spain
H. Graafsma, H. Hirsemann, E. Welter
Deutsches Elektronen-Synchrotron DESY, Hamburg, Germany
M. Porro, Ca'Foscari University, Venice, Italy
S. Chatterji, E.N. Gimenez, S. Scully, Diamond Light Source Ltd, Oxfordshire, United Kingdom
C. Cohen, E. Collet, T. Martin
European Synchrotron Radiation Facility ESRF, Grenoble, France
A. Balerna, The National Institute for Nuclear Physics INFN, Frascati, Italy
P. Bell, M. Cascella, K. Klementiev, Ch. Ward, MAX IV Laboratory, Lund, Sweden
B. Schmitt, PSI Center for Photon Science, Villigen, Switzerland
T. Kolodziej, National Synchrotron Radiation Centre SOLARIS, Kraków, Poland
M. Chauvin, N. Goyal, F.J. Iguaz, Synchrotron SOLEIL, Saint-Aubin, France
R. Menk, Elettra Sincrotrone Trieste, Trieste, Italy
S. Aplin, M. Porro, M. Turcato, European XFEL, Schenefeld, Germany

Abstract

As part of the European LEAPS-INNOV project, a new generation of high-purity Germanium detectors has been developed for synchrotron applications requiring spectroscopic capabilities. This novel design focuses on the development of monolithic multi-element Germanium detectors for X-ray Absorption Fine Structure (XAFS) and X-ray Fluorescence Spectroscopy (XRF) applications. This article presents the thermo-mechanical simulation results of the final detector prototype, based on Finite Element Analysis (FEA). These results are compared with the first experimental data obtained in the laboratory. Numerical calculations were carried out using ANSYS software, simulating combined thermal and mechanical effects under cryogenic and vacuum conditions. The numerical studies presented here represent an extension and update of previous work conducted during the development of this project.

BACKGROUND

In the context of the European project LEAPS-INNOV, work package 2 [1], a new generation of Germanium detectors has been designed for X-ray Absorption Fine Structure (XAFS) experiments. Two detector prototypes have been developed, based on simulation studies to optimize their performance. Each prototype is equipped with a 10-element monolithic HPGe sensor, one with 5 mm^2 area pixels and another with 20 mm^2 area pixels. In addition, a new electronic chain has been designed, allowing crosstalk and charge-sharing correction, and enabling the processing of higher count rates ranging from 20 $kcps/mm^2$ up to 250 $kcps/mm^2$. During the thermo-mechanical design phase, numerical simulations were performed using ANSYS software, with initial results reported in previous studies [2, 3]. This paper presents new thermal results of the final model, considering modifications added to the previous models, and compares some of the numerical results with actual experimental values obtained from commissioning tests carried out at the SOLEIL and ESRF [4, 5].

GEOMETRIC DESCRIPTION

Figure 1 shows the Germanium detector, highlighting its main components. The prototype consists of three parts: (i) the Detector Head, which houses the Germanium crystal (21x21x4 mm^3) and its mechanical holder, the front-end electronics, and the beryllium window; (ii) the Cooling System, composed of the cryocooler, copper braid, copper arm, copper holder, and the arm holder; and (iii) the Vacuum Chamber.

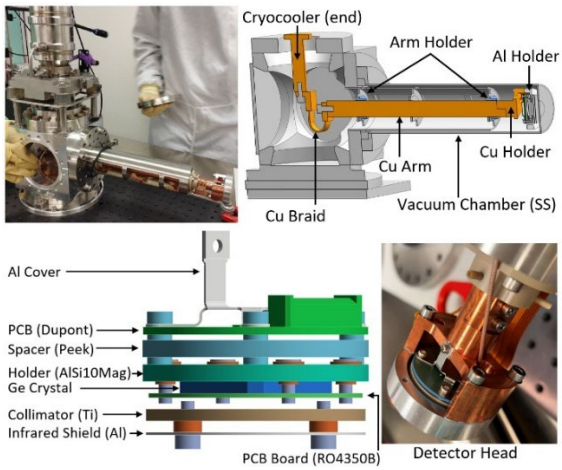

Figure 1: Germanium detector. Details of main parts (top) and components of the Detector Head (bottom).

†mquispe@cells.es

ISBN: 978-3-95450-263-9 ISSN: 2673-5520 doi: 10.18429/JACoW-MEDSI2025-THP16

ConFlat® VACUUM FLANGE APPLICATION AND ANALYSIS IN VARIOUS NON-CIRCULAR FLANGE GEOMETRIES*

M. Seegitz, H. Brodsky, A. Kudler, P. Palecek, R. Todd
Brookhaven National Laboratory, Upton, NY, USA

Abstract

The National Synchrotron Light Source II (NSLS-II) facility at Brookhaven National Laboratory uses an ultra-high vacuum (UHV) system to operate, which typically uses circular ConFlat (CF) flanges to connect vacuum components together. With varying equipment design restrictions, the implementation of non-circular CF flanges is being studied as a possible alternative, as it has been used in other accelerators. Here, an analysis of noncircular CF flanges was conducted to identify sealing problems associated with such flanges, particularly at the HEX beamline. Autodesk Inventor and ANSYS Workbench were used to create models and conduct finite element analysis (FEA) simulations, respectively. Parameters relating to the flange rigidity and geometry were performed to find problem areas. The results suggest that the geometry, combined with plastic deformation of the CF knife-edge and uneven pressure distribution, may contribute to the overall sealing failure.

INTRODUCTION

The ConFlat (CF) flange first developed at Varian Associates in 1961, has proven to be remarkably reliable [1]. The CF flange has been successfully modified to other shapes. At CERN, a separate rectangular CF flange was specially designed to withstand fully bakeable UHV conditions and was successfully implemented at CERN's Proton Synchrotron accelerator [2]. The Cornell High Energy Synchrotron Source (CHESS) has also made modified versions of the circular CF flange that include oval radio frequency (RF) seals [3]. Moreover, commercially available rectangular ConFlat flanges are also available [4].

With care, rectangular shaped CF flanges have been used at exit locations successfully. However, these rectangular flanges have been prone to a higher rate of sealing failures when compared to the circular CFs. A larger version of this flange designed for the High Energy Engineering X-ray Scattering (HEX) beamline exhibited an even greater number of sealing failures, leading to this investigation.

The flange assembly is shown in Fig 1. The analysis looks to uncover potential issues of the rectangular flange using finite element analysis (FEA) software as well as careful laboratory prototype testing and measurements. The results of which may lead to better possible design improvements and sealing reliability.

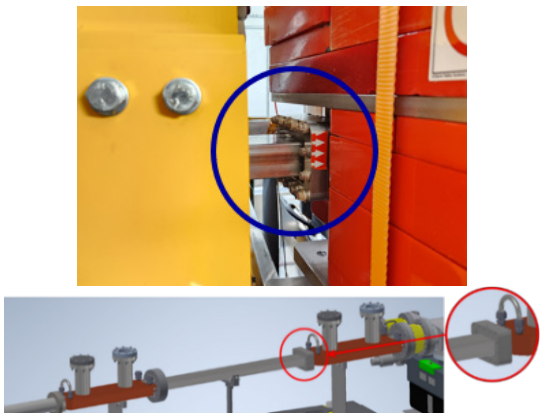

Figure 1: Assembly of HEX beamline extraction without magnets showing location of the rectangular CF flange.

EXPERIMENTAL

ANSYS Simulation Conditions

Since the gaskets in question are made of quarter-hard C101 copper, the material had to be incorporated into the simulation via the material data library in ANSYS Workbench. Because the gasket would plastically deform, the material included a multilinear isotropic hardening object, where plastic strain and stress data would be included in the calculations. Likewise, the flange inserts and receivers in the model were made of a general stainless steel (SS) alloy defined by ANSYS or a 304L stainless steel material defined similarly to that of the copper alloy [5]. Figure 2 below shows the graph in which strain hardening data was found.

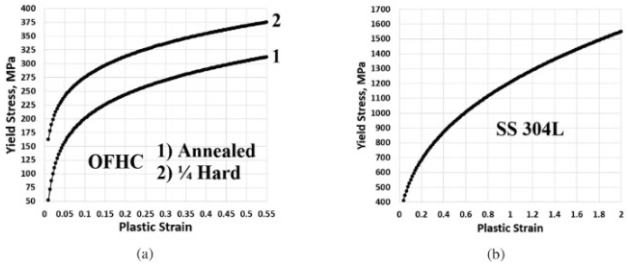

Figure 2. Hardening curves for a) annealed and ¼ hard gaskets and b) a SS 304L stainless steel flange.

A series of frictional contacts were included along the faces of the gasket, knife-edges (on the flange inserts) and flange receiver connected to each other. All frictional contacts were given a frictional coefficient of 0.2.

With respect to mesh, a global mesh size of 3.0 mm was applied. Additionally, a body sizing of 0.3 mm was applied to the gasket. Both knife edges were given a face sizing of

*Not Export Controlled - The research described herein is Fundamental Research as defined in EAR (15 CFR §734.8), or Part 810 (10 CFR §810.3), as applicable, and as described in the USD (AT&L) memoranda on Fundamental Research, dated May 24, 2010, and on Contracted Fundamental Research, dated June 26, 2008.

ISBN: 978-3-95450-263-9 ISSN: 2673-5520 doi: 10.18429/JACoW-MEDSI2025-THP18

DESIGNING A 3-AXIS DELTA ROBOT CAPABLE OF SUB-NANOMETRE STABILITY FOR A SYNCHROTRON FLAGSHIP BEAMLINE

S. Beamish†, J. H. Kelly, C. Bovo, D. Tillin, S. Davies, D. Burn
Diamond Light Source, Didcot, UK

Abstract

Understanding the structure of quantum materials is essential for unlocking the next generation of low-cost, energy-efficient devices. To achieve this, a state-of-the-art Coherent Soft X-ray Imaging and Diffraction (CSXID) beamline is currently under development at Diamond Light Source. At the heart of the endstation will be a three-axis delta robot capable of manipulating samples with sub-nanometre RMS (root-mean-square) stability under cryogenic conditions. This work presents the mechatronics process applied to design this delta robot, from initial concepts to a manufacturable assembly and a fully simulated closed-loop control system. The results demonstrate the power of the mechatronics process to predict system performance and enable a right-first-time approach.

THE CHALLENGE

As the demand for studying samples in greater detail increases, the limiting factor in imaging performance increasingly becomes the vibrational stability of the sample. One such example is the study of quantum materials, which requires nano-scale imaging to facilitate this scientific research.

The QMI (Quantum Materials Imaging) endstation, part of the CSXID beamline is currently under development as part of Diamond II. This endstation demands a sample stability of 0.5 nm RMS relative to the Fresnel zone plate in both the X and Y axes (where Z-axis is along beam direction). Additionally, the scanner must have an X-Y travel range of ±2 mm, along with a Z travel range of ±0.2 mm.

Further increasing complexity, the system must also operate in high vacuum (10^{-8} mbar), with sample cryo-cooling, a variable magnetic field, and dual-axis sample rotation for 3D scanning.

DESIGN PROCESS

To meet the stringent performance requirements, a structured and iterative mechatronics design methodology was employed. This approach systematically integrates mechanical, electronic, and control system design to reduce development risk and ensure the specification is met at each step [1].

The process, illustrated in Fig. 1, emphasizes rapid concept evaluation through a staged go/no-go decision framework. Early-stage concepts are assessed by applying fundamental physics and design principles, allowing infeasible solutions to be efficiently eliminated before significant resources are committed. This contrasts with some traditional linear design workflows, which often risk late-stage redesigns due to overlooked constraints.

A distinguishing feature of this methodology is the incorporation of comprehensive system simulations at the final stages. These simulations account for real-world disturbances, such as floor vibrations and amplifier noise, providing predictive insight into closed-loop performance. While this requires upfront investment in gathering accurate data, it significantly enhances confidence in achieving a right-first time build.

Previous systems at Diamond Light Source have been developed using this design philosophy, including the I14 Delta Robot [2] and DLS Concept Maglev Stage [3]. This project utilises and refines the same process.

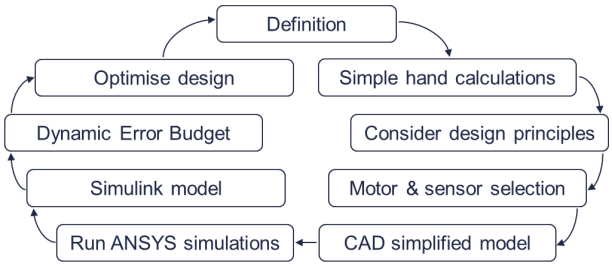

Figure 1: Mechatronics design process.

KEY ELEMENTS OF DESIGN

The design centres around an orthogonal delta robot with compliant flexure mechanisms. This has been proven effective for the I14 Delta Robot, which allowed millimetre scale travel range whilst also providing nano-scale stability. Flexure based systems achieve this due to their zero backlash and the capability to maximise out-of-plane stiffness by intelligently selecting the flexure geometry.

Linear voice coils provide actuation, while 12 interferometers track the positions of the sample and zone plate across six degrees of freedom. These interferometers are mounted on an Invar metrology frame to minimise thermal distortion. Floor vibrations are suppressed using passive isolators and three-axis tuned mass dampers located in each corner of the scanner base plate. Voice coil cooling is achieved via conduction to an external water-cooled heat sink.

As highlighted by the mechatronics design process, these decisions were made by applying analytical equations on elements of the design. For example, calculating the peak stress, and therefore factor of safety, in each flexure for different notched flexure widths and hinge parameters (β, being the thickness of a notch divided by its diameter [4]), with the case for Ti6Al4V shown in Fig. 2.

† scott.beamish@diamond.ac.uk

ISBN: 978-3-95450-263-9 ISSN: 2673-5520 doi: 10.18429/JACoW-MEDSI2025-THP25

TUNING FEA MODELS OF THE ALS-U LATTICE MAGNETS SUPPORTS USING EXPERIMENTAL MODAL ANALYSIS*

R. Johnson†, A. Allézy
Lawrence Berkeley National Laboratory, Berkeley, USA

Abstract

The Advanced Light Source Upgrade (ALS-U) project will deliver a beam 100x brighter than the existing Advanced Light Source (ALS) beam. In order to achieve this, the root mean squared (RMS) displacement levels above 10 Hz for all magnets in a sector of the storage ring, shall be on average <200 nm along the electron beam direction and <35 nm in both transverse directions. Vibration measurements were performed on a prototype raft to inform on the expected performance of the production rafts. This paper details the approach chosen to tune the prototype finite element analysis (FEA) model using the measurements. First, spring constant parameters representing the stiffness of the storage ring supports were tuned to match the predicted mode frequencies, shapes and damping coefficients to impact hammer measurements. Predicted levels at the magnets were then validated with measurements on the prototype raft. The production raft types are predicted to meet the displacement level requirements.

NEW STORAGE RING FOR THE ALS

In order to deliver the required stability of <200 nm along the electron beam direction and <35 nm in both transverse directions, the magnets aimed to have first natural frequencies (FNF) >100 Hz and the full raft system >40 Hz. These requirements and the following validation approach are similar to other 4th generation light sources [1].

The storage ring magnet lattice consists of 12 sectors. Each sector is comprised of 31 electromagnets supported across 4 different rafts (Fig. 1). A raft is comprised of a steel sandwiched core which interfaces to welded plinths and baseplate through 4x Airlock KSC-515 load levellers. This baseplate is in turn bolted to an embedded plate which is grouted to the ALS floor.

Figure 1: Standard ALS-U storage ring sector.

At the time of impact hammer testing, 4x production magnet were not available, and therefore represented by a magnet mass simulator (MMS). The only production magnet in the impact hammer test was the BENDC first article (Fig. 2).

* The Advanced Light Source Upgrade Project and this work are supported by the Director, Office of Science, Office of Basic Energy Sciences, of the U.S. Department of Energy the Department of Energy (DOE) Office of Science at Lawrence Berkeley National Laboratory under Contract No. DE-AC02-05CH11231

† rpj@lbl.gov

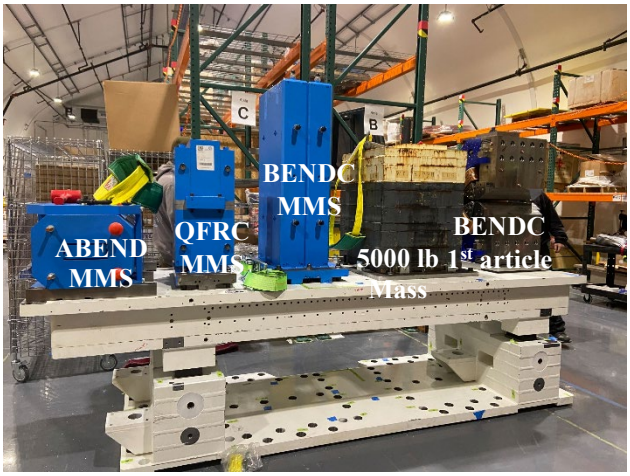

Figure 2: Storage ring prototype raft, configured for impact hammer testing.

IMPACT HAMMER TESTING

Test Set Up

A prototype raft was built and tested in a building outside the ALS. The baseplate was freely mounted on three M36 spherical washers. Three PCB model 356A32 accelerometers were used to capture the response from a 3 lb impact hammer B&K type 8208 at two excitation locations. A total of 80 measurement points were captured to generate 240x FRF's [2]. Feeding the ANSYS modal FEA to FEMTools, accelerometer and excitation locations (Fig. 3) were identified to maximize the modal participation factors. Responses were collected over a frequency of 0-450 Hz. The established coordinate system is transverse: X, vertical: Y, beamline: Z.

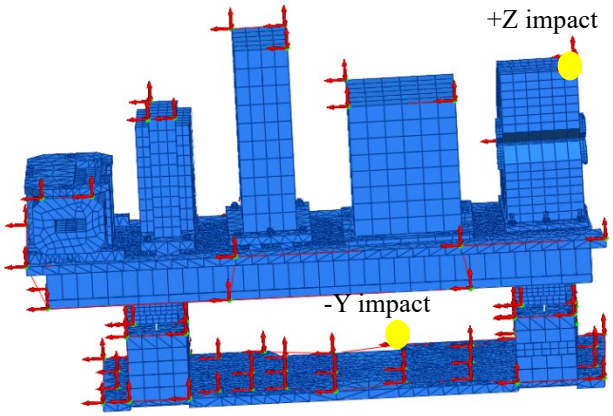

Figure 3: Measurement and excitation location overlaid on FEA model.

ISBN: 978-3-95450-263-9 ISSN: 2673-5520 doi: 10.18429/JACoW-MEDSI2025-THP26

IN-SITU VIBRATION MEASUREMENTS FOR EVALUATING IMPACT OF LOW CONDUCTIVITY WATER INDUCED VIBRATION ON ADVANCED LIGHT SOURCE (ALS-U) ACCUMULATOR RING MAGNETS AND ELECTRON BEAM POSITIONING MONITORS*

R. Johnson†, D. Zaytsev, A. Allézy
Lawrence Berkeley National Laboratory, Berkeley, CA, USA

Abstract

Maximum vibration limits for the magnets of the accumulator ring (AR) for the Advanced Light Source Upgrade (ALS-U) project are <1 um in the transverse direction (X), <0.2 µm in the vertical direction (Y), and <1 µm in the beam direction (Z). For the beam position monitors (BPM), it is <140 nm in X, Y and Z.

Since the ALS-U project is reusing the existing tunnel for the new AR and storage ring, a combination of floor mounted and wall mounted AR supports stands are used. With the AR now installed in the current ALS storage ring tunnel, cooling flow induced vibration measurements were conducted. This paper presents the results of a 2 week measurement campaign with accelerometers on the AR magnets and BPM's in the tunnel while the current ALS storage ring is running. Results are compared to the FEA predictions and to the requirements.

THE ALS-U PROJECT

As part of the construction of a 4th generation synchrotron at the Advanced Light Source (ALS), an Accumulator Ring (AR) is installed during planned extended shutdowns. This will allow the AR to be commissioned while the current ALS is still operating. With the AR recently installed, any design changes that increase risk to the vibrational stability of the ring can be properly assessed with experimental vibration analysis, and mitigated. Past work on flow induced vibration has found induced vibrations are detrimental to stability once turbulent flow is reached [1-5]. While the ALS-U AR flow regime is not expected to be turbulent, a redesign requiring mounting of the low conductivity manifold directly on the raft supports caused a risk evaluation.

Design

The AR is mounted to the inner shield wall using bolted interface plates (Fig. 1). Epoxy shims are placed between the interface plate and wall. Welded rectangular steel beams create the frame base support. Using a 6-strut support system (Fig. 2), the AR raft is mounted to this base support. The AR raft is a welded unit of steel plates and rectangular steel tubing. Vertical support studs interface the AR magnets and the AR raft (Fig. 3).

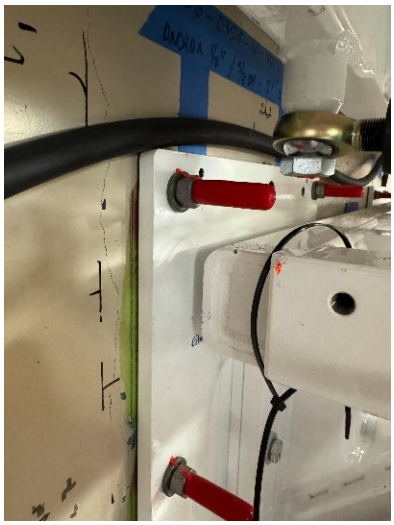

Figure 1: AR raft baseplate to ring wall bolted connection.

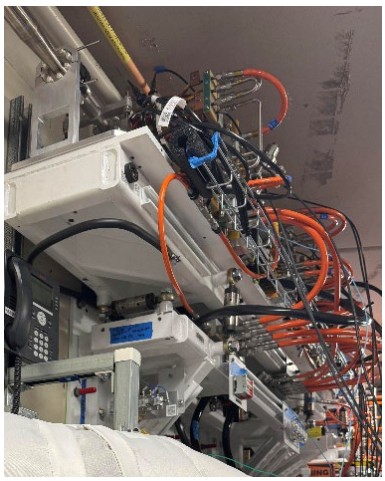

Figure 2: AR raft 4 weldment to raft support via 6 struts.

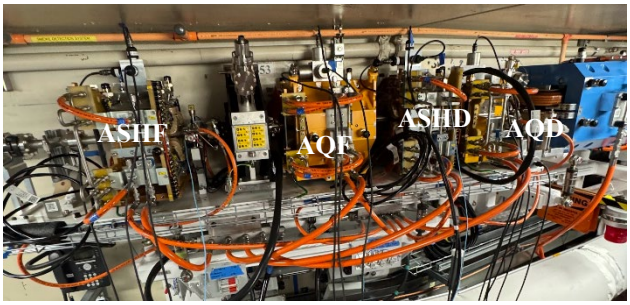

Figure 3: AR raft 4 mounted to the wall.

* The Advanced Light Source Upgrade Project and this work are supported by the Director, Office of Science, Office of Basic Energy Sciences, of the U.S. Department of Energy the Department of Energy (DOE) Office of Science at Lawrence Berkeley National Laboratory under Contract No. DE-AC02-05CH11231
† rpj@lbl.gov

ISBN: 978-3-95450-263-9 ISSN: 2673-5520 doi: 10.18429/JACoW-MEDSI2025-THP27

EXTENDED TRAVEL RANGE AND PARALLEL-DECOUPLED COMPLIANT POSITIONING MECHANISM FOR MEDIUM ENERGY RESOLUTION MONOCHROMATOR AT HEPS

Lu Zhang, Hao Liang†,1, Wei Xu[1], Yunsheng Zhang, Yang Yang, Zheng Sun, Yuanshu Lu, Dashan Shen, Shan Zhang, Xiaobao Deng, Weifan Sheng, Ming Li
Institute of High Energy Physics, Beijing, China,
[1]also at University of Chinese Academy of Sciences, School of Physics, Beijing, China

Abstract

We developed a novel medium energy resolution monochromator (MRM) for Resonant Inelastic X-ray Scattering (RIXS) experiments at the High Energy Photon Source (HEPS) featuring an integrated flexible high-precision positioning system that surpasses conventional designs. Our rotation platform delivers unprecedented performance with a travel range of hundreds of milliradians - three times greater than existing systems - while maintaining sub-microradian precision, with potential for nano-radian resolution if an additional simple configuration is developed. The breakthrough innovation is our two-axis rotation mechanism using parallel decoupled architecture that uniquely combines structural rigidity with precise motion control, solving the longstanding challenge of spatial motion decoupling while enhancing stability. Rigorous simulation and testing confirm all performance metrics exceed design targets. This technology not only meets the exacting requirements for monochromators but extends high-precision capabilities in high-vacuum environments, with our parallel decoupling principle offering transformative potential across multiple precision engineering applications.

INTRODUCTION

The RIXS experimental technique, implemented at synchrotron radiation facilities, offers energy resolutions in the tens of meV and has become an essential research tool in diverse fields such as semiconductors, high-temperature superconductivity, catalysis, and geophysics [1]. The HEPS currently under construction, is the first fourth-generation synchrotron light source in Asia. For its RIXS experiment, a target energy resolution of 70 meV is established, which necessitates a monochromator equipped with multi-dimensional, high-precision crystal attitude adjustment capabilities and excellent stability.

Regarding the structural design of such MRM, most existing light sources either adopt configurations similar to those of high energy resolution monochromators or utilize platforms constructed from stacked industrial stages [2]. The former approach is often overly complex and provides an insufficient angular range, failing to meet the large-range adjustment demands of medium resolution applications [3, 4]. The latter approach, based on stacked stages, presents challenges including excessive overall mass and the high cost of vacuum-compatible platforms.

†lianghao@ihep.ac.cn

To address the requirement for precise three-axis angular adjustment of the crystals, we have designed and developed a novel configuration. This configuration incorporates a large-range rotation stage for the pitch adjustment and a parallel-kinematic, decoupled platform for the roll and yaw adjustments. In this paper, we present the detailed mechanical design of this monochromator and its two integrated high-precision attitude adjustment mechanisms. Furthermore, we report the experimental test results, including the resolution, travel range, and stability of the system.

MECHANICAL DESIGN

The medium-energy-resolution monochromator consists of three main parts: a granite base, a vacuum chamber, and the crystal attitude adjustment mechanisms. As illustrated in Fig. 1, the entire assembly is supported by a granite base resting on Airloc wedge mounts, which allow for three-degree-of-freedom adjustments: ±5 mm in vertical displacement, ±8.7 mrad of roll (about the beam axis), and ±5.8 mrad of yaw (about the vertical axis). The granite base is topped with a honeycomb breadboard for mounting the vacuum chamber and other components. The vacuum chamber is supported by four short, robust cylindrical legs. Inside, the crystal assembly platform is supported by three separate pillars fed from below, ensuring it remains isolated from the chamber walls to prevent position drift caused by chamber deformation.

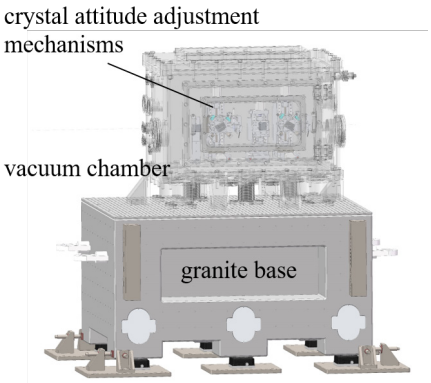

Figure 1: Mechanical design of the MRM.

The monochromator accommodates two channel-cut crystals, each manipulated by an identical, independent adjustment mechanism. As shown in Fig. 2, each mechanism provides five degrees of freedom. Two coarse-adjustment axes, perpendicular to the beam direction, are driven by standard motor-leadscrew linear stages, providing a travel

ISBN: 978-3-95450-263-9 ISSN: 2673-5520 doi: 10.18429/JACoW-MEDSI2025-THP28

FE-ANALYSES AS THE KEY TO SUCCESSFUL HIGH-TEMPERATURE BRAZING OF COMPLEX COMPONENTS

M. Lemke, A. Ermakov, S. Vilcins DESY, Hamburg, Germany

Abstract

Alongside welding, high-temperature vacuum brazing is one of the most used joining processes. At the Deutsches Elektronen Synchrotron (DESY) is a well-equipped workshop area with vacuum brazing furnaces located. Several components for beampipe parts, high-frequency components or diagnostic components made from a wide range of materials have been brazed there, sometimes for an ultra-high vacuum application. Unfortunately, it also happens that these components are defective after brazing. And the cause is often very difficult to find. As in this example the component is made of high-alloy stainless steel. A brazed component has already been successfully serially produced. For another use case a modification has been made. A small series of six pieces was produced and brazed at DESY. This report describes the research into the causes for the defects by using FE-Analyses. We present FE-Analyses as a very powerful tool for detecting errors early on in the design process that could potentially lead to the component being rejected. All results will be presented. On top practical tips for vacuum brazing will be given.

INTRODUCTION

Vacuum brazing (Mathot, 2008) [1] is one of the most common techniques to join structures in accelerators and other related components. In this process, the parts which has to be joined and the braze material are under vacuum and heated to a temperature where the braze material melts and flows throughout the joint area by capillary action between the base materials (Ramani, 2005) [2]. This process is excellent for bonding different materials in a vacuum-compatible manner. In regard of metals various types of stainless steel, copper and titanium are possible pairing partners. Additionally, metal-ceramic connections can be realized by brazing, too. Challenges in the use of the vacuum brazing process are different: coefficients of thermal expansion, wetting behavior and possible residual stresses of the materials. These residual stresses are caused by previous manufacturing processes or manufacturing-related influences. In addition, there are challenges regarding the final, brazed component. For example, components are subject to extremely high requirements in terms of low deformation, tight tolerances, purity, magnetic permeability and surface quality. Due to different coefficients of thermal expansion by brazing to different materials, manufactured gaps in joint zones can getting wider at brazing temperature which directly leads to insufficient joints and especially with vacuum components – vacuum leakages. Furthermore, component stresses and varying wall thicknesses for stainless steel components are critical while using copper-based braze material. This effect is known as liquid metal embrittlement LME [3], which played an important role in the case described here, as the braze material was pure copper. The vacuum brazing processes in general require a large amount of experience, present a number of challenges, and have numerous influencing factors that must be controllable and repeatable.

In our specific case, some dimensions of the Dark Current Monitor (DCM, a vacuum component) are changed. The original DCM was already in series production for another accelerator. A 2D forged 316LN material was used. The brazing was carried out using pure copper wire. In addition to the actual brazing on the component, two small pipe attachments for subsequent Conflat (CF) flanges were brazed in the same brazing step using the same copper braze material. (Fig. 1)

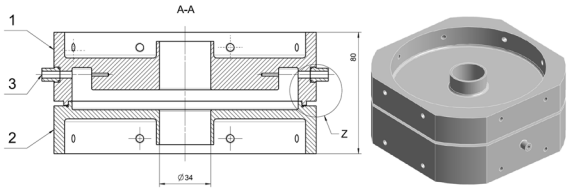

Figure 1: Technical drawing and 3D-model of the modified DCM, courtesy by M. Pelzer DESY, MDI.

DEFECTS AT THE DCM STRUCURE AFTER VACCUUM BRAZING

In our accident case, the vacuum components made of 316LN were brazed with pure copper at a brazing temperature of 1110 °C. There was a visible crack, filled up with braze material on both vertical sides of the DCM structure after the brazing process. For this reason, the crack must be occurred in the phase of heating the DCM structure. This crack is shown in the following Fig. 2. Therefore, the relevant temperature range for the investigation in the heating phase are between room temperature and 1110 °C.

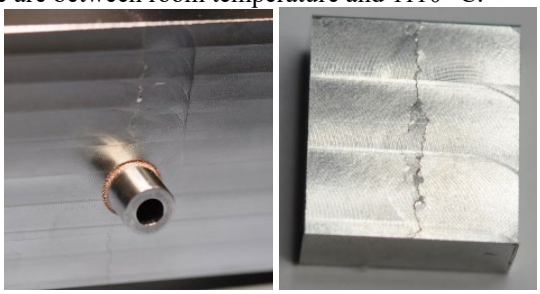

Figure 2: Crack filled with braze material.

FE-ANALYSIS, METHODS AND MATERIAL

Simulating vacuum brazing processes for specific component geometries in a time-dependent, thermal FE-Analysis is a suitable method for supporting the definition of the brazing process in terms of temperature-time cycle, adjusting the batch size, and positioning individual parts locally.

ISBN: 978-3-95450-263-9 ISSN: 2673-5520 doi: 10.18429/JACoW-MEDSI2025-THP29

FEA SIMULATIONS FOR THE REUSE OF FRONT-END COMPONENTS PETRA IV

J. Seltmann†, H. Bienert
Deutsches Elektronen-Synchrotron DESY, Hamburg, Germany

Abstract

The DESY upgrade project PETRA IV includes a major change of design parameters for all components in the ring as well as in the beamlines. Especially the white beam high heat load components currently in use in PETRA III have to be evaluated for their reusability. A case study of a front-end power slit is presented in this paper to show the necessary steps. From given ring and undulator parameters the heat load profiles are calculated. They are imported into ANSYS Workbench using a method to apply heat flux even on freeform surfaces. The FEA model then allows to evaluate cooling water parameters as well as temperatures, deformations and von Mises stresses for all components.

BOUNDARY CONDITIONS

Light Source

The PETRA ring is the largest synchrotron light source with 2.3 km circumference. PETRA IV will be a new 6 GeV X-ray source based on a hybrid seven-bend achromat (H7BA) lattice that enables highest brightness with a very high degree of coherence [1].

The biggest differences to the operation with PETRA III for the front-end design will be the increase in electron beam current to 200 mA and the use of longer undulators. For this study the parameters for a cryogenic permanent magnet undulator (CPMU) with a magnetic period of 18 mm as operated by the ESRF for example will be used (Table 1). This won't be the most powerful insertion device at PETRA IV (UE65 - APPLE-II) but a possible candidate to fit the demands of several future beamlines. These changes will more than double the peak power and the max power density when compared to the UE65 at 100 mA at PETRA III.

There are two kinds of apertures in the PETRA front-ends. Fixed apertures are abbreviated BL and movable apertures are called power slits (PS).

The beam profile is calculated with SPECTRA (ver. 11.1.2) [2] for the position of the main power slit (PS1) to assure a good resolution at this position (Fig. 1). This profile is then rescaled to the first aperture BL1 and evaluated for the absorbed heat load for the cases:

- On-axis beam.
- Horizontal orbit deviation of max 200 µrad.
- Vertical orbit deviation of max 100 µrad.
- Combination of hor, and vert, orbit deviations.

Table 1: PETRA IV Storage Ring and CPMU Parameters

Parameter	Unit	Value
Beam energy	GeV	6.0
Beam current	mA	200
Circumference	m	2304
Magn. period length	mm	18
Device length	m	3.8
K_{max}	-	1.76
Peak power	kW	18.9
Max power density	kW/mrad²	603

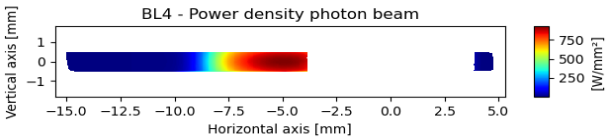

Figure 1: BL4 beam profile.

The "unused" parts of the beam profile are then passed to the next aperture and so on resulting in Table 2 to estimate the power deposition in each aperture. Up to BL4 the front-ends will be built similarly for all beamlines but will deviate for the remaining parts, depending on their experimental hall.

Material

All apertures will be made from GlidCop® as this has proven successful at PETRA III. The cooling channels are machined into the outside of the aperture bodies which are

Table 2: Power on Front-end Apertures for Missteered Electron Beam Trajectories in PETRA IV Extension Buildings

Aperture	Distance from Undulator [m]	Size [mm]	On-axis Beam [W]	Hor. Angle 100 µrad [W]	Hor. Angle 200 µrad [W]	Vert. Angle 100 µrad [W]	Hor. 200 µrad, Vert. 100µrad [W]
BL1	8.37	9	0.3	2.2	22.0	0.4	22.9
BL2	13.6	12	7.6	25.8	106.7	12.1	121.3
BL3	21.3	15	57	108.3	695.3	90.9	1053.4
PS1 (Vgap)	24.34	1.0	12944	12879	12288	17681	16642
BL4 (Hgap)	24.85	8	136.3	1471.7	3715.4	92.9	598
BL5 (Hgap)	40.08	8	1263	1433.7	1277.1	228	201.2
PS2	41.24	-1.0	4389	2877	691	692	157.6

† Joern.seltmann@desy.de

ISBN: 978-3-95450-263-9 ISSN: 2673-5520 doi: 10.18429/JACoW-MEDSI2025-THP34

HIGH HEAT LOAD ANNEALED PYROLYTIC GRAPHITE FILTER FOR THE MATERIALS SCIENCE BEAMLINE AT SESAME

M. AL-Najdawi[†,1], M. Abdellatief[1,2]
[1]SESAME, Allan, Jordan
[2]Diamond Light Source, Didcot, United Kingdom

Abstract

The Materials Science Beamline has historically relied on a rotating filter system for beam attenuation, which introduced mechanical complexity, risk of failure, thermal instabilities, and high outgassing during conditioning. To address these limitations, we have developed a new fixed filter assembly using highly oriented annealed pyrolytic graphite, chosen for its excellent thermal conductivity and low outgassing characteristics. By eliminating moving parts, the fixed filter improves thermo-mechanical stability and reduces operational interruptions.

INTRODUCTION

An X-ray beam attenuation system is an essential component of hard X-ray beamlines, particularly those based on wigglers, which produce very high power that can damage X-ray optics if not properly managed. The attenuation system serves to control the beam flux and reduce the heat load by absorbing low-energy X-rays, thereby protecting the optical components of the beamline.

Different synchrotron beamlines employ various designs and materials for attenuation. For example, some use rotating filters [1] to distribute the power over a larger surface area, while others rely on fixed filter sets. The Materials Science beamline at SESAME [2, 3] previously employed a rotating filter system [4], which had also been implemented at the Materials Science beamline of the Swiss Light Source [5] before its major upgrade. Although this system was effective in reducing the power to safe levels, the rotating filter concept has several drawbacks, including mechanical complexity, risk of mechanical failure, thermal instabilities, and high outgassing during conditioning.

To overcome these issues and challenges, a fixed filter design featuring a 1 mm annealed pyro-graphite filter material has been developed. This material offers exceptional in-plane thermal conductivity, low coefficient of thermal expansion (CTE), and excellent vacuum compatibility. This paper describes the design requirements, material selection process, finite element analysis (FEA) simulations, and expected performance of the new filter.

DESIGN REQUIREMENTS

The fixed filter was required to meet the following specifications:

- Operate in ultra-high vacuum (UHV) conditions ($< 1\times10^{-9}$ mbar).
- Withstand beam power densities up to 21.7 W/mm^2 (worst-case).
- Maintain mechanical stresses below material yield strength.
- Operate continuously without moving parts.

The selected highly oriented annealed pyrolytic graphite (HOAPG) [6] is produced under controlled vacuum conditions using a chemical vapor deposition (CVD) process, followed by annealing to achieve the desired thermal properties. This material offers exceptionally high in-plane thermal conductivity (up to ~1700 W/m·K), low density, zero porosity, and negligible outgassing. Furthermore, it can be lapped and polished to a mirror-like surface finish. Table 1 presents a comparison between HOAPG and other commonly used filter materials.

Table 1: Common Materials Properties Used as Filters

Property	HO APG	Glassy Carbon	Pyro-graphite	Be
Thermal Conductivity XY (W/m·K)	1700	6.3	700	182
Thermal Conductivity Z (W/m·K)	7	6.3	3.5	182
CTE ($\times10^{-6}$/K)	0.5	2.6	6.5	11
Density (g/cm^3)	2.2	1.42	1.8	1.85

† Mohammad.alnajdawi@sesame.org.jo

ISBN: 978-3-95450-263-9 ISSN: 2673-5520 doi: 10.18429/JACoW-MEDSI2025-THP35

HIGH-STABILITY DOUBLE MULTILAYER MONOCHROMATOR WITH GRAVITY-DRIVEN WATER COOLING FOR THE SDB BEAMLINE AT HEPS*

Hao Liang†,1,2, Yuanshu Lu[1], Yang Yang[1], Yunsheng Zhang[1], Lu Zhang[1], Bingbing Zhang[1,2], Changrui Zhang[1], Shuaipeng Yue[1,2], Zhen Hong[1,2], Xiaobao Deng[1], Zheng Sun[1], Ming Li[1,2], Weifan Sheng[1,2],
[1]Institute of High Energy Physics, Beijing, China
[2]University of Chinese Academy of Sciences, Beijing, China

Abstract

Multilayer monochromators are commonly employed in photon hungry synchrotron beamlines to deliver intense, monochromatic X-ray beams. We present the design, validation, and beamline integration of a high-stability, high energy (20-70 keV) double multilayer monochromator developed for the Structure Dynamics Beamline at HEPS. A special gravity-driven water-cooling system, coupled with a unique indium-gallium interface for clamping and cooling, was developed to suppress vibrational disturbances. A vibration level as low as 5.5 nrad RMS within a bandwidth of 0.5 Hz-25 kHz under cooling was measured by laser interferometry. Experimental validation confirmed a clamping-induced deformation about 68 nrad RMS. The system has been successfully installed and tested with synchrotron beam, meeting requirements of the beamline, validated the new design.

INTRODUCTION

The Structure Dynamics Beamline (SDB) at HEPS [1] focuses on the in-situ monitoring of ultrafast irreversible processes, including but not limited to dynamic loading and advanced manufacturing fields [2]. A pink beam mode covers an energy range of 20-70 keV with an integral intensity of more than 2×10^{15} photons/s and a spot size of 5 μm. To achieve this, a Horizontal deflecting Double Multilayer Monochromator (HDMM) is placed at 38.5 m of the beamline as shown in Fig. 1. The requirements of the experimental methods require high sampling speed, that brings extremely challenge for the mechanical design of the system, especially in stability.

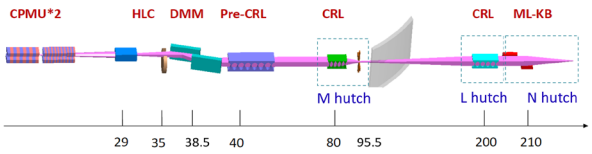

Figure 1: SDB layout.

The main parameters of the HDMM are listed in Table 1. There will be 2 multilayer optics to keep the beam travel in the same direction, each has 3 stripes of multilayers on a silicon substrate. The 3 stripes have different d-space to cover different energy range, from low to high, which reduces the Bragg angle range and the length of the optics.

The monochromator works in Pseudo-Channel-cut mode, that means when tuning the Bragg angle, the beam will move slightly in horizontal direction. This is acceptable as the beamline only carries out experiments at fixed energy.

The requirement of stability in pitch is 50 nrad in the frequency range of 0.1 Hz~10 kHz, which is very demanding and requires special consideration, as to our best knowledge no such high frequency range result is ever reported.

The optics will be water cooled as the heat load is only 65 W. The total slope error of the optics needs to be less than 0.5 μrad RMS including thermal deformation, clamping deformation, substrate and coating slope errors.

In this work, we will present the design of the HDMM, the special water-cooling system and the surface slope error and stability test results.

Table 1: Parameter Specifications of the HDMM

Item	Parameter
Optics	Multilayer, 3 stripes
Energy range	20～70 keV
Bragg angle range	4.12～4.62 mrad
Working mode	Pseudo-Channel-cut mode
Beam offset	Horizontal, ~10 mm
Minimum energy step	10 eV @ 20 keV
Beam height	1400 mm
Beam size (V×H)	1.386 mm×1.386 mm
Relative pitch stability	＜50 nrad RMS (0.1 Hz~10 kHz)
Maximum heat load	65 W
Coolant	Water
Total slope error	<0.5μrad RMS

* Work supported by National Development and Reform Commission (NDRC)
† email address: lianghao@ihep.ac.cn

ISBN: 978-3-95450-263-9 ISSN: 2673-5520 doi: 10.18429/JACoW-MEDSI2025-THP39

MECHANICAL DESIGN OF A FLEXIBLE BUNCH COMPRESSOR FOR SHINE LINAC

F. Gao, T. T. Zhen†, D. Gu, C. Chen, R. B. Deng, Z. Q. Jiang, S. Sun, M. Zhang
Shanghai Advanced Research Institute, Chinese Academy of Sciences, Shanghai, China

Abstract

The SHINE linear accelerator is designed to enhance the electron beam peak current to 1.5 kA at 100 pC through a two-stage bunch length compression process. The magnetic compression support platform (movable chicane) functions as a specialized electromechanically-controlled structure in the linear accelerator tunnel, serving to house critical components including fixed magnetic compression section magnets, vacuum systems, and beam diagnostics. The magnetic bunch compressor (BC) vacuum chamber consists of two side arms and a central section connected by flexible vacuum bellows. The central section, equipped with two middle dipoles on a movable frame, can shift vertically using servomotors (micrometer-scale control). This design allows adjusting the beam path from 0 mm to 438 mm displacement, equivalent to bending angles of 0° to 5°. These platforms are strategically implemented at BC1/BC2/BC3 positions within the linear accelerator lattice.

INTRODUCTION

The accelerator, schematically illustrated in Fig. 1, consists of an electron gun, a laser heater, four accelerating section groups (L1–L4), three bunch compressors (BC1/BC2/BC3), and a dechirper section [1-3]. BC1 was integrated into the SHINE linac at 270 MeV. The magnetic bunch compressor's physics design employs an asymmetric four-dipole chicane configuration. It's used to compress the bunch length and thereby increase peak current by utilizing the beam's correlated energy spread.

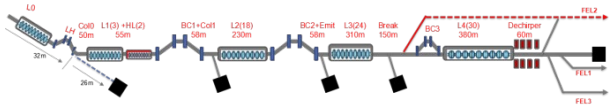

Figure 1: The schematic layout of the 3-BC lattice.

BUNCH COMPRESSOR OVERVIEW

The BC1 support system, installed in the SHINE tunnel, comprises four dipole magnets (DM), two quadrupoles, two corrector magnets, a beam position monitor (BPM), a collimator, and a profile scan wire. All beam diagnostics maintain fixed positions relative to the central dipoles. Figure 2 depicts the schematic layout of the BC lattice. Key parameters of the BC1 support system are summarized in Table 1.

The end dipole magnets are suspended from the tunnel ceiling via co-frame supports, while the two central magnets translate vertically through moving supports that rotate about the end magnets' center. The nominal operating angle is 4.51°, with a maximum angle of 5° corresponding to a 438 mm vertical displacement of the central magnets. A schematic diagram illustrating the kinematic principle of the bunch compressor (BC) support structure is provided in Figure 3. The direction of movement follows the direction of gravity, which can effectively eliminate mechanical backlash.

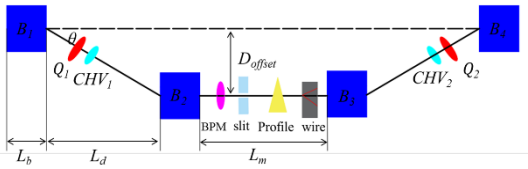

Figure 2: The schematic layout of the BC lattice.

Table 1: Key Parameters of the BC1 Support System

	L_b [m]	L_d [m]	L_m [m]	D_{offset} [m]	θ [°]	Aperture diameter of Quad [mm]
BC1	0.15	4.85	1.8	0.394	4.51	100

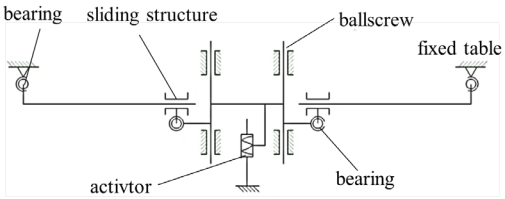

Figure 3: Schematic diagram of the kinematic principle.

MECHANICAL DESIGN

The BC1 support system comprises two suspension supports at each end, a ground-supported moving platform at the center, and two connecting trusses, as illustrated in Fig. 4. The ground-based moving support system includes a grouted foundation, a movable table, a support frame, four linear displacement sensors, and four servo motors, etc., as depicted in Fig. 5.

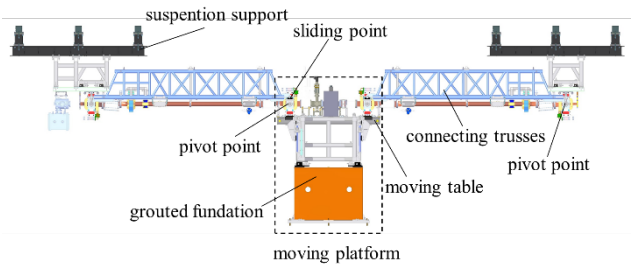

Figure 4: 3D modelling of BC1 support system.

† zhentt@sari.ac.cn

ISBN: 978-3-95450-263-9 ISSN: 2673-5520 doi: 10.18429/JACoW-MEDSI2025-THP40

MINIMIZATION OF THE HEAT-INDUCED DEFORMATION IN THE PREFOCUSING MIRROR FOR THE ELETTRA 2.0 nanoESCA/NANOSPECTROSCOPY BEAMLINE

G. Scrimali*
Elettra Sincrotrone Trieste S.C.p.A., Trieste, Italy

Abstract

As part of the Elettra storage ring upgrade to 4th generation standards, the Nanospectroscopy/nanoESCA beamline is replacing its prefocusing mirror. The new mirror is a 100 mm x 40 mm x 40 mm monocristalline silicon piece, optimized for the maximum heatload produced by the 25 eV horizontal polarity of the beamline's undulators (100.4 mm period, kx = 7.3). This paper presents the layout and strategy followed to ensure a high-quality photon delivery as well as and the calculations and the optimization process of the mirror geometry. To minimize the deformations, a notched, top-side cooling design was chosen, with an almost full-illumination of the top surface. The contact length between the cooling circuit and the mirror was optimized shorter than the mirror length, leading to slightly higher temperatures in the mirror extremities, but more preferable heatload-induced slope. Slits positioned before and after the mirror select only the center and least affected portion of the reflected radiation. Additional simulations confirmed that the optimized design performs equally well or better at higher photon energies.

INTRODUCTION

The "Nanospectroscopy" and "NanoESCA" beamlines at Elettra provide advanced experimental platforms for investigating surfaces, interfaces, and nanostructured materials. Operating in the soft X-ray range (25–1500 eV), they support a wide user community in materials science, nanotechnology, and magnetism [1, 2].

As part of the Elettra 2.0 upgrade, the beamline prefocusing mirror was redesigned. This paper outlines its optimization and the optical strategy adopted to ensure high-quality photon delivery to the beamline's endstations. A key design driver was ensuring uniform out-of-focus illumination for large-area studies while maintaining high-resolution in-focus microscopy. At 25 eV, this required strict control of slope errors and thermally induced deformations, which are the subject of the following analyses.

PREFOCUSING MIRROR ASSEMBLY

The aim of this study was to minimize the effects of heat-induced residual local distortions that generate aberrations that cannot be compensated by the downstream optics. All calculations and simulations presented in this work, unless stated otherwise, were performed for the case of 25 eV, where the undulators deliver the maximum power to the mirror (74 W) and the strongest heat-induced deformations occur.

Optical Layout

The beamline source consists of two identical elliptical undulators, each 2 m long, with a minimum magnetic gap of 19 mm, with λ = 100 mm and kx = 7.3. For the purposes of the analyses, the emitted power was calculated using the parameters of the upgraded Elettra 2.0 storage ring [3]. The emitted radiation is shaped by a fixed mask positioned at 9.8 m from the source, reducing it to a solid angle of 200 × 200 μrad²; a first set of slits at 11 m reduces the vertical acceptance, bringing the beam to 200 × 100 μrad². At 16 m, the prefocusing mirror chamber (PFMC) houses a toroidal mirror at a grazing angle of 1.75°. After the PFMC, another set of slits removes the outer portions of the reflected beam, restricting the transmitted light to the maximum beamline acceptance† of 100 × 100 μrad². This sequence ensures that only the central, most uniform portion of the beam is transmitted to the monochromator, improving the downstream optical performance. The beam finally reaches the monocromator, before continuing towards the experimental station. A scheme illustrating the layout is shown in Fig. 1.

Mirror and Footprint Geometry

The prefocusing mirror (PFM) is a toroidal element machined from a 100 mm × 40 mm × 40 mm monocrystalline silicon block with an Au coating on the optical surface, defined by a meridional radius R = 116 m and a sagittal radius r = 15 cm. As shown in Fig. 1, the mirror is mounted vertically, reflecting the radiation in the horizontal plane.

To minimize the deformations and maintain beam stability and uniformity, the "smart cuts" approach [4-6] is used in the PFM substrate shape: two side notches are combined with a top-side cooling to strategically steer the deformations, stabilizing and flattening the optical surface. The notches run along the entire PFM length and are described by three parameters: the distance from the reflective surface, d_{top}, the depth and height of the notch, d_n and h_n respectively.

The mirror is cooled by water, flowing through two cooling blocks pressed against its sides with the interposition of indium foil to assure good contact. The length of the cooling blocks, l_{cool}, is optimized and is

* giulio.scrimali@elettra.eu

† The maximum beamline acceptance of 100 x 100 μrad² is set by the monocromator's mirrors dimensions. The fixed mask aperture was chosen to be larger to render possible future upgrades to the beamline.

ISBN: 978-3-95450-263-9 ISSN: 2673-5520 doi: 10.18429/JACoW-MEDSI2025-THP42

NSLS-II MAGNETRON COATING SYSTEM UPGRADE

P. Palecek[1], C. Hetzel[1], R. Todd[1], W. Waldron[2]
[1]Brookhaven National Laboratory, Upton, NY, USA
[2]Lawrence Berkeley National Laboratory, Berkeley, CA, USA

Abstract

Subsequent to the commissioning of NSLS-II, the Vacuum Group established a vertical magnetron coating facility to support continued NSLS-II operations and research activities. Some of the early projects included titanium coating injection kicker ceramic chambers as well as NEG coating standard vacuum chambers. This coating facility was also used to apply copper-oxide coating to the APS-U Injection Strip-line Kickers to manage thermal loads. While these efforts proved successful, the coating system was upgraded with a moveable, higher field-strength water-cooled solenoid to allow small aperture coating of varying length. The upgraded facility was used to develop the titanium coating for the ALS-U injection kickers and will also be used to test small aperture NEG coatings for a potential upgrade to NSLS-II. The coating system can now coat chambers up to 2m in length which will allow for photon stimulated desorption measurements here at NSLS-II. The upgrade to this facility will be described in detail along with the results of the ALS-U coating effort.

INITIAL SETUP AND RUNS

At its inception, the NSLS-II Magnetron Coating Facility was purpose built to coat titanium on the NSLS-II Ceramic Kicker Chambers. The system was comprised of a single, air-cooled solenoid with a maximum field of 250G, sitting 6' tall with an inner diameter of 10". That sat upon a custom built 80/20 frame structure (Fig. 1). Integrated into this frame were all the vacuum components (TMP, rough pump, gauging, etc.), the control electronics (high voltage DC PS, low voltage DC PS, VGC, and bakeout controllers), and also a controls PLC. This was all looped into a custom designed/coded software package that would control each system (Fig. 2).

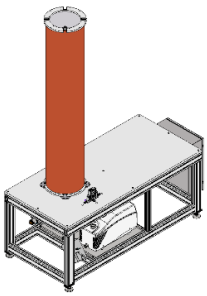

Figure 1. Early design of NSLS-II Magnetron Coating System.

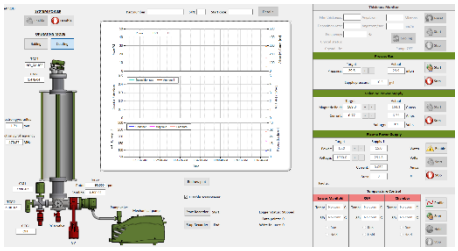

Figure 2. Sample picture of controls software.

This initial setup was able to complete a multitude of runs and geometries. These included titanium coating on the NSLS-II Ceramic Kickers [1], CuO coating on both the APS-U Stripline Kickers and Blades [2], and in-house NEG development of Ti-Va-Zr (Fig. 3).

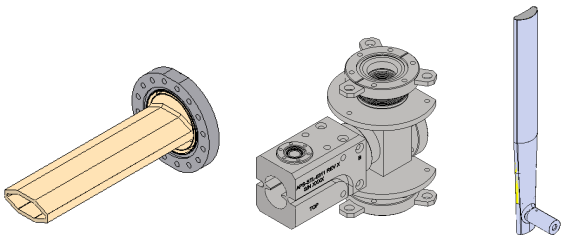

Figure 3. Half-section views of NSLS-II Ceramics, APS-U Stripline Kickers and Blades, respectively.

UPGRADE AND CURRENT SETUP

With the receipt of the ALS-U Ceramic Kicker Chambers, it was quickly apparent that the air-cooled magnet was not capable of completeing the job. During the initial titanium runs, the plasma could not be contained to the chamber proper, but instead chose to propagate into only the end spools of the setup, depicted in Fig. 4.

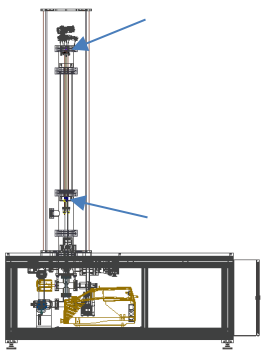

Figure 4. Arrows depict plasma placement in chamber while running air-cooled solenoid during initial testing of ALS-U Ceramic Kicker Chambers.

ISBN: 978-3-95450-263-9 ISSN: 2673-5520 doi: 10.18429/JACoW-MEDSI2025-THP43

NUMERICAL SIMULATION AND THERMAL OPTIMIZATION OF A CATALYSIS CHAMBER FOR THE MIRAS BEAMLINE AT ALBA SYNCHROTRON

A. Jacquet†
ENSTA, Brest, France
A. Carballedo, J. J. Casas, C. Colldelram, B. A. Francisco, M. Quispe, I. Yousef
ALBA – CELLS Synchrotron, Cerdanyola del Vallès, Spain
P. Concepcion, J. Zamarripa
Instituto de Tecnología Química, Universitat Politècnica de València, València, Spain

Abstract

In the context of the development plan for the MIRAS beamline at the ALBA Synchrotron (Infrared Microspectroscopy Beamline), a dedicated experimental chamber has been designed for the study of catalytic reactions using synchrotron-based infrared spectroscopy. This chamber is designed to operate with a reactive gas mixture composed of O_2, H_2, CO, and an inert gas such as Ar, at pressures up to 20 bar, while maintaining sample temperatures between 480 ºC and 500 ºC. To meet these operational requirements, a study strategy based on numerical simulations has been defined. This work presents all the numerical details considered in the simulations. Computational fluid dynamics (CFD) analyses were performed using the ANSYS WORKEBENCH suite, incorporating turbulence modeling, vacuum boundary conditions, and combined forced and natural convection. Three design configurations were evaluated, followed by detailed parametric studies, including mesh sensitivity analysis and simulations under extreme thermal conditions. The final configuration meets all specified operational and thermal mechanical constraints, ensuring reliable performance under synchrotron operating conditions.

INTRODUCTION

The MIRAS beamline at the ALBA Synchrotron is dedicated to infrared spectroscopy and microscopy and aims to extend its capabilities toward catalysis research in the mid and far infrared range. For this purpose, a new catalysis chamber is being developed to operate with reactive gases including O_2, H_2, and CO, as well as inert gases such as argon, at pressures up to 20 bar. The chamber must maintain sample temperatures between 480 ºC and 500 ºC with a maximum gradient of 10 ºC, while keeping external wall temperatures below 70 ºC to ensure operational safety. Achieving these specifications requires precise thermal management that accounts for conduction through metallic components, convection in both pressurized gases and vacuum, and radiation between heated surfaces.

This article complements the work presented in reference [1], which introduced three chamber configurations and presented initial results. Here, the focus is on configuration C3, the most advanced design incorporating integrated water-cooling circuits along with an additional top cooling pipe (Fig. 1).

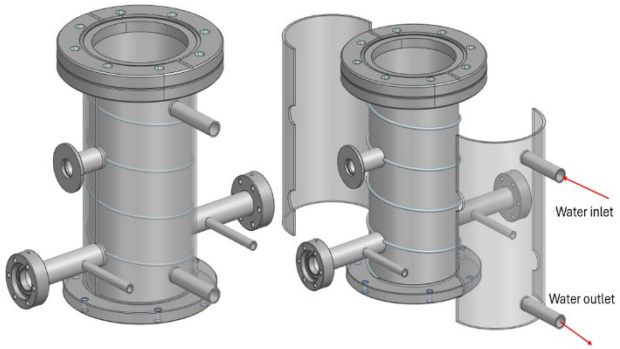

Figure 1: Third model illustrating the water-cooling system (left) and the water inlet and outlet (right).

This study provides a detailed account of the numerical methodology, boundary conditions, thermal contact modeling, and mesh refinement, which were only briefly discussed in the previous publication.

SIMULATIONS

Thermal Contacts

Contact regions, particularly between the sample holder, heat exchanger, coil heaters, and base plates, were explicitly modeled. Thermal Contact Conductance (TCC) was included to account for imperfect contact between solids [2]. TCC quantifies the interface's ability to conduct heat.

The value of the TCC is introduced into the model indirectly, through the definition of an effective thermal conductivity ($K_{effective}$) in a thin solid layer of thickness dx, which acts as the interfacial material. This approach is derived from a thermal balance in the interfacial region, where the heat transfer (Q) across the area A is governed by Eqs. (1) and (2):

$$Q = TCC\ A\ \Delta T_i \tag{1}$$

$$Q = A\ K_{effective}\ \frac{\Delta T_i}{dx} \tag{2}$$

Where ΔT_i is the temperature gradient at the interface. From the thermal balance, the effective thermal conductivity is defined as indicated in Eq. (3):

†auxane.jacquet@gmail.com

ISBN: 978-3-95450-263-9 ISSN: 2673-5520 doi: 10.18429/JACoW-MEDSI2025-THP44

SIMULATION APPROACHES FOR MAGNET DESIGN IN THE ALBA II SYNCHROTRON UPGRADE*

B. A. Francisco†, P. Salmerón, B. Zhang, V. Massana, M. Quispe
ALBA Synchrotron Light Source, Cerdanyola del Vallès, Spain

Abstract

ALBA 01 is the prototype project to improve the fourth-generation upgrade of the ALBA synchrotron - ALBA II, developed by ALBA CELLS (Barcelona, Spain). To achieve its targeted increase in photon beam brilliance and coherence, the new storage ring requires precise validation and optimization of its magnetic structures. The majority of the designs of ALBA 01 are based on the 6BA A2L002b lattice and includes magnet families as bending, antibending, quadrupoles, sextupoles and correctors—totaling around 640 units, including electromagnets and permanent magnets.

This work presents the development of static structural simulations, considering two different solvers, based on the values obtained from the magnetic design specifications. Each tool is employed to predict field distribution, magnetic forces, and mechanical loads, as well as to provide boundary conditions for coupled magneto-structural analysis.

The capabilities and limitations of each approach are discussed, with emphasis on meshing, post-processing, and CAD integration. The convergence of results obtained from the different software packages is presented, along with the associated uncertainties and cross-validation procedures. Finally, the next steps of development are outlined.

INTRODUCTION

ALBA II is the fourth-generation upgrade of the ALBA synchrotron, operated by ALBA-CELLS, designed for an energy of 3 GeV and a natural emittance of 185 pm·rad, while using the same tunnel as the current accelerator. Achieving these goals required a full redesign of the storage ring, including replacement and optimization of the magnetic systems.

The Six-Bend Achromat (6BA A2L002b) lattice—comprising about 640 magnetic units [1]—was adopted as the reference for most of the prototype developments (ALBA 01). In this configuration, some magnets are positioned only 1 mm from the vacuum chamber, imposing extremely tight fabrication and assembly tolerances to prevent interference or misalignment.

Under such conditions, even minor deformations or displacements may compromise ring stability, degrade beam quality, or induce chamber stresses. The increased magnet density may lead to cross-talk, potentially amplifying forces from neighboring units, while the larger height-to-width ratio could reduce intrinsic structural stability.

The explicit consideration of magnetic forces in the structural analyses of ALBA 01 is being addressed in the current development phase. *OPERA™* [2] has been employed to perform the magnetic studies and, although it provides accurate field and force calculations, it is not specifically designed for structural analysis. Therefore, current efforts are focused on investigating methodologies to incorporate these effects into the simulations, with the goal of establishing a fully coupled magneto-mechanical framework.

In this study, we explore alternative coupling strategies between magnetic and mechanical simulations, aiming to implement a fully integrated magneto-mechanical methodology into the magnet development process. Two approaches were tested:

- Integration of ANSYS® Maxwell with Static Structural, via force data transfer;
- The combination of ANSYS® Magnetostatic and Static Structural modules within the Mechanical environment.

In both workflows, the geometric models correspond to four bending magnets. The magnetic simulations were calibrated against the results obtained with *OPERA™*, after which the resulting force maps were extracted and applied as boundary conditions in the subsequent structural analyses. While modal, thermal, and other types of simulations were also conducted as part of the magnet design project, the present discussion is restricted to the static structural analysis of the ALBA 01 prototype bending magnets, as this provides the most direct assessment of the impact of magnetic forces. Moreover, this analysis not only addresses the dipoles developed during the initial project phase but also establishes a methodological framework applicable to the entire set of magnets foreseen for the accelerator upgrade.

MAGNET DESIGN AND REQUIREMENTS

Magnet development starts with preliminary magnetic designs based on the target field profile, which define the required materials and dimensions. The engineering group ensures that these designs also meet the mechanical, assembly, and manufacturing requirements.

In the context of this accelerator upgrade, the mechanical development of the magnets involves three main aspects. First, since the new accelerator is designed with the same tunnel as the previous one, there is a significant increase in the compactness of magnets. As shown in Fig. 1, in a 12.8 m (22.5° arc section), ALBA consists of 49 % iron and 51 % air, whereas the ALBA II design (lattice 6BA A2L002b) reaches 80 % iron and only 20 % air [3]. This condition requires

* Work supported by the Spanish MCIN and Catalan Government, and co-funded by the European Union – NextGenerationEU project ICTS-MRR-2021-02-CELLS from the Recovery and Resilience Mechanism.
† bdeabreu@cells.es

ISBN: 978-3-95450-263-9 ISSN: 2673-5520 doi: 10.18429/JACoW-MEDSI2025-THP45

PARALLEL FLEXURE-BASED RADSI INSTRUMENT FOR CURVED X-RAY MIRROR METROLOGY

L. Lienhard†, C. Austin, W. Xu, M. Idir, S. Hulbert, E. Nazaretski, D. Coburn, T. Wang, L. Huang
NSLS-II, Brookhaven National Laboratory, Upton, NY, USA

Abstract

New high-resolution X-ray beamlines demand reflective optics with higher surface profile accuracy to achieve diffraction-limited focusing. This necessitates advanced metrology instruments capable of delivering repeatable measurements in the nanometer to sub-nanometer range. Slope ranges exceeding 15 mrad (0.86°) and greater pose significant challenges for mirror metrology using conventional interferometric methods especially on shorter mirrors with low radius of curvature (<20 m). To address this, we present a new Relative Angle Determinable Stitching Interferometry (RADSI) instrument featuring a parallel flexure-based mechanical design. This approach enhances vibration and thermal stability while maintaining a compact and lightweight system. Initial measurements of a cylindrical mirror with a 16 m radius of curvature and a slope range of 5 mrad demonstrate nanometer-level repeatability. Comprehensive system characterization suggests the potential for achieving sub-nanometer repeatability with further refinement to the instrument.

INTRODUCTION

Synchrotron X-ray beamlines are constantly looking to improve the quality of mirror-based focusing optics necessary for reaching state-of-the-art focusing resolutions, targeting tens of nanometers or even sub-10 nanometers [1-3]. Achieving diffraction-limited focusing properties for X-ray mirrors in Kirkpatrick-Baez (KB) geometry requires elliptical surface profile accuracy on the order of 1 nm [4]. To achieve smaller focal sizes, optical configurations with high Numerical Aperture (NA) elliptical mirrors are necessary, often resulting in total slope ranges exceeding 15 mrad. Such steep slope requirements pose significant challenges for interferometric metrology methods [5-8].

Relative Angle Determinable Stitching Interferometry (RADSI) addresses these challenges by utilizing a Fizeau interferometer and a reference flat mirror to measure curved elliptical mirrors through sub-aperture stitching with the stitching angles determined from the reference flat mirror [9, 10]. In stitching interferometry, to reconstruct the whole surface topology, the test mirror is gradually rotated in steps to align a portion of its surface normal with the interferometer, ensuring low-density interference fringes suitable for measuring and stitching with sufficient overlap. The instrument concept and Fizeau camera view is shown in Fig. 1.

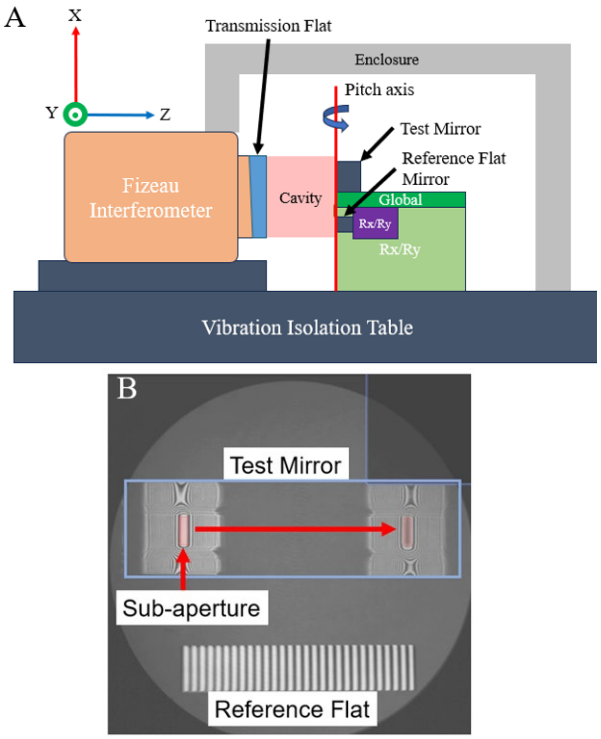

Figure 1: NSLS-II RADSI Instrument Design. (A) Conceptual sketch of the instrument showing motion axes. The global stage moves both the test mirror and reference flat together, while the reference flat also has its own independent stage to null fringes. (B) Fizeau interferometer field of view: Both test mirror in sub-apertures and reference flat are captured at the same time. Superimposed image shows starting and end sub-apertures as the mirror is tilted.

Achieving nanometer-level measurement accuracy in RADSI demands exceptional relative stability between the test mirror and reference mirror throughout the measurement process, which can last up to two hours or longer. This requires a metrology instrument with robust vibration and thermal stability performance while also allowing for relatively large angular travel requirements to measure mirrors with a total slope range of 15 mrad or greater.

To meet these requirements, we designed and developed a parallel flexure-based RADSI metrology instrument. This design offers enhanced stability and precision, making it well-suited for measuring curved X-ray mirrors.

MECHANICAL DESIGN

The RADSI instrument consists of a global stage to orient the test mirror and a nested reference stage to orient

† llienhard@bnl.gov

ISBN: 978-3-95450-263-9 ISSN: 2673-5520 doi: 10.18429/JACoW-MEDSI2025-THP47

PUMPING STATION FOR UCV AND UHV COMPONENTS IN THE EUROPEAN XFEL CLEANROOM

J. Ohnesorge*, J. Eidam, M. Dommach, European XFEL GmbH, Schenefeld, Germany

Abstract

The European XFEL (X-ray Free-Electron Laser) is a research facility that generates ultra-short X-ray flashes for scientific experiments across various fields. Operating at MHz repetition rates, it produces coherent femtosecond X-ray pulses with unprecedented brilliance in the energy range of 250 eV to 25 keV. The facility consists of a linear accelerator and three photon beamlines in underground tunnels.

To protect the sensitive optical components, such as mirrors that guide the X-ray beam to the experimental stations, strict contamination control within the photon beamlines is essential. A cleanroom is therefore required to handle critical components, ensuring that all equipment near the mirrors remains particle-free. Many of these components must meet ultra-clean vacuum (UCV) and ultra-high vacuum (UHV) standards to prevent contamination.

This paper presents a newly designed pumping station for cleanroom applications. It enables standard vacuum tests, including leak testing and residual gas analysis (RGA), while minimizing contamination risks. To maintain cleanroom integrity, the pumping station is housed in a separate technical room and features remote operation capabilities.

INTRODUCTION

UCV and UHV requirements are essential for maintaining the performance and lifetime of optical components in X-ray free-electron laser facilities. Mirrors and beam transport elements are particularly sensitive to particle and hydrocarbon contamination, and therefore must be assembled and qualified in an ISO 5 cleanroom environment [1, 2].

To address this need, a dedicated pumping station was developed for the European XFEL cleanroom. It provides a local connection port for vacuum testing directly within the cleanroom, enabling leak tests and residual gas analysis.

UCV AND UHV REQUIREMENTS

To ensure that components meet the strict standards for ultra-clean and ultra-high vacuum operation, several acceptance criteria must be fulfilled. These requirements follow the established XFEL UHV guidelines [3].

Particle Cleanliness

The particle level inside critical components must be verified using a particle counter. A turbulent flow of ionized nitrogen is introduced into the component, and the particle counter is positioned at the exhaust. The number of particles must not exceed the maximum levels permitted by ISO 14644-1 Class 5.

* joshua.ohnesorge@xfel.eu

Leak Tightness and Residual Gas Analysis (RGA)

Leak testing and residual gas analysis are essential steps to demonstrate the suitability of components for UHV operation. A low leak rate ensures that no external gases enter the vacuum system during operation, while residual gas analysis provides detailed information about the cleanliness and outgassing behavior of the tested parts.

The integral leak rate of the tested component must not exceed 1×10^{-10} mbarls^{-1}.

In addition, an RGA spectrum is recorded to identify the chemical composition of the residual gas. Acceptance criteria for unbaked vacuum systems include:

- The mass 18 peak of a leak-free system must reach a pressure below 5×10^{-8} mbar.
- After 15 h of pumping, all mass peaks between 18 and 44 must be at least 100 times lower than the mass 18 peak, with the exception of masses 28, 32, and 44.
- All mass peaks from 45 up to at least 100 must be 1000 times lower than the mass 18 peak.

CLEANING PROCEDURES

To comply with the UCV and UHV requirements described above, all components must be thoroughly cleaned before entering the cleanroom and undergoing qualification at the pumping station. Since a wide variety of components with different materials and geometries are used, several cleaning approaches are applied depending on the specific requirements and material compatibility.

Washing Machine

Large or complex components are cleaned using a dedicated lab washing machine, which is loaded from the preparation laboratory and unloaded on the clean side inside the cleanroom. The system offers multiple cleaning programs optimized for different materials and surface conditions.

Ultrasonic Bath

For smaller components, ultrasonic baths are employed. Depending on the material, various cleaning chemicals are used to ensure effective removal of contaminants. This method provides flexibility for treating delicate parts.

Vacuum Oven

When required, a vacuum oven located inside the cleanroom is available to dry components after wet cleaning procedures. This ensures that no residues remain on the surface and prepares the components for subsequent vacuum testing.

ISBN: 978-3-95450-263-9 ISSN: 2673-5520 doi: 10.18429/JACoW-MEDSI2025-THP51

SIMULATION STUDY ON THE MOTION PROCESS OF THE COPPER FOIL TENSIONING DEVICE IN THE VACUUM UNDULATOR*

Hongcui Wang, Wei Zhang†, Shudong Zhou, Ya Zhu
Shanghai Advanced Research Institute, Chinese Academy of Sciences, Shanghai, China

Abstract

In order to reduce the impedance of the electron beam, flexible and smooth transition plates are typically employed in vacuum undulators to establish a connection between the copper foil on the magnetic array and the vacuum chamber flange. Traditional transition plates, while effective for the vertical movement of magnetic arrays, fail to account for the dynamic movement of magnetic arrays that can shift vertically, horizontally, and along the beam direction. To address this limitation, a specialized copper foil tensioning device has been designed and analyzed through simulations. This device ensures a stable electrical connection between the magnetic array and the vacuum chamber flange while allowing for adaptive movement.

INTRODUCTION

The Shanghai Advanced Research Institute (SARI) of the Chinese Academy of Sciences has developed a mechanical structure for a double-period in-vacuum undulator, featuring a magnet array capable of three-dimensional movement [1]. The conventional transition plate is typically a curved thin metal sheet [2-4] , which permits only limited vertical displacement in conjunction with the movement of the magnetic array. In contrast, the copper foil tensioning device proposed in this study allows for substantial displacement in both the vertical and horizontal directions, while permitting limited displacement along the beam direction. The core components of the copper foil tensioning device are the torsion springs, spiral springs, and tension springs， which connect the moving magnetic array with the stationary vacuum chamber flange. All springs operate within their linear elastic ranges, ensuring full reversibility of motion.

MECHANICAL STRUCTURE

The mechanical structure of the copper foil tensioning device is illustrated in Fig. 1. One end of the copper foil is wound around a roller, while the opposite end is secured to the flange of the vacuum chamber. Spiral springs located at both ends of the roller apply a reverse torque, enabling the copper foil to be extended and retracted as needed. The sliding guide is mounted on the steel girder which can only move vertically and along the beam direction. Two tension springs, one on each side, connect the roller to the steel girder, ensuring that continuous contact is maintained between the roller and the copper plate of the torsion spring, even as the rolled copper foil's diameter varies. Given that tension springs are widely used and well understood, this study focuses specifically on modeling the behavior of torsion and spiral springs.

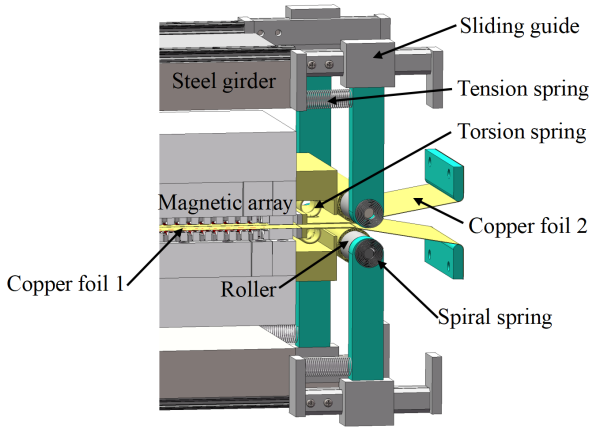

Figure 1: Mechanical structure of copper foil tensioning device.

Torsion Spring

The two straight arms of the torsion spring are each welded to a copper plate, as illustrated in Fig. 2. Copper plate 1 is mounted at the end of the magnetic array. The torsion spring serves two distinct functions:

Tensioning the Copper Foil 1 In Fig. 2, the red dotted line indicates the initial position of copper plate 2. Its left end is connected to copper foil 1, and the plate rotates to a horizontal position under the tension from the foil. At this stage, the force F applied by the torsion spring on copper foil 1 can be expressed as $F = \frac{k \cdot \theta}{r}$, where k is the spring stiffness, θ is the rotation angle, and r represents the force arm.

Maintaining Contact with the Roller The right end of the copper plate 2 is pressed downward by the roller. This results in a reaction force that ensures continuous contact between copper plate 2 and the roller. As a result, a smooth transition is formed between copper plate 2 and the copper foil 2.

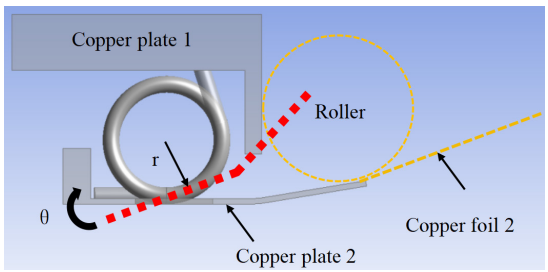

Figure 2: Torsion spring structure.

When the undulator undergoes lateral movement, the roller remains stationary, while the torsion spring moves

* Work supported by Shanghai Advanced Research Institute.
† zhangwei@sari.ac.cn

ISBN: 978-3-95450-263-9 ISSN: 2673-5520 doi: 10.18429/JACoW-MEDSI2025-THP52

STABILITY EVALUATION OF A DOUBLE CRYSTAL MONOCHROMATOR USING AN OPTICAL LINEAR ENCODER

M. Okui†, [1, 2], N. Yato[1], D. Nagata[1], Y. Ikeya[1], A. Shimoguchi[1], H. Fukuzawa[3], H. Yamane[3], J. Yoshida[4], T. Nakamura[3, 4]
[1]Technical Division, Kohzu Precision Co. Ltd., Kawasaki, Japan
[2]LASTI, University of Hyogo, Hyogo, Japan
[3]Department of Beamline, Photon Science Innovation Center, Sendai, Japan
[4]SRIS, Tohoku University, Sendai, Japan

Abstract

A dedicated jig with a high-speed optical linear encoder was developed to evaluate the intrinsic mechanical stability of a double crystal monochromator (DCM) in a standalone configuration. This novel method avoids the convolutional effects of beamline optics, allowing for a direct assessment of the monochromator's performance. The system was applied to a symmetrical layout double crystal monochromator (SDCM), demonstrating its exceptional stability. At a Bragg angle of 10°, the pitching stability was measured to be 17.15 nrad (RMS), which is significantly better than previous reports. Fast Fourier Transform (FFT) analysis revealed a vibration peak at 290–300 Hz, providing new insights into the system's performance limits. These results validate the effectiveness of our measurement system in diagnosing and improving the stability of high-performance monochromators.

INTRODUCTION

The stability of the normal vector of the two crystals of double crystal monochromators (DCMs) is a critical factor for next-generation light sources, particularly those utilizing nanometer-scale, high-brilliance X-ray beams. Maintaining a stable output beam position is essential for high-precision experiments and any angular instability in the monochromator can directly impact the quality of the experimental data.

Previous studies [1, 2] have addressed this challenge through various methods, including the development of advanced control systems. For example, a Symmetrical layout double crystal monochromator (SDCM) with an electronic cam control system was developed to maintain a fixed beam height over a wide Bragg angle range, as detailed in a related study [3–5]. While these prior works have contributed significantly to beam stability, a major challenge has been the difficulty in isolating and evaluating the intrinsic stability of the monochromator itself. Measurements using the X-ray beam often represent a convolution of instabilities originating from the electron source, the front-end optics, and the monochromator, making it difficult to pinpoint the root cause of the instability.

To address this limitation, this paper introduces a novel approach for evaluating monochromator stability. We have utilized a standalone measurement system with an optical linear encoder to directly assess the pitching and rolling stability of a SDCM. The SDCM, whose conceptual design minimizes moment changes during rotation [5, 6], was developed. This method allows for a precise evaluation of the monochromator's mechanical performance in isolation, independent of external beamline-related factors. The primary objective of this study is to demonstrate the exceptional performance of the symmetric layout DCM by quantitatively measuring its intrinsic stability under various operational conditions.

EXPERIMENTAL SETUP

The positional stability of the SDCM was evaluated using a newly developed standalone measurement system, a method also utilized and validated in a previous peer-reviewed study [3]. This system consists of an optical linear encoder (Renishaw REXT20USA255) and a high-speed data acquisition unit. The encoder was mounted in a custom-designed bracket to measure the linear displacement of the double crystals. This setup allows for precise monitoring of the pitching and rolling motions of the monochromator.

The measurement system's resolution is 8 nrad, and its detection limit is greater than 16 nrad. All data were acquired at a sampling rate of 2048 Hz, with the acquisition time set to 4 seconds for each measurement. The monochromator was operated with a water-cooling system at a flow rate of 2.2 l/min. The analysis was performed at three different Bragg angles (10°, 40°, and 70°) to investigate the stability under various operational conditions. The measured values, such as the root-mean-square (RMS) stability, should therefore be interpreted with consideration for the measurement system's inherent resolution and detection limits.

RESULTS

The SDCM's stability was evaluated using the newly developed standalone measurement system at Bragg angles of 10°, 40°, and 70° (2048 Hz sampling).

Figure 1 illustrates the temporal behavior of the monochromator's intrinsic mechanical stability in pitching and rolling directions, showing consistent performance without significant long-term drifts. The RMS stability was measured to be 17.15 nrad for the 10° pitching data, reinforcing the key finding from the abstract. The full data set for all measurements is summarized in Table 1.

† okui@kohzu.co.jp

ISBN: 978-3-95450-263-9 ISSN: 2673-5520 doi: 10.18429/JACoW-MEDSI2025-THP54

THE FIRST PARTICLE-FREE BEAM STOP FOR THE ESS SUPERCONDUCTING LINAC

Elena Donegani*,[1], Artur Gevorgyan[1], Juan Herranz[2], Anders Olsson[1]
[1]European Spallation Source (ESS) Lund, Sweden
[2]Proactive R&D, Barcelona, Spain

Abstract

For the ESS superconducting linac, a compact beam stop for [21, 100] MeV protons was designed instead of a bulky beam dump. Its mass is 60 kg, its length 1200 mm (perpendicular to the beamline), and the cylindrical beam-intercepting part fits into a CF160 flange. In the most thermally demanding beam mode (40 MeV, 50 µs, 1 Hz, 62.5 mA), thermomechanical calculations predict a peak temperature of 685 °C in the graphite core that is enclosed in a TZM shell. The beam stop is water-cooled, equipped with thermocouples and movable by a pneumatic actuator. The beam stop was manufactured by Proactive R&D in Spain and shipped under vacuum to ESS in Sweden. The assembly, tests and metrology measurements were performed in an ISO5 cleanroom. During August 2024, the beam stop was installed with a dedicated cart in the ESS beamline, surrounded by a portable cleanroom to maintain a particle-free environment next to superconducting cavities.

The results of the commissioning with beam and the main challenges (e.g. the ISO5 requirements, unconventional brazing and demanding engineering tolerances) are summarized and useful for the design of future particle-free devices intercepting high-power beams.

INTRODUCTION

The European Spallation Source (ESS, [1]) is a new facility under construction in Lund (Sweden). Once fully operative, the ESS will be the world's most powerful accelerator-based neutron source. The ESS accelerator is an extremely compact proton linac that will deliver 2.86 ms long proton pulses, at a repetition rate of 14 Hz with a nominal proton current of 62.5 mA. One of the main challenges is to design and install particle-free devices that not only withstand the high-power proton beam, but also fit in the limited space both inside and outside the vacuum vessel. The literature about particle-free insertable devices is limited; therefore, this contribution summarizes challenges and solutions for the first particle-free beam stop [2] that was designed, installed and operated in the first section (SPK1) of the ESS superconducting linac (see Fig. 1). In the following sections, the emphasis is on the vacuum requirements and the corresponding tests that have driven the design, manufacturing, tests and installation of the particle-free beam stop.

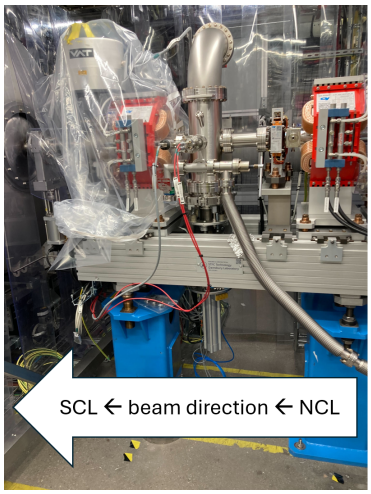

Figure 1: Photo of the SPK1 beam stop vertically installed next to the first cryomodule of the ESS superconducting linac (SCL, on the left), and in between the two red quadrupoles.

VACUUM REQUIREMENTS

The SPK1 beam stop is the first particle-free beam stop installed in the superconducting ESS linac. It should be noted that rigorous control of particulate contamination is mandatory to achieve and maintain the high accelerating gradient (up to 10 MV/m in the case of the ESS SPK section). The Vacuum Requirements (VR) are summarized as follows:

- VR1 Virtual leaks must be avoided in the first place i.e. in the design phase.
- VR2 The leak tightness of each component must be checked, quantified and below < 10^{-10} mbar·L/s.
- VR3 All components must be degreased, rinsed, dried, cleaned and controlled in particles.
- VR4 No signs of contamination must be experimentally demonstrated via RGA scans i.e. the presence must be ruled out for CO, CO_2 and hydrocarbons.
- VR5 During the operation with beam, the outgassing must remain below 10^{-7} mbar·L/s.

DESIGN AND MANUFACTURING

The SPK1 beam stop was designed at ESS for the most demanding beam power of 700 W (corresponding to: 100 MeV protons, 10 mA, 50 µs, 1 Hz, 14 Hz). The detailed design was developed by ESS in collaboration with Proactive R&D in Spain; it results also from the design and operational experience gained with the ESS DTL4 Faraday cup [3], both devices having a graphite core and a TZM entrance window. Graphite and TZM were selected because of their physical

* elena.donegani@ess.eu

ISBN: 978-3-95450-263-9 ISSN: 2673-5520 doi: 10.18429/JACoW-MEDSI2025-THP55

THE NEW NANOMOTION LABORATORY AT ALBA

J. L. Frieiro†, N. B. Pereira, N. González, C. Colldelram, J. Nicolàs
ALBA Synchrotron, Cerdanyola del Vallès, Spain

Abstract

ALBA synchrotron has built and recently opened a new laboratory for Nanomotion tasks, which will gain relevance in the upcoming years as the upgrade to a 4th generation facility, ALBA II, commences. The laboratory is operated as a clean room built in the Experimental Hall to profit from the main slab isolation of vibrations.

This work shows the dedicated spaces, installations and capabilities of the Nanomotion laboratory and the commissioning results of its environment demonstrating the design specifications achieved. In addition, the involvement of the laboratory in different projects at ALBA is introduced.

INTRODUCTION

With the upgrade of ALBA to ALBA II, a 4th generation facility [1], on the horizon, a new Nanomotion laboratory has recently been built. This laboratory will focus on researching, developing, and commissioning high-performance motion and positioning instrumentation, control systems, and synchronization between components. The space is also equipped with optimal conditions for the assembly of beamline components that require a controlled environment, such as mirrors.

The laboratory is constructed as a clean room, with control of particles, temperature, pressure, and humidity. The structure is constructed over the main slab of the facility, thereby benefiting from the vibration isolation it provides.

This work introduces the current state of the Nanomotion laboratory, focusing on its different spaces, installations, and capabilities. The preliminary results of the laboratory environment conditions, which are currently under commissioning, are also presented, along with their target specifications. Finally, the various projects in which the laboratory is currently engaged are delineated, showing its potential future contributions to the advancement of ALBA.

LOCATION AND SPACES

The Nanomotion laboratory is built on the main slab of ALBA. It occupies the position of BL17, which would otherwise be left unused as it collides with the truck entrance for large equipment, rendering a space for a very short beamline (Fig. 1a).

As an additional benefit, the main slab of ALBA is isolated from the main ground, providing lower floor vibrations. The situation of the laboratory over this slab serves two purposes: work with improved stability conditions and in a space resembling the working conditions of the beamlines.

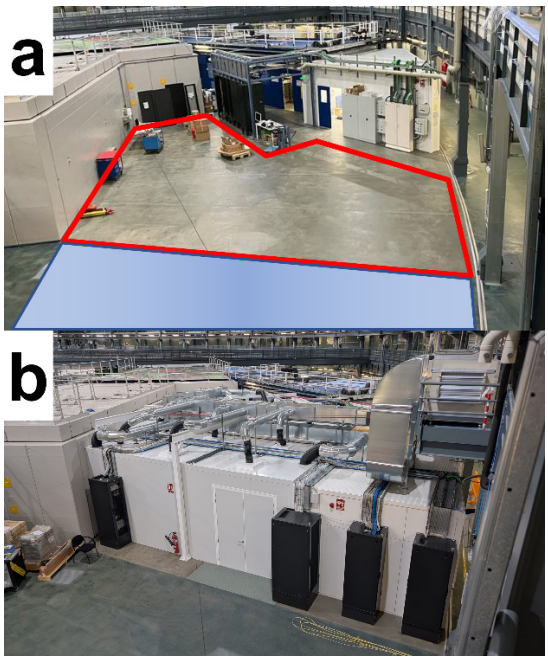

Figure 1: a) Available space before the construction of the laboratory. In red, the perimeter for the laboratory. In blue, the truck entrance. b) The exterior of the laboratory built.

The laboratory is distributed into three areas (Fig. 2), two dedicated for the clean room and another one for the operation of the laboratory.

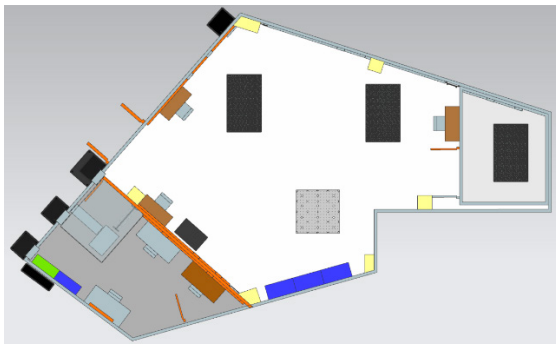

Figure 2: CAD layout of the laboratory.

Main Clean Room

The largest area is the main workspace of the laboratory (Fig. 3). It includes two 1.2×2 m^2 optical tables used for the majority of the work. A 1.5×1.5 m^2 floor plate is also embedded in the floor, providing a working surface for large equipment in case the environment of the laboratory is necessary. Last, three workstations with connection to PCs can be already used from inside to setup the different works and test while inside. The space has been planned and equipped with the future installation of two additional tables in mind.

† jfrieiro@cells.es

ISBN: 978-3-95450-263-9 ISSN: 2673-5520 doi: 10.18429/JACoW-MEDSI2025-THP58

PROTOTYPING FOR THE ALBA II VACUUM SYSTEM*

R. Parise†, P. Ros, L. Carvajal, O. Traver, J. Álvarez, G. Peña, L. Ribó, J. Boyer, P. Salmeron, B. Francisco, L. Nikitina, J. Ladrera, A. Fontanet, B. Zhang, M. Ning, V. Massana, L. Torino, M. Carlà, O. Blanco, T. Günzel, Z. Martí, I. Bellafont, M. Quispe, M. Llonch, N. Gonzalez, G. Benedetti, F. Fernandez, J. Marcos, U. Iriso, J. Casas, F. Perez, M. Pont, C. Colldelram
ALBA Synchrotron, Cerdanyola del Vallès, Spain

Abstract

ALBA is working on the ALBA II upgrade to transform the current storage ring, in operation since 2012, into a 4th-generation diffraction-limited synchrotron light source. The vacuum system is designed for a compact geometry with tight magnet apertures, where synchrotron power is distributed directly onto the chamber walls. Nevertheless, crotch absorbers will be used at key locations. Due to the low conductivity in such small chambers, the entire ring will be NEG coated to accelerate vacuum conditioning and achieve the required ultimate pressure. Most of the vacuum chambers of the 268.8 m long ring, divided into 16 arcs of 12.8 m each, will be made of OFHC-Cu or CuCrZr to dissipate synchrotron radiation and reduce resistive wall impedance. The chambers will have a nominal internal diameter of 16 mm, a minimum wall thickness of 1 mm, and clearances of up to 0.5 mm from magnet poles. Launched in 2021, the upgrade includes an R&D program focused on prototyping critical components. This contribution presents the overall vacuum system status, the design and production of vacuum prototypes, and initial component tests.

INTRODUCTION

ALBA II is a major upgrade of the ALBA synchrotron light source in Spain, aiming to transform its storage ring into a fourth-generation, diffraction-limited facility [1]. The upgrade replaces the current Double-Bend Achromat lattice with a compact Multi-Bend Achromat layout, while reusing much of the existing infrastructure.

A prototyping program, called ALBA01, was launched when the working design was based on a 6-bend achromat (6BA) lattice. Despite later transitioning to a 5BA configuration [2], the prototypes remain valid for manufacturing, testing, and assembly validation. Features expected for the 5BA layout were incorporated wherever possible. This early freeze was a strategic decision to reduce project risk and ensure timely use of committed funding before December 2025. This paper presents the current vacuum system design, details of the prototypes manufactured to date, and the strategy to adapt them to the evolving 5BA layout.

ALBA II VACUUM SYSTEM CONCEPT

The ALBA II vacuum system is being designed to meet the requirements of a 4-gen synchrotron light source: low beam impedance, mechanical compatibility with a densely packed lattice, and vacuum levels below 1×10^{-9} mbar in under then 100 Ah of conditioning.

To address these competing constraints, the baseline solution adopts a hybrid approach:

- NEG-coated copper round chambers with an internal diameter of 16 mm will be used in most sections to minimize resistive wall impedance and allow distributed pumping.
- A conventional antechamber design will be implemented locally to manage synchrotron radiation (SR) power and accommodate photon absorbers and pumping elements.
- Stainless-steel (SS) chambers will be used in corrector magnet locations to increase orbit feedback bandwidth and magnetic transparency.

The small aperture, defined by the minimum magnet aperture diameter of 20 mm, combined with the tight magnet layout, with separations between the effective length of adjacent magnets as small as 40 mm [3], results in poor vacuum conductance and limited space for distributed pumping. To compensate, the entire storage ring will be NEG coated, with *ex-situ* activation during the sector pre-assembly. Synrad+ and Molflow+ simulations [4] indicate that, with this strategy, an average pressure of 2.4×10^{-10} mbar CO-equivalent can be reached after 100 Ah of accumulated beam dose for the long dipole chamber, as shown in Fig. 1.

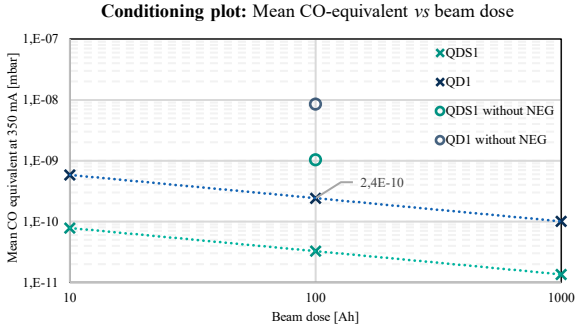

Figure 1: Conditioning plot for the chamber prototypes.

Another key feature is the use of Matsumoto-Ohtsuka (MO) type flanges [5], which offer compact sealing with good alignment repeatability and have been adopted successfully in other light sources operating with small aperture chambers.

The overall layout consists of 16 arcs, each approximately 12.8 m long, supported by 5 girders [6], forming a ring of 268.8 m in total circumference [7]. Each arc will be equipped with a set of ion pumps located near the photon absorbers, typically rated at 75 l/s, to provide local pumping and complement the distributed NEG pumping.

* Work supported by Spanish MCIN and the European Union – Next Generation EU project 28.50.460D.74903 from the Recovery and Resilience Mechanism.
† rparise@cells.es

ISBN: 978-3-95450-263-9 ISSN: 2673-5520 doi: 10.18429/JACoW-MEDSI2025-THP59

VERIFICATION OF SPring-8-II VACUUM SYSTEM PROTOTYPE CHAMBER

K. Tamura†,1,2, H. Dewa[1], M. Masaki[1], T. Masuda[1], M. Oishi[1,2], H. Ota[1], M. Shoji[1,2], S. Takano[1,2], Y. Taniuchi[1], Y. Ueda[1], T. Watanabe[1,2],
[1]Japan Synchrotron Radiation Research Institute (JASRI), Sayo, Hyogo, Japan
[2]RIKEN SPring-8 Center (RSC), Sayo, Hyogo, Japan

Abstract

The SPring-8-II project, upgrading SPring-8 to a 4th generation light source, has started in FY2024. The project requires a vacuum system compatible with compact, reduced-aperture magnets, ensuring sufficient beam lifetime and operational flexibility. An efficient pumping system has been introduced for obtaining long enough beam lifetime, where photon stimulated desorption gas around discretely distributed photon absorbers is locally evacuated by discrete NEG pumps. A low coupling impedance vacuum system has been designed by optimizing chamber geometry, etc., to enable various operation modes. Prior to mass production of vacuum components, prototypes of the main vacuum chambers were fabricated for performance verification with magnet arrays. These tests validated the procedure for rapid installation and vacuum commissioning without in-situ baking, checked for interference with other equipment, and verified the required vacuum performance.

INTRODUCTION

SPring-8-II is a major upgrade project [1, 2] of the third generation light source SPring-8. This project aims to achieve excellent light source performance, while preserving the same level of high beam stability and machine reliability as those achieved by the current SPring-8. Simultaneously we aim to reduce power consumption of the light source machine. The SPring-8-II project has started in FY2024. The current SPring-8 will be shut down after summer 2027 and replacement of the accelerator components will be conducted for almost one year. After beam commissioning of the SPring-8-II storage ring, user operation is scheduled to resume in April 2029. Main parameters of SPring-8-II are shown in Table 1 together with those of the current SPring-8.

Table 1: Main Parameters of SPring-8-II and SPring-8

Parameter	SPring-8-II	SPring-8
Lattice type	5-bend	2-bend
Energy [GeV]	6	8
Stored Current [mA]	200	100
Circumference [m]	1435.43	1435.95
Emittance [pm rad]	< 100	2,400

We will reuse the existing ring tunnel and beamlines, so SPring-8-II is designed to have the same cell number of 48 as SPring-8. Among them, 34 cells are called normal cells. 2 cells are designed for beam injection, 4 are called a long straight section without bending magnets, and 8 on both sides of the four long straights are used for matching beam optics. Prior to mass production of vacuum components, prototypes of the main vacuum chambers of the normal cell have been fabricated and tested. Through the fabrication and construction of the vacuum chambers, interference checks with magnets and overall vacuum tests, we confirmed the validity of our vacuum design and construction procedures.

This paper presents the outline of the vacuum system of the SPring-8-II storage ring, and prototype verification results for the SPring-8-II vacuum system.

VACUUM SYSTEM

In designing the vacuum system of the SPring-8-II storage ring, we have many challenges to solve such as 1) adaptation to narrow bore magnets assembled with a high packing factor, 2) achievement of low pressure enough to obtain a sufficient beam lifetime, 3) realization of smooth inner surface and low resistive wall impedance. Furthermore, it is necessary to replace the accelerator components within a short period of approximately one year. High reliability, robustness, and maintainability are also required. In addition, these challenges must be solved while keeping the cost as low as reasonably achievable.

As a solution to these challenges, we employed small aperture, thin-walled stainless steel vacuum chamber and discrete photon absorbers equipped with a compact, cartridge type NEG pump nearby. This scheme can localize photon stimulated desorption (PSD) gas source around the photon absorber, and realize the effective evacuation of the PSD gas for compensation of low conductance of small size vacuum chamber. In addition, by adopting a rhombic shape for the cross section of the beam chamber, we have realized the vacuum system with low resistive wall impedance without copper plating on the inner surface of the beam chamber. In order to complete the installation of the vacuum equipment in a short period, we adopted the procedure that omits in-situ baking inside the tunnel, and instead performs pre-baking outside the tunnel, installation inside the tunnel, rough pumping down by turbo molecular pumps (TMPs), and NEG activation. For this reason, changing from the previous design [3, 4], we divided each cell into chambers of a manageable length. Furthermore, with the aim of reducing costs and ensuring robustness and maintainability, we reviewed the structure, materials and manufacturing methods of various types of vacuum equipment.

† tamura@spring8.or.jp

ISBN: 978-3-95450-263-9 ISSN: 2673-5520 doi: 10.18429/JACoW-MEDSI2025-THP62

MODULAR SENSOR SUPPORTS FOR PRECISION ALIGNMENT OF HL-LHC COMPONENTS

M. Sosin*, P. Biedrawa, C. Casarotto[1], A. Herty, J. Kampp,
M. Noir, V. Rude, CERN, Geneva, Switzerland
[1]also at Technical University of Denmark, Kongens Lyngby, Denmark

Abstract

The High Luminosity Large Hadron Collider (HL-LHC) is an ambitious upgrade project to increase the LHC collision rate, significantly enhancing the physics discovery potential of the present LHC beyond 2030. As part of this effort, new components must be aligned within an elliptical 1σ tolerance envelope, with radii of 0.17 mm vertically and 0.33 mm radially over 420 m around the two high luminosity experiments ATLAS and CMS. To meet these stringent requirements, all components will be equipped with micrometric alignment sensors, including 276 Wire Positioning Sensors and 148 Hydrostatic Levelling Sensors. These sensors must be rigidly attached to the component structures and accurately pre-adjusted relative to external reference networks. These requirements led CERN's geodetic metrology group to develop a modular support system. This system ensures an ergonomic adjustment of sensors, a long-term positional stability, and a robustness against mechanical constraints. This paper presents the design approach and the results of the final testing and validation of the modular sensor support solution.

INTRODUCTION

The High Luminosity Large Hadron Collider (HL-LHC) is an upgrade to the current LHC to increase the instantaneous collision rate by a factor of five relative to its original design values [1]. Achieving this goal requires a major enhancement of the accelerator infrastructure, including the replacement of approximately 1.2 km of beam lines with new high-performance components. Key technological innovations—such as next-generation superconducting magnets, compact superconducting radio-frequency cavities, and other advanced systems—will be installed primarily in the long straight sections (LSS) around the ATLAS and CMS experiments. To preserve beam stability and maximise luminosity, these components must be positioned with unprecendeted precision: within an elliptical standard deviation envelope with radii of 0.17 mm vertically and 0.33 mm radially over a 420 m span [2].

To meet these stringent tolerances while minimising the exposure of personnel in high-radiation areas, the Full Remote Alignment System (FRAS) will be deployed [3]. FRAS enables continuous position monitoring and micrometric remote adjustment of 76 HL-LHC beam line components installed in the tunnel. Each component is equipped with high-precision alignment sensors to determine its position, coupled with motorised actuators providing a transverse adjustment range of ± 2.5 mm. This architecture allows operators to maintain alignment performance without requiring frequent in-situ intervention.

Two types of sensors are central to FRAS operation: the Wire Positioning System (WPS), which measures transverse offsets relative to a reference wire, and the Hydrostatic Levelling System (HLS), which determines vertical offset from a water level reference (cf. Fig. 1). Their reliable performance requires a stable, adjustable, and cost-optimised mounting solution, given that more than 420 sensors will have to be installed.

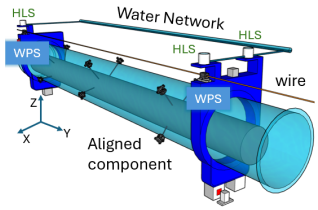

Figure 1: WPS and HLS sensors for component alignment.

This role is carried out by the sensor supports—dedicated mechanical interfaces that mount the WPS and HLS instruments onto the so-called Sensor Support Bracket (SSB) welded to the components (cf. Fig. 2). The sensor supports provide a critical link between the aligned component structure and the high-precision alignment instrumentation of the FRAS.

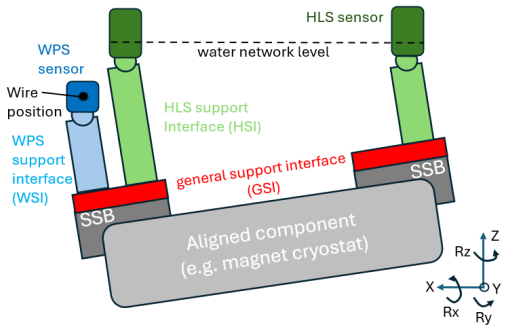

Figure 2: Schematic of sensors installation on the component and role of the supports.

DESIGN REQUIREMENTS

The design requirements are derived from HL-LHC alignment tolerances and operational needs, ensuring the sensor

* mateusz.sosin@cern.ch

ISBN: 978-3-95450-263-9 ISSN: 2673-5520 doi: 10.18429/JACoW-MEDSI2025-THP63

QUALIFICATION OF SERIAL PRODUCTION OF JIGS FOR THE UNIVERSAL ADJUSTMENT PLATFORMS FOR THE HIGH LUMINOSITY PROJECT

M. Noir*,1, M. Sosin†,1, N. Bendotti[1], B. Marcin Pudlo[1], L. Sjöberg[2]
[1]CERN, Geneva, Switzerland
[2]Kungliga Tekniska Högskolan (KTH), Stockholm, Sweden

Abstract

As part of the High Luminosity LHC (HL-LHC) project, a modular platform with 6 degrees of freedom, the Universal Adjustment Platform (UAP), has been developed. This platform, based on standardized micrometric adjustment jigs, enables the precise alignment of accelerator components weighing up to 2000 kg. Following the successful validation of a fully functional prototype, serial production of the standardized components began in 2025. To ensure quality and to meet the stringent requirements, a validation test sequence—based on a specially designed test bench—was established. This sequence allows the verification of the series production (140 vertical jigs and 70 radial jigs) including their micrometric backlash and behavior under nominal load. This paper presents the testing methodology for such a qualification and the results obtained.

INTRODUCTION

The upcoming High Luminosity upgrade of the CERN Large Hadron Collider (HL-LHC) aims to increase the machine's operating luminosity by a factor of five [1]. This target imposes stringent alignment requirements on accelerator components located along the 420 m Long Straight Sections (LSS) situated around the ATLAS and CMS experiment.

The alignment of the HL-LHC is realized through the Full Remote Alignment System (FRAS) project [2]. FRAS enables continuous monitoring of component positions and micrometric remote adjustments of 76 beam line elements installed in the tunnel. Each element is equipped with high-precision alignment sensors for position determination and mounted on motorized jacks or standardized platforms.

A dedicated platform solution has been implemented for components with a mass below 2000 kg. In this case, the in-house-developed Universal Adjustment Platform (UAP) [3] provides precise six-degree-of-freedom (DoF) positioning. After installation, these platforms will be motorized to enable fully remote operation [4].

Following the successful functional validation of prototypes in 2024, a series of 35 UAPs was produced in 2025 to support the HL-LHC collimators and masks. Each platform integrates micrometric actuation jigs specifically designed for the CERN application.

* michel.noir@cern.ch
† mateusz.sosin@cern.ch

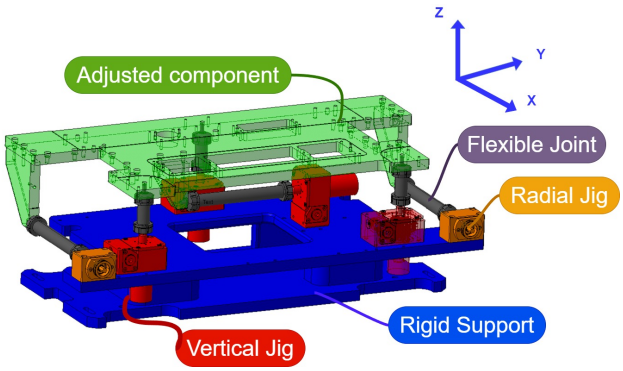

Figure 1: Jigs position in UAP Platform.

The production batch — comprising 70 radial jigs and 140 vertical jigs — underwent intensive post-assembly testing by the manufacturer on a dedicated bench. The key parameters and corresponding test results are presented in this paper.

VERTICAL AND RADIAL JIGS - KEY UAP's ELEMENTS

The UAP platform is derived from the Stewart platform concept. Adjustment in all six degrees of freedom is achieved using two radial jigs, which control the radial position and yaw of the component, and four vertical jigs. Of the vertical jigs, three define the vertical position, pitch, and roll, while the fourth controls the longitudinal position (Fig. 1). As the performance of the complete UAP depends primarily on the precision of each jig, the following functionalities were identified as critical for serial production:

- Jigs shall be able to sustain the component load with sufficient safety margins. This implies to perform load tests at 150 % of the nominal system load.
- Jigs shall be compatible with the motorization system, requiring a limited and repeatable actuation torque both with and without load.
- Jigs shall allow micrometric positioning. This implies that the full system backlash has to be as low as possible.

Due to their nominal load and installation orientation within the UAP, the radial and vertical jigs have distinct designs (Fig. 2):

- The radial jig is based on a precisely machined metric lead-screw with a fine pitch.
- The vertical jig is composed of a first worm gear reduction and a trapezoidal lead-screw as output.

ISBN: 978-3-95450-263-9 ISSN: 2673-5520 doi: 10.18429/JACoW-MEDSI2025-FROA02

DEVELOPMENT OF NON-EVAPORABLE GETTER (NEG): SET-UP AND CHARACTERIZATION

U. Ruiz de Gopegui, E. G-Berasategui
TEKNIKER, Basque Research and Technology Alliance (BRTA), Eibar, Gipuzkoa, Spain

Abstract

Achieving Ultra High Vacuum (UHV) conditions is crucial for the operations of particle accelerators or synchrotron facilities. One effective approach to reach these conditions is the applications of TiZrV Non-Evaporable Getter (NEG) thin films coatings on copper and stainless-steel beam pipes. In this work, we report on the development of a coating setup designed for 40mm and 16mm diameter, 1-meter-long pipes. The influence of sputtering pressure and working gas on the coating properties has been investigated. The coated pipes have been characterized in a setup based on the aperture method and Monte Carlo simulations have been carried out to determine coating sticking factor. The elemental composition, structure, hydrogen pumping speed, and CO saturation have been also evaluated

INTRODUCTION

NEG sputtering coatings based on TiZrV alloys are extensively employed along accelerator beamlines to provide distributed pumping solutions and maintain extreme ultra-high vacuum (XUHV) conditions—typically 10^{-12} mbar—in low-conductance chambers. These coatings play a crucial role in ensuring stable beam delivery and extending the lifetime of beamline components [1]. TiZrV coatings significantly reduce desorption yields for gases such as H_2, CH_4, CO_2, and CO [2], as well as photon and electron stimulated desorption yields [3, 4], and secondary electron yield [5] Their application inside beam guides chambers simplifies vacuum system design, enabling longer beam guides, reduced cross-sections, and more complex geometries. This facilitates higher particle energies and precision experiments, reducing beam losses. After saturation, NEG coatings are reactivated, to revert NEG coating to metallic state, at relatively low temperatures (~180ºC) making them compatible with materials such as aluminium and copper [6]. To further enhance their performance and extend their operational lifetime, additional research is needed. To this end, four different sputtering pressures—1 mbar, 5×10^{-1} mbar, 5×10^{-2} mbar, and 5×10^{-3} mbar—along with two sputtering gases, argon (Ar) and krypton (Kr), have been analysed. Their influence on the coatings' morphology, thickness, composition, and pumping properties has been evaluated.

NEG COATINGS SET UP

A NEG coatings deposition system was designed, UHV compatible with a base pressure of less than $5x10^{-9}$ mbar and a turbomolecular dry pumping station. The working pressure can be between $2x10^{-3}$ to 1 mbar using Ar or Kr. The gas control is made with a UHV variable leak rate valve which keeps constant gas flow during the process. The whole system can be baked up to 150 ºC whereas substrate can be heated up to 300 ºC. The magnetic field has been designed to be up to 600 G within 1m length. DC and Pulsed-DC sputtering can be done with powers up to 100 W. Sputtered material is 0.5-1 mm diameter twisted wires of Ti, Zr and V. The system has an RGA (0-100 amu) for vacuum quality control prior deposition. Coated tube dimensions were 40 mm and 16 mm diameter, and 1 meter length (Fig. 1).

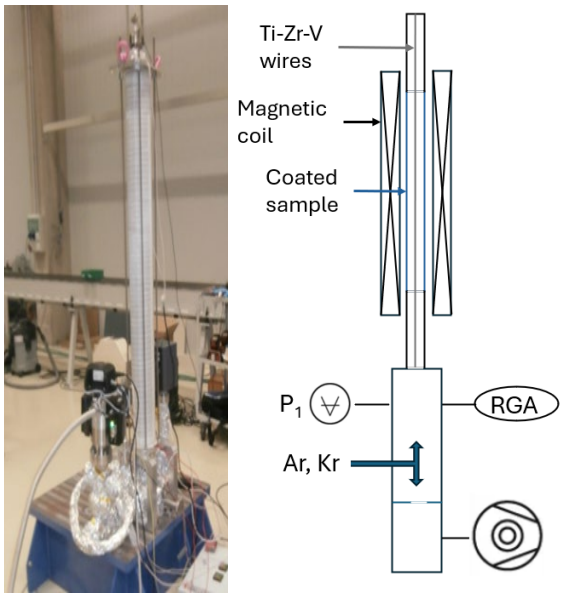

Figure 1: NEG coating set up at TEKNIKER.

COATING CHARACTERIZATION

Thickness and morphology of the coatings were analysed using Scanning Electron Microscopy (SEM) on silicon and stainless-steel samples positioned at both ends of the tubular specimens. Coating adhesion was evaluated on the stainless-steel samples. Coating material composition was performed by means of EDS into silicon samples and GDOES into stainless steel samples. Grain size analysis was performed by means of XRD.

For the sticking factor analysis, a characterization system was designed. The characterization equipment is a UHV compatible with a base pressure of less than $5x10^{-9}$ mbar (Fig. 2). The system has a turbomolecular dry pumping station. The whole system can be baked up to 150 ºC and the tested sample can be activated between 150 and 300 ºC. The system is based on the aperture method where the pressure is kept constant at the pumping side, whereas the pressure of the test sample side is registered. Working Hydrogen gas pressure can be maintained from $1x10^{-7}$ to $1x10^{-4}$ mbar with a UHV variable leak rate valve. The system has an RGA (0-100 amu) connected to the test sample

ISBN: 978-3-95450-263-9 ISSN: 2673-5520 doi: 10.18429/JACoW-MEDSI2025-FROB01

TEST BENCH FOR DEVELOPMENT OF COOLING MECHANISM OF THE FIRST OPTICAL CRYSTAL TOWARDS SPring-8-II

K. Tsubota[1], H. Kishimoto[1], Y. Senba[1,2], H. Yamazaki[1,2], H. Ohashi[†,1,2]
[1]Japan Synchrotron Radiation Research Institute, Hyogo, Japan
[2]RIKEN SPring-8 Center, Hyogo, Japan

Abstract

Thermal distortion of the first optical element under high heat load is a key issue for synchrotron beamlines, and it becomes particularly demanding for SPring-8-II of the 4th generation light source. To address this, we developed a test bench that reproduces beamline conditions while enabling offline interferometric observation of thermal distortion in cryogenically cooled crystals. As a demonstration, we tested the standard cooling holder used in cryogenically cooled Si monochromators at SPring-8, and the results were in good agreement with thermo-mechanical simulations by introducing a single effective interfacial heat transfer coefficient, with the absorbed power implemented as volumetric heating in silicon based on the measured absorption depth. This validates the approach and supports the design of ultra-stable first optical elements for SPring-8-II.

INTRODUCTION

Since the early development of third-generation synchrotron radiation sources, thermal distortion of the first optical crystal has been recognized as a major challenge. Many studies have addressed this problem by direct measurement of crystal deformation [1, 2], finite-element simulations [3, 4], or comparisons between experiments and modelling [5, 6]. More recently, new cooling schemes have been proposed based on simulations [7], and stringent wavefront preservation requirements have been quantified for FEL applications [8]. These studies collectively demonstrated that thermal effects not only reduce flux but also degrade the wavefront, compromising focusing and coherence.

At SPring-8, high-heat-load LN_2 (Liquid Nitrogen)-cooled double-crystal monochromators (DCMs) have been extensively investigated using Talbot interferometry and FEM analysis [9]. The feedback from beamline evaluations and simulations enabled improvements in holder design, leading to the standardization of crystal holders capable of handling synchrotron radiation power up to 700 W [9]. This iterative approach of experiment and modelling has proven effective, but relying solely on beamline tests is limited by available beam time and experimental constraints.

With the upgrade to SPring-8-II, the requirements for thermal management will become even more demanding. The facility will operate as a 4th generation light source (4GLS) with low emittance [10]. To take advantage of this property, beamline optics are expected to directly accept the bright source. The electron energy will decrease from 8 GeV to 6 GeV, extending the low-energy limit of x-ray monochromators from 4.9 keV to 2.1 keV, while the stored current will double from 100 mA to 200 mA. These changes will significantly increase the absorbed power density in the first crystal. Thermal distortion of crystal monochromators directly affects beamline performance: in DCMs, the parallelism of the two crystals can be adjusted to tolerate some distortion, whereas monolithic channel-cut monochromators (CCMs), though intrinsically vibration-free and therefore promising as 4GLS monochromators, cannot compensate for distortion of the first crystal, leading to reduced throughput. In both cases, apparent source shifts and wavefront degradation occur when the first crystal is distorted. At SPring-8-II, where even higher brilliance is expected, establishing reliable countermeasures against heat load on the first optical crystal will be particularly crucial [9].

Thermo-mechanical analysis of cooling schemes has long been recognized as a useful approach. However, achieving reliable predictive power requires accurate engineering parameters, such as the effective heat transfer coefficient at the crystal–holder interface. Such coefficients have previously been measured using small contact samples in offline experiments at SPring-8 [10], but the results varied widely depending on surface pressure, flatness, and interlayers. Therefore, more realistic evaluations with actual holders are needed. To address this, we have developed a dedicated test bench that reproduces beamline heat-load conditions while allowing flexible offline measurements. This enables quantitative evaluation of crystal deformation and validation of thermo-mechanical models, providing a foundation for developing ultra-stable first optical elements for SPring-8-II.

TEST BENCH CONFIGURATION

As shown in Fig. 1, the setup consists of LN_2 supply lines for cryogenic cooling, a high-power infrared (IR) laser to simulate the X-ray heat load, and a Fizeau interferometer for high-sensitivity surface deformation measurements.

The penetration depth of X-rays in Si strongly depends on photon energy. For example, in a typical high-power insertion device at SPring-8, X-rays near 10 keV make a major contribution to the absorbed heat load, penetrating approximately 0.1–0.2 mm into Si. As a representative model, we therefore selected an infrared wavelength with a comparable absorption depth. Since Si shows markedly reduced infrared transmittance at cryogenic temperatures and its thermal expansion coefficient changes sign near 130 K, the absorption depth in the liquid-nitrogen to 200 K range was particularly important. Transmission and reflectance

† hohashi@spring8.or.jp